MICROBIAL COMMUNITY ANALYSIS FOR DENITRIFYING BIOFILTERS

BY

JENNIFER MALIA ANDRUS

DISSERTATION

Submitted in partial fulfillment of the requirements
for the degree of Doctor of Philosophy in Agricultural and Biological Engineering
in the Graduate College of the
University of Illinois at Urbana-Champaign, 2011

Urbana, Illinois

Doctoral Committee:

Professor Yuanhui Zhang, Chair
Assistant Professor Luis F. Rodriguez, co-Director of Research
Research Assistant Professor Julie L. Zilles, co-Director of Research
Associate Professor Richard A. C. Cooke
Assistant Professor Angela D. Kent

ABSTRACT

Denitrifying biofilters are a promising and low-maintenance technology for removing nitrate from agricultural drainage, capable of removing 50-80% of annual nitrate loads. Because increased riverine nitrate concentrations are correlated with indicators of eutrophy and degradation of coastal waters, including a large hypoxic zone in the Gulf of Mexico (Turner and Rabalais 1994; Lohrenz et al. 1997; Rabalais and Turner 2001), denitrifying biofilters have the potential to substantially improve surface water quality. However, our understanding of ecological factors influencing biofilter performance was limited. Therefore, in this study, the microbial community of the biofilter was described using several different techniques. Denitrifying enzyme assays with inhibition showed that denitrification is primarily mediated by bacterial populations, but that fungi are also indirectly important. These assays also showed that denitrification occurs both on the surface of the biofilter woodchip media and in biofilter water, and that washing woodchips in buffer solution was able to remove cells for further study. Sample preparation methodology for use with FISH was developed using vortexing of samples with glass beads to aid in removing cells from woodchip debris. Community fingerprint techniques using ARISA and *nosZ* t-RFLP were also developed to provide high throughput bacterial and denitrifying community data.

The spatial structure of microbial communities in a biofilter was characterized using mapping of ecological metrics, MDS plots, and a new geostatistical method—ANOSIM-GS—developed for this research. ANOSIM-GS provides a robust way to characterize the variation of ecological communities with separation of space or time. Using these tools,

significant spatial variability in overall bacterial (ARISA) community spatial structure were observed across sampling depth and in the direction of biofilter flow, but not in the direction of cross-flow. Bacterial community correlation distances of 6.1 m at the 0.76 m biofilter depth, and 10.7 m at the 1.52 m biofilter depth were calculated. No significant spatial structure in the denitrifying (*nosZ* t-RFLP) community was observed.

Time-series data were collected from three biofilter sites beginning in November 2008, including performance, microbial community, and environmental data. Using ANOSIM-GS, bacterial and fungal communities (ARISA and fARISA) were shown to have temporal structure. Bacterial communities in all three biofilters showed a correlation time of approximately 125 d and signs of annual cyclic patterning. Correlation times in fungal communities were more variable, between 100-200 d, and annual cyclical patterning was less. Communities were also structured by space in the time-series data. Analysis of the relationships between community, performance characteristics, and environmental variables yielded several results. A subset of 39 bacterial and fungal populations accounted for 80% of the community variation both between and within biofilter sites, and several of these populations were significantly associated with variation in nitrate removal. Microbial community composition was found to be structured by changes in temperature, inlet nitrate, pH, moisture content, and depth (distal controls on denitrification). Additionally, nitrate removal was also significantly affected by COD, DO, flow, temperature, and moisture, apart from the influence of any of these parameters on microbial community structure (proximal controls on denitrification). These results suggest that inoculation of well-performing species, or changes in the biofilter environment, either to restructure

community composition or to improve the denitrification rate of those populations already present, may improve biofilter performance.

ACKNOWLEDGEMENTS

I'd like to extend my sincere thanks to the many people who made this work possible:

- To Dr. Yuanhui Zhang, for letting me find my own path and specialty
- To Drs. Luis Rodriguez, Julie Zilles, and Angela Kent, for letting me coerce them into this crazy research project and turning it into something of substance. I also thank these three for lending me use their facilities, their expertise, their patience, and their time. In particular, Dr. Zilles has shown amazing dedication to reading and editing written work and to mentoring my progress
- To Dr. Richard Cooke for developing the denitrifying biofilters in the first place and for letting me conduct my work on them
- To Dr. Michael Hirschi for providing the best advice at the most challenging times and for letting me be who I am
- To the undergraduate and fellow graduate students that have spent countless hours with me sampling and in lab work: in particular Matt Porter, Nick Bartolerio, Ariane Peralta, and Sara Paver.
- To my funding agencies: the USDA National Needs Fellowship and the National Science Foundation.
- And finally to the people to whom this dissertation belongs more than it does to me—you know who you are.

TABLE OF CONTENTS

1. INTRODUCTION

Today, we face unparalleled challenges in sustaining the function of the environment while promoting positive development of our societies and economies. We as a society are attempting to provide energy, clean water, and food for seven billion people, a substantial portion of which live in developing countries and whose demand for a higher standard of living will only increase. At the same time, aspects of our previous development and technologies have resulted in global climate change, habitat destruction, and pollution of the water and air. We are under pressure to find effective, efficient, and low-impact technologies that will improve our ability to provide for ourselves, to clean up our environments, or to ideally do both.

1.1 ECOLOGICAL ENGINEERING

Ecological engineering is a promising field with the potential to address many of these challenges. Ecological engineering design seeks to manage the self-organization of ecosystems such that they carry out desired functions (Kangas, 2004; Mitsch and Jorgensen, 2004). The resulting technologies are frequently more environmentally sustainable than traditional solutions because they harness the natural functions of ecosystems. Therefore, they typically require little maintenance and few to no inputs, and are usually solar powered. Designed ecosystems also have the potential to adapt to changing conditions.

Because ecology is the branch of science that underpins ecological engineering, typical design strategies have been developed based on ecological principles. These strategies include the manipulation of state variables to promote certain populations or

interactions, periodic perturbation of some environmental conditions to encourage system robustness, seeding with communities from ecosystems similar in function to that desired to increase the probability that appropriately preadapted populations are present, and encouraging diversity at all scales under the supposition that diversity will increase system stability.

However, the same complexities that make these systems desirable also make them difficult to understand, design, and control. Traditionally engineers have sought precise control and predictive capability. However, because ecological engineering involves complex biological systems with the capability of self-organization, control and reliability are challenges. Currently no theoretical approaches beyond the use of the above design principles have been developed, leading some engineers to eschew the field as lacking rigor and precision. A more mature understanding of how to design and control engineered ecosystems, how to translate ecology and systems theory to application, is necessary.

This dissertation focuses on a particular engineered ecosystem—denitrifying biofilters—as a system to be optimized in its own right, but also as a test case for ecological engineering in general.

1.2 Denitrifying Biofilters

One environmental challenge we currently face is that of reduction of water quality due to agricultural practices. Along with sediments, animal wastes, herbicides, and pesticides, one major contribution to water quality degradation is nitrogenous fertilizer residues, which enter surface waters through runoff and subsurface (tile) drainage. Increases in riverine nitrate concentrations due to these inputs are correlated with

indicators of eutrophication and degradation of coastal waters (Turner and Rabalais, 1994; Lohrenz et al., 1997; Rabalais and Turner, 2001). Because ocean ecosystems are typically nitrogen limited, high levels of inorganic nitrogen discharged into the Gulf of Mexico via the Mississippi River system sharply increase biotic activity. When these organisms die, the oxygen demand caused by their decomposition creates an annual recurrence of a hypoxic zone off the off the Louisiana coast each summer during summer stratification (Rabalais and Turner, 2001). This hypoxic zone affects the ecology and economy of the Gulf Coast. Although historic evidence indicates that a hypoxic zone existed before modern agriculture, the size of the hypoxic zone has increased substantially with increased application of agricultural fertilizers in the Mississippi River basin. USGS research estimates that agricultural sources in Mississippi River basin watersheds account for greater than 70% of delivered nitrogen to the Gulf of Mexico (Alexander et al., 2008). Of this, corn and soybeans are the largest contributors (52% of exported nitrogen).

Here, in our region of Central Illinois, subsurface, or tile, drainage is a major pathway for nitrogen discharge; it is estimated that 25-41% of annual precipitation and 15-42% of annual fertilizer application is discharged through tile drains in Central Illinois (David and Gentry, 2000). In fact, watersheds draining into the Illinois River carry the highest nitrogen loads in the country (16-24 mg/L NO_3^- on average) (Mitchell et al., 2000). Control of nitrogen discharge in the upper Midwest sub-basins of the Mississippi River could therefore improve coastal ecosytem health in the Gulf of Mexico (Rabalais et al., 2002). Furthermore, similar hypoxic, or "dead" zones, are increasing worldwide (Diaz and Rosenberg, 2008), a phenomenon which is driving environmental advocates and

policymakers to seek technologies and ecosystem processes that can mitigate nitrate pollution (Brezonik et al., 1999).

Applying ecological engineering to this problem has resulted in the development of subsurface denitrifying biofilters (Cooke et al., 2001; Wildman, 2002; Doheny, 2003; Chun et al., 2010; Woli et al., 2010). These biofilters are an effective, low-cost, low-maintenance technology that reduces nitrate loading onto surface waters. Direct reduction of fertilizer use does not necessarily reduce nitrate loads to surface waters (e.g. Keeney and Deluca, 1993; Jaynes et al., 2008). However, by instead harnessing the metabolism of denitrifying soil microorganisms, aqueous inorganic nitrogen can be removed.

While fertilizer use is not point source pollution, subsurface drains provide excellent pseudo-point sources for control of nitrate pollution. In areas of tile drainage, applied nitrate that would ordinarily be leached into groundwater or transformed by the natural denitrification of soil microorganisms is instead diverted to drainage ditches and then into surface waters. Denitrifying biofilters, consisting of a control structure and a buried volume of woodchips colonized by native soil microorganisms, can be installed at drain outlets to remove nitrate before it is discharged.

In multi-year field trials, biofilters have reduced nitrate loads by 40-90% annually (Woli et al., 2010). Much of the remaining effluent nitrate load were discharged during the winter and spring; during the summer and autumn the biofilters were capable of substantial nitrate removal even during periods of high flow. Broad implementation of the biofilter technology could result in considerable reduction of agricultural nitrate loading to surface waters in the Mississippi River basin, without requiring large monetary investment or decreasing agricultural yields.

However, our understanding of the environmental parameters and biological interactions that impact the performance of the biofilters is limited. Therefore, from an engineering perspective, our ability to design and control the biofilters is imprecise. Certainly, previous work on the biofilter has focused on optimizing design from a traditional engineering perspective, evaluating design parameters including retention time, biofilter medium, biofilter shape, and water depth (Wildman, 2002; Doheny, 2003). However, these parameters do not fully explain the performance of the field-trial biofilters; performance variation exists between biofilters, the time required to establish denitrification capability varies, and biofilter performance under high flow conditions is inconsistent within and between biofilters. Because the biofilters are engineered ecosystems, further advancements in their design and control will depend on a more fundamental understanding of the underlying ecology.

1.3 GOALS OF THIS WORK

The limitations faced in designing denitrifying biofilters are characteristic of many designed ecosystems, where multiple species interactions are used to provide functional and resilient technologies. In this work, I sought both to better understand the ecosystem of the biofilter so as to improve its design and functionality, and to also use it as a test case for engineered ecosystems in general. Because microbial communities have fast dynamics, I had an opportunity in this study to assess the impact of extant ecological engineering principles and to explore the development of better measurement and predictive tools for engineered ecosystems.

The specific objectives of this research were to:

1. Develop theoretical and technical methodology for characterizing the microbial community of biofilter ecosystems
2. More generally, experiment with different ways of measuring and assessing engineered ecosystems
3. Track changes in microbial community and environmental parameters in the biofilter over space and time.
4. Describe the interactions between microbial community, environmental parameters, and function
5. Identify those parameters influential to community and nitrate removal that might be exploited for optimization of biofilter design and/or operation

1.4 Organization of This Work

The work that resulted from these objectives is presented in several sections. In Chapter 2, I discuss theoretical background from several disciplines that were drawn from in this research. In Chapter 3, I present the specific methodology used for experiments and analysis. The results of these studies and their implications are discussed in Chapter 4. Finally in Chapter 5, I offer an overall evaluation of the research and suggestions for its extension.

2. LITERATURE REVIEW

The work presented in this dissertation is multidisciplinary; its methodology and background are drawn from a number of fields not typically connected. The purpose of this section is to introduce fundamental concepts and information from each of these areas, and to explain their relevance to each other in the context of the research that was conducted. In this section, I discuss the history and current state of the biofilter technology (Sections 2.1), the level of understanding of its function prior to this study (Section 2.1.3) basic concepts of microbial ecology and how to measure microbial ecosystems (Section 2.2), and methods of statistical analysis that can be applied to these measurements (Sections 2.3 and 2.4).

2.1 BIOFILTERS AND DENITRIFICATION

The denitrifying biofilters that are the subject of this study use the denitrifying pathway of microorganisms to remove nitrate from water. Denitrification is part of the biogeochemical nitrogen cycle, the series of mechanisms by which nitrogen is transformed from atmospheric nitrogen into ionic and organic forms that are usable by biological organisms and then is converted back to gaseous nitrogen. The major steps of the cycle are mediated by microorganisms.

2.1.1 Denitrification and parameters that influence it

The reduction of nitrate occurs both to incorporate nitrogen into cellular molecules (assimilatory pathway) and to serve as an electron sink for cellular respiration (dissimilatory pathway) (For reviews of denitrification biochemistry, see Knowles, 1982;

Zumft, 1997). The pathway that is used by the denitrifying biofilters is a specific form of the dissimilatory pathway in which successive reductions of nitrogen species ultimately lead to nitrogen gas (N_2). This pathway is mediated by four separate enzymes that may or may not be present in the same organism: different organisms therefore may produce different denitrification products.

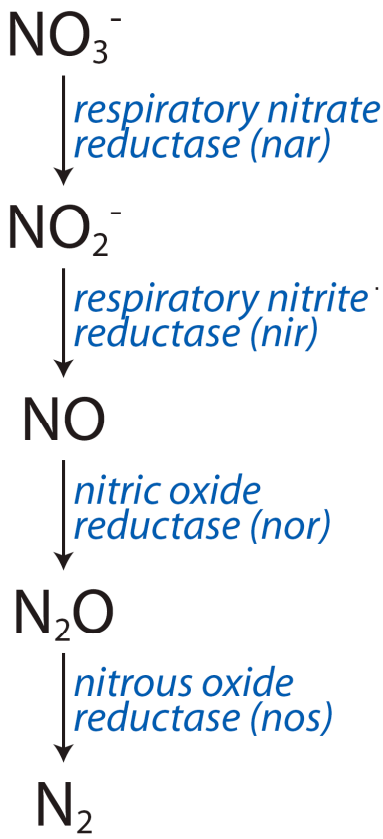

Figure 1. Diagram of dissimilatory denitrification sensu stricto. Blue labels indicate enzymes responsible for each transformation step and a gene associated with each each enzyme (in parentheses).

Denitrifying organisms belong to a wide range of groups and genera with a variety of physiological characteristics (Zumft, 1997). Species of bacteria, archaea, and fungi have all been found to denitrify. Within the bacterial world, denitrifiers are more frequent in the alpha and beta classes of *Proteobacteria*, but there is no discernible pattern of taxonomic distribution. Physiologically, most denitrifiers are aerobic, heterotrophic bacteria that use

nitrate as an electron acceptor under anoxic conditions. Psuedomonads have been the most heavily studied denitrifiers since there are a large number of them within the genus. However, denitrification can occur in S, H, and N-oxidizing lithotrophs, and even phototrophs. Some organisms (notably *Thiosphaera pantotropha* and *Paracoccus denitrificans*) denitrify aerobically. A large number of fungi have also been found to denitrify, but there has been comparatively little investigation in this area. In the biofilter system used in this study, as well as in systems like it, denitrifying organisms are naturally seeded from microbial populations in the soil.

The ecological conditions affecting denitrification in soils have been well-characterized. Firestone (1982) specified three requirements for denitrification to occur:

1. the presence of microorganisms that are capable of producing the required enzymes
2. a suitable carbon source to fuel the anabolism
3. the absence of oxygen and the presence of oxidized nitrogen compounds capable of acting as an electron acceptor

In addition to these necessary conditions, temperature, pH, Eh, and the presence of heavy metals (Chang and Broadbent, 1982) and pesticides (Grant and Payne, 1982) affect the rate of denitrification. Bremner and Shaw (1958) found that denitrification rates increase with temperature between 2-25°C, increase slightly until 60°C, and then decrease significantly above this 60°C. Denitrification occurs over a pH range of 3.5-11.2 (Cady and Bartholomew, 1961), however there appear to be optima for many species. For example, Wang et al. (1995) found that the optimum temperature for denitrification for *Pseudomonas denitrificans* is 38°C, and the optimum pH is 7.4-7.6 for nitrate reduction and

7.2-7.3 for nitrite reduction. Acidic conditions appear to favor NO and N_2O production (Bollag et al., 1973). Some evidence also exists that finer soil texture and higher moisture contents enhance denitrification (Weier et al., 1993); anoxic conditions may be more likely to exist in these environments. Denitrification has been found to occur in oxygen concentrations of 4 to 17% O_2 and at redox potentials of 300-650 mV (Firestone, 1982).

The carbon (electron) source has a critical role in denitrification. Beauchamp et al. (1989) summarized research investigating the impact of carbon source on denitrification. While denitrifying organisms can use a broad set of organic compounds as carbon (electron) sources, under denitrifying conditions, usable carbon compounds may be restricted. In particular, decomposition of complex carbon sources appears to be much slower under anoxic conditions than oxic conditions. Therefore, carbon compounds containing higher levels of lignins and organic N complexes yield usable carbon more slowly that they would under aerobic conditions.

Presumably due to differences in ability to break down complex substrates, interspecies dependences have been found in denitrification whereby one organism degrades the initial substrate and a second uses the byproducts of the first reaction. The first reaction may use nitrogen oxides as electron acceptors or may be a fermentation reaction (as in the decomposition of manure or cellulose). Although these interactions are not unique to denitrification, they are useful in the context of encouraging microbial denitrification for technical application. Knowles (2005) found that interspecies commensal association can occur with methanogens. Beauchamp et al. (1989) also relates that electron supply per mole of carbon impacts denitrification rates.

Denitrification in soils is typically limited by available carbon. In the rooting zone, carbon substrates exuded by the plant and depleted oxygen appear to increase denitrification capacity (Firestone, 1982; Beauchamp et al., 1989; Myrold and Tiedje ,1985); however, below the rooting zone organic carbon is frequently too low to support significant denitrification (Parkin and Meisinger, 1989; Yeomans et al., 1992). Although these last two studies found that addition of plant residues to the soil surface promotes denitrification in subsoils, this result was short-lived; most of the organic carbon in the residues was rapidly degraded and little reached or remained in the subsoils (Parkin and Meisinger, 1989; Yeomans et al., 1992).

More recently, molecular techniques have yielded additional information about the relationship between environmental conditions, denitrifying organisms, and denitrification function. Wallenstein et al. (2006b) reviewed work pertaining to environmental controls on denitrifying communities and rates. They defined two categories of controls: "distal controls", which affect long-term composition of denitrifying microbial communities, and "proximal controls" that affect the instantaneous rate of denitrification. Wallenstein's metaanalysis of previous studies revealed that distal controls on denitrification include patterns of carbon availability, pH, and the range of moisture and temperature to which the system is exposed. Of note was the assessment that denitrifying community structure and abundance are primarily controlled by factors other than nitrate, presumably because most denitrifiers are facultative anaerobes and do not always require nitrate. An analysis of previous research further shows that the relative activity of denitrification enzymes is sometimes driven by environmental proximal controls, but is also sometimes driven by the composition of the denitrifying community (Wallenstein et al., 2006b). Specifically, strong

seasonal shifts in denitrifying populations are common and that the distribution of populations with capability for the various steps of denitrification is variable. The ability to perform steps in the denitrification pathway is typically detected by the presence of genes coding for enzymes in the pathway. The *nosZ* gene (which codes for the enzyme nitrous oxide reductase), for example, is more cosmopolitan than *nir* genes (which code for the enzyme nitrite reductase), and its distribution is less affected by distal controls.

2.1.2 Biological nitrate remediation systems

There have been many systems designed to harness the denitrifying microbial pathway to remove nitrate from various water streams. Municipal wastewater treatment plants have long relied on both nitrifying and denitrifying microbial action in activated sludge systems, membranes, or other reactors to remove nitrogen from drinking water (Mateju et al., 1992; Tchobanoglous et al., 2003). More recently, in situ biological denitrification technologies have been investigated for treating septic systems (Ritter and Eastburn, 1988), groundwater (Robertson and Cherry, 1995; Robertson et al., 2000, 2008 Schipper et al., 2004, 2005; Schipper and Vojvodic-Vukovic, 1998, 2000, 2001), landfill leachate (Robertson and Anderson, 1999) stormwater runoff (Kim et al., 2003), and agricultural drainage (Cooke et al., 2001; Jaynes et al., 2004, 2008; Moorman et al., 2010; Woli et al., 2010). Because denitrification is limited by organic carbon substrate availability (Ritter and Eastburn, 1988), these systems encourage denitrification by adding various organic substrates such as corn oil (Hunter et al., 1997), primary alcohols (Sikora and Keeney, 1976; Janda et al., 1988; Weier et al., 1994), cotton (Volokita et al., 1996b; Soares et al., 2000), newspaper (Volokita et al., 1996a), jute (Wakatsuki et al., 1993), and, more commonly, straw, sawdust, or woodchips (Ritter and Eastburn, 1988; Robertson and

Cherry, 1995; Schipper and Vojvodic-Vukovic, 1998, 2000, 2001; Robertson and Anderson, 1999; Robertson et al., 2000, 2008, 2010; Cooke et al., 2001; Jaynes et al., 2004, 2008; Schipper et al., 2004, 2005, 2010; Cameron and Schipper, 2010; Elgood et al., 2010; Greenan et al., 2006; Moorman et al., 2010; Woli et al., 2010;). Oakley et al. (2010) found that out of various technologies designed for decentralized remediation of aqueous nitrate, denitrifying biofilters most reliably removed nitrate to a <10 mg/L compliance level.

For long-term in situ denitrification applications, generally porous barriers of solid, lignocellulosic substrates emplaced in the water flow path are the most successful. Liquid substrates will be continuously washed from the system and therefore require high-maintenance dosing mechanisms that are more appropriate to unit wastewater processes (Doheny, 2003; Mateju et al., 1992), although Hunter et al. (1997) found that corn oil may remain adhered to soil particles for up to a year. Carbon sources with low concentrations of lignins such as straw or cotton have been found to promote high rates of denitrification in laboratory scale reactors but have limited longevity as they decompose more quickly (Greenan et al., 2006; Vogan, 1993). Carbon sources that contain higher levels of slowly-decomposing lignin, such as wood, newspaper, or corncobs, therefore have been most widely used. Grinding this type of carbon source appeared to increase denitrification rates over at least 180 days (Greenan et al. 2006). In a longer-term study (10-23 months), Cameron and Schipper (2010) found that corncobs provided a 3-6.5 fold increase in denitrification rates over wood (with a retention time of 33-54 h), but were uncertain as to whether this increase would result in a shortened medium life. Cameron and Schipper also found that woodchips of larger particle size (tested range: sawdust – 61 mm particle size) resulted in higher biofilter porosity and, in some cases, higher nitrogen removal rates, over

smaller woodchip particle sizes. No difference was found between the properties of hard and soft woods.

Several different configurations of in situ biological denitrification systems using lignocellulosic media have been designed. One design creates a denitrifying "wall" or "curtain" to intercept laterally flowing groundwater by excavating soil perpendicular to the flow, mixing it with sawdust and returning it to the ground (Starr and Cherry 1994; Schipper and Vojvodic-Vukovic 1998, 2000; Schipper et al., 2004, 2005). Alternatively, infiltration beds of cellulosic material layered with sand have been used to intercept nutrient-laden effluent prior to infiltration into the ground (Robertson and Cherry, 1995; Robertson and Anderson, 1999). A number of different designs have been devised for remediating high-nitrate agricultural tile drainage, where high flow rates are common, before discharge into surface waters. One configuration treats drainage as it enters drainage ditches and streams by piping it through a series of 200 L barrels containing sand and organic matter (Blowes et al., 1994). Another type of design uses ground trenches filled with layers of sand and/or organic matter through which drainage flows in a upflow or lateral path before discharge to surface water (Cooke et al., 2001; van Driel et al., 2006; Woli et al., 2010; Elgood et al., 2010; Robertson, 2010; Schipper et al., 2010). Finally, one method seeks to treat water before it reaches the tile drains by surrounding sections of tile with woodchips such that water flows through the woochips as it enters the tile (Jaynes et al., 2008; Jaynes et al., 2004; Moorman et al., 2010).

Performance of the above in situ systems is generally very good. Schipper and et al. (2010) summarize the characteristics of the various denitrifying biofilter designs. From a metaanalysis of previous research, they report nitrate removal in the range of 0.01-3.6 g-

$Nm^{-3}d^{-1}$ for denitrification walls and 2-22 g- $Nm^{-3}d^{-1}$ for denitrification beds or trenches. Design retention times were typically on the order of hours to days. This metaanalysis also revealed that nitrate removal was increased by increased carbon substrate supply and by increased temperature, which was reported as the predominant variable. The kinetics of nitrate removal was generally found to be of zero-order under non-limiting nitrate conditions. Schipper et al. (2010) furthermore state that although ^{15}N-enrichment of media and the results of denitrification assays are consistent with the microbial denitrification pathway as the mechanism of nitrate removal in biofilters, further work in their microbial ecology is needed.

One important aspect of these in situ systems is that they show excellent longevity. Schipper et al. (2001) report that their denitrifying wall system maintains removal rates of 5-15 mg/l after five years of operation. Robertson et al. (2000, 2008) have undertaken more thorough analyses of the long-term performance of their system. After seven years of operation, their denitrifying walls exhibited 57-91% nitrate reduction, and it was found that only 2-3% of the carbon in the media had been used (Robertson et al., 2000). After fifteen years, the nitrate removal rates had only fallen to half that of the first year. Removal of the wood particle substrate decreased denitrification rates by 80%, indicating that the original media still provided the majority of the carbon source (Robertson et al., 2008). By testing woodchip media of varying ages, Robertson (2010) also showed that nitrate removal of woodchip media decreases by about 50% in the first year of operation, but afterward the rate is relatively stable for at least 7 years. Moorman (2010) found that the decomposition rate of woodchip media was associated with hydrologic conditions: media

at a continuously inundated depth (sustained anaerobic conditions) decomposed roughly seven times more slowly than media at periodically inundated depths.

2.1.3 History of the biofilter systems used in this study

The biofilters used in the present study belong to the "ground trench" category of designs for agricultural drainage described above. These systems consist of a trench filled with woodchips near the tile drain outlet through which tile effluent flows before being discharged into drainage ditches. The denitrifying biofilters have gone through several design iterations to improve their function.

Lab-scale up-flow biofilters were first used to determine the effect of hydraulic retention time and carbon source on nitrate (Cooke et al., 2001; Doheny, 2003). 10 mm gravel coated with corn oil or ethanol, and chopped corncobs or oak wood chips alone or mixed with gravel were tested as packing media. It was found that wood chips mixed with gravel was the best performing media, but that chopped corn cobs with gravel also removed significant nitrate. Consistent with the findings of other groups, the retention time necessary to treat tile water nitrate increased with both increased influent concentration and decreased temperature. A denitrification model using a Gompertz equation modified by the Arrhenius equation was developed to assist in sizing biofilters for particular conditions. According to the model, typical tile water with 20 mg/L nitrate would require 10 hours retention time in a woodchip biofilter and 12 hours in a corncob biofilter for adequate treatment at 10°C.

Wildman (2002) investigated the impact of limestone addition and soil overburden (depth of soil above biofilter media) on the performance of a lab-scale biofilter, developed instrumentation for measuring tile flow, and determined the optimum configuration of

inlet and outlet pipes. Additionally, the performance of field-installed biofilters was assessed. It was found that the addition of limestone to increase pH did not significantly affect nitrate removal in the biofilters.

Wildman also found that as head difference through the biofilter was increased, maximum flow rate was more strongly enhanced by longer inlet pipe extension into the biofilter. A set of curves was developed showing the maximum flow rate for different lengths of outlet pipe extension into the biofilter medium at various head differences. The length of inlet and outlet extension was not found to impact retention time, which was solely controlled by biofilter size. It was also determined that the addition of gravel does not significantly enhance the maximum achievable flow rate by itself, but that the addition of gravel enhances the ability of the biofilter to withstand soil overburden. Based on trial results, a mixture of 75% woodchips and 25% 25mm pea gravel was recommended.

For Wildman's study (2002), field biofilters were installed in several locations across central Illinois. These biofilters consist of a volume of woodchip medium approximately 24 in wide buried 12-24 in below the drainage pipe (a total of about 4-6 ft deep). A lateral pipe extends from the tile drain into the biofilter and an exit pipe releases treated water to a receiving body. Field biofilters were found to reduce nitrate by 3-11% in the first few months, increasing to 95-100% thereafter. This start-up period was thought to be due to the time required to establish an assemblage of denitrifying bacteria. A drop in measured dissolved oxygen across the biofilter indicated that oxygen was depleted to produce anoxic conditions within the reactor.

Over the years of development of the denitrifying biofilter systems, a number of biofilters have been installed in various field locations. However, although most are still in

Table 1. Installed biofilters under current study in Central Illinois.

Location	Site code used in this study (where applicable)	County	Shape	Size	Wood type	Loading Density (ha drainage/m^2 biofilter surface area)
Decatur, IL	FP07	Macon	square	6.1 m x 6.1 m	soft	6.54
Deland, IL		Piatt	rectangular	28.3 m x 3 m	soft	13.1
Amenia, IL		Piatt	rectangular	12.2 m x 3.1 m	hard	16.3
Decatur, IL	FP03	Macon	linear	24.4 m x 1.5 m	soft	17.4
Bloomington, IL		McLean	rectangular	12.2 m x 3.1 m	soft	21.8
Deland, IL		Piatt	rectangular	17.1 m x 3.1 m	soft	30.5
Deland, IL	DE01	Piatt	rectangular	12.2 m x 3.1 m	soft	37.0
Mount Zion, IL		Macon	rectangular	12.2 m x 3.1 m	soft	76.2

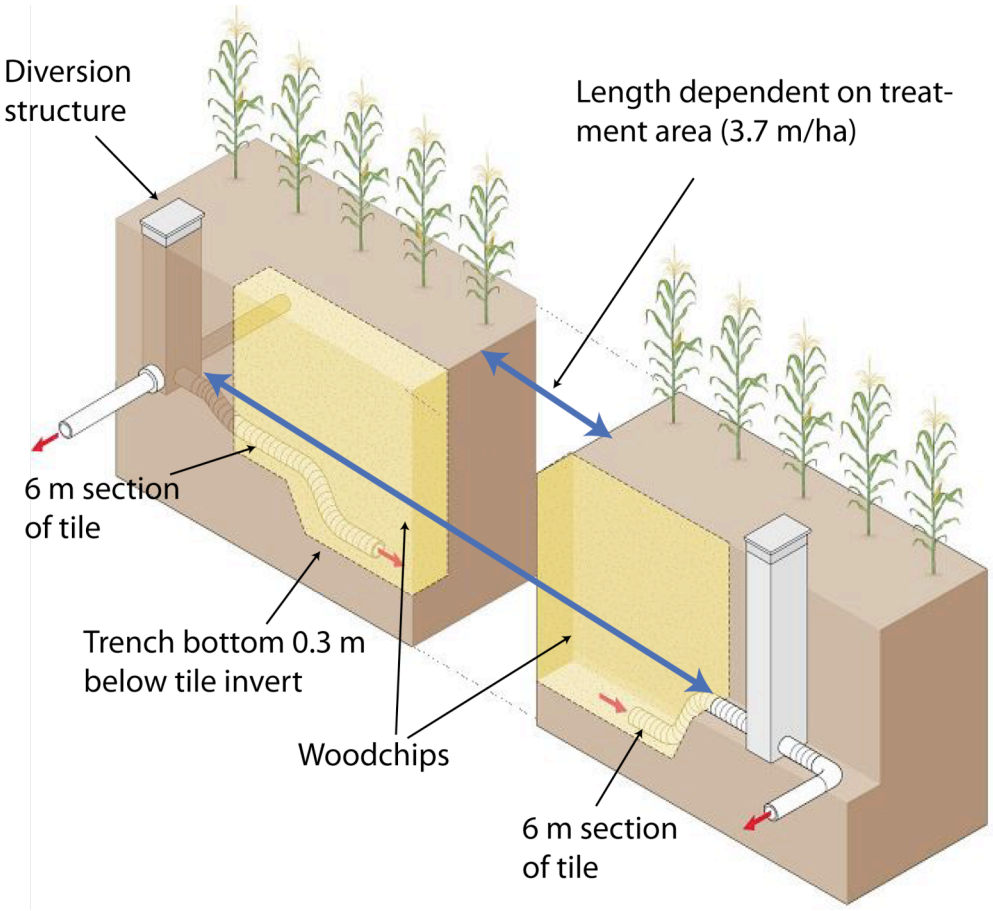

Figure 2. Biofilter schematic. As shown in Rodrigue (2006)

operation, some have been decommissioned from research and are not now under the management of the research team. Currently there are several biofilters in central

Illinois that are still under investigation (Table 1). The most recent design of these reactors is shown in Figure 2. Chun et al. (2010) investigated the hydrodynamic characteristics of of the FP07 field biofilter site. Using a random walk modeling methodology, Chun et al. estimated the longitudinal dispersivity to be 10.2 cm, the transverse dispersivity to be 1.13 cm, the first-order decay coefficient to be 0.01 h^{-1}, and the effective porosity to be 0.79. Under a high nitrate loading experiment (269.9 gN), 47% of input nitrate was removed and under a retention time of approximately 4.4 h.

For another field site (DE01), nitrate removal efficiency and N_2O gas production was evaluated in the years 2008 and 2009 (Woli et al., 2010). The biofilter was found to have varying efficiency (between 12 and 99.5% reduction of nitrate), and a typical removal rate of 6.4 gN m^{-3} d^{-1}. For 2008, the overall reduction in nitrate load was 23%, and for 2009, the overall reduction in nitrate load was 50%. At the average flow rate (0.15 cm d^{-1}), retention time in the system was calculated to be 1.4 hr when the biofilter had a depth of 61 cm, and 2.6 hrs when the biofilter was at a depth of 100 cm. At a higher flow rate of 0.5 cm d^{-1}, retention time was calculated as 26 and 50 min for the 61 cm and 100 cm depths, respectively. The observed N_2O flux from the system was between 0.01-0.13 mg m^{-2} h^{-1} (negligible), and no difference was noted among locations in the biofilter. CO_2 flux from the system (a proxy measurement for the decomposition of wood) was observed to range from 4.4 to 4.5 gC $m^{-2}h^{-1}$, suggesting substantial microbial activity and decomposition of wood in the biofilter.

2.2 Microbial Community Theory and Measurement

To this point, the biofilters used in this study have been considered "black box" systems (Tiedje et al., 1999), optimized solely on traditional engineering variables such as retention time or flow control. However, the functional part of an engineered ecosystem is the ecological community. A community is an assemblage of populations of different organisms that live together in a particular environment. A community together with its environment forms an ecosystem—for ecological engineers, this is the designed ecosystem. Because one strategy ecological engineers use is to allow communities to develop via self-design, characterization of the resultant community and the processes and conditions that drive its formation are important to optimize this process and to improve the performance of the system.

2.2.1 Role and variation of microbial community in ecosystems

One reason that describing a microbial community is important for ecological engineers is that the composition of a microbial community substantially influences both microbial services in an ecosystem (Bell et al., 2005) and the function of macroorganisms and the ecosystem overall (McGrady-Steed et al., 1997; Naeem and Li, 1997; van der Heijden et al., 1998). Specifically, increased biodiversity in microbial communities was shown to enhance ecosystem reliability, productivity and predictability, as well as to influence the composition of macroorganisms (McGrady-Steed et al., 1997; Naeem and Li, 1997; van der Heijden et al., 1998). Effects of microbial community on ecosystem function appear to persist over time, so that the historical microbial community impacts current ecosystem properties (McGrady-Steed et al., 1997; Naeem and Li, 1997; van der Heijden et

al., 1998). These findings imply that a thorough understanding of the microbial community should substantially improve our ability to manage and design ecosystems. Furthermore, consistent with the theories that diversity enhances stability of ecosystem function (see "Role of diversity and evenness in stability" below), some research suggests that the stability of microbially-mediated processes depends on the level of functional redundancy amongst microbial populations and upon their relative abilities to tolerate environmental variability (Schimel and Gulledge, 1998).

An important characteristic of microbial communities is that, despite the fact that microorganisms typically are not thought to be dispersal limited, they exhibit substantial heterogeneity over space and time. Microbial spatial variation has been documented at global and regional scales (eg, latitude or ocean depth) to the centimeter scale, and adheres to the same type of taxa-area relationship as macroorganisms (Green et al., 2004; Horner-Devine et al., 2004b). In particular, the spatial heterogeneity of soil microorganisms at the plot and local level has been shown to interfere with accurately describing microbial communities (Ellingsoe and Johnsen, 2002; Franklin et al., 2002; Franklin and Mills, 2003; Kang and Mills, 2006). Martiny et al. (2006) summarized the literature examining the biogeography of microorganisms and hypothesized that the same spatial processes affecting macroorganisms also affect microorganisms, but that these effects are of the scale of microorganism size. Martiny et al. (2006) also suggest that this variation is due both to selection by the current environment (the "Baas-Becking" hypothesis) but also to historical environmental factors.

Microorganisms, in common with macroorganisms, also exhibit temporal heterogeneity driven by seasonal and longer-term environmental variation, dynamic food

web interactions, and ecosystem succession. This microbial temporal variation has been described in terrestrial, lake, river, and marine ecosystems (Stepanauskas et al., 2003; Yannarell et al., 2003; Kent et al., 2004, 2007; Wardle et al., 2004; Bardgett et al., 2005; Crump and Hobbie, 2005; Pinhassi and Hagstrom, 2000; Shade et al., 2010). Both the top-down (ie, predators (Kent et al. 2006)) and the bottom-up (ie, availability of resources (Paver and Kent, 2010)) type of food web interactions appear to be influential in determining microbial community. Of particular interest for engineers, differences in the activity and composition of microbial functional groups have also been seen with long-term anthropogenic manipulations of environmental conditions, such as different agricultural treatments, on the half-century scale (Enwall et al., 2005).

2.2.2 Characterizing ecological community

Although there has been continued debate as to what specifically constitutes a community (Jackson, 1994), ecologists generally characterize communities in terms of which species are present and in what proportion; which guilds/functional groups these species occupy, and the food webs that portray relationships among species. Communities also are considered to have associated properties such as productivity (the rate of conversion of solar energy to biomass), stability (how much the community changes over time), stage in succession (the progression of communities to greater efficiency and relative stability), and spatial distribution (Legendre and Legendre, 1998; Ricklefs, 2008).

Comparisons among different communities is complicated by varying structure, sampling efficiency, and functionality. Several metrics have therefore been developed to enable characterization and assessment of communities, and comparisons among communities.

Diversity and evenness

The most basic understanding of a community is at the diversity level (the proportions of species that are present). Various measures of diversity have been proposed (see Legendre and Legendre, 1998), with the general form

$$N_a = \exp(H_a) \tag{1}$$

where N_a is the entropy number corresponding to the diversity index, and H_a is the argument. This general form corresponds to the different measures of information entropy (Shannon and and Weaver, 1963). The zeroth entropy number corresponds to the species richness, that is the number of species present, q:

$$\begin{aligned} H_0 &= \log q \\ N_0 &= q \end{aligned} \tag{2}$$

The first entropy number is Shannon's classical information entropy, sometimes referred to as the Shannon-Weiner index or the Shannon-Weaver index:

$$H_1 = -\sum_{i=1}^{n} p_i \log p_i \tag{3}$$

where p_i is the proportion of the total number of individuals that belongs to species *i.* This metric is maximized when all species have equal numbers of individuals. The second entropy number corresponds to Simpson's index, which gives the probability that two interacting individuals are of the same species:

$$H_2 = D = -\log \sum_{i=1}^{n} p_i^2 \tag{4}$$

Lloyd and Ghelardi (1964) proposed developing a metric to more specifically describe the shape of the distribution of species in a community, or evenness. There are numerous evenness metrics (see Legendre and Legendre, 1998), the most frequently used

of which is Pielou's *J*. This metric measures how evenly distributed the community population is by comparing the calculated Shannon index to its maximum value (achieved when all species are equally distributed):

$$J = \frac{H}{H_{\max}} = \frac{H_1}{H_0} \tag{5}$$

Role of diversity and evenness in stability

Ecologists have debated the role of biological diversity in ecosystem stability for decades. Historically, it has been argued that biodiversity enhances ecosystem stability and resiliency (Macarthur, 1955; Elton and Elton, 1958; Odum, 1971). More recent analyses using mathematical models have shown that in certain circumstances diversity has a destabilizing effect on communities, and that there is potentially an ideal range of diversity from the perspective of community stability (May, 1973; Pimm et al., 1991).

In response to these opposing viewpoints on the stability of community structure several researchers have instead focused on the stability of ecosystem function rather than explicit food web interactions. These analyses have shown that while higher diversity may destabilize certain populations, it may enhance redundancy of function by providing more species capable of performing particular functional tasks within an ecosystem (Walker, 1992; Borrvall et al., 2000; Gunderson, 2000; Loreau et al., 2001; Hooper et al., 2005).

With respect to the concepts of stability and redundancy in microbial ecosystems, Allison and Martiny (2008) have summarized current thought on the topic and have conducted a meta-analysis of studies of microbial community reaction to disturbance. Firstly, they define three important concepts: resistance (the degree to which a community remains unchanged in the face of disturbance), resilience (the rate at which a community

returns to its previous state after disturbance), and functional redundancy (the ability of a different microbial group to carry out a particular process at the same rate under the same conditions). From their meta-analysis, they argue that, despite the overwhelming diversity of microorganisms in many systems, the majority of studies show that microbial communities are generally sensitive to disturbance (not resistant), are not resilient within the scope of a few years, and that at least some microbial taxa are not functionally redundant. However, in communities with a large number of taxa (high diversity), a "portfolio effect" may occur in which functional decrease in one taxa is averaged with a functional increase in another to result in consistent functionality. The extent to which microbial community diversity contributes to responses in resistance, resilience, and functional redundancy is still unclear.

The potential roles of community structure in ecosystem functional stability underscores its importance from an ecological engineering perspective. Because the objective of ecological engineering is to design stable ecosystems that provide particular functionality, diversity and evenness measures of engineered ecosystems may prove to be important metrics.

Metrics of community similarity

Apart from comparing diversity and evenness characteristics, ecologists can compare the species composition of communities to differentiate them. Frequently it is useful to condense species differences into a single metric that expresses the similarity between two communities, typically taking values between 0 and 1, with 1 representing perfect similarity between samples and 0 representing perfect dissimilarity. Several of these measures of community distance have been proposed and are in general use (for

review, see (Faith et al., 1987) and (Gower and Legendre, 1986)). Two of the most popular metrics used in microbial community analysis are described below.

Jaccard's index operates on community analysis data that is expressed as a species being either present (1) or absent (0). It measures the proportion of species shared at the site to all species existing at either site:

$$J = \frac{M_{11}}{M_{01} + M_{10} + M_{11}} \tag{6}$$

where M_{11} are species that appear at both sites, and M_{10} and M_{01} are species that appear at only the first site or only the second site, respectively.

Using a slightly different concept of similarity, the Bray-Curtis dissimiliarity metric *BC* measures the ratio of turnover of species between two communities to the total species richness (Bray and Curtis, 1957):

$$BC_{ij} = \frac{\sum_{k=1}^{n}(x_{ik} - x_{ij})}{\sum_{k=1}^{n}(x_{ik} + x_{ij})} \tag{7}$$

where x is abundance, k is a particular species or population within a community of n populations, and i and j are different samples. Unlike the Jaccard index, the Bray-Curtis metric can be used with community data either coded by presence or absence, or by species abundance.

Measuring microbial communities

For many years, identification of groups and species in microbial communities was performed by removing samples from an environment, culturing extracted microorganisms in appropriate nutrients and media, and then characterizing them by their morphology or

metabolism. However, in the last twenty years, it has been shown that microorganisms are in general difficult to culture and that many of them have been misclassified by using morphology to characterize them (Woese, 1987; Ward et al., 1990; Ovreas, 2000; Floyd et al., 2005). Traditional community analyses miss a substantial portion of microorganisms present in a sample. This discrepancy was both discovered and, to an increasing extent, resolved by modern molecular techniques that analyze nucleic acids and other cellular molecules for phylogenic identification (Torsvik et al., 1990; Pace, 1997).

There are two basic approaches to molecular analysis: extraction of or in situ examination of characteristic cellular molecules. Extracted cellular molecules can be sequenced, probed or otherwise analyzed to provide information about cellular identity. Most of these analyses study RNA or DNA containing both highly variable and highly conserved sequences related to taxonomy or functional capabilities. *In situ* detection relies upon labeling characteristic molecules of intact cells with fluorescence, dyes, or radioactivity, and visualizing these labels microscopically. This type of analysis can preserve the spatial relationships within a community or environment, and can therefore be useful under certain circumstances (Amann et al., 1990). In this study, I adapted both community analysis approaches for application to samples collected from denitrifying biofilters.

Using extracted DNA, automated ribosomal intergenic spacer analysis (ARISA) (Fisher and Triplett, 1999; Manter and Vivanco, 2007) and terminal restriction length polymorphism (t-RFLP (Liu et al., 1997)) was used to characterize the bacterial and fungal communities in the biofilter. For ARISA, DNA from the 16S-23S rRNA intergenic spacer region (a section of DNA that separates sequences coding for ribosomes) is copied many

times (amplified) and these copies are labeled fluorescently. Because this region is highly variable by taxonomy, the copied DNA fragments are of different lengths. t-RFLP was carried out on the *nosZ* gene to describe the community of denitrifiers that possess the genes encoding the enzyme for the final transformation in the denitrification pathway. Like ARISA, the t-RFLP analysis amplifies a target region of DNA and labels the amplified fragments with a fluorescent dye at one end. After this step, however, the fragments are cut with restriction enzymes to create different fragment lengths based on sequence heterogeneity. Primers for t-RFLP have been developed for most of the genes in the denitrification pathway, including *narG* (Philippot et al., 2002), *nirS/nirK* (Braker et al., 2000), *norB* (Braker and Tiedje, 2003), and *nosZ* (Rosch et al., 2002; Rich et al., 2003). In both ARISA and t-RFLP, separation of the differently-sized DNA fragments using a capillary electrophoresis instrument with a fluorescence detector allows visualization of the proportions of different discrete populations of microorganisms in a community, producing "community fingerprint".

Fluorescence *in situ* hybridization (FISH, Amman et al., 1990; Lipski et al., 2001) was developed for use with the biofilter samples as an *in situ* method. FISH uses oligonucleotide probes complementary to rRNA specific for particular groups or species. These probes are fluorescently labeled and hybridized to intact but fixed cells. If the sequence of the ribosomal DNA is complementary to the oligonucleotide probe, hybridization of the probe to the ribosomes produces a fluorescent cell that can be visualized under epifluorescence microscopy, enabling quantification of target organisms.

2.2.3 Microbial community analysis of biofilters and denitrifying systems

Several methods of community analysis have been applied to engineered and natural systems similar to the denitrifying biofilters, although none to denitrifying biofilter systems themselves. Systems similar to the denitrifying biofilters include waste gas biofilters, remediation systems for wastewater nitrate, agricultural soils, and wetlands. Below is a summary of relevant community analysis research that has been conducted on such systems.

To my knowledge, the only microbial community analysis performed on a biofiltration system similar to our denitrifying biofilter was that of a zero-valent iron permeable reactive barrier (Gu et al., 2002). The microbial community was analyzed by fatty acid composition and DNA sequences specific to several functional groups or genes (sulfate-reducing bacteria, *nirS*, *nirK*, and methanogens). In this work, the microbial community was found to be more diverse and of greater overall abundance in the barrier by 1-3 orders of magnitude as compared to the surrounding soils. Over time the composition of the microbial community was found to change; specifically diversity increased as the biofilter aged. Differences in community were also seen at different points in the flowpath of the biofilter: cell counts were greater upstream of the iron treatment (inlet side) and proportions of major microbial groups were varied.

Other methods have also been used to perform community analysis on engineered systems designed to remove nitrate from wastewater (denitrifying sand filters, Mergaert et al., 2001; fixed bed denitrification reactors, Neef et al., 1996; activated sludge reactor, Hoshino et al., 2005). In these analyses, isolates with denitrifying functionality were

identified and taxonomically classified and/or classified into groups associated with various stages of or locations in the system.

Similarly to the denitrifying biofilters, nitrate removal from water also occurs in wetlands (constructed or natural), and the microbial ecology of these have been the subject of a growing body of research. Gutknecht et al. (2006) summarizes research focusing on the microbial structure and function of wetlands. Their meta-analysis revealed that hydrology and substrate availability are consistently shown to be controlling variables in wetland performance and microbial structure. Furthermore, wetland denitrification functionality is influenced by hydrologic regime, temperature, seasonality, type and availability of substrates, and plant type and presence. The extent to which these are also distal controls on microbial community composition is the subject of current study.

Some studies have investigated relationships between performance, microbial community, and hydrology. These types of relationships may be of importance for the denitrifying biofilter system, which sees large fluctuations in hydrology over the course of a year. Ishida et al. (2006) showed that while dampened flow fluctuations and extended residence time in wetlands resulted in better nitrate removal, these conditions did not select for a bacterial community that was inherently better at nitrate removal. Although bacterial communities were different between wetlands conditioned to different hydrologic regimes, and between locations along the flowpath of each wetland, these different communities removed nitrate at a similar rate when exposed to high retention times and steady flow. In a similar vein, Kim et al. (2008) found that short-term drought impacts communities of different types of wetlands differently. Drought did not significantly affect the abundance (by gene count) or community composition of bacteria or

of *nirS* denitrifiers in riparian wetlands, whereas bacterial communities from bogs and fens were significantly altered in abundance or in composition after short-term drought.

Stres et al. (2008) similarly studied the influence of temperature and soil water content on microbial communities in fen microcosms. Bacterial and *nosZ* communities were not found to appreciably change in response to increased temperature or soil moisture, although temporal shifts in the *nosZ* community were observed.

A number of studies have investigated the changes in community structure of constructed versus natural wetlands. For example, D'Angelo et al. (2005) found only slight differences in microbial community using fatty-acid methyl ester analysis (FAME) between natural reference wetlands and mitigation (constructed) wetlands, although both varied seasonally. The unexpected similarity was attributed to similar environmental conditions at each site. However, Peralta et al. (2010) found substantial differences between natural and restored (constructed) wetlands. While seasonal shifts were again noted, both bacterial and denitrifying (*nosZ*) communities were significantly different between natural and restored sites and were influenced by moisture, TOC, TN, and nitrate. In addition, denitrification potential was significantly higher in reference wetlands, variation that could be explained by a combination of bacterial community composition, nitrate, ammonium, C:N ratio, and pH. These findings may be relevant to denitrifying biofilters, as they show that engineered denitrifying ecosystems may be different from the natural systems they emulate, and also that environmental parameters can both drive community composition and performance in denitrifying systems

Finally, because the denitrifying biofilters investigated in this dissertation are passively seeded from the surrounding soils, a discussion of studies of the microbial

community of denitrifying agricultural soils is relevant. Cavigelli and Robertson (2000) first presented findings suggesting that diversity is not necessarily functionally redundant; that is, that the denitrification capabilities of different communities may not be the same. Controlling for major environmental conditions, they found that the denitrification potential and ratio of denitrification products of soils from an agricultural field and from a successional meadow were significantly different. Furthermore, soil denitrification showed different sensitivities to environmental parameters: agricultural soils were more sensitive to oxygen, and successional soils were more sensitive to pH. The authors concluded that these differences could only be due to variation in community composition.

Further studies comparing agricultural soils to other nearby soils revealed significant differences in community composition. Rich and Myrold (2004) found that the denitrifying (*nosZ*) community composition was significantly different between agricultural and riparian soils and creek sediment. Agricultural soils showed the highest diversity (mean 24) and evenness of denitrifiers (0.86) of all sites, and the lowest ratio of N_2O production to N_2 production (rN_2O). Furthermore, communities from different locations within the agricultural plots were statistically different. Likewise, Stres et al. (2004) found that denitrifying (*nosZ*) communities in native and agricultural soils in Michigan were significantly different. Again, agricultural soils showed the higher diversity of *nosZ* denitrifiers (104 distinct populations between two digests).

The abundance of denitrifiers (rather than their composition) has also recently been investigated by quantitative PCR (qPCR). Henry et al. (2006) determined that denitrifying (*nosZ*) communities make up less than 5% of the total bacterial community in soil. Dandie et al. (2008) studied the spatial and temporal variation of denitrifier abundance in

agricultural soils. They found that sites differed in *nosZ* abundance, but that there was little change in abundances of denitrifiers (*nosZ*, *nirK*, and *cnorB*) and all bacteria over time. Results also showed that abundances and denitrifying activity, and abundances and environmental parameters were decoupled.

In light of these findings, it appears that denitrification is more related to community composition than to abundance of denitrifiers. In fact, an examination of *nirK* genes extracted from agricultural soil and derived from mRNA transcripts showed that present and active denitrifying populations are different (Wertz et al., 2009). The authors also found that a few populations were responsible for most of the denitrification and that these populations did not change over time and space, even when the whole *nirK* population changed.

Some attention has been focused on the effects of environment on the development of microbial communities in denitrifying agricultural soils. Enwall et al. (2005), for example, studied the effect of long-term fertilization on bacterial community composition and denitrifying (*nosZ* and *narG*) community composition in agricultural soils. Both bacterial and denitrifying communities showed significant differences between ammonium sulfate and organic fertilizers. Denitrification and overall respiration rates were also higher in plots treated with organic fertilizer. Braker et al. (2010) also found that temperature significantly influenced the denitrifying (*nirS/nirK*) community of agricultural soils. In the study, increased temperature led to enhanced denitrification activity, higher abundances of denitrifiers, and different community compositions. Interestingly isolates possessing *nirS/nirK* genes were also shown to have the full denitrification pathway.

Although the community analyses described in this section do not give information that is specific or directly applicable to the function of denitrifying biofilter system, they give useful comparisons in both methodology and results. Furthermore, environmental parameters shown to be important in those systems that denitrify offer insights into possibly influential factors in the denitrifying biofilter.

2.3 Statistical Analysis of Microbial Communities

In this work I sought to develop methodology to assess the microbial communities within denitrifying biofilter sites and their variation with environmental and operational parameters. To describe whether differences in community or variations with time and space are significant, appropriate statistical tests are critical. Below, I discuss the application of statistical tests to microbial datasets.

2.3.1 ANOSIM (analysis of similarity)

Comparison of similarity indices can be used to statistically test for differences in community structure. One method frequently used for microbial communities is the analysis of similarity (ANOSIM) (Clarke and Green, 1988; Clarke, 1993). ANOSIM tests for statistically significant differences between community groups selected *a priori* (such as different sites or treatments). To create the ANOSIM statistic, a matrix of the similarity coefficients between each pair of samples is created, and this matrix is transformed to reflect the rank order of the similarities. The test statistic, *R*, is then calculated from the following equation:

$$R = \frac{r_b - r_w}{\frac{1}{4}(n(n-1))} \tag{8}$$

where r_b is the mean rank of similarities between groups (average rank of similarities between community assemblages in different groups of samples), r_w is the mean rank of similarities within groups (similarities between community assemblages in the same group), and n is the total number of samples. The statistic gives a value between -1 and 1, with 0 indicating that there are no differences in community similarity between groups, and 1 indicating that all communities within a group are more similar than they are to samples not in the group. Negative values are atypical, but indicate that members of the group are more different from each other than to samples not in the group. The significance of this test statistic is calculated by repeatedly permuting the samples into random groups of the same sizes as the test groups and comparing the value of R of these permutations with that of the original data. The proportion of random permutations that have values of R greater than the R of the test data is the significance. It is important to note that relatively small values of R can be significant but may not necessary represent strong differences between groups.

2.4 Geostatistical and Multivariate Analysis of Ecology

Legendre and Legendre (1998) suggest that ecological heterogeneity is a functional property of an ecosystem, and should therefore be studied in its own right. Given that microbial communities are both major mediators of ecological services and exhibit substantial temporal and spatial heterogeneity, analysis of these communities should include dynamic and spatially structured aspects in their analysis.

2.4.1 Autocorrelation and ecology

The field of geostatistics was originally developed to assess spatial heterogeneity in mineral deposits for the mining industry, however, it has been applied to numerous disciplines, including ecology (Goovaerts, 1997; Legendre and Legendre, 1998). Geostatistical analyses are designed to characterize spatial structure and variability. Initial analyses—sometimes called exploratory data analysis—typically focus on establishing the extent to which a value may be accurately predicted based on nearby measurements (autocorrelation). Exploratory analyses also evaluate whether autocorrelation is the same in all directions (isotropic) or has a particular directionality (anisotropic), and the range over which this autocorrelation operates. Although the results of these analyses are frequently then used in more complex methods such as predictive mapping (kriging) or simulations, they are valuable in their own right. In our particular case, knowledge of the spatial or temporal structure of a microbial community, or the lack thereof, can help one to i) apply statistical analyses appropriately, ii) devise sampling schemes, and iii) develop hypotheses and identify correlations between biological functions and environmental parameters.

Autocorrelation can be described by a geostatistical structure function, which plots some measure of similarity between sample points against their Euclidean separation distance. Different types of structure function use different measures of similarity, or *statistics*. The most typical forms are the semivariogram (γ) and correlogram (C), shown below:

$$\gamma(h) = \frac{1}{2N(h)} \sum_{a=1}^{N(h)} \left| z_i - z_j \right|^2$$
$$C(h) = \frac{1}{N(h)} \sum_{a=1}^{N-h} (z_i - \bar{z})(z_j - \bar{z}) \qquad (9, 10)$$

where h is a particular separation distance, N is the number of pairs with separation distance h, and z_i and z_j are the attribute values at the sample locations that make up a pair. For a semivariogram, the statistic chosen is mathematical distance, and for the correlogram the statistic is Pearson's correlation coefficient.

Structure functions have been frequently been used to characterize spatial patterns in macro-ecological data. Legendre and Fortin (1989), Rossi et al. (1992), and Kent et al. (2006) all review geostatistical methodology for the purposes of ecology. These reviews highlight that fact that most ecological datasets are autocorrelated and that it is important to remove autocorrelation trends in typical statistical analyses. They also provide background on typical and more specialized methods of assessing spatial structure (including robust and cross variants of variograms and correlograms and useful data transformations), on methods to test causal models (such as the Mantel test, see below), and methodology for mapping and interpolation.

The majority of applications of geostatistics to ecology have been to study macroecological, and typically univariate, datasets. Much less frequently, individual microbial populations or groups have been tested for spatial structure. Semivariograms to document spatial structure or co-variation with environmental parameters have been constructed using whole bacterial density or counts (Franklin and Mills, 2003; Franklin et al., 2002; Nunan et al., 2003), functional activity (Grundmann and Debouzie, 2000; Gonod et al., 2006; Tuckfield and McArthur, 2008; Krause et al., 2009), counts of a particular

microbial species or group (Dandurand et al., 1997; Collins et al., 2003; Lilleskov et al., 2004; Barnes et al., 2007), or groups defined by fatty-acid methyl ester (FAME) profiles (Cavigelli et al., 1995; Ritz et al., 2004; Saetre and Baath, 2000; Torneman et al., 2008). Several groups also used structure functions to then produce interpolated maps of microbial populations or groups (Orum et al., 1999; Collins et al., 2003; Philippot et al., 2009; Pickles et al., 2010).

Although analysis of the spatial and temporal dynamics of particular populations can provide important ecological information, ecological community data are typically multivariate. That is, description of community is an assembly of abundances of many populations. Because most geostatistical analyses are designed for univariate data, analysis of community data requires modification of typical approaches to allow for multivariate data.

2.4.2 Multivariate approaches for geostatistical analyses

Several approaches have been devised to apply geostatistical tools to multivariate community data. These approaches have mostly been developed and used for macroecological datasets (see Kent et al., 2006; Ettema and Wardle, 2002 for reviews), with some exceptions as noted below.

A frequent option has been to use ordination analysis (such as principle components analysis (PCA), correspondence analysis (CA), or canonical correspondence analysis (CCA)) to reduce the dimension of community data. Here, communities are ordinated along one or more axes according to some measure of similarity of behavior, and their position along one of these axes (the axis scores) are used as the attribute in univariate geostatistical methods (Legendre and Legendre, 1998; Legendre and Fortin, 1989). This method was

used by Saetre and Baath (2000), Franklin et al. (2002) and Franklin and Mills (2003) to create interpolated maps showing the spatial structuring of soil communities characterized using FAME analysis and analyses of DNA, respectively. Mouser et al. (2005) also used this technique to evaluate the spatial dynamics of bacteria and archaea communities assessed with the community fingerprints in contaminated groundwater wells. For Mouser's research, cross-variograms were constructed to show community co-variation with hydrologic and chemical properties, and kriged maps showing variation of PCA scores were created.

Instead of reducing the dimensionality of data to a univariate attribute, several groups have instead proposed to substitute a dissimilarity metric for the mathematical distance in a semivariogram ("dissimogram" or "pseudovariogram," (Mistral et al., 2000; Mackas, 1984)), or, to more simply plot the dissimilarity of each pair against separation distance ("distance decay," (Nekola and White, 1999)). The dissimogram therefore has a form very similar to the semivariogram:

$$\gamma(h) = \frac{1}{2N(h)} \sum_{a=1}^{N(h)} D_{ij}^{\ 2} \qquad (11)$$

where D_{ij} is a dissimilarity metric between samples *i* and *j*, and can be modeled with equations that are similar to those used to model semivariograms. Distance decay, however, takes the form of a scatter plot (typically log scale) and must be modeled with a linear fit. Mackas (1984) developed the pseudovariogram method to describe the spatial structure of marine phytoplankton, but it also has been used to characterize communities of soil bacteria (Franklin et al., 2002; Franklin and Mills, 2003). The spatial distribution of soil fungi has been similarly assessed using the distance decay method (Green et al., 2004).

Another widely-used approach to analyze multivariate spatial data is the Mantel correlogram, based on Mantel's test (Mantel, 1967). The statistic tests the correlation between two or more distance matrices (a matrix where position *ij* refers to the distance between some samples *i* and *j*). These distance matrices may refer to community dissimilarity (as in the Sorensen or Jaccard metric), geographical distance, or any other variety of distance/dissimilarity. The statistic itself is a normalized extension of Pearson's correlation coefficient, a simple cross-product term:

$$r = \frac{1}{(n-1)} \sum_{i=1}^{n} \sum_{j=1}^{n} \frac{(x_{ij} - \bar{x})}{s_x} \frac{(y_{ij} - \bar{y})}{s_y} \qquad (12)$$

where *x* and *y* are distances in the first and second matrix, respectively, measured between sample *i* and *j*, *n* is the number of elements in the distance matrices (*=m(m-1)/2* for *m* samples), and *s* is the standard deviation. The statistic ranges from -1 (negatively correlated) to 1 (positively correlated), with a statistic of zero indicating no correlation, although the magnitude of correlation can be small even when highly significant statistically. (Whether such correlations are meaningful is a separate question.) Testing the significance of the statistic is achieved via permutation (permuting the rows and columns randomly over many iterations and generating a distribution of statistic values for these random permutations (see Manly, 1991). The Mantel test may be used to test the correlation of ecological communities with environmental variation or with a predictive model. By adding an additional distance matrix to the analysis, the contribution of two separate environmental variables may be separately tested (the "partial Mantel" test, see (Legendre and Legendre 1998).

To form the Mantel correlogram, the dataset is partitioned by distance class and the statistic calculated for each class:

$$r(h) = \frac{1}{(n(h)-1)} \sum_{i,j \in h} \frac{(x_{ij} - \bar{x})}{s_x} \frac{(y_{ij} - \bar{y})}{s_y} \quad (13)$$

where *h* is a particular separation distance, and *n(h)* is the number of pairs having that separation distance. Graphing these statistics against separation distance produces an analogue of the correlogram. Cho and Tiedje (2000) used Mantel correlograms to study the spatial structure of groups of different strains of fluorescent *Pseudomonas* as described by genetic differences. A similar procedure was used by Lilleskov et al. (2004) to show patterns of colonization of ectomycorrhizal fungi.

More intricate methods involving complex matrix manipulations have also been proposed to handle multivariate ecological datasets. Wagner has developed several tools for multivariate plant community analysis. As a basis, she proposes using a variogram matrix, a three-dimensional matrix made up of elements of variance C_{ijh}, where *i* and *j* are species and *h* is the distance class (Wagner 2003). By summing elements of the matrix in various ways, the community variance can be partitioned into spatial components at three levels: individual species, community composition, and species richness. At the community composition level, a composite variogram (the "variogram of complementarity") can be formed as the summation of the normalized variograms of each species. By using this methodology, PCA, CA, and CCA results can similarly be partitioned by distance. These scores can be then graphed against separation distance to characterize spatial variation due to environmental gradients and that due to biotic autocorrelation (Wagner, 2004).

Couteron and Ollier (2005) expanded upon this framework to produce a generalized method of partitioning multivariate ordinations of various types by using different normalization and lighting options. Nanos et al. (2005) further developed Wagner's methodology by producing kriged maps using principle component scores calculated for specific separation distances.

A slightly different approach was taken by Lichstein (2007), who proposed using multiple regression on distance matrices (MRM), an extension of the partial Mantel test, for multivariate ecological data. In this method, distance matrices of separate explanatory characteristics are used as regression variables to model community dissimilarity. By using matrices defined by membership in a specific distance class, autocorrelation at various spatial scales can be tested and visualized.

The methods using complex matrix calculations described above are novel and have not yet found popular use in ecology. To my knowledge, none have been applied to microbial datasets.

2.4.3 Limitations of current multivariate methods

While useful in many circumstances, the current approaches each have limitations that may reduce their appropriateness for large microbial datasets. Partitioning of community variability by PCA or CCA, for example, flattens population data and may result in artifacts from the ordination method in the spatial analysis. Additionally, several of the methods suffer from assuming a parametric variable response. Mantel correlograms, variograms of complementarity, the proposed multiscale ordinations, and the distance decay method all standardize variables by their mean and standard deviations, and variograms of complementarity are based on the variance/covariance matrix. However,

both ecological populations and their resultant similarity indices tend to be non-normal (Clarke, 1993; Mcardle et al., 1990). In particular, population distributions are commonly skewed and contain many zeroes, which can result in inaccurate estimates of standard deviation and variance/covariance (Olson, 1974; Faith et al., 1987; Mcardle et al. ,1990; Obrien, 1992).

Although use of similarity metrics lessens the effects of non-normality in statistical analyses, their properties are dependent upon the metric chosen and any prior transformation of data, so that their own statistical behavior and their robustness to non-normal population data varies (Faith et al., 1987; Clarke ,1993). Also because these variations with metric and transformation occur, spatial analyses using similarity metrics directly in their computation (distance decay, dissimograms, Mantel correlogram) are not precisely comparable unless the same metric and transformation are used. Furthermore, several approaches present difficulties in determining the shape and or autocorrelation range of the data. Mantel correlograms and distance decay plots assume a linear correlation between distance and similarity, which may obscure or distort spatial relationships. However, using rank transformation of the similarity metric before performing analyses can ameliorate or lessen the effects of non-normality and non-linearity.

Finally, methods involving direct analysis of population data (variograms of complementarity, multiscale ordinations, and multiple regressions) can be cumbersome and/or computationally intensive with the large datasets typical of microbial ecology. For these methods, regressions with many variables, and particularly permutation tests for significance can be computationally time-consuming.

2.5 SUMMARY

In this section I discussed background information relevant to denitrification, biofilters, microbial community analyses, and statistical tests applied to technology. The intersection of these subjects provides the framework for the experiments of and tools created in this research.

3. EXPERIMENTAL METHODS

To characterize the microbial communities in denitrifying biofilters I pursued several different analyses, including one that was devised for this project, using samples of woodchips and water from four different biofilters. I began by trying to describe some basic aspects of the biofilter denitrification activity using a denitrifying enzyme assay. Using these results, I optimized two different approaches for characterizing the different types of microorganisms from the biofilter: fluorescence in-situ hybridization, and analysis of extracted DNA using ARISA and t-RFLP. I employed the second of these approaches to characterize spatial and temporal variation of community. To further analyze this data, I also developed a new statistical method for testing for community variation across time and space. This chapter describes the sampling and collection methodology, the analysis techniques used, and the development of the new statistical test ANOSIM-GS.

3.1 BIOFILTER SAMPLING

3.1.1 Study sites

Four different biofilter locations, installed and maintained by Dr. Richard Cooke and his laboratory at the University of Illinois, were used in this study. As described in Section 2.1.3, the biofilters are woodchip-filled trenches installed in line with a subsurface drainage system, between the tile outlet and discharge into a drainage ditch or wetland. The dimensions and configurations of each biofilter were designed based on the drainage area and conditions at each site, as well as to incorporate design improvements. Table 2 lists the biofilter sites used in this study, along with their dimensions and drainage area, and the

analyses conducted. The dimensions reflect differences in design. The AB03 and FP03 biofilter sites are considered one-dimensional flow biofilters, with a narrow width-to-length ratio. The DE01 and FP07 biofilters were designed to be two-dimensional flow biofilters, with either a wide rectangular (DE01) or square (FP07) shape. The two-dimensional biofilters are a later design, created as an improvement in nitrate removal efficiency. All biofilters used in this study had a depth of approximately 0.3 m (1 ft) below the tile line for the duration of the study. At the AB03 site, this depth included a soil cover of 0.64 m. The woodchip medium in each of the biofilters is woodchip of mixed origin.

Table 2. List of Biofilter Study Sites.

Site	Location	Drainage Area	Soil Overburden?	Dimensions, width x length x depth	Analyses Applied
AB03	Hume, IL	5.0 ha	Yes	1.5 m x 27 m x 1.8 m	DEA, FISH
DE01 (AE05)*	Deland, IL	6.1 ha	No	3.1 m x 12.4 m x 2.2 m	Time Series, FISH
FP03	Decatur, IL	5.0 ha	No	1.5 m x 30.5 m x 1.8 m	Spatial analysis, FISH, Time Series
FP07	Decatur, IL	2.0 ha	No	6.1 m x 6.1 m x 1.5 m	DEA, Time Series, FISH

*Biofilter site DE01 is referred to in some previous unpublished data as AE05/06.

3.1.2 General practices for biofilter woodchip and water sample collection

Biofilter woodchips and water were collected for analysis of microorganisms. Biofilter woodchips at a particular depth were accessed either by using a 10.2 cm-diameter soil auger or through a biofilter sampling port (see below). Woodchips were removed from the auger using autoclaved forceps rinsed in ethanol. Woodchips were removed from ports using the holding pin of the port apparatus, which is usually in contact with the woodchip sample location, so that cross-contamination of samples was minimized. Woodchip samples were placed in autoclaved, 250 ml Nalgene bottles, transported on ice to the laboratory, and stored at 4°C until analysis.

Water samples were obtained from the auger hole or port using a 125 ml Nalgene bottle attached to a sampling pole. For water samples used in denitrifying enzyme assays (DEA) or FISH analysis, the sample collection bottle was rinsed twice in the sample biofilter water, and the third volume was transferred to an autoclaved 125 ml bottle. For the time series dataset, a pole apparatus was constructed that allowed the autoclaved sample bottle to be placed directly onto the pole. Using this apparatus, the bottle was dipped into the port to collect the sample directly. Water samples were transported on ice to the laboratory for further analysis. Water samples used for chemical analysis were preserved with 36 mM H_2SO_4 to prevent transformation of chemical species by microorganisms present in the sample or by redox reactions.

For analyses of woodchip microbial communities, microorganisms were removed from the woodchip samples by washing with Ringer's solution (0.9% NaCL, 0.042% KCL, 0.024% $NaHCO_3$) (Friedrich et al., 2003). Briefly, a standardized mass (variable by analysis type as described in the following sections) was placed into a volume of Ringer's solution and this mixture was shaken for a particular period, after which the woodchips were discarded and the wash (containing microorganisms) was used for further analyses. Details of the washing methodology varied by analysis type (see Sections 3.1.3, 3.1.4, and 3.1.5).

3.1.3 Sample collection for denitrifying enzyme and FISH analyses

Individual samples were collected by soil auger for denitrifying enzyme analyses (DEA) and FISH analyses. Woodchip samples for DEA protocol development were collected from the AB03 biofilter in the fall and winter of 2006/2007 in the middle of the biofilter at a depth of approximately 0.76 m. For these samples only, sample woodchips were stored

at room temperature until use. Final DEA inhibition tests were carried out on woodchip and water samples collected from the FP07 biofilter on 16 July and 7 August 2007. These woodchip samples were collected at approximately 3.8 m from the biofilter head and 2.3 m west of the eastern edge at a depth of ~1 m. The water samples were pumped from a co-located water sampling well installed for a previous study. The sample collection hose for the well extended to the full depth of the biofilter (1.5 m). Samples were stored at 4°C. DEA analyses to assess the production of N_2O gas by the biofilters was conducted using samples collected from the DE01 biofilter on 6 April 2008.

Samples were collected for FISH at various times from all four biofilters as well as from a number of other biofilter sites not used in this study. Samples were collected from depths where woodchips were inundated. Sampling locations were recorded as approximate areas within the biofilter. Microorganisms were removed by washing with Ringer solution and preserved as detailed below (details varied by analysis type, see Sections 3.1.3, 3.1.4, and 3.1.5).

3.1.4 Spatial dataset

To assess the spatial variability of the microbial community in a biofilter, a comprehensive, spatially explicit sample collection scheme was designed for the FP03 biofilter. Samples were collected on 16 March 2007. This biofilter consists of an L-shaped, one-dimensional flow design (approximately 21.3 m on the long arm and 9.1 m on the short arm) that is roughly 1.5 m wide and 1.8 m deep, filled with woodchips. The biofilter was installed in the summer of 2005. Flow through the biofilter on the day of the study was on average 0.5182 L/s, with a retention time of approximately 2.5 hr. The biofilter historically

has received inlet nitrate concentrations of between 0 and 8 mg-N/L, and has exhibited nitrate concentration reduction between 50 and 100% (variable with flow rate). Typical annual nitrate load reduction is around 90%.

Woodchip samples were taken at 2.75 m intervals along the length and 0.45 m intervals along the width of the biofilter, and were taken at two depths, 0.76 m and 1.52 m (Figure 3). Sample transect locations were labeled 1-12 (starting from biofilter inlet), and positions along a transect were labeled A-C (from south to north at the inlet). The woodchip medium was partially degraded, with pieces between 1 to 300 mm in width, and these pieces were sometimes mixed with soil particles that had washed into the biofilter. Woodchip samples were collected by soil auger as described above. At most locations, the woodchip sample volume was 250 ml. To assess whether there was significant community variation at a small scale, at several locations, a larger (approximately 700 ml) sample was placed into a plastic container, shaken to mix the sample, and an additional 250 ml subsample was taken from the container. This container was rinsed with ethanol between samples to avoid cross-contamination. Because the biofilter was not of uniform width, several sample locations at the edges were outside the biofilter boundary and augering removed soil instead woodchips. At these locations, no sample was collected.

After transport on ice, microorganisms were washed from the woodchips by standardizing the mass of woodchips in each sample bottle to 20g. Ringer solution (125 ml) was added and the contents were shaken vigorously for 30 s to remove cells (adapted from (Friedrich et al., 2003)). 1 ml aliquots of this wash were then pipetted from the middle of the bottle into 2ml microfuge tubes. Aliquots were concentrated 4-fold by

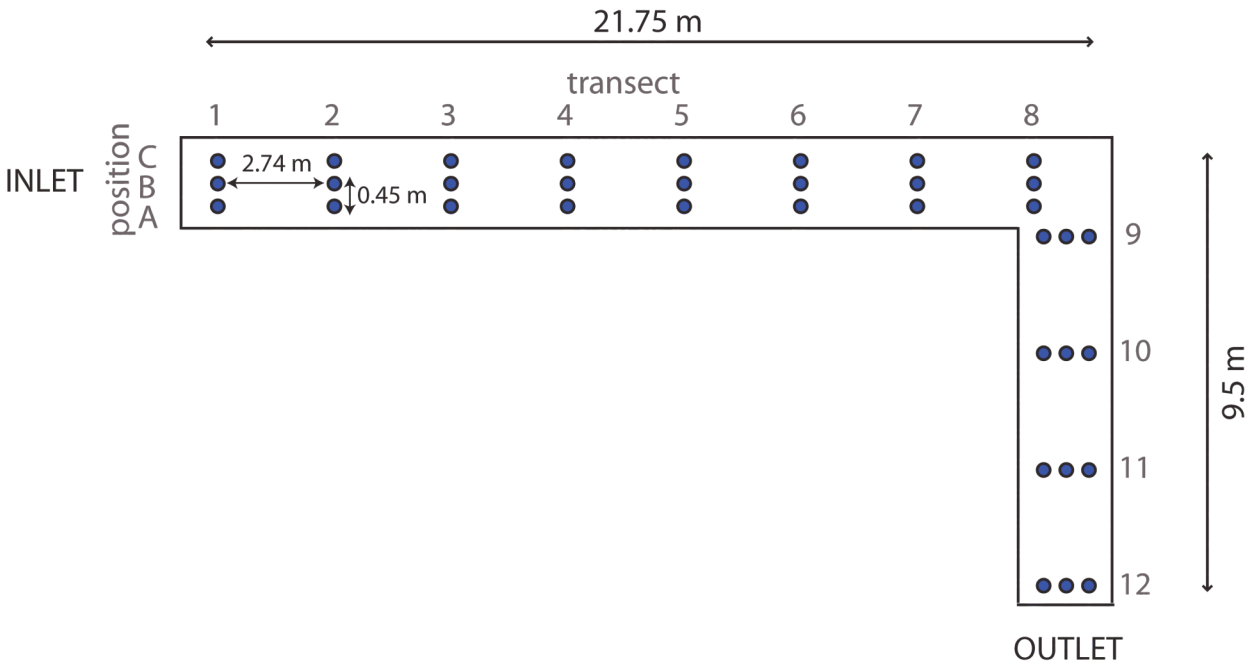

Figure 3. Sampling schematic for spatial study of microbial community in the FP03 biofilter. Sampling locations are represented by blue circles. At each location, a sample was taken at 0.76 m depth and at 1.52 m depth.

centrifuging at 5000 x g and resuspending the resulting pellet into 250 μl of sterile Ringer solution. Samples were stored at -80°C until DNA extraction.

3.1.5 Time series dataset

Time series data were collected to track the variation of microbial communities over time and to discern their relationships with environmental variables. Biofilters FP03, DE01 and FP07 were selected for the study, as these biofilters represent all three configurations of currently installed biofilters—one-dimensional flow, and rectangular and square two-dimensional flow, respectively. Sampling ports constructed from 3- and 4-inch diameter PVC pipe were installed into these three biofilters on 13 November, 2008 (Figure 4). The ports are designed such that the two pipes are fitted one inside the other; the inner pipe is filled with woodchips excavated from the port installation and can be lifted easily from

inside the outer pipe, which remains permanently in the ground. The bottom of the inner pipe is capped with a removable grate to allow woodchip samples to be collected from the bottom of the pipe. Both pipes are perforated at the bottom such that water can flow through to maximize the similarity between the environmental conditions that the woodchips are exposed to inside and exterior to the port. Ports were installed at a 0.76 m depth every 6.1 m along the flowpath (according to the range of similarity calculated in the spatial analysis study). Additionally, two ports at a 1.52 m depth were installed in each biofilter. Beginning in mid-December, 2008 (to allow the woodchips in the ports to equilibrate with the surrounding community), woodchip and water samples (where inundated) were collected from the bottom of these ports every 1 to 4 weeks. After each sampling, additional woodchips from the area immediately adjacent to each port were added to the top of the port.

For community analyses of woodchips, cells were washed from woodchips with buffer solution. Woodchips suspended in buffer were subjected to vortex agitation including 5, 5 mm glass beads to remove as many cells from the woodchips as possible (Whiteley et al. 2003). Specifically, Ringer solution (110 ml) was added to sample woodchips standardized to 30 g in the collection bottles. The filled collection bottles were incubated at 20°C overnight on a rotary shaker. Washes were then centrifuged for 3 min at 5000 x g, the supernatant was decanted off. To the concentrated sediment, five sterile 5 mm glass beads and 2.5 ml of 1X PBS (phosphate-buffered saline) were placed in a 50 ml centrifuge tube. The mixture was vortexed for 2 min at maximum speed, then centrifuged at 750 x g for 5 minutes to remove woodchip debris. The supernatant was removed and

partitioned into two aliquots of 0.3 ml for fixation for FISH (see below) and two aliquots of 0.9 ml, which were stored at -20°C for DNA extraction.

To connect microbial community to environmental variation, environmental parameters from the sample locations were also measured. Temperature and dissolved oxygen (if water was present) were measured inside the sampling ports at the time of sampling with a YSI model 55 combination dissolved oxygen and temperature probe (YSI, Yellow Springs, OH). Water samples were tested for nitrates (nitrate + nitrite) using the automated hydrazine reduction method (EPA method 353.1) in the Water Quality Laboratory in the Department of Agricultural and Biological Engineering. Chemical Oxygen Demand (COD) of water samples was performed using the dichromate reduction method (EPA method 410.4). Additionally, a portion of the sample woodchips was used to measure the moisture content of the woodchip media according to ASTM method C566.

Data not directly collected through this study were also used for some analysis methods. Biofilter inlet and outlet nitrate and nitrite measurements collected in a separate study (again using EPA method 353.1) were used to calculate nitrate removal performance (defined as difference in mg/L nitrate across the biofilter); flow measurements from this same study were also used as environmental parameters (Richard Cooke, unpublished data). These data do not completely span the length of the study. Weather data, including maximum, minimum, and average temperature, precipitation, humidity, and growing-degree days were collected from Weather Underground (www.wunderground.com). Weekly averages of these data were calculated by Matthew Porter.

For statistical analyses, several environmental parameters were processed to obtain the best estimates for sample dates or locations. For ports that were not inundated with

water, water quality measurements (NO_3, DO, COD, pH) were used from the nearest inundated port, with preference for the nearest upstream port (with no consideration for port depth). Where available, flow data was reported on an hourly basis. Instantaneous flow was taken as the flow in the hour between 11 am and 12 pm on the date of sampling (as samples were typically taken during the mid-day or afternoon depending on weather). 1 d, 4 d, 7 d, and 14 d flow averages were taken as the arithmetic average of flow data in the previous 1 d, 4 d, 7 d, or 14 d. Inlet and outlet nitrate measurement dates frequently did not correspond to the woodchip sampling dates in this study and were absent for some portions of the study. To create a best estimate of inlet and outlet nitrate for the woodchip sampling dates, nitrate data was linearly interpolated between available samples. Rodrigue (2006) found that tile nitrate was typically consistent over a month. However, we assumed that microbial activity and community composition may have a much more rapid variation. Therefore, a cutoff of one month was selected for interpolation of inlet nitrate data, and two weeks for the interpolation of the outlet nitrate data; sample data were not used for interpolation when they were separated by more than the appropriate cutoff period from the true sample. Sample dates for which there was no appropriate data to interpolate from were excluded from analyses using performance data.

3.2 Denitrifying Enzyme Assay

Because both bacteria and fungi have been found to have denitrification capability, to determine the organisms responsible for denitrification, I inhibited either bacteria or fungi in woodchip samples and measured the denitrification activity. I also tested for the denitrification activity in biofilter and inlet water samples, and in woodchip wash samples.

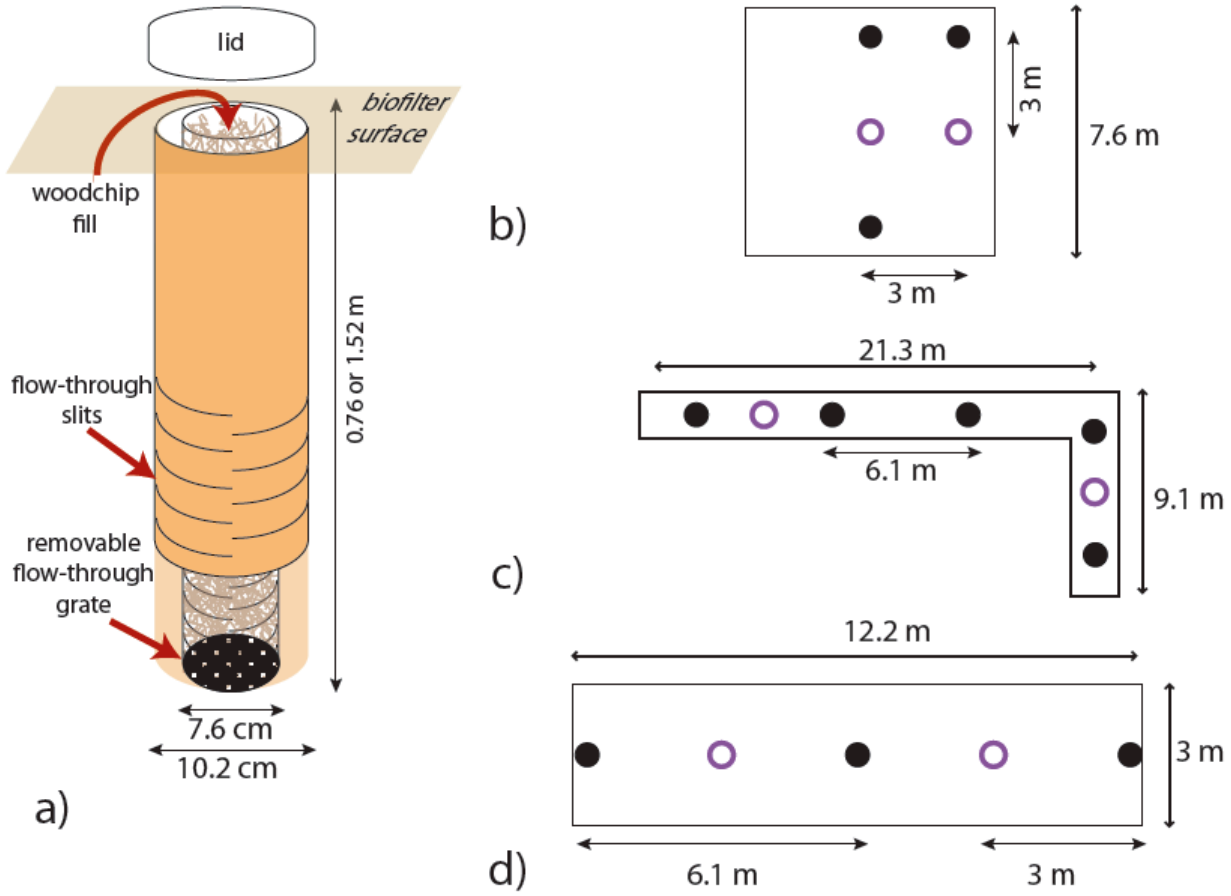

Figure 4. Sampling port and location schematic. a. Sampling port construction schematic. b-d. Sampling port locations at the FP07, FP03, and DE01 biofilters, respectively. Black circles indicate 0.76 m depth ports, open purple circles indicate 1.52 m depth ports.

Finally, I used DEA to investigate whether denitrification was complete in the biofilters or whether N_2O gas (a greenhouse gas) was produced in situ.

The denitrifying enzyme analysis (DEA) is based on Tiedje et al. (1989). For each woodchip DEA test, 25 g of sample woodchips were placed into a 125 ml Ehrlenmeyer flask. 30 ml of reaction solution was added. For the method optimization, this solution contained 1 mM NO_3^-, 1 mM glucose, and any inhibitors (see below) in ddH_2O. 1 mM NO_3^- (14 mg/l NO_3-N) is within typical concentrations of nitrate in tile drain effluent in Illinois

(16-24 mg/l NO_3-N, Mitchell et al., 2000). For most analyses, glucose was omitted (to more closely approximate biofilter conditions) and the 1 mM NO_3^- was added to biofilter water. Chloramphenicol, used by Tiedje et al. (1989) to extend the period of linear accumulation of N_2O, was not included in the reaction mixture because the objective was not to analyze kinetics, but to characterize the proportion of total denitrification due to a particular domain.

Sample flasks were covered with a rubber septum stopper and the flask headspace was then altered using sterile needles. First, the flask atmosphere was removed with a lab vacuum, then flasks were flushed with N_2 gas for 2 minutes. Finally, 10 ml of acetylene gas was injected into the headspace to give a concentration of approximately 20% acetylene. Flasks were then incubated overnight (between 12-15 hours) on a rotary shaker at room temperature (20°C); at this length of reaction, nitrate concentration was limiting.

A gas syringe was used to extract 250 µl from the headspace and this sample was analyzed for N_2O, CO_2, and acetylene using a Hewlett Packard 5890 gas chromatograph equipped with a thermal conductivity detector. The chromatograph setup included a 0.75 ml gas sampling loop and a Porapak N (2 m x 0.32 cm; 30 ml/min) separation column. Helium was the carrier gas and Ar/CH_4 was used as the makeup gas at a total rate of 60 ml/min. Linear regression of standards (taken at least once every three days) was used to determine the N_2O concentration (ppm) of DEA samples. The detection limit of the instrument was approximately 50 ppm N_2O, with the region of linearity beginning at approximately 100 ppm. CO_2 results were compared by peak area only.

Soil sampled from the AB03 site was used as a positive control. Negative controls were created by sequentially microwaving and autoclaving sample flasks (woodchips and

reaction solution) for 30 s and 70 min (liquid cycle), respectively. Tetracycline and cycloheximide were used to inhibit bacteria or fungi, respectively. To determine the concentrations of inhibitors necessary to fully inhibit samples, DEA tests were run with increasing concentrations of each inhibitor until denitrification activity ceased to change. Woodchips from biofilter AB03 were used for the optimization of the DEA method and inhibitors. For the final inhibition analyses, inhibitor concentrations of 40 mg cycloheximide per g of woodchips (1 g total per flask) and 45 mg tetracycline per g of woodchips (1.125 g total per flask) from the FP07 biofilter were used.

The denitrifying capacity of woodchip washes was tested to determine the efficacy of removing denitrifying cells. Biofilter water samples and woodchip washes from the FP07 site were also analyzed with the DEA procedure. Woodchip washes were prepared by placing 25g of woodchips in 125 ml of sterile Ringer's solution (0.9% NaCl, 0.042% KCl, 0.024% $NaHCO_3$), and shaking at room temperature for periods of 30 min, 1 hr, or overnight. For the DEA analysis, 30 ml of either this wash solution or biofilter water was placed into a flask without woodchips and spiked with 1 mM NO_3^-. Half of the woodchip washes also received an addition of 1 mM glucose to the reaction mixture to determine if electron donor was a limiting factor. The effect of adding glass beads to enhance cell removal during the woodchip wash was also tested by adding five 2 mm glass beads to duplicates of the 30 min and overnight wash durations.

To test whether N_2O gas would ordinarily be produced by the biofilters in-situ, a DEA analysis using woodchips from the DE01 site was performed as usual except that half of the test samples received no acetylene. In this way, any N_2O produced in the flasks would be attributed to incomplete denitrification of the woodchip microbial community.

3.3 FLUORESCENCE IN-SITU HYBRIDIZATION

To visually characterize the composition of the biofilter community, I optimized methodology for fluorescence in-situ hybridization (FISH) (Amman et al., 1990). Our basic protocol for FISH was based on work completed by (Zhou 2007) in the application of FISH to environmental samples from swine farms. This is described directly below. The majority of experimentation with FISH had the purpose of optimizing the fixation and slide preparation protocols such that woodchip debris and autofluorescence was reduced to an acceptable level.

3.3.1 Basic practices

Cells from woodchip washes were fixed according to two separate methodologies using ethanol and paraformaldehyde (PFA) (as described in de los Reyes et al., 1997). For ethanol fixation, 0.3 ml of woodchip wash was incubated with 0.3 ml of 100% ethanol and incubated for two hours on ice. Samples were then centrifuged at 5000 x g for 3 min and resuspended in 0.3 ml of a one to one mixture of phosphate buffered saline (130 mM NaCl, 10 mM sodium phosphate) and ethanol (PBS:EtOH). For PFA fixation, 0.3 ml of woodchip wash was incubated with 0.9 ml of 4% PFA for 30 min at room temperature. Samples were then centrifuged at 5000 x g for 3 min and resuspended in 1 X PBS twice. After the third spin, samples were resuspended in 0.3 ml PBS: EtOH. Samples fixed using both methods were stored at -20°C until used in FISH.

FISH probes specific for several different groups were applied to samples to attempt a broad characterization of the biofilter community. Three domain –level probes were used: Bac338 (S-D-Bact-0338-a-A-18, Cy3-labeled, (Amann et al., 1990; Daims et al., 1999),

Arch915 (S-D-Arch-0915-a-A-20, Alexa 488-labeled, (Stahl and Amann, 1991), and Euk516 (Amann et al., 1990). Three additional probes specific for Proteobacteria were used: aProt19 (S-Sc-aProt-0019-a-A-17, Cy3-labeled), bProt1027 (L-C-bProt-1027-a-A-17, FAM-labeled), and gProt1027 (L-C-gProt-1027-a-A-17, FAM-labeled) (Manz et al., 1992).

FISH was conducted as optimized and reported in Zhou (2007). Prepared slides (variations described in Section 3.3.2) were sequentially dehydrated by washing for three minutes each in 50%, 80%, and 95% ethanol. Into each well was pipetted 25-30 μl of hybridization solution. This solution consisted of 0.1 mM probe (plus 0.1 mM unlabeled competitor probe for bProt1027 and gProt1027), 0.9 M NaCl, 20 mM Tris buffer (pH 7.2), 0.01% sodium dodecyl sulfate (SDS), and a varying concentration of formamide depending on the probe. For the Bac338, aPro19, and Euk516 probes, a 20% formamide concentration was used. For the bPro1027 and gPro1027 probes, a 35% formamide concentration was used.

Slides were then placed with filter papers moistened in 1M NaCl solution in 50 ml centrifuge tubes. The tubes were incubated at 46°C for 2h, after which slides were rinsed 2-3 times with 1 ml of a preheated wash buffer and incubated with the wash buffer for 20 min at 48°C. This wash buffer contained 20 mM of Tris (pH 8), 0.01% SDS, and a specific concentration of NaCl. For the Bac338, aPro19, and Euk516 probes, 167.5 mM NaCl was used. For the bPro1027 and gPro1027 probes, 46.6 mM NaCl was used. Slides were then washed 2-3 times with 1 ml distilled deionized water (ddH_2O) and air-dried.

Slides were counter-stained with 1 μg/ml 4',6-diamidino-2-phenylindole (DAPI, Sigma Chemical, St. Louis, MO) in the dark for 5 min to provide non-specific cell counts.

After staining, slides were rinsed twice with ddH_2O and air-dried. 3 μl of Citifluor (Marivac Limited, Halifax, Nova Scotia) per well was used for antifading.

Hybridized and stained cells were examined using a Zeiss Axioscop 40 (Carl Zeiss, Oberkochen, Germany) under 630x magnification. Three separate filters were used to visualize fluorescence of different stains: a near UV excitation filter (excitation 350 nm/emission 460 nm, Chroma Technology Corp, Model 31000, Rockingham, VT) for DAPI, a green filter set (excitation 480 nm/emission 535 nm, Chroma Technology Corp, Model 41001, Rockingham, VT) for FAM and Alexa488, and a red filter set (excitation 535 nm/emission 610 nm, Chroma Technology Corp, Model 41002, Rockingham, VT) for Cy3. Greyscale images were taken using an AxioCam MRm (Carl Zeiss MicroImaging, Inc. Thornwood, NY) with varying exposure times. Exploratory image analysis was conducted using the program Visilog (version 6 Noesis, Les Ulis, France).

3.3.2 Sample and slide preparation investigations

Wood, in common with soil, exhibits fluorescence at wavelengths near those at which FISH stains are visualized. Several different variations in preparation were tried to minimize this autofluorescence while maximizing cell counts and separation on sample slides.

To optimize the number of cells visible in the microscope field, dilutions and concentrations of woodchip wash were tested. Dilutions of 1:5, 1:10, 1:25, and 1:50 in PBS:EtOH were tried with the FISH protocol. The woodchip wash was also concentrated up to 100 times by centrifuging the wash in 50 ml centrifuge tubes at 25,000 x g for 5 min and resuspending in 1 X PBS before sample fixation.

To test whether different methods of preparing slides would produce better distribution and separation of cells, direct spotting of the fixed cells onto slides (1-6 μl) was compared with a filtration method. The filtration method consisted of filtering full strength woodchip wash or a 1:50 dilution through a black 0.22 μm pore size polycarbonate membranes (25 mm diameter, Osmonics, Minnetonka, MN) and then manually transferring the filtered cells by pressing the filter onto a gelatin-coated slide.

Removal of debris was also attempted using several methods. Prefiltration was tested by filtering samples through 1.5–10 μm prefilters before spotting. Sonication to break up wood particles and clumps of cells was also tried. Samples at full strength or diluted up to 50 times were sonicated on ice for 1 minute at 250 W (5 s pulse on/off) using a sonic dismembrator (Fisher Scientific Model 500, Pittsburgh PA). Cells were then transferred by filtration as described above or concentrated by centrifugation and resuspended in PBS:EtOH before spotting directly onto slides. A slow centrifugation (300 x g) for 3 minutes to remove large particles was additionally tested. Finally, vortexing with glass beads for to dislodge cells from woodchip particles was tried (Whiteley et al., 2003). 50x concentrated woodchip wash was transferred to a 15 ml centrifuge tube with four, 5mm glass beads and 2 ml PBS. The centrifuge tube was vortexed at maximum speed for 2 min, then centrifuged at 750 x g for 6 min to remove sediment but leave cells in solution. The supernatant was removed, concentrated by centrifuge at 16,800 x g, and resuspended in 300 μl PBS:EtOH.

The effect of different slide coatings on the adhesion of cells was also investigated. Slides were soaked in 10% KOH in ethanol for an hour, rinsed and air-dried. For a gelatin coating, slides were then dipped in a 0.1% gelatin, 0.01% chromium potassium sulfate

solution at 60°C and air-dried vertically, following the protocol by Amannet al. (1990). Agarose coating was achieved by adding 20 μl of 0.1% agarose to the 1 μl sample while spotting. Both low-melting-temperature and high-melting-temperature agarose was used.

To reduce the effects of autofluorescence, treatments with sodium pyrophosphate ($NaPP_i$) (Kobabe et al., 2004) and lysozyme (Thurnheer et al., 2004) were tested. 1 M $NaPP_i$ was used to dilute samples 1:1 before spotting or incubated 1:1 with samples overnight. To test the effect of lysozyme, a 5 mg/ml solution of lysozyme was spotted over the sample on the slide for 15 or 30 min. Alternatively, the lysozyme solution was incubated with an equal volume of sample for 15 minutes; the mixture was then centrifuged at maximum speed for 3 min, the supernatant removed, and the pellet resuspended in PBS:EtOH.

Success of these preparation methods was assessed by qualitative inspection and, in some cases, manual counting of cells or image processing by Visilog.

3.4 COMMUNITY FINGERPRINTING

Concurrently, methodology was developed to characterize microbial communities using community fingerprints. For these methods, DNA was extracted from cells washed from woodchip samples so that the bacterial, fungal, and denitrifying communities could be described using ARISA and t-RFLP.

DNA was extracted from 250 μl of woodchip wash using the FastDNA kit (MP Biomedicals, Solon, OH). For the spatial analysis dataset, the wash was concentrated 4x. For the time series dataset, woodchip washes processed with glass bead vortexing (see section 3.1.5 for description) were used. Success of the extraction was confirmed with gel

electrophoresis for selected samples. For the spatial dataset samples analyzed with ARISA, extracted DNA was used directly in the ARISA method (see below). For the remainder of the analyses, contaminants were removed from woodchip-wash extracted DNA using cetyl trimethyl ammonium bromide (CTAB) (Sambrook and Russell, 2001).

Bacterial communities were characterized using ARISA (Fisher and Triplett, 1999) as described previously (Kent et al., 2004). ARISA PCR reactions were performed using 1μl of extracted DNA (containing varying concentrations of DNA, on average ~10 ng/μl) and 0.4 μM each of the 1406f (5' TGYACACACCGCCCGT 3', universal 16S rRNA gene) and 23Sr (5' GGGTTBCCCCATTCRG 3', bacteria-specific 23S rRNA gene) primers. The reaction mixture included 1X Tris buffer (pH 8.3), 0.25 mM dNTPs, 2.5 mM $MgCl_2$, and 0.25 mM BSA. The 1406f primer was labeled on the 5' end using the phosphoramidite dye 6-FAM. PCR was conducted in a MasterCycler Gradient thermocycler (Eppendorf, Hauppauge, NY) with an initial denaturation at 94°C for 2 min, followed by 30 cycles of 94°C for 35s, 55°C for 45s, and 72°C for 120s, with a final extension at 72°C for 2 min.

Samples of DNA from the time series were also used to characterize fungal communities (Matthew Porter, unpublished data) using fungal ARISA (Manter and Vivanco, 2007). fARISA PCR reactions were performed with 1 μl of extracted DNA and the ITS1F (5'-CTTGGTCATTTAGAGGAAGTAA-3') and ITS4 (5'CAGGAGACTTGTACACGGTCCCAG-3') primers.

The bacteria capable of performing denitrification were measured using t-RFLP of the *nosZ* gene (Liu et al., 1997; Rich et al., 2003; Peralta et al., 2010) which encodes the catalytic subunit of nitrous oxide reductase. PCR reactions contained 50 mM Tris (pH 8.0), 250 μg of bovine serum albumin per ml, 2.0 mM $MgCl_2$, 200 μM of each dNTP, 20 pmol of

each primer, 2.5 U of Taq polymerase (Promega), and ~100 ng (10 μl) of woodchip-wash-extracted DNA. The primers used for *nosZ* t-RFLP were *nosZ*-F-1181 (5' CGCTGTTCITCGACAGYCAG 3') and *nosZ*-R-1880 (5' ATGTGCAKIGCRTGGCAGAA 3) (Rich et al. 2003). The 1181f primer was labeled with 6-FAM at the 5' end. PCR was conducted in a MasterCycler Gradient thermocycler (Eppendorf, Hauppauge, NY) with an initial denaturation at 94°C for 3 min, followed by 25 cycles of 94°C for 45s, 56°C for 60s, and 72°C for 120s, with a final extension at 72°C for 7 min. For each DNA sample, PCR product from two 50 μl PCR reactions was concentrated and purified using the Qiagen MinElute PCR purification kit (Qiagen, Valencia, CA). Combined and purified PCR products were digested in single-enzyme restriction digests containing *AluI*, *HhaI*, and *MboI* (New England Biolabs, Ipswich, MA). Digests contained 10 μl of DNA product, 1 μl 10x Buffer 4 (New England Biolabs, Ipswich, MA), 0.2 μl 100X BSA, 0.5 μl enzyme, and 8.3 μl water, and were incubated overnight at 54°C.

For each ARISA and *nosZ* t-RFLP PCR reaction, fragment profiles were created using denaturing capillary electrophoresis, performed by the W. M. Keck Center for Functional Genomics (Urbana, IL) with an ABI 3730xl Genetic Analyzer (Applied Biosystems Inc., Foster City, CA). Electrophoresis conditions were 15 kV and 63˚C with a running time of 120 min using the POP-7 polymer. The internal standard for ARISA PCR reactions was a custom Rhodamine X-labeled, 100- to 2000-bp size standard (Bioventures). ABI GeneScan ROX-1000 (Applied Biosystems) was used as the internal size standard for *nosZ* t-RFLP reactions. ARISA and *nosZ* t-RFLP profiles were analyzed using GeneMarker 1.7 (SoftGenetics, State College, PA). Fluorescence cutoffs of 300 and 100 relative fluorescence units were used for ARISA and *nosZ* t-RFLP profiles, respectively, to include the maximum

number of peaks and exclude background noise. In addition, profiles with low overall fluorescence were individually examined and obvious peaks that were below the fluorescence cutoff were manually included. Profiles with maximum signal strength (peak area) of less than 10% of the average maximum signal strength for all ARISA profiles or all *nosZ* t-RFLP profiles (as appropriate) were excluded entirely from analysis. The signal strength of each peak was normalized to the total fluorescence of each profile to control for signal detection variations between runs. Where several profiles were concatenated (as for t-RFLP *nosZ* digests), normalization was constrained to each individual profile. Each peak was therefore expressed as a proportion of the total observed community (Rees et al., 2004; Yannarell and Triplett, 2005).

3.5 COMMUNITY MEASUREMENTS AND STATISTICS

The community diversity measures of richness (number of taxa) and evenness (Pielou's *J*) were calculated for each community fingerprint sample using relative fluorescence as a proxy for abundance. Specific taxa here are defined as ARISA/t-RFLP fragments of the same fragment length. Spatial plots of these measurements were created using the GS-Lib program LocMap (Deutsch and Journel, 1997). Statistical analyses of these values were conducted using the statistical software "R."

To further compare the community composition of each biofilter sample, the Bray-Curtis similarity coefficient (Bray and Curtis, 1957; Legendre and Legendre, 1998) was calculated between ARISA profiles and between *nosZ* t-RFLP profiles. The Bray-Curtis metric is a value between 0 and 1, with 1 representing complete similarity between samples and 0 representing complete dissimilarity:

$$BC_{ij} = \frac{\sum_{k=1}^{n}(x_{ik} - x_{ij})}{\sum_{k=1}^{n}(x_{ik} + x_{ij})}$$

where *k* is a particular taxa, and *i* and *j* are different samples.

A matrix of Bray-Curtis dissimilarities for all possible sample pairs was generated for both the ARISA and the t-RFLP data separately. Because abundance in population data can sometimes have non-normal distribution (Clarke and Green, 1988), profiles processed by the GeneMarker software were also transformed to a binary array indicating either presence or absence of a fragment (ie, Sørenson's dissimilarity metric), and a second set of dissimilarity matrices were constructed from this presence-absence data.

Dissimilarity matrices were analyzed using four different methods: non-metric multidimensional scaling (MDS plots), analysis of similarity (ANOSIM) between various sample groups, the geostatistical analysis of similarity (ANOSIM-GS), and Mantel tests. (Non-metric) MDS plots, a visual representation of community similarities between samples (Rees et al., 2004; Yannarell et al., 2003), were generated from the dissimilarity matrices using PRIMER 6.0 (Plymouth Marine Laboratory) or the "vegdist" function in the "vegan" package (version 1.17-4) of the statistical program R (version 2.11.1 for Mac). Additionally, PRIMER was used to conduct analysis of similarity (ANOSIM) (Clarke and Green, 1988; Clarke, 1993) on the similarity matrices to evaluate the similarity of the bacterial community composition in various groups of samples. ANOSIM was used to test the hypothesis that communities from the same group were more similar to each other than to those from a different group—the null hypothesis being that there is no difference between sample groups. Some analyses were also conducted with two-way, crossed

ANOSIM. To characterize the spatial or temporal structure of communities, dissimilarity matrices were analyzed with ANOSIM-GS. The methodology and parameters used for ANOSIM-GS are fully explained in Section 3.5.1. To test the strength of relationship between community composition or abundance of particular populations and other parameters, Mantel tests or partial Mantel tests (Legendre and Legendre, 1998; Mantel, 1967) were conducted between dissimilarity matrices and distance matrices of time, space, or environmental parameters. Mantel tests were performed using the "mantel" function in the package "vegan" for R, with 1000 permutations and using the Spearman rank coefficient. Parameters were standardized using the "scale" function before Euclidean distance matrices were constructed with the "vegdist" function of "vegan." When a dissimilarity matrix was created for an individual population, the Euclidean distance was also used.

Representative taxa within bacterial, fungal, and denitrifier communities (based on ARISA, fARISA, and *nosZ* t-RFLP profiles) were identified using the BVStep function (Clarke and Warwick, 1998) in PRIMER 6.0 (Plymouth Marine Laboratory, Plymouth, UK). Two variants of this analysis were performed: across all sites, and for each individual site. All samples of each community type, either for all sites or by site, were included in each analysis, and the following parameters were used: correlation coefficient = Spearman rank, random selection with 6 restarts, $\rho > 0.8$, $\Delta\rho < 0.001$.

Correspondence analysis was performed on bacterial and fungal community data based on ARISA and fARISA profiles. Both unconstrained (indirect gradient) analyses, and analyses constrained with only the variable of nitrate removal (direct gradient) were conducted using all populations of a particular community. Environmental parameters

available for correspondence analysis include inlet and outlet nitrate, instantaneous flow, a 14 d rolling average flow, nitrate and temperature in sampling ports, COD, DO, moisture content (%), pH, depth, weekly mean temperature and precipitation, average growing degree days in the month of sampling, and average humidity. Apart from nitrate removal, these parameters were not used as constraining variables, but only projected onto constructed plots. Data for constrained plots were restricted to those with nitrate removal measurements. Correspondence analyses were carried out using the "cca" function of the package "vegan" for R. Environmental parameters were fit onto the plots using the "envfit" function of "vegan." For this function, samples for which specific environmental parameters were missing were omitted from the analysis (na.rm = TRUE; no parameters extrapolated to the nearest port were used). Only representative populations were visualized on the correspondence analysis plots, all others were masked.

To confirm relationships between environmental variables, Spearman rank correlation tests were used to account for data non-normality. These tests were carried out using the "cor.test" function of the "stats" package of R, with the parameter "method" set to "spearman." Furthermore, to assess whether differences between environmental variables at different sites and/or times existed, the Kruskal-Wallis rank sum test for differences (Kruskal and Wallis, 1952) and multiple comparison test after Kruskal-Wallis was used (Siegel and Castellan, 1988). These tests were carried out using the "kruskal.test" function of the "stats" package of R, and the "kruskalmc" function of the "pgirmess" package of R, both excluding null values (na.rm = TRUE).

3.5.1 Development and use of the ANOSIM-GS method

To assess the spatial and temporal structure of biofilter microbial communities, a new method, ANOSIM-GS, was developed as an amalgamation of the ANOSIM statistical test and the geostatistical correlogram.

For the ANOSIM-GS method, I use the community comparison statistic *R* of ANOSIM to create a geostatistical structure function. To construct the structure function, pairs of samples are separated into groups defined by their physical or temporal separation distance (distance classes). The ANOSIM *R* statistic is then calculated separately for each distance class, testing whether sample pairs separated by a particular distance are more similar than those separated by any other distance:

$$R(h) = \frac{r_b(h) - r_w(h)}{\frac{1}{4}(n(h)(n(h)-1))} \qquad \text{(Eq. 14)}$$

where h is the separation distance of the distance class, $n(h)$ is the number of pairs in the distance class, $r_b(h)$ is the mean rank of similarities of pairs *not* in the distance class ("between"), and $r_w(h)$ is the mean rank of similarities of pairs in the distance class ("within").

This modified R test statistic results in testing a slightly different hypothesis than in the traditional ANOSIM application. The traditional ANOSIM metric tests whether pairs of samples belonging to the same a priori group are more similar than those belonging to different groups. In the ANOSIM-GS application, the R statistic tests whether pairs of samples that are separated by a particular geographical or temporal distance are more similar than those that those that are separated by a different distance. Thus, in the ANOSIM-GS analysis, samples themselves do not belong to a group, but rather, particular

pairings of samples belong to a group (the distance class). A global test for significance of the ANOSIM-GS analysis is made by determining if at least one distance class has an *R* value that is significant at the $\alpha'=\alpha/\nu$ significance level, according to the Bonferroni method of correcting for multiple tests (Legendre and Fortin, 1989; Cooper, 1968; Oden, 1984), where ν is the number of distance classes tested. To visualize the ANOSIM-GS analysis, the *R* statistic and the significances of the ANOSIM statistic at each distance class are plotted against their separation distance. The *R* statistic plot shows the basic structure of the correlations (similar to a Mantel correlogram) and the significance plot can be modeled to calculate the range of correlation.

Conventional semivariograms are typically fit to a standard model to determine the range, or maximum distance at which samples are similar. The ANOSIM-GS plot of significances, however, does not resemble traditional semivariograms in shape, but rather curves sharply upward. Therefore, a model based on the Gaussian curve was developed. To adapt the form to represent the ANOSIM-GS curve, the complement was used. Additionally, because the inclines and the centers of the ANOSIM-GS curves are variable and represent properties of the spatial or temporal structure, variables accounting for these parameters were introduced to give:

$$\gamma^s(h) = \begin{cases} 0, h < C_C \\ C_H\left[1 - \exp\left(-\frac{(h - C_C)^2}{C_I {C_W}^2}\right), h \geq C_C\right] \end{cases} \quad (15)$$

where *h* is the lag separation, C_H, C_C, C_I, and C_w are the curve height, center, incline, and width, respectively. The parameter C_H (the curve height) represents the significance value of the largest lag class (that is, the maximum *p*-value as lag distances tend toward infinity).

Traditionally, the range (maximum correlation distance) of a semivariogram is given by the lag distance at which the semivariogram model reaches 95% of its height. Because the ANOSIM-GS analysis plots significance rather than variance, the range was chosen to be the lag distance at which the model reaches the α level (in this case 0.05). Sample pairs of a lag greater than this distance should therefore not be statistically autocorrelated.

To automate the construction of ANOSIM-GS plots, a computer program coded in Python (version 2.5.4) was created in collaboration with Timothy Kuehlhorn, based in part on the *gamv* program of the FORTRAN geostatistics package GS-Lib (Deutsch and Journel, 1998). To enable comparison to the ANOSIM-GS method, additional code for the algorithm was also developed to calculate the dissimogram (Mistral et al., 2000), Mantel correlogram (Oden and Sokal, 1986), and variogram of complementarity (Wagner, 2003). Permutation tests were included for each metric to assess statistical significance. Validation of the program was carried out by calculating variograms of each type for a dummy dataset using an Excel spreadsheet and comparing the results to those of the program. Models were also fit for the dissimogram and variogram of complementarity in Excel using an exponential variogram model:

$$g(h) = N + S\left[1 - \exp\left(\frac{-3h}{R}\right)\right]$$

where N, S, and R are parameters representing the nugget, sill, and range of the variogram, respectively. To fit the model, a solver function was used to minimize the squared error of each lag class, weighted by the number of pairs in the lag class.

The ANOSIM-GS program was applied to community fingerprints from both the spatial and time series dataset to describe spatial and temporal variation in biofilter communities.

For the spatial dataset, both ARISA and *nosZ* t-RFLP data were analyzed, using both the normalized abundance and presence-absence Bray-Curtis matrices separately. Samples were also separated within these matrices by depth and analyzed again with ANOSIM-GS. Plots were constructed either specifying pairs in the direction of the biofilter flow (with parameters azimuth = 90 degrees, azimuth tolerance = 5 degrees) or omnidirectionally (azimuth = 90 degrees, azimuth tolerance = 180 degrees). For all (both omnidirectional and anisotropic) analyses the following further parameters were used: lag number = 6, lag separation distance = 2.74 m, lag tolerance = 1.37 m, azimuth bandwidth = 1.52 m, dip angle = 0 degrees, dip tolerance = 0 degrees, and dip bandwidth = 3 m. Comparison graphs using the spatial dataset were also constructed using the dissimogram, variogram of complementarity, and Mantel correlogram methods.

Because the FP03 site is L-shaped, the flow does not follow a constant direction. Therefore, for ANOSIM-GS analyses specifying in the direction of flow, a location file was constructed reporting location as if the biofilter were straightened into a line, but retaining correct distance between sampling locations along the flowpath. ANOSIM-GS plots were modeled with a Gaussian curve model as described above. Model parameters were optimized with the Excel function solver, such that the sum of the mathematical difference between the model and the empirical value, weighted by the number of pairs in the class, was minimized.

For the time series dataset, ARISA and FARISA (Matthew Porter, unpublished data) community fingerprints were used. Similarity matrices were created with abundance data separately for each biofilter. Similarity matrices were further subdivided by sample depth. Each similarity matrix was analyzed using ANOSIM-GS with distance classes defined by days separating samples. Distance classes were restricted to pairs from the sample location separated by the specified number of days. Lag sizes were optimized, testing 7, 10, 14, 21, and 38 days, with 21 days found to give the optimal curve shape. The analysis parameters were as follows: lag number = 29, lag separation distance = 21 d, lag tolerance = 10.5 d. Azimuth and dip parameters are not applicable to temporal ANOSIM-GS analyses (any input is ignored).

4. RESULTS AND DISCUSSION

In this section, I present the results of a number of different analyses of the microbial community in denitrifying biofilters. These analyses include denitrifying enzyme assays experimentation with biofilter sample preparation protocols for FISH analysis, the development of a geostatistical method for analyzing spatial and temporal structure in microbial communities, an analysis of the spatial structure of microbial communities in the biofilter, and an investigation into the relationships between community, performance, and environment in a set of time-series data.

4.1 DENITRIFYING ENZYME ASSAYS

At the outset of this research, I sought to understand some basic characteristics of the biofilter community. While it was known that denitrification occurred in the biofilters, where in the system and by what sort of organisms was unknown. In particular, because many types of microorganisms can perform denitrification it was important to narrow the scope of further analyses to a particular group (in particular, bacteria or fungi). Denitrification enzyme assays, which quantify the amount of denitrification observed in samples under ideal conditions, were therefore carried out on samples from different types of biofilter samples, under different sample preparation schemes and with varying levels of inhibitors to help elucidate some basic information about biofilter communities. This section relates the results of these analyses.

4.1.1 Adaptation and optimization of DEA for biofilter samples

Although denitrifying enzyme analyses are well-developed for use with soils (Tiedje et al., 1989), adaptation of the protocol for the woodchips required the optimization of the negative control and the level of biological inhibitors that was necessary for woodchip samples. A negative control is required for comparison with experimental samples. In this case, because the objective was to quantify the amount of denitification activity from microorganisms, a control containing sterilized reaction media (no living microorganisms) was needed. Repeated cycles of autoclaving were insufficient to eliminate all denitrification within sample flasks, although N_2O production was considerably reduced. Because fungi were suspected to be responsible for residual denitrification, the addition of microwaving to autoclaving the negative control was tested (Wainwright et al. 1980). I evaluated inhibition of denitrification activity following durations of 30 s or 60 s of microwaving followed by 70 or 140 min of autoclaving (a 70 min liquid autoclave cycle once or twice). Microwaving (30 or 60 s) completely eliminated production of N_2O (indicating inhibition of denitrification). CO_2 production, however, was decreased but not eliminated following microwave treatment. The shortest effective treatment, 30 s of microwaving followed by 70 min of autoclaving, was used to prepare the negative control sample for all analyses. I hypothesize that autoclaving was not sufficient to prevent denitrification because cells may be shielded within woodchips, or there may be resistant spores present. The destruction of spores was also offered as an explanation for the efficacy of Wainwright's (1980) microwave treatment.

To investigate the relative denitrification activity of fungi and bacteria, inhibitors were used to block the activity of one or the other. The concentration of inhibitors used in

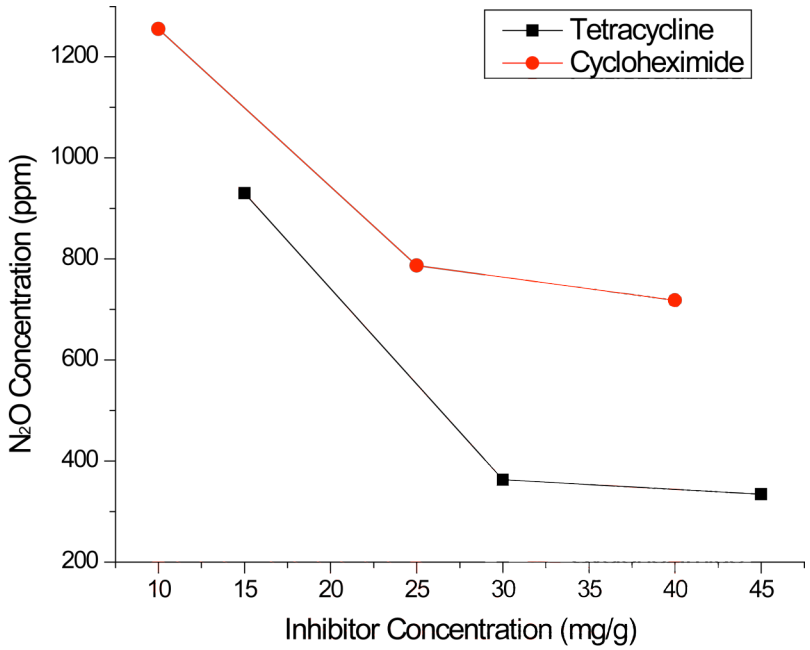

Figure 5. Optimization of tetracycline and cycloheximide concentrations in DEA analyses of biofilter woodchips. Assays included 25 g woodchip sample, 30 ml of 1 mM NO_3^-, 1 mM glucose. Samples were purged of oxygen and 10% acetylene gas added before being incubated with shaking overnight at room temperature. Each data point represents one assay.

this study also required optimization. Figure 5 shows the effect of tetracycline and cycloheximide on N_2O production. The concentration of N_2O appears to level out when inhibitor concentrations exceed the 20 to 30 mg/g-woodchips inhibitor range. Based upon these results, the remainder of the inhibition studies included 40 mg/g-woodchips cycloheximide and 45 mg/g-woodchips tetracycline. These concentrations are approximately 2-4 times in excess of published concentrations for inhibition of soil microorganisms (Susyan et al., 2005). A relatively high concentration of inhibitors may be required because of the difficulty of penetration into the woodchips. One additional and unexpected result from this optimization is that tetracycline inhibition increased CO_2 production within the flasks up to six times. This might be due to removing bacterial competition, allowing the fungi present to grow much more quickly and therefore increasing the CO_2 produced by fungal metabolism. This is supported by the observation

that flasks where bacterial populations were inhibited with tetracycline showed a rapid growth of fungi over the woodchip within 2-3 days following the tests.

4.1.2 DEA analyses of biofilter woodchip samples

DEA tests on biofilter woodchip samples were designed not to calculate denitrification rates under ideal conditions, but to ascertain the contribution of bacteria and fungi to denitrifying activity under typical biofilter conditions. Therefore, DEA was conducted with unfiltered biofilter water amended with 1 mM nitrate as the liquid phase. No glucose was added to better approximate biofilter conditions, in which no carbon sources external to the biofilter system would be present.

Results from denitrification enzyme assays where inhibitors were used to block denitrification activity from either fungi or bacteria suggest that both bacterial and fungal microorganisms are important to denitrification in the biofilters (Figure 6a). There was considerable variability in overall denitrification activity between the July and August sample dates. This may be caused by differing environmental conditions on the sampling dates. The July sampling date was preceded by rains and the biofilter was moist through almost the entire profile, and inundated below 0.76 m. The August weather was much drier and warmer, and the biofilter was mostly dry; water was only found deeper than 1.52 m. Denitrifying activity requires the presence of nitrate and the absence of oxygen, therefore, wetter weather (which would increase the volume of the biofilter which is submerged and therefore exposed to less oxygen) would increase the moisture content of the woodchips and proportion of these that were submerged. Samples were collected from approximately 1 m depth. At this depth, inundation is not consistent, so increased moisture from precipitation events may be influential to denitrifying activity. Although

DEA was carried out in moist conditions with sufficient nitrate (so lower denitrification rates cannot be directly attributed to in situ environmental conditions), differing weather and hydrologic conditions may influence the composition or abundance of denitrifiying organisms present in samples. Alternatively, because glucose (as an electron donor) was not added to these assays, samples from the August sample may be substrate limited. July rains may have leached much of the soluble carbon from the woodchips, reducing that present in the August samples.

Despite differences in overall activity, there was a similar pattern of inhibition for the two sampling dates. Tetracycline-inhibited flasks showed nearly no denitrification activity—approximately 50 ppm (roughly at detection limit, and below linear quantitation). This suggests that bacterial denitrification is the predominant mechanism for nitrate reduction. If there were significant fungally-mediated denitrification, there would be significant denitrification under tetracycline inhibition.

Surprisingly, cycloheximide-inhibited flasks also showed a considerable reduction in observed denitrification (Figure 5). Addition of cycloheximide reduced denitrifying activity by 60-80% compared to uninhibited flasks. Although tetracycline inhibition suggests that the actual denitrification is mediated by bacteria, it seems that fungal activity also contributes in some way to denitrification. The most likely mechanism of this enhancement is that fungal decomposition of the woodchips release additional substrate molecules for bacterial metabolism. However, other mechanisms are possible. One way to test whether fungi release additional substrate would be to conduct inhibition studies in the presence of an excess of glucose (rather than a 1:1 glucose:nitrate ratio, as is sometimes used). Under these conditions, if fungal control on denitrification is only through

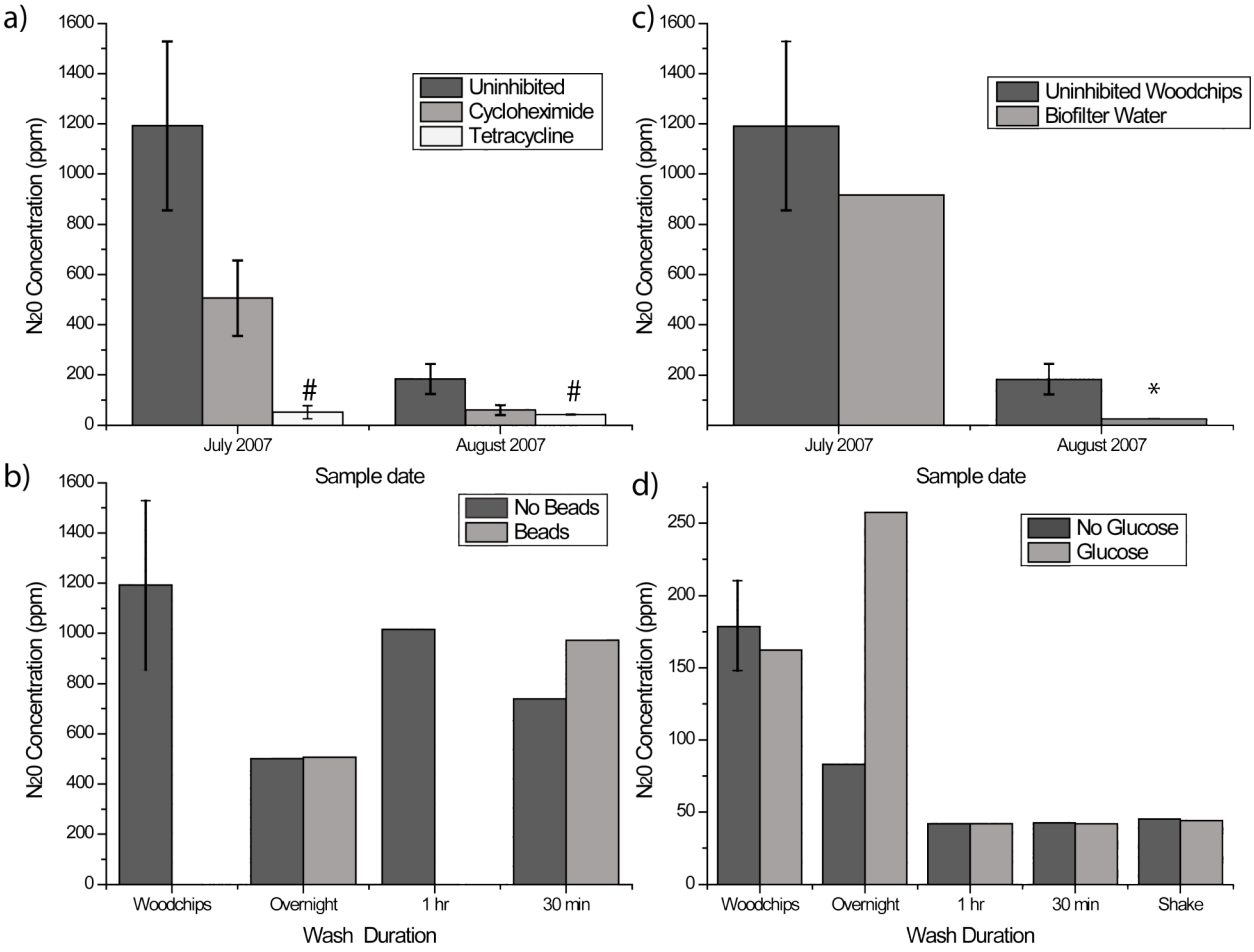

Figure 6. DEA analyses using woodchips, biofilter water, and woodchip washes. a) inhibition studies, with woodchips uninhibited, or inhibited with 40 mg/g cycloheximide or 45 mg/g tetracycline (no glucose added); b) comparison of washes processed with and without glass beads (July sample, no glucose added); c) comparison of activity in woodchips, and biofilter water (no glucose added); d) comparison of samples analyzed in the presence of or without glucose (August sample—note different scale). Error bars represent standard deviation of three replicates; all other data represent a single assay. # denotes measurment below linear response (<100ppm), * denotes measurment below detection limit (<50ppm).

production of substrate, no decrease in denitrification under fungal inhibition should be observed.

These conclusions are somewhat limited by the variation in overall activity between the two sample dates. Because the overall denitrification of the August samples is low, there is less certainty for the relative effect caused by inhibitors. In particular, for the August samples, inhibition with cycloheximide results in a greater reduction of denitrification relative to uninhibited levels than for the July samples (75.2±8.2% reduction

versus 57.6±17.4% reduction in denitrification). This is exacerbated by the fact that there were only two August cycloheximide-inhibited measurements (due to lack of sufficient cycloheximide) rather than triplicate measurements. At such a low overall activity level, small measurement variations can substantially alter the relative results. Yet, pattern alone is a reasonable indication that both bacteria and fungi play significant roles in the biofilter, with bacteria apparently the predominant denitrifying domain.

4.1.3 DEA of woodchip washes and biofilter water samples

DEA was also used to measure the denitrifying activity in biofilter water and in washes of woodchips in Ringer solution. The biofilter water was analyzed for two reasons. First, it served as the underlying matrix for the woodchip inhibition samples; that is, unfiltered biofilter water rather than distilled water was used in the analyses to more closely approximate the biofilter conditions. Second, I wished to partition the contribution of surface woodchip microorganisms and detached microorganisms to denitrifying activity. In addition, woodchip wash solutions were tested to ascertain if washing the woodchips was an effective way to remove denitrifying organisms for further study and to optimize the wash duration was for this procedure.

DEA analyses with biofilter water samples and woodchip washes indicate that denitrifying microorganisms are present in both solutions. Figure 6b shows N_2O production from woodchips in biofilter water and biofilter water only. Although the level of activity is again substantially different for the two sampling dates, both the July and August samples showed denitrifying activity in biofilter water samples and woodchip washes; however, the relative activity of the biofilter water and the wash was substantially

different on each sampling day. These results suggest that microorganisms both in the biofilter water and on the woodchip matrix contribute to denitrification in the biofilters.

Additionally, the amount of denitrifiers in the biofilter water may also be important to the overall denitrifying activity. For the July sample, the denitrifying activity of the biofilter water represents 76.9±37% of the total uninhibited activity; for the August sample, this drops to 13.8±6.8%. It is therefore possible that the amount of denitrifying microorganisms on the woodchips is relatively constant but that the population in the aqueous phase varies with flow rate and retention time, however I did not collect measurements of bacterial biomass to confirm this. This may also explain the variability in overall activity and proportional calculations between sample dates. Experiments to better quantify temporal variation in denitrifying activity in woodchips and biofilter water are needed to support this theory.

DEA of woodchip washes (Figure 6c-d) show that the washing protocol removes denitrifying organisms from the woodchips. The effect of wash duration was variable. In the July sample, a 1 hr wash produced the highest level of denitrifying activity in washes (Figure 6c); in the August sample, the overnight wash performed the best (Figure 6d). From this data, an overall best performing wash duration could not be distinguished, however, all durations of wash (including shaking the sample vigorously for 1 min) removed some denitrifying organisms from the woodchips. The effect of adding glass beads to aid washing cells from woodchips was also tested (Figure 6c). The results indicated that there was no clear gain in recovery of denitrifying activity from using glass beads, as the overnight wash showed no improvement with beads and the 30 min wash showed some, but did not substantially increase in activity. As I later discovered, more

vigorous agitation with glass beads using a vortex mixer does improve removal of cells from woodchip particles (see Section 4.2); this may be because the shaker used for the washes did not create enough movement with the beads to dislodge cells from the chips.

Another important result was that in one case a greater amount of denitrification was observed from a wash than from the woodchip/biofilter water combination (Figure 6d, overnight wash). This is a puzzling result without clear causes. Because glucose was added, cells removed from woodchip surfaces may have the ability to grow overnight, resulting in greater denitrification activity. Or perhaps this is simply error in the methodology. This may be a subject of further experiments, as the present methodology was only designed to establish whether washing could remove cells (showing denitrifying activity) from woodchips, not to quantify the level of recovery.

Although most of my analyses did not include glucose (to better approximate biofilter conditions), DEA analyses are typically conducted in the presence of glucose as an electron donor. To determine if this addition was required or if sufficient carbon substrate was present in wash samples to support denitrification in the presence of added nitrate, I tested the denitrification activity of samples with and without glucose addition (Figure 6d). The shorter wash periods appeared to be unaffected by glucose content, however, the overnight wash showed a small increase in activity with the addition of glucose to the DEA reaction solution. This may be due to additional cells washed from the woodchips or to some overnight growth of bacteria. That denitrification activity is observed without addition of glucose and that similar activity is generally observed with and without glucose addition suggests that at least some molecules capable of acting as electron donors are washed from the woodchips during the wash process.

4.1.4 Analyses for potential in-situ N_2O production

One concern about using denitrification to remove nitrate from surface waters is the potential production of N_2O gas, a greenhouse gas. N_2O gas can be produced in denitrification if no, or not enough, denitrifying species have the enzyme nitrous oxide reductase—that is, when denitrification is not complete. To evaluate the potential for incomplete denitrification by denitrifying organisms in the biofilter, I conducted DEA on woodchips both in the presence of and without acetylene gas. Acetylene gas is typically used in DEA to inhibit nitrous oxide reductase, resulting in the accumulation of the intermediate product N_2O gas, which is more readily measured by gas chromatography, rather than N_2 gas, whose measurement is confounded by the large amount of N_2 in the atmosphere. By not adding acetylene gas, denitrification proceeds without inhibition, so the only the N_2O gas that is produced by incomplete denitrification is present and measured.

Minimal N_2O production (below detection limit) was observed in the absence of acetylene gas for both woodchip or biofilter inlet water samples while substantially higher N_2O production was observed in samples inhibited with acetylene (Figure 7). In situ N_2O production due to incomplete denitrification should therefore be minimal, with the majority of denitrification proceeding completely to N_2 in the biofilter system.

To make sure that acetylene addition only inhibited the last step of denitrification and not other metabolic functions, I also measured the CO_2 production of the reactions as a proxy measurement for overall metabolism (Figure 7). CO_2 production was comparable between those samples receiving acetylene and those under no inhibition. Therefore, the

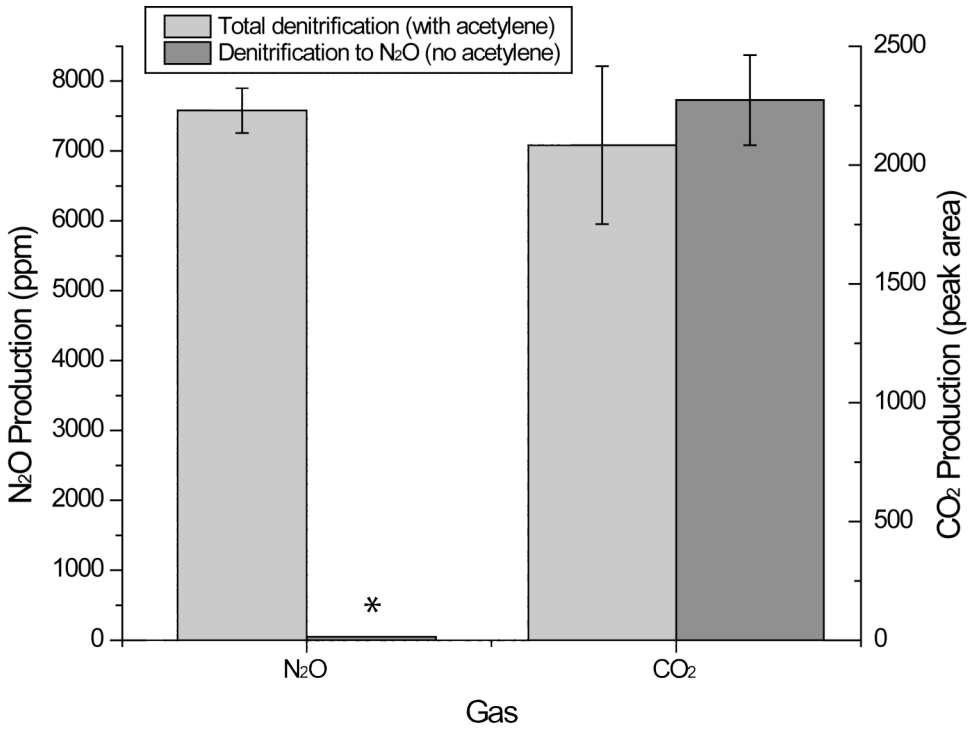

Figure 7. DEA analyses of biofilter woodchips in the presence and without acetylene gas (10% of atmosphere). Assays included 25 g dry woodchips and 50 ml of 1 mM nitrate. Error bars represent standard deviation of triplicate samples. * indicates measurements below detection limit (<50 ppm).

concentration of acetylene did not appear to cause additional effects on metabolism beyond the inhibition of nitrous oxide reductase.

4.1.5 Implications

In these tests, the denitrifying enzyme assay (DEA) was used to characterize the types of organisms responsible for denitrification in subsurface biofilters and to evaluate the removal of cells by washing for use in other methods. I was successfully able to adapt the DEA method for biofilter samples, although a relatively high concentration of inhibitors was required to effectively inhibit bacteria and fungi. I also found that woodchip washes remove at least some cells for further analysis, a technique that was used later in this research.

DEA analyses showed that both bacteria and fungi contribute to the denitrification function of the system. It appears that bacteria directly mediate denitrification while fungi contribute indirectly, possibly through decomposition of the woodchips and subsequent release of carbon substrate for bacterial use or by providing other beneficial compounds. These results are consistent with the findings of Myrold and Posavatz (2007), who showed by selective inhibition that bacteria were more important than fungi for nitrate flux in soil. Conversely, Laughlin and Stevens (2002) found that fungal species performed most of the denitrification in a grassland environment in Ireland. However, relative contributions of fungi and bacteria to overall biomass and activity in soils appear to be variable by location and environment (D'Angelo et al., 2005; Bailey et al., 2002; Kageyama et al., 2008).

Results of the DEA analyses also indicated that denitrifying microorganisms exist both on the woodchips and in the water within the biofilter. This suggests that denitrification occurs in both the attached and free-living fractions of the biofilter habitat. Although this description of the microbial ecosystem is reductive, it was an important step in understanding the functioning of the biofilter. Recognizing the types of organisms responsible and the sites of denitrification may also help to make decisions about biofilter management and improvement, such as predicting biofilter response to pesticide or other chemical additions or optimizing flow for basic rates. Results of these preliminary analyses also enabled us to choose appropriate techniques for molecular analysis.

The data presented here also suggest that there can be differences in denitrifying activity over time. I hypothesize that this is linked to environmental conditions and that biofilter communities are variable in total abundance and community composition over time. Given that environmental parameters such as temperature and moisture have been

shown to be important for denitrifying rates and communities (Wallenstein et al., 2006b; Gutknecht et al., 2006), a shift in activity between the July and August samples is not unreasonable. However, because only two sampling dates were used in this study, more analyses need to be performed to say anything conclusive about dynamics of denitrification activity in the biofilters.

This research also suggests that N_2O production in the denitrifying system is low. Agricultural soils have been shown to have lower N_2O:N_2 production ratios (ranging from 0.16~0.29) than similar riparian areas or sediments (Cavigelli and Robertson, 2000; Rich and Myrold, 2004). Because the denitrifying biofilter is passively seeded from such soils, a relatively low N_2O:N_2 ratio is consistent with these findings. However, our system showed even lower N_2O:N_2 than typical agricultural soils. My results are also in agreement with recent work by Woli et al. (2010) and Elgood et al. (2010) who have measured minimal N_2O production in biofilter systems. More controlled and repeated studies from several biofilter locations or in situ measurements are needed to confirm that these are representative results, and to discern their cause.

4.2 FISH PROTOCOL DEVELOPMENT

DEA tests were successful in describing the relative contributions of fungi and bacteria to denitrification in biofilters. To further refine our understanding of biofilter microbial communities and their relationship to environmental and performance variables, methodology was required that could characterize more specific microbial groups. I optimized two types of methods for use with woodchip samples: characterization of whole

cells (using FISH) and analysis of extracted DNA (using t-RFLP and ARISA; See Sections 4.4 and 4.5).

Creating a successful FISH protocol was challenging. Our main difficulties with the FISH procedure were the high levels of autofluorescence from woodchip debris and low cell density in samples. The FISH technique uses fluorescent oligonucleotide probes to count cells and to calculate percentages of cells that belong to a particular group. Background fluorescence makes it difficult to identify and enumerate target cells. Furthermore, low cell density leads to a lower probability of finding rare cell types and also to less confidence in the composition of samples. The challenges of autofluorescence and low cell density appear to be due to the woodchip media. Autofluorescence is not atypical in environmental samples such as soils and sediments (Hahn et al., 1992; Zarda et al., 1997; Bertaux et al., 2007; Eickhorst and Tippkoetter, 2008). However, in comparison to soil, woodchip debris in the sample washes has larger particle sizes and a lower overall abundance of microorganisms. Additionally, the ability of probes to penetrate into surface biofilms on woodchip particles may be adversely affected by larger particle size and the characteristics of wood itself.

Various strategies have been used with soil and sediment samples to attenuate autofluorescence and/or increase target fluorescence, including dispersal by sonication (Shelley and Perry, 2000; Lam and Cowen, 2004; Danovaro et al., 2001), addition of pyrophosphate to quench autofluorescence (Lindahl, 1996), and use of lysozyme to increase cell permeability to probes (Thurnheer et al., 2004). I experimented with these and a number of other slide preparation techniques to increase cell counts and remove (or reduce) autofluorescence in woodchip wash samples (Table 3). Several results were of

Table 3. Results of experimental FISH slide preparations.

Slide Preparation Technique	Qualitative Result
Spotting directly onto slide	Good retention of cells but large amounts of debris
Filtration of sample onto 0.2 μm filter, pressing filter against slide	Substantial reduction in cell count
Use of PFA vs EtOH fixation methods	No consistent differences between the methods
Sonication of diluted sample	Reduction of debris, but some concurrent reduction in cell count
Addition of $NaPP_i$ to samples	No noticeable reduction in autofluorescence
Concentration of woodchip wash up to 50X	Increased cell counts, but also increased debris
Prefiltering through a 1.5 to 10 μm filters	Untenable reduction in cell count
Slow centrifuge (800-3000 rpm)	Separation of large quantities of fungal-looking cells (visible by DAPI) that do not adhere well to FISH slide, few discernable bacteria
Different coating of FISH slides (gelatin, low- or high-melting temperature agarose)	Gelatin-coated slides showed least background fluorescence
Lysozyme pretreatment (on slide or in microtube)	Pretreatment in microtube showed increased signal for DAPI, but not for labeled probes; slide treatment showed no discernable difference
Vortexing sample with glass beads followed by slow centrifuge	Increased cell counts and clarity, substantially reduced background fluorescence

note. Firstly, the slide preparation techniques that were previously successful in reducing autofluorescence and enhancing cell visualization in soil with our same hybridization protocol (use of sodium pyrophosphate to dilute the sample, sonication, filtration onto a 0.2 μm filter and pressing this filter onto a gelatin-coated slide (Zhou et al., 2007)) were ineffective for woodchip samples. Autofluorescence was not reduced using this technique, possibly due to limited penetration of the sodium pyrophosphate into the woodchip debris or the effectiveness of sodium pyrophosphate on the wood material. Additionally, cell counts were very low using this protocol. I found that spotting sample directly onto the slide instead increased our cell density by 5-20x. This may be due to cells adhering strongly to large debris particles (noted visually in many samples), which might limit their separation from debris by sonication and reduce transfer to the slide following filtration. Prefiltering through larger pore size filters to retain debris but permit bacteria to pass through likewise was unsuccessful, again possibly because bacteria adhered closely to large debris particles.

Lysozyme pretreatments showed limited effectiveness in increasing fluorescence intensity (Figure 8). Specifically, treatment of woodchip wash with 1 X lysozyme in microtubes for 15 minutes appeared to increase cell permeability to DAPI staining. However, only a very slight improvement was seen for intensity of fluorescent probe response in relation to background fluorescence.

From our range of experiments, I was successful in developing a slide preparation protocol that enabled clear visualization of target cells with lowered background. First, I found that concentration of woodchip wash samples of at least 25x, optimally 50x, is required to get useable cell counts. Alone, this concentration step increased debris to a level that would completely obfuscate probe detection. However, the addition of vortexing the concentrated woodchip wash with 5 mm glass beads, slowly centrifuging the results to remove large debris, and using the supernatant for FISH dramatically improved cell counts and separation (Figure 9). The vortexing step appeared to effectively dislodge bacteria from wood particles; in comparison to tests not using this step bacterial cell counts were much higher. Without vortexing large amounts of fungal-type cells were instead visible (images not shown). No consistent differences in the target fluorescence or background were observed among samples fixed with the ethanol or PFA mixation methods (de los Reyes et al., 1997).

Using the slide preparation protocol described above, FISH was conducted on selected samples from the FP03 and DE01 biofilters using a broad spectrum of group probes. A visual inspection of FISH images revealed several general results. First, there was approximately 80% coverage of the bacterial probe (Bac-338) to most samples (Figure 9d), indicating that the majority of cells visible were bacterial. In contrast, there was little,

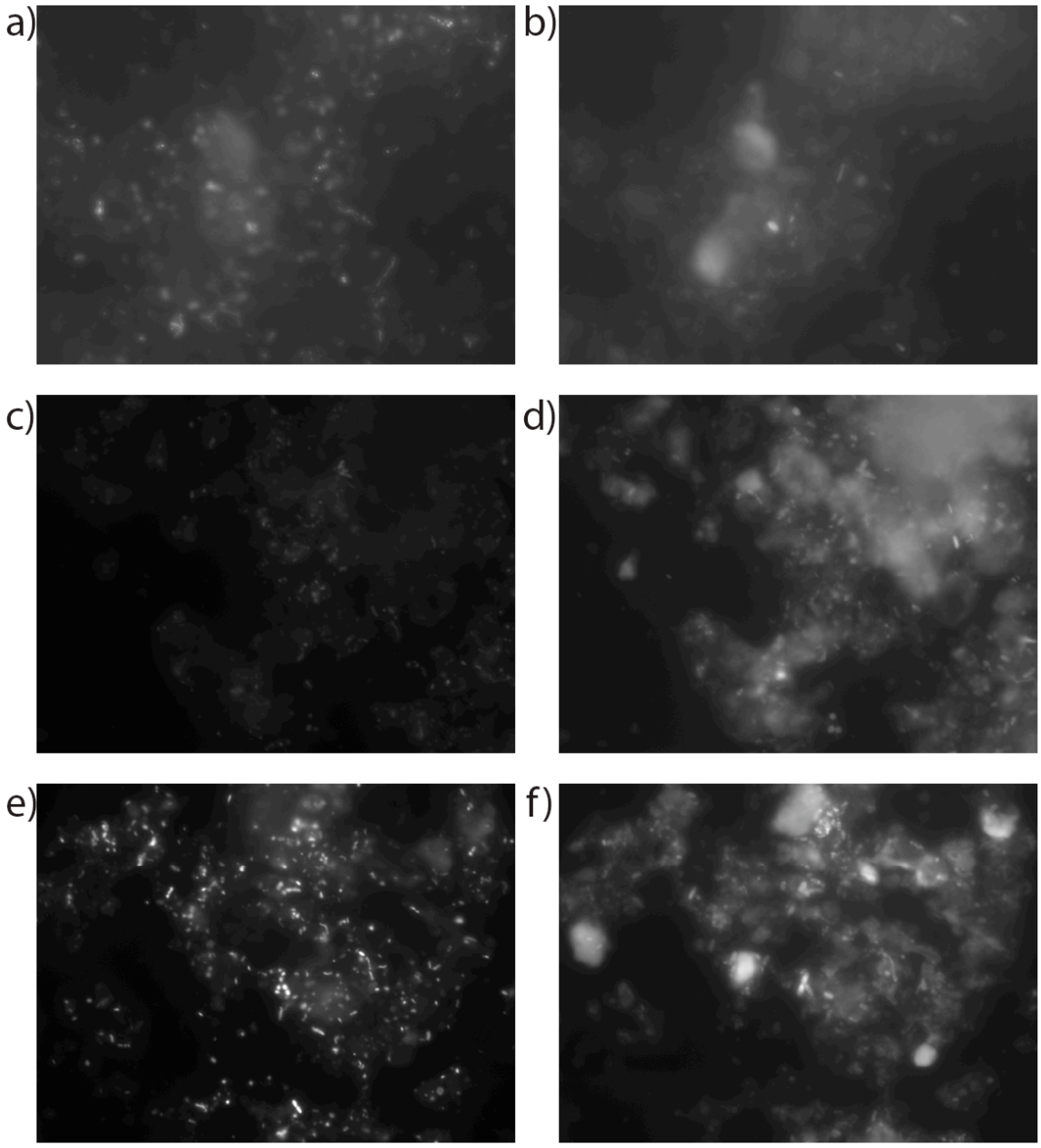

Figure 8. Microscope images of cells from woodchip samples analyzed with FISH under differing levels of lysozyme treatment. a-b) DAPI and Bac-338 probe with no treatment; c-d) DAPI and Bac-338, spotting lysozyme onto slide for 30 min; e-f) DAPI and Bac-338 incubating lysozyme with sample in microtube for 15 min.

if any, discernable hybridization with the eukaryotic probe (EUK) on test samples. This probe showed strong fluorescence with yeast standards and DEA tests indicated that fungi are present in woodchip samples. Because fungi frequently constitute a substantial amount of microbiota in agricultural soils (Frey et al., 1999) and because fungal fruiting

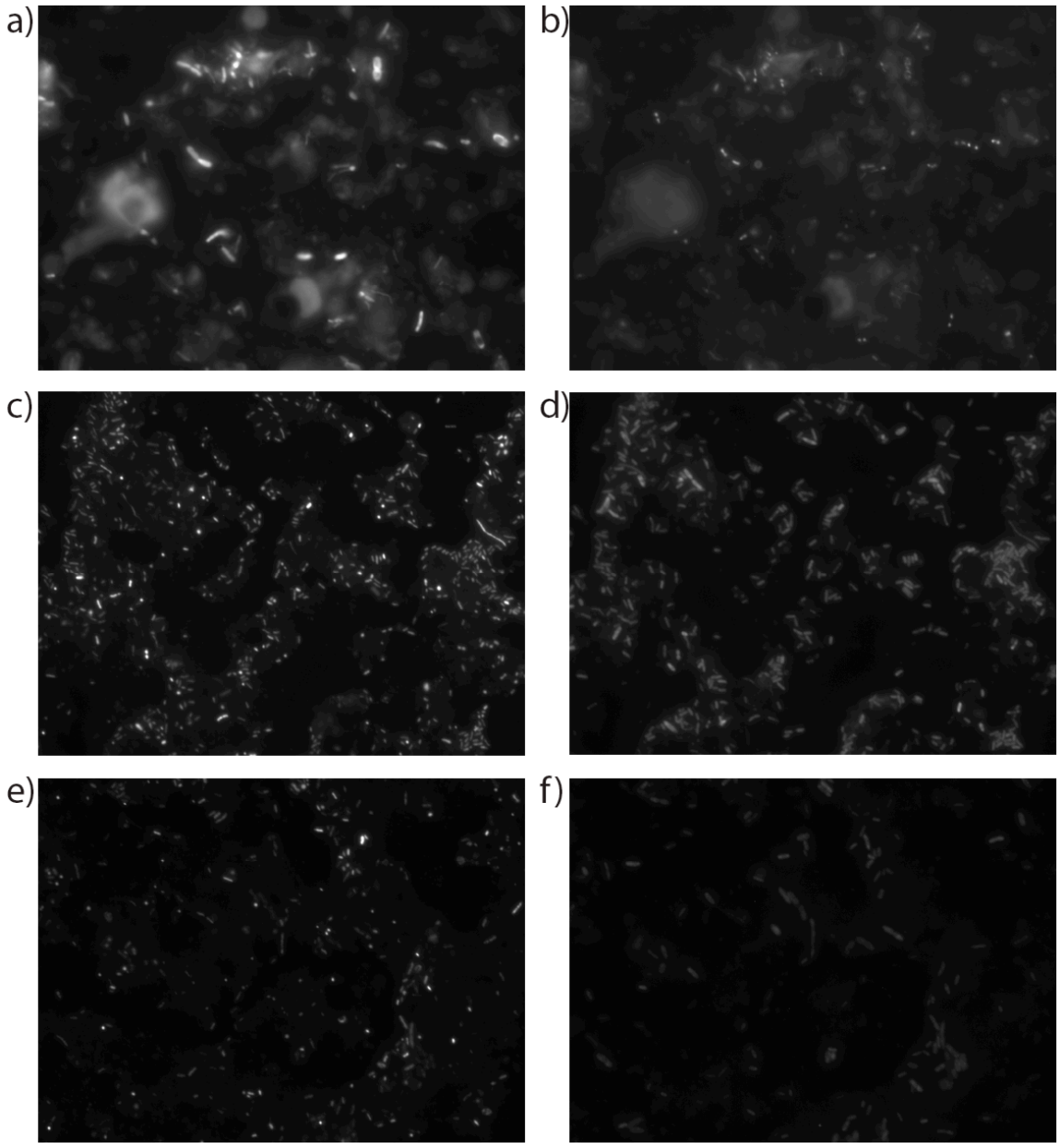

Figure 9. Microscope images of cells from woodchip samples analyzed with FISH under differing levels of vortexing with glass beads. a-b) FISH slides with no bead vortexing, 25x concentration, a) DAPI stain and b) Bac-338 probe; c-f) FISH slides with bead vortexing, c) DAPI stain and d) Bac-338 probe, e) DAPI stain and f) γ-Proteobacteria. Samples from FP03 biofilter, 20 Mar 08.

bodies have been often observed at biofilter sites, this result suggests that our sample fixation and preparation methodology does not preserve intact fungal cells well.

Second, a qualitative assessment showed that the majority of cells in the samples tested hybridized with γ-Proteobacteria (e.g. Figure 9f), indicating a high percentage of

cells belonged to this group of bacteria. Other probes specific for archaea, high- and low-GC bacteria, α-Proteobacteria, and β-Proteobacteria resulted in low hybridization with samples. Because I was unable to create consistent standards for these groups, it is unclear if the results are due to low probe hybridization under the methods used, or if they reflect actual low abundance of the particular groups in the tested samples. Although some studies indicate that γ-Proteobacteria make up a comparatively small percentage of bacteria in soil (Zarda et al., 1997; Spain et al., 2009), recent analysis of DNA libraries of soil extracts suggests that γ-Proteobacteria are up to 34% of total soil bacteria, with *Pseudomonas* species making up approximately 2% (Janssen, 2006).

The optimized FISH methodology presented here should enable future examination of biofilter samples for the presence of particular bacterial groups. Images produced from our experiments were tested for their ability to be used with automated analysis (using the software Visilog) and performed well. Because the t-RFLP and ARISA methodologies that were developed in parallel with these experiments proved to be rapid and effective, they became the avenue of data collection for most of this research. However, samples collected from the FP03, FP07, and DE01 biofilters for the time-series dataset were all fixed for future use with the FISH protocol. This should enable the extension of the method to a larger set of samples in the future.

4.3 ANOSIM-GS ALGORITHM AND PROGRAM

Whichever method of community description one uses, microbial communities are frequently observed fo be dynamic in space and time (Martiny et al., 2006; Horner-Devine et al., 2004a, see Section 2.2.1) and quantitative analysis of this variability is necessary to

describe the spatial and temporal structure of microbial communities in biofilters more quantitatively. To this end, a method combining a geostatistical structure function with the ANOSIM metric was developed. The ANOSIM metric, which tests whether groups of samples have statistically similar communities, is a widely used choice; it has been shown empirically to be a robust analysis for the large and sparse community datasets typical in microbial ecology (Clarke, 1993, times cited on Web of Science as of October, 2010: 2,662). Additionally, because ANOSIM uses rank-transformed ecological similarity metrics, the effects of non-normal distribution and non-linear associations are avoided. By using ANOSIM as the statistic in a geostatistical structure function, the resultant plots (ANOSIM-GS) show the variation of community similarity as a function of the separation distance—either geographical space or time—between pairs of samples.

A computer program automating the production of ANOSIM-GS plots was developed. In this section, I discuss the structure of the program algorithm, guidelines for its use, and compare it to other multidimensional statistical methods.

4.3.1 The ANOSIM-GS Algorithm

An algorithm based on the *gamv* program of the FORTRAN geostatistics program GS-Lib (Deutsch and Journel, 1998), was created to perform the ANOSIM-GS analysis. The *gamv* program, given an input file detailing location and univariate data at each sample point, sorts pairs of samples into classes defined by lag (separation) distance h and calculates a variogram metric of the user's choice for each class. Analysis for anisotropy (differences in spatial structure in different directions) can be performed by choosing particular directions along the surface (azimuth) and in the depth direction (dip angle) in

which pairs must be oriented. The number and spacing of the distance classes, as well as the desired azimuth, are specified by a user-defined parameter file.

For the new ANOSIM-GS variogram, the original algorithm was altered to accept a similarity matrix instead of univariate data, to allow the user to choose between a spatial or temporal analysis, and to create the ANOSIM-GS plot. The new algorithm was implemented in Python (version 2.5.4). The analysis steps of the program are as follows:

1. The parameter file, location file, and similarity matrix are read by the program.
2. The similarity matrix is rank-transformed.
3. For each sample pair:
    a. the separation distance and lag class is determined,
    b. (for spatial analyses) the angle between the pair is checked to assess whether it falls into the specified directions, and
    c. (for temporal analyses) the pair is checked to ensure samples are from the same location.
4. If the pair meets the sorting criteria, the rank of the pair is added to the "within" sum for its class and to the "between" sum for every other class. A count of pairs within each class is kept.
5. When all pairs have been sorted, for each class:
    a. the average "within" and "between" ranks are calculated,
    b. the *R* statistic is calculated, and
    c. the significance of the *R* statistic is determined by permutation. For the permutation test, groups with the same number of pairs as

the test class are randomly chosen from all sample pairs, and for each random group, the *R* statistic is calculated and compared to the *R* statistic of the test class. The process is repeated 10,000 times, and the percentage of R values of random groups that were higher than the R value of the test class is calculated as the significance of the statistic. Therefore, a lower p indicates greater significance.

6. The lag class, average separation distance of the class, number of pairs in the class, R statistic for that class, and statistical significance of the R statistic are outputted into a file.

4.3.2 Guidelines for ANOSIM-GS use

Figure 10 shows the general procedure for analyzing a dataset with ANOSIM-GS and some guidelines for effective use. In practice, the ANOSIM-GS method has much in common with many geostatistical structure functions. As with traditional semivariograms or correlograms, accurate visualization of spatial or temporal structure with ANOSIM-GS is reliant upon the choice of appropriate analysis parameters and on using enough data to have statistical confidence. For ANOSIM-GS, I add to these usage guidelines a discussion of the choice of ecological similarity matrix used. These are discussed below and illustrated with bacterial community data from the spatial dataset (FP03, March of 2007).

This dataset is comprised of samples collected from the FP03 biofilter on 16 March 2007. 250 ml samples of woodchips were taken according to a regular sampling grid, spaced every 2.7 m in the direction of biofilter flow, every 0.46 m in the cross flow, and at two depths (0.76 m and 1.52 m). At several locations, a 250 ml sample was composited

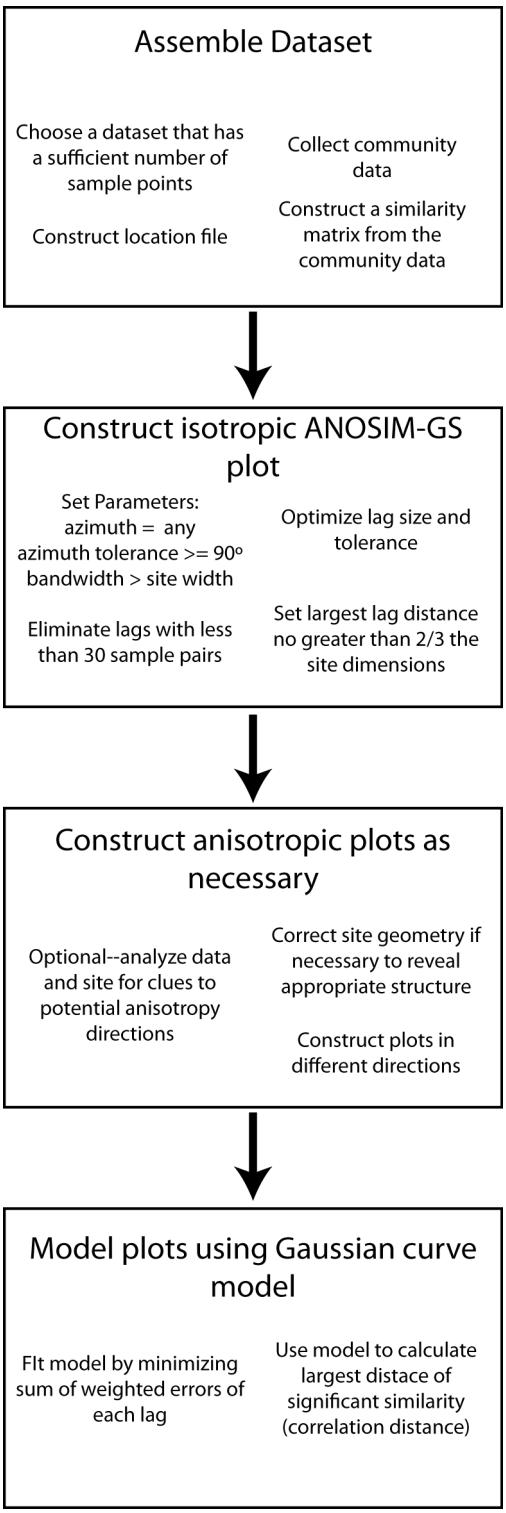

Figure 10. Schematic of ANOSIM-GS use.

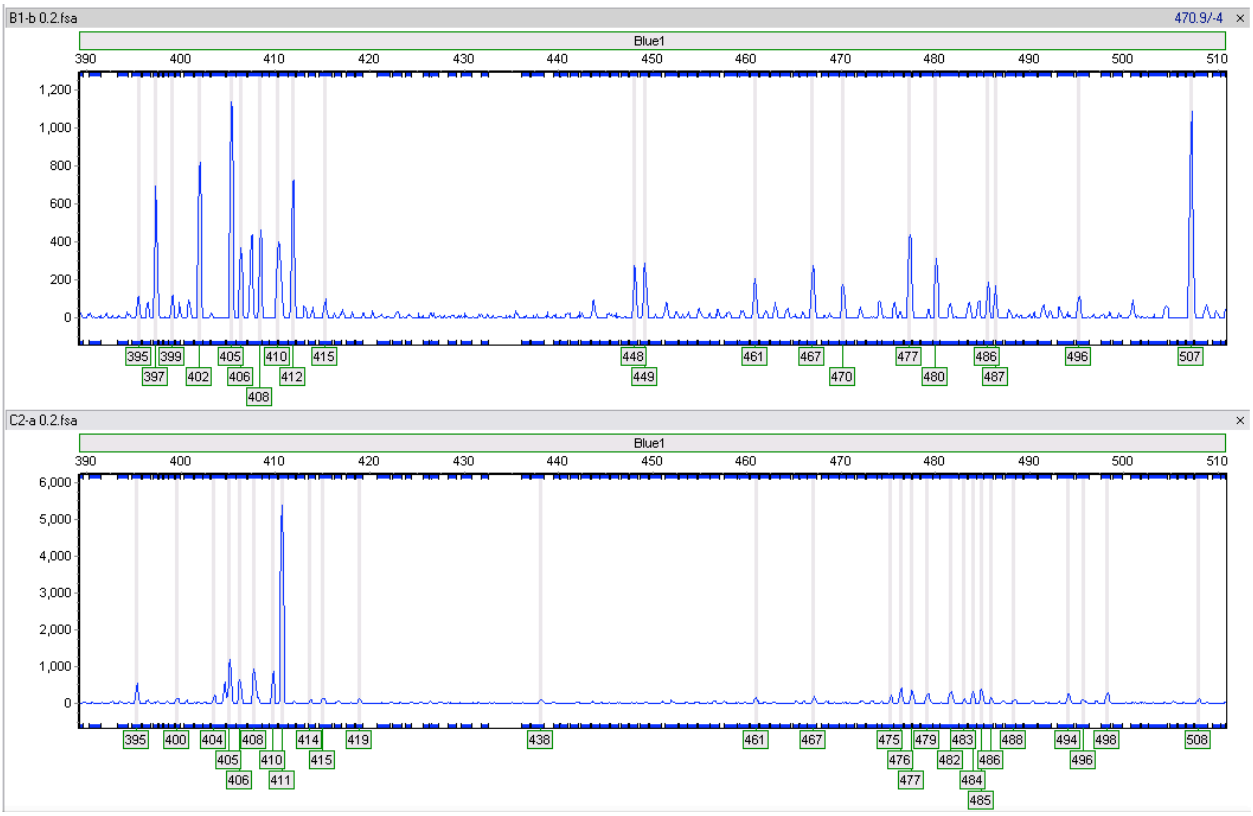

Figure 11. Portions of ARISA community fingerprints from two biofilter samples. Horizontal axes represent the DNA fragment length in base pairs corresponding a distinct population. Vertical axes are the fluorescence intensity, a proxy measurement for abundance of the population. Samples taken on 16 March, 2007 from the FP03 biofilter. ARISA fragments processed with GeneMarker version 1.75.

from a larger sample (approximately 700 ml). Figure 3 shows this sampling scheme. ARISA and *nosZ* community fingerprints were created from these samples (Figure 11) and used to compare overall bacterial communities (ARISA) and denitrifier populations (*nosZ*) from different locations within the biofilter. From such data, it is possible to compare the relative abundance of each distinct microbial population in the overall community.

The significance of the results of applying the ANOSIM-GS technique to the spatial dataset is fully described in Section 4.4.3, in this section I confine my remarks to the development of the methodology and comparison of resultant ANOSIM-GS output to analyses conducted with alternative methodologies.

Characteristics of the dataset

The size and distribution of the dataset are important to the resolution and extent of spatial structure that can be visualized. A general rule of thumb for construction of structure function plots to ensure that calculated values are truly representative is that every distance class should contain at least 30 sample pairs (Journel and Huijbregts, 1978); Legendre and Fortin (1989) argue this requires at least 30 total samples. Anisotropic structure function plots should only be constructed when there are enough pairs in the direction of the azimuth to satisfy this requirement. Analysis of spatial structure by structure functions such as the ANOSIM-GS method are only accurate over approximately 2/3 the total dimension of the dataset in the direction of analysis and cannot discern spatial structure at a scale smaller than the sample spacing.

Lag size and tolerance

As with other structure function plots, trial and error is necessary to produce an ANOSIM-GS plot that most clearly reveals structure (Deutsch and Journel, 1998). The two parameters that most substantially influence whether structure is clearly visible are the interval between distance classes (lag size) and the width of the distance classes (lag tolerance). The optimal lag size will adequately capture changes in similarity with separation distance. Plots with lag sizes too small will be erratically shaped, those with lag sizes too large will not show changes in significance at their smallest resolution. The smallest appropriate lag size corresponds to the smallest physical distance between samples. The lag tolerance can be half the lag size (so that every sample pair falls into one class), less than half the lag size (so that some pairs do not fall into a class), or greater than half the lag size (so that some pairs fall into multiple classes). Choice of tolerance allows

for inclusion of all data (in the first case), for heightened specificity in a lag class (in the second case), or for smoothing of the plot (in the third case).

As an example, Figure 12 shows ANOSIM-GS plots for lag sizes of 0.46 m to 3.66 m using tolerances of half the specified lag size. With increasing lag size, the plots progressively become less chaotic and more smoothed. From these results I see the effect of sampling grid size on optimal lag size. For the spatial dataset, the grid size is 2.74 m in the flowpath direction, 0.46 m in the cross-flowpath direction, and 0.76 m in the depth direction. For the smaller lag sizes, the number of pairs in each lag class varied substantially, resulting in differences in the significance. In contrast, the plot using lag size equaling the predominant grid size (2.74 m) is smooth and Gaussian-shaped with a sharp incline. The plot with a lag size of 3.66 m is also Gaussian-shaped, but fails to capture the spatial features as clearly. A lag size of 2.74 m is therefore optimal in this case.

Direction parameters

User-supplied parameters determine whether a lag class includes pairs of samples irrespective of direction (omnidirectional) or only those pairs that are related in a particular direction (to show anisotropy). These parameters include the direction of the analysis along the surface (azimuth), the tolerance in this direction (azimuth tolerance), and the perpendicular distance from the azimuth allowed (bandwidth) (Figure 13). Similarly, parameters related to the requisite deflection from the surface in the depth direction (dip angle, dip tolerance, and dip bandwidth) can also be defined. For omnidirectional plots, the choice of direction is irrelevant; tolerances are set to >90° and the bandwidths set to the width/depth of the site so as to include all sample pairs. Assessment of the direction of anisotropy is largely trial and error, but can be informed by

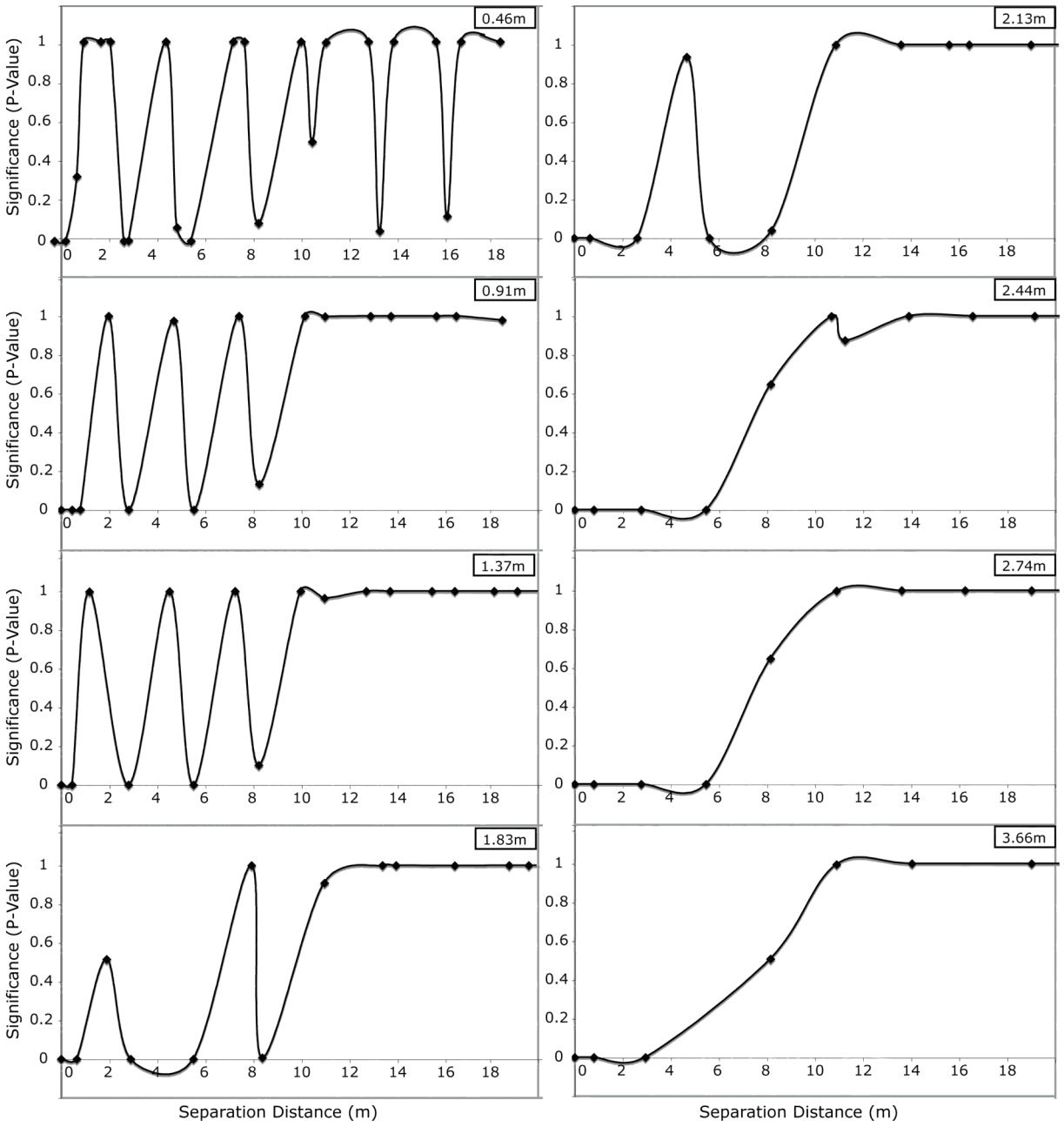

Figure 12. ANOSIM P-value plots showing optimization of lag size using bacterial community data from the FP03 biofilter site. Plots are constructed with variable lag sizes, denoted in the upper right-hand corner of each plot. The 2.74 m lag size gave the smoothest significance curve that still retained the majority of major shape features.

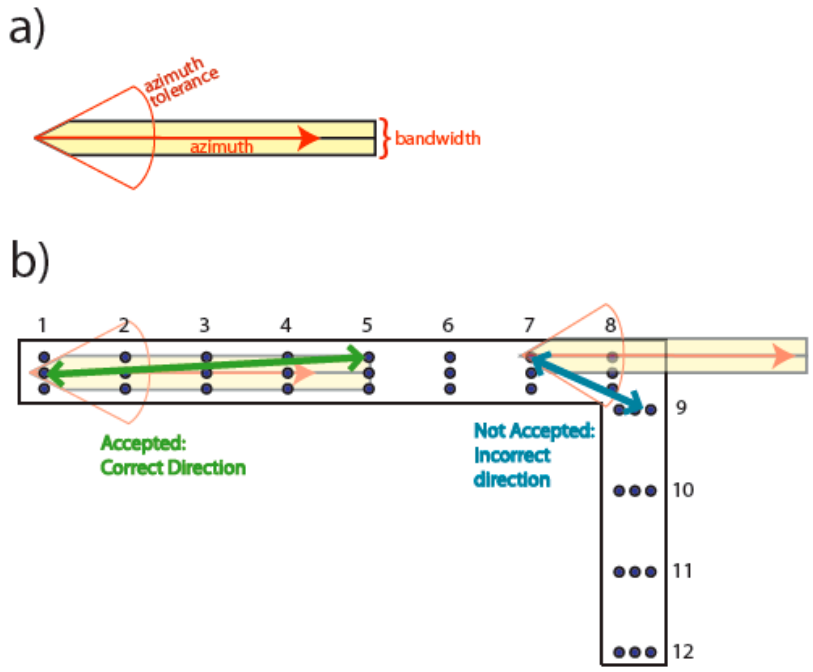

Figure 13. Illustration of directional parameters and their application: a) azimuth, azimuth tolerance, and bandwidth; b) application of directional parameters to a dataset including an accepted and a rejected sample pair. The vector between samples in the accepted pair is both within the defined azimuth tolerance and the bandwidth. However, although the vector between samples in the rejected pair is within the azimuth tolerance, it is outside of the bandwidth.

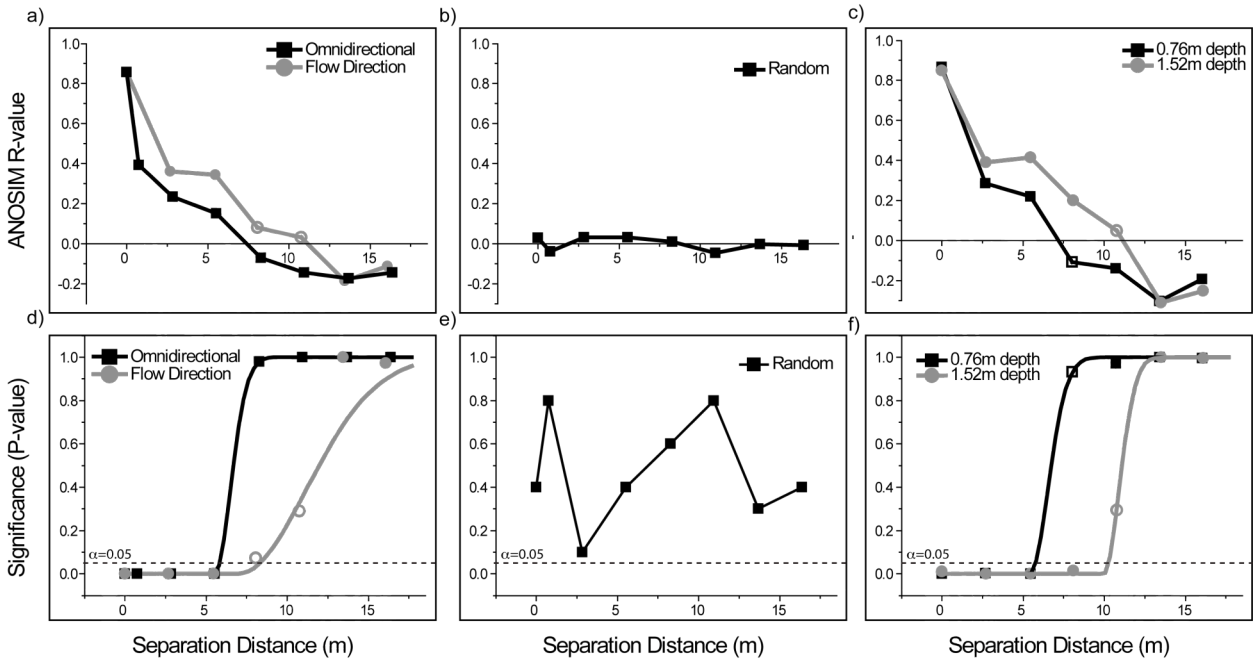

Figure 14. ANOSIM-GS (Eq. 14) plots using: a) and d) bacterial community spatial data analyzed omnidirectionally and in the direction of flow; b) and e) randomized data; and c) and f) biofilter community data separated by depth, analyzed in the flow direction. Closed symbols denote lags that are significantly similar ($p<0.05$) or dissimilar ($p>0.95$), open symbols show lags that are not significant.

site information or preliminary analysis. As the FP03 biofilter has a strong directionality of flow, I suspected anisotropy in the direction of flow. Both types of plots were constructed for the biofilter dataset (Figure 14). For the isotropic (omnidirectional) plot, parameters were chosen to encompass all sample pairs. Because of the shape of the biofilter site, production of anisotropic plots in the flowpath direction required alteration of the location data. To account for the L-shape of the biofilter flowpath, I altered the location file for the biofilter data so that the positions of the vertical arm of the L appeared as if the biofilter were straight. Separation distances between sample locations were kept consistent with the original data. For the directional plots, I restricted pairs to the same depth (dip angle and tolerance of 0°) and in the flow direction (azimuth 90°). Because samples were tightly spaced in the 0° (cross-flow) direction, a narrow angle was necessary to isolate spatial structure in the direction of flow. Therefore, an azimuth tolerance of 5°, and a bandwidth of 1.5 m were chosen.

Transformation of abundance data

One of the advantages of the ANOSIM-GS method is the ability to use a similarity metric and data transformations that are appropriate to the community dataset. These choices are made before input into the ANOSIM-GS program, however, it is important to assess the choice of similarity metric and transformation on the resultant plots. For example, community similarity metrics constructed using presence-absence data provide a more conservative, but possibly more distorted, estimate of community similarity than those constructed with abundance data, because abundance-based ecological community datasets are often statistically skewed and zero-inflated (Mcardle et al., 1990). To test the effect of transformation of community data on ANOSIM-GS plots constructed from the

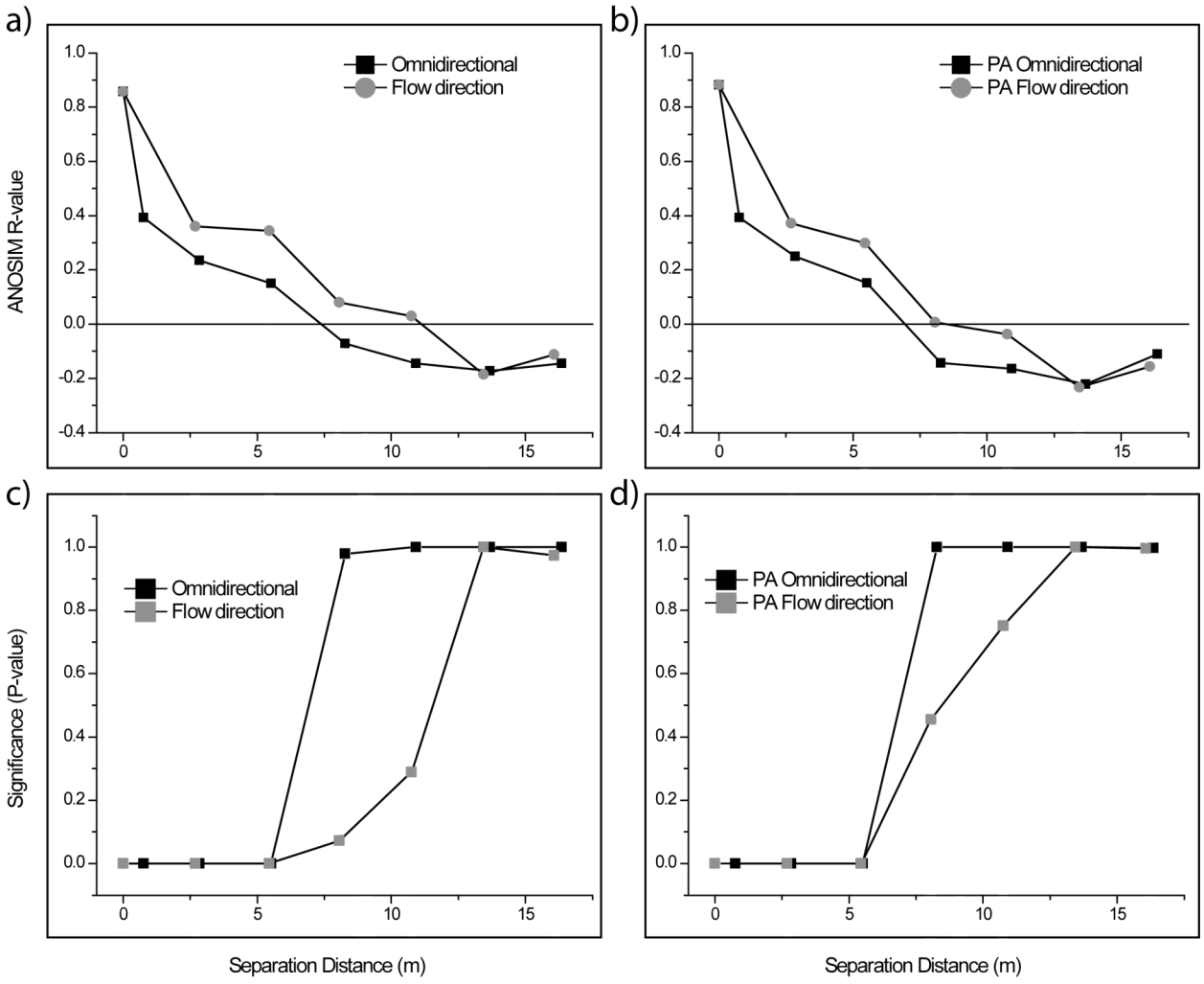

Figure 15. Comparison of ANOSIM-GS (Eq. 14) plots using abundance or presence-absence community data from the spatial dataset: a) R plot using abundance data; b) R plot using presence-absence data; c) significance plot using abundance data; and d) significance plot using presence-absence data.

spatial dataset, I compared omnidirectional and flowpath-directional plots constructed with community similarities derived from relative abundance data and from presence-absence data (Figure 15). There were no appreciable differences between these plots at either depth. Therefore, I chose to retain the abundance information.

4.3.3 Comparison to alternative approaches

To compare the ANOSIM-GS method with previously developed multivariate approaches, I used the spatial dataset with the same parameters used to create the above ANOSIM-GS plots to create plots of several other analysis types. These included distance decay plots, dissimograms, variograms of complementarity, and Mantel correlograms (Figure 16).

The ANOSIM-GS plots showed several major spatial attributes of the dataset (Figure 14). Although these are discussed at more length in Section 4.4.3, briefly, the spatial structure of the FP03 communities shows anisotropy in the direction of flow and a difference in spatial structure at the 0.76 m and the 1.52 m depth. The correlation ranges at these two different depths were calculated to be 8.5 m at 0.76 m and 10.3 m at 1.52 m.

Applying the distance decay method to the FP03 spatial dataset (Figure 16) revealed slight differences in slope and intercept for each analysis group, however, the method does not allow for calculation of a definitive correlation range, and the number of points in the plots made a clear pattern difficult to ascertain. Figure 16 also shows the results of several other geostatistical analysis methods as applied to the spatial dataset. The majority of these methods were able to distinguish differences in the community spatial structure from anisotropy and at different depths. However, the ranges and shapes of perceived correlation using these different methods were inconsistent. Ranges resulting from exponential models applied to the dissimograms and variograms of complementarity were not similar, and neither were they consistent with the ranges calculated from the ANOSIM-GS method (Figure 16). The variogram of complementarity predicts a lower correlation range compared to the ANOSIM-GS method and is not able to discern a coherent spatial

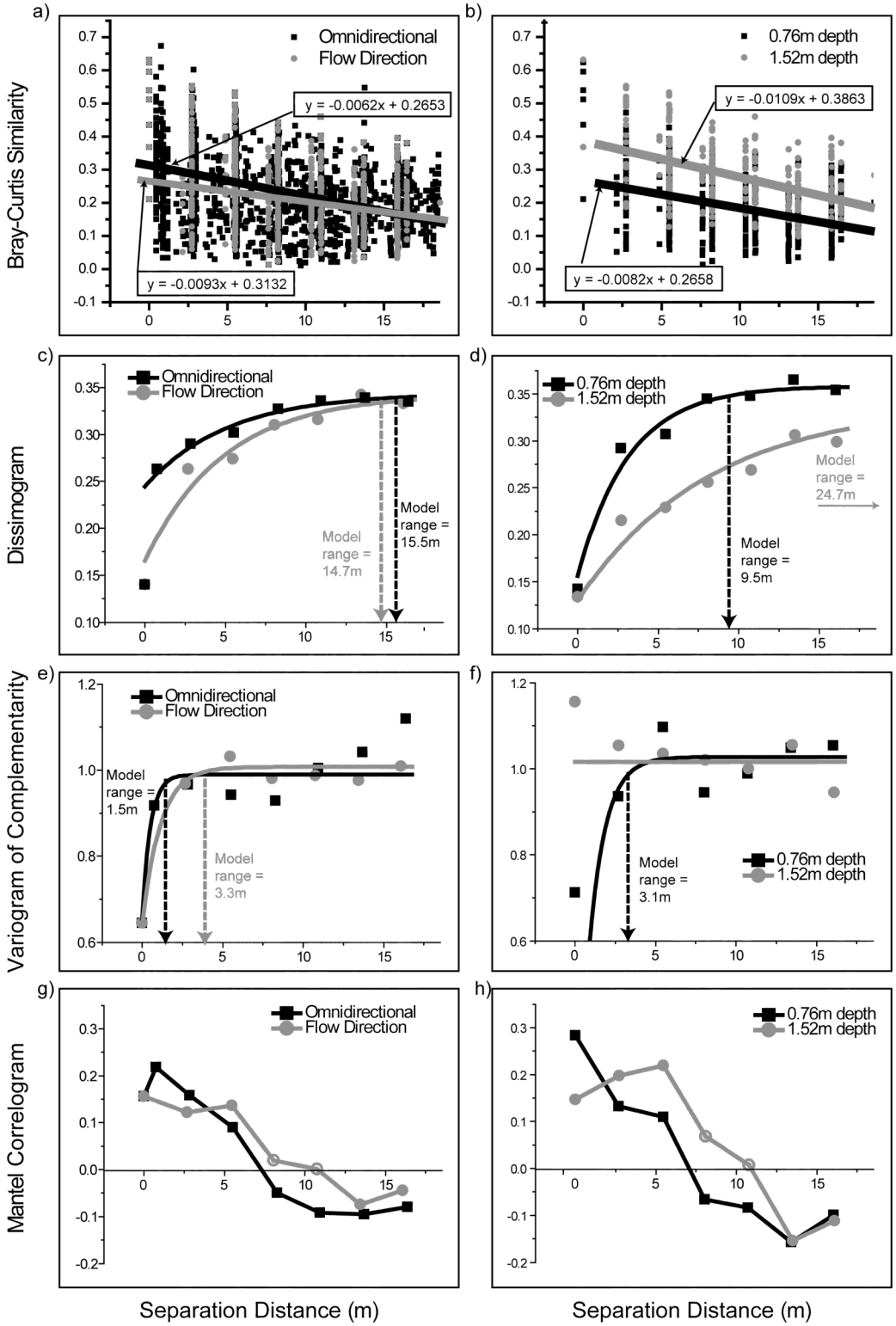

Figure 16. Multivariate analysis plots of bacterial community samples from the FP07 biofilter (March 2007): a) distance decay plots using all data; b) distance decay plots by depth; c) dissimograms using all data; d) dissimograms by depth; e) variograms of complementarity using all data; f) variograms of complementarity by depth; g) Mantel correlograms using all data; h) Mantel correlograms by depth. In h), closed symbols denote significant lags, while open symbols denote lags not significant in permutation tests.

pattern for sample pairs at the 1.52 m depth. The modeled ranges of the anisotropic dissimograms, in contrast, are higher than those modeled from the ANOSIM-GS plots (Figure 16). For both the omnidirectional variogram of complementarity and the omnidirectional dissimogram, the second lag class (an average distance of approximately 0.76 m) appeared to strongly influence the model; this lag class was the only one to include sample pairs along the width of the same transect and therefore may exhibit greater variability than other classes.

Measures of significance from permutation tests also did not correspond to the modeled ranges. For variograms of complementarity, significant lags in the omnidirectional plot extend past the modeled range, for the flowpath-directional and 0.76 m depth plots, they do not extend to it, and for the 1.52 m depth no significantly correlated lag classes were found.

The Mantel correlograms, on the other hand, have similar shape and pattern of significance to the ANOSIM-GS correlation plots. Differences in the significance of lag classes do occur in the fourth and fifth lag classes (the inflection points of the plots), with the ANOSIM-GS correlation plots showing a greater correlation range. The Mantel correlograms also show potential effects of the linear correlation assumption: in both the omnidirectional and directional plot at the 1.52 m depth, the Mantel correlogram increases after the first lag class where the ANOSIM-GS correlation plot does not. Using rank-transformed similarity data for the Mantel correlogram may improve this result.

Each of the tested alternative methods additionally showed differences between plots derived from presence-absence data and those derived from abundance data (data not shown); differences in modeled correlation ranges of up to 21.5 m were noted. A

further consideration is that the computation time required to calculate the variogram of complementarity was substantially larger than that needed to run the other analyses. The computational intensity could be minimized by reducing the number of permutations in the significance testing, but at the expense of the power of the test.

4.3.4 Implications of the ANOSIM-GS method

The ANOSIM-GS method provides researchers a flexible and robust means to evaluate the spatial structure of complex ecological communities. Although the test was designed to handle spatial data from biofilter community analysis, the method only requires data with a distance and a similarity component, and is therefore applicable to both spatial and temporal analysis of many types of multivariate data. The program used to prepare the similarity matrix and the choice of similarity metric are also not constrained (see Gower & Legendre, 1986, for a comparison of similarity metrics). The statistical test used in ANOSIM-GS is non-parametric and able to accommodate non-linear associations. This is particularly important because many ecological datasets, including raw abundance data and community similarities, exhibit non-normal behavior (McArdle et al., 1990; Clark and Green, 1988). Transformation of community data can somewhat correct for non-normality, but use of a non-parametric test avoids this necessity and is more robust.

In comparison, most of the alternative multivariate methods tested above either do not provide the capability of determining correlation range (distance decay), or show inconsistencies in calculated correlation ranges or shape with different parameters or datasets (dissimogram, variogram of complementarity), perhaps due to effects of non-normality or model sensitivity. The use of presence/absence data versus abundance data showed particular influence on ranges calculated by these methods, but did not

substantially change the results of the ANOSIM-GS analysis. Additionally, the ANOSIM-GS correlation plots, while very similar to the widely-accepted Mantel correlograms, appeared to reduce variation in the shorter lag classes potentially caused by non-linearity and provided a definitive correlation range. Using rank-transformed similarity matrices in Mantel correlograms will circumvent issues of non-linearity, however, modeling of correlation range in Mantel correlograms is typically not done. Furthermore, the ANOSIM-GS method is suited especially well to large microbial datasets (both in terms of sample numbers and numbers of community populations), whereas the variogram of complementarity proved to be very cumbersome for more than 30 or so populations.

However, the ANOSIM-GS method is limited to visualization of spatial structure (in terms of geographic or temporal distance) of communities. While this method can suggest relationships with environmental parameters, it cannot directly calculate whether communities are correlated with particular environmental parameters, as is possible with a partial Mantel test. I also cannot use the spatial structure that is elucidated from ANOSIM-GS plots to create interpolated maps or other geostatistical applications, as is possible with variograms created with principle components or Wagner's variogram matrix methods (of which the variogram of complementarity is a component). The variogram matrix method can also construct cross-correlograms of individual populations and variograms of population richness. However, the tradeoff is that these analyses are unwieldy for complex microbial communities.

Assuming that ecological heterogeneity is, as Legendre (1993) suggests, functional, ANOSIM-GS analysis can help to reveal ecosystem structure and its underlying sources. Based on their shape and correlation distances, ANOSIM-GS plots can suggest the influence

of environmental gradients and patterns (ecological niche) or limits in dispersion between appropriate habitats. Focusing spatial analysis in different directions or on different subsets of data can enhance the visualization of these influences. In the case of the example biofilter dataset, ANOSIM-GS plots were consistent with the hydraulic characteristics of the biofilter, which exhibits essentially one-dimensional flow in the longitudinal direction but has differing regimes of inundation at different depths. The flowpath structure could suggest that changes in dissolved oxygen or other nutrients are important influences on the biofilter's bacterial community. The differences between depths may also be related to the flow regime. The 1.52 m depth is continually inundated, while the 0.76 m depth is subject to irregular inundation. Inundation could influence the community structure through decreased oxygen and through increased dispersion of bacterial communities.

Spatial analysis through the ANOSIM-GS method also offers the more immediately practical result of guiding sampling design. Because ecological heterogeneity is the rule rather than the exception in natural systems, it is important to assess the scope of this variation before conducting experiments involving ecological communities. Correlation distance can assist the researcher to choose a sampling scheme that is reasonably comprehensive but not superfluous. In the case of the example dataset, I determined that approximately 6.1 m was the most conservative estimate of the correlation distance. The resultant sampling for the time-series dataset uses different sampling distances for each depth design (in the flow direction every 6.1 m at 0.76 m, and at least two samples across a biofilter at the 1.52 m depth) as informed by the corresponding ANOSIM-GS plots.

4.4 Analyses of the Spatial Dataset

A major step in the description and understanding of microbial communities in biofilter systems was to assess their spatial variability. As previously discussed, a characterization of spatial variation and structure in ecosystems is useful both to design further sampling schemes but also to elucidate potential relationships and functional properties of the system. In this section, I discuss the results of several analyses showing spatial variability and relationships within samples taken from the FP03 biofilter site in March, 2007.

4.4.1 Location mapping and ecological metrics

Figure 17 shows maps of ecological metrics calculated from ARISA and *nosZ* t-RFLP profiles. The maps show both the number of observed bacterial and denitrifying populations (recovered population richness) and their evenness at each sample location, with a separate map for each depth. 504 distinct bacterial populations (ARISA fragments) were recovered from the biofilter. The number of ARISA fragments in a sample ranged from 7 to 157, with a median value of 54. Observed population evenness across the biofilter varied from 0.46 to 0.97, with a median value of 0.91. Both variables appeared to exhibit patterns of variation through the biofilter. Paired t-tests of samples at the same location but different depths showed that evenness ($p=0.0165$) was significantly higher at the 1.52 m depth than at the 0.76 m depth. No significant difference was found between the bacterial richness observed at the two depths. Using ANOVA, the effect of distance from the biofilter inlet (transect) and position within a transect was tested. Bacterial richness was observed to vary significantly by transect ($p=0.009$) but not by position within the

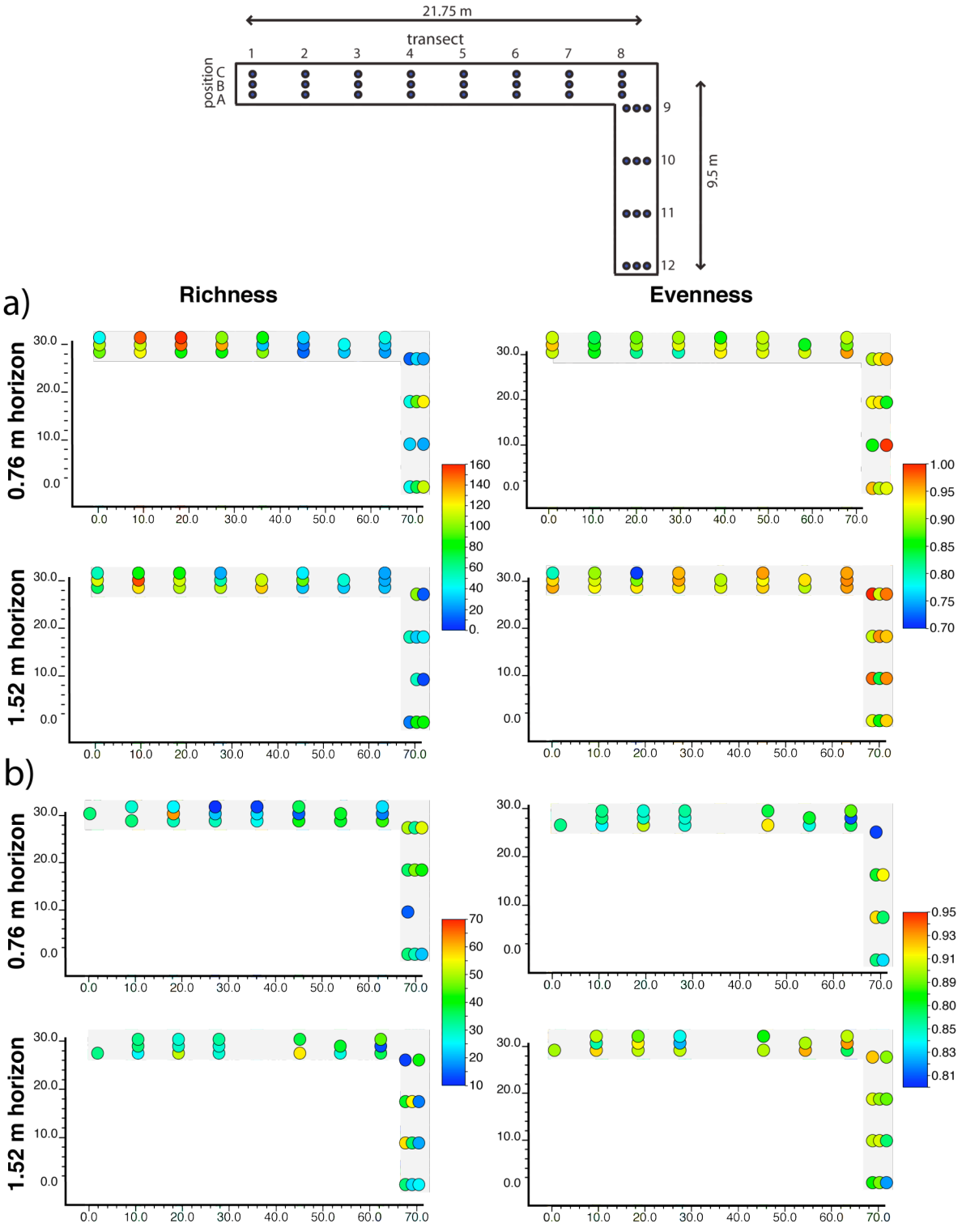

Figure 17. Aerial map of FP03 biofilter sampling scheme and ecological metrics at sample locations: a) recovered bacterial (ARISA) richness and evenness at the 0.76 m and 1.52 m depth; b) richness and evenness of recovered *nosZ* t-RFs at the 0.76 m and 1.52 m depth. Points represent richness or evenness at one sample location. Flow through the biofilter proceeds from upper left to bottom right.

transect (p=0.213).

Nesting the effects of transect within depth improved the model (p=0.008). Sample population evenness was not significantly affected by transect (p=0.412) or position (p=0.770). These results were consistent with examination of the raw ARISA profiles, in which peaks around 440bp increased with transect number, while peaks around the 750-800 bp range decreased with transect number. Profiles were also notably less diverse at transects farther from the inlet.

The number of observed *nosZ* t-RFs summed across all three digests was 110, with the number in each sample ranging from 10 to 64 (median of 33). Because individual species may produce a specific fragment for each digest, the total observed *nosZ* t-RFs does not translate directly to overall denitrifying species richness; it can be estimated that the number of denitrifying populations is approximately one-third of this, or a median of 11. The evenness of *nosZ* communities had a mean of 0.89, varying between 0.80 and 0.94. Although evenness appeared to be higher for *nosZ* populations than for the overall bacterial populations, t-tests indicated that there was no significant difference between the evenness for these two types of populations (p=0.191). In contrast to the overall bacterial populations, however, observed *nosZ* t-RF richness and evenness were fairly consistent across the biofilter. Paired t-tests confirmed that there is not a significant difference between *nosZ* t-RF richness (p=0.173) observed at the two depths. However, population evenness is slightly but significantly higher at the 1.52 m depth than at the 0.76 m depth (p=0.031). ANOVA showed that there are no significant differences in richness or evenness at different transects or positions. However, it is important to note that because the

resolution of *nosZ* t-RFLP is relatively coarse to that of ARISA, the technique may be less capable of resolving existing patterns than ARISA.

4.4.2 Community similarity analyses

To visualize patterns of whole bacterial and denitrifying community differences across the biofilter and test the significance of these differences, I used two approaches: non-metric multidimensional scaling (MDS) plots followed by the ANOSIM statistical test (to determine if different groupings of samples showed different community compositions), and ANOSIM-GS (to determine the spatial structure of the biofilter microbial community). Figure 18 shows MDS plots for the whole bacterial community and the denitrifying (*nosZ*) community, coded by sample transect, depth, and position within the transect, and Table 4 shows the results of ANOSIM tests between different groups of samples.

Bacterial (ARISA) community

Because sample size has been shown to affect consistency in recovered microbial populations in soil (Kang and Mills, 2006), I firstly tested the effect on bacterial community composition of taking a subsample (~125 ml) from a larger, homogenized sample of approximately (~700 ml) at several sample sites. Compositing from a larger volume did not significantly change the observed community (ANOSIM R=-0.5, p=1.000). Using only the non-composited samples, MDS plots reveal differences in bacterial community by transect (the flow direction) and depth, but not by position along the transect (the cross-flow direction) (Figure 18). The MDS plot of ARISA results coded by transect (Figure 18a)

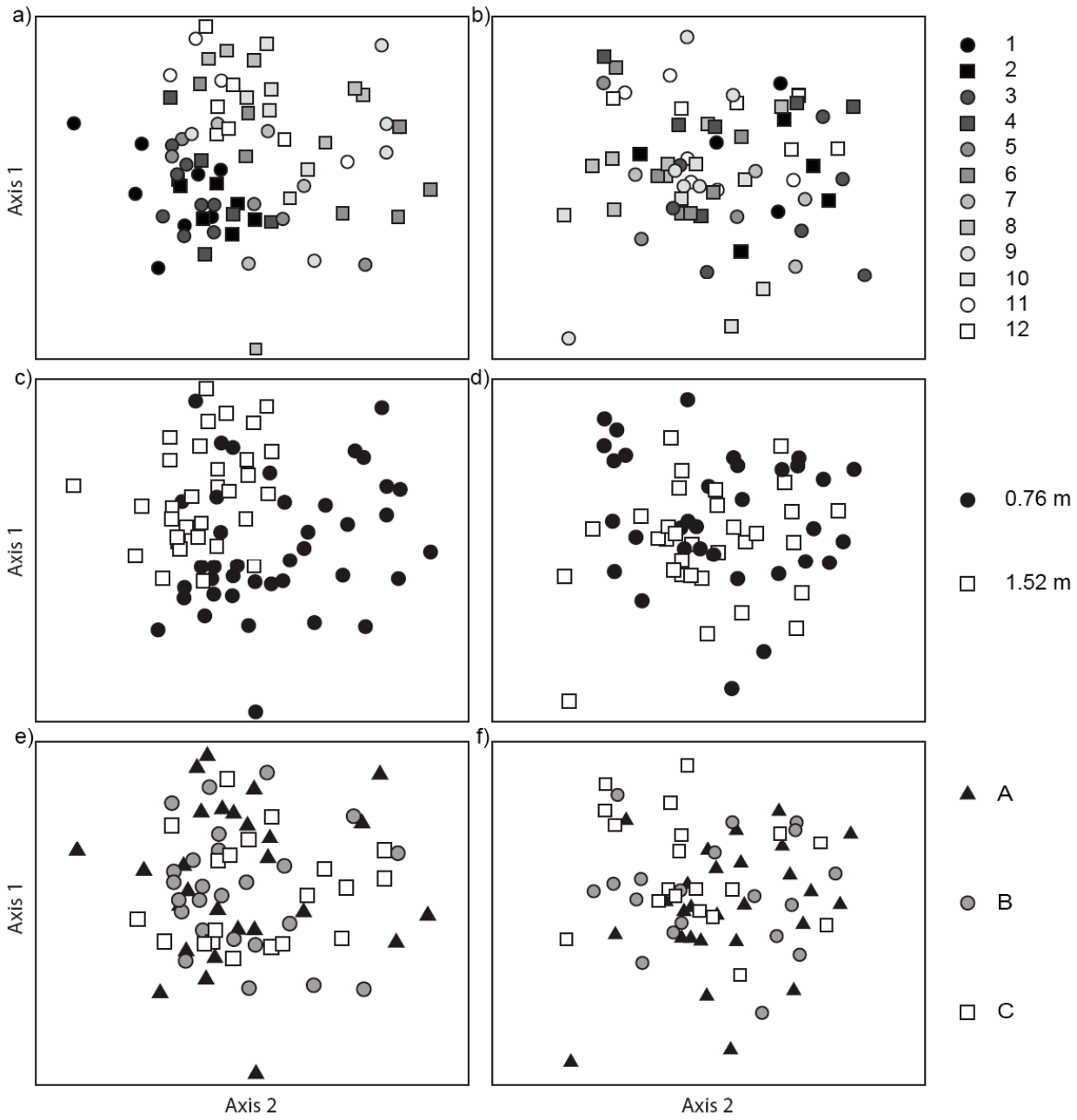

Figure 18. Non-metric multidimensional scaling plots of whole bacterial and denitrifying communities: bacterial (ARISA) communities with samples coded by transect (a), depth (c), or position along a transect (e); denitrifying (*nosZ* t-RFLP) communities with samples coded by transect (b), depth (d), or position along a transect (f). Distance between plotted samples represents community difference between samples. Axes represent a theoretical ordination space.

Table 4. Summary of ANOSIM tests between community sample groups.

Groups compared	Controlling for difference in ("crossed" model)	R	Significance (p-value)
Bacterial (ARISA) community:			
Depth	Transect	0.273	0.030*
All Transects	Depth	0.458	0.001**
All Transects	Cross-flow position	0.578	0.001**
All Positions	Transect	0.421	0.001**
Position A, Position B	--	0.288	0.028*
Position A, Position C	--	0.650	0.001**
Position B, Position C	--	0.483	0.050*
Denitrifying (*nosZ* t-RFLP) community:			
Depth	--	0.042	0.034*
All Transects	Cross-flow position	0.175	0.021*
Transect 2, Transect 8	Cross-flow position	0.719	0.022*
Transect 2, Transect 11	Cross-flow position	0.651	0.022*
Transect 6, Transect 12	Cross-flow position	0.802	0.022*
Transect 8, Transect 12	Cross-flow position	0.603	0.033*
Transect 7, Transect 8	Cross-flow position	0.673	0.033*
All Positions	Transect	0.302	0.011*
Position A, Position B	Transect	0.300	0.035*
Position A, Position C	Transect	0.239	0.033*
Position B, Position C	Transect	0.279	0.077

Cross-flow position and transect are as shown in Figure 3.
* denotes significance at the 0.05 level; ** denotes significance at the 0.001 level

shows that samples from the same transect tend to cluster in the same vicinity, suggesting that bacterial community composition is similar within each transect, and changes with transect. However, these transect clusters overlap those of other transects, and community similarity within a transect appears to decrease with increasing transect number. Additionally, clusters of samples from adjacent transects are mostly positioned closer together than those from transects located farther apart; there is a general sample position trend from the lower left-hand corner to the upper right-hand corner of the plot with increasing transect number. In ANOSIM tests controlling for position or depth differences (crossed analysis), samples from different transects were significantly different (Table 4). Pairwise ANOSIM comparisons showed 16 transect pairs that were statistically different, mostly between pairs that were separated by four or more transects.

There is also a clear pattern in the MDS plot for the whole bacterial community coded by depth (Figure 18c). In ANOSIM tests controlling for transect differences (crossed analyses), samples at the two different depths were significantly different (Table 4).

However, the MDS plot coded by position along a transect (cross-flow direction) showed no discernable pattern (Figure 18e). Despite this, controlling for differences in transect (crossed analysis) revealed that positions along a transect were weakly, but significantly, different (Table 4). Pairwise comparisons for different positions within a transect showed that all three were significantly different from each other, but that the strongest differences were between position A and position C. These differences are not apparent in the MDS plots because variation in the cross-flow direction (position) is obscured by variation in the direction of flow (transect).

Denitrifying (nosZ t-RFLP) community

In contrast, MDS plots constructed from denitrifying communities (*nosZ* t-RFLP) show no observable patterns by transect, depth, or position within a transect. ANOSIM tests, however, indicate several differences between specific sample groups (Table 4). These tests show that there is no difference between samples collected at different depths (R is very low, even though p value is significant). However, using a crossed model to control for differences by transect and position, there were moderate, but significant, overall community differences between transects and also between positions within a transect (Table 4). Within this test, pairwise analyses showed that position A was significantly different from B and C, but that B and C are not significantly different. Pairwise tests between transects showed several substantial and significant differences, mostly involving samples from transects 2, 8, and 12.

4.4.3 ANOSIM-GS analysis of the spatial dataset

To further evaluate the presence and characteristics of community geographical variation spatial structure within the biofilter, I used the ANOSIM-GS method as described in Section 4.3. Figure 14 shows ANOSIM-GS plots for the whole bacterial (ARISA) community. Because the ANOSIM tests showed that spatial community variation occurred by depth, plots were created both using data from both depths (Figure 14a,d) and also separately for data from each depth (Figure 14c,f).

Figure 14a shows R-plots using all data. In the first case, sample pairs in all directions were used (an "omnidirectional" plot). Because MDS and ANOSIM analysis showed that significant community differences by transect, in the second case the analysis was restricted to only sample pairs parallel to the direction of flow through the biofilter (an anisotropic plot in the direction of flow). Because only pairs of samples of the same position are parallel to the direction of flow, the analysis parameters also restricted sample pairs to those of the same position along a transect (A, B, or C). The plots in Figure 14a show that community similarity between sample pairs decreases with increasing separation distance; the R statistic is positive and significant for the first three points. Differences in the shapes of the omnidirectional and flow direction plots show that there is anisotropy in the spatial structure; in the omnidirectional plot the R statistic is smaller for the same separation distance. Differences in the modeled Gaussian shape between the two ANOSIM P-value plots (Figure 14d) show anisotropy in the community spatial structure of the biofilter; p-values in the flow-direction model increased at a larger separation distance than in the omnidirectional model. For the omnidirectional ANOSIM-GS analysis, the

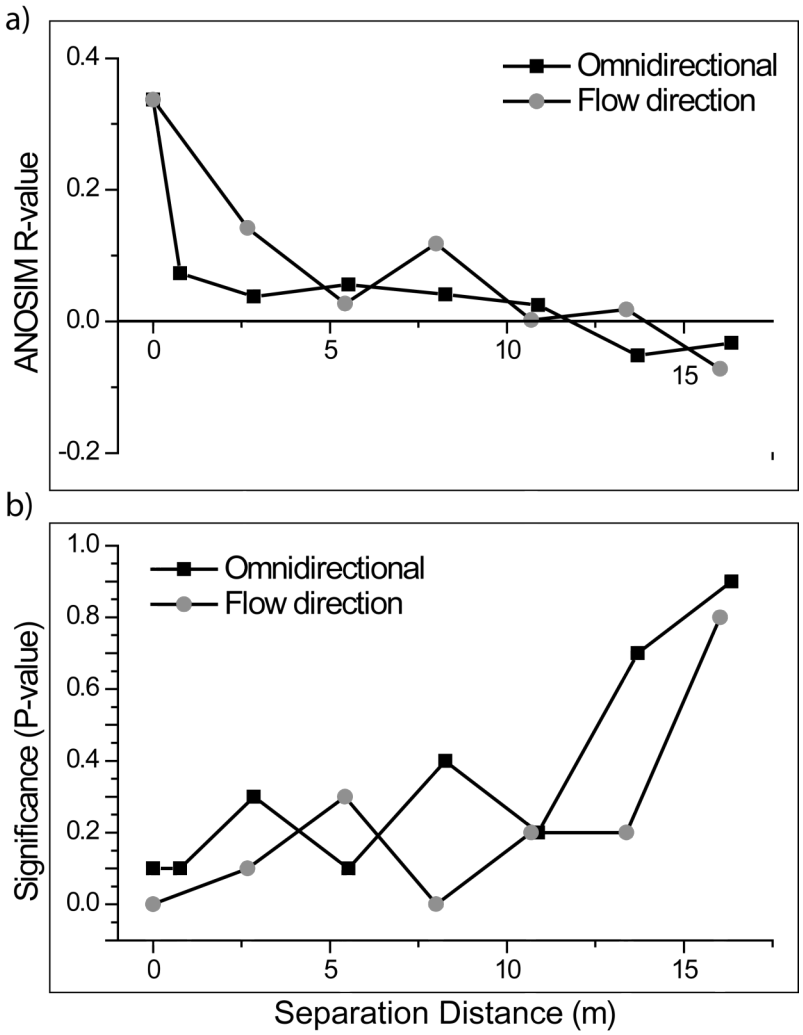

Figure 19. ANOSIM-GS plots of denitrifying (*nosZ* t-RFLP) communities from the spatial dataset: a) R plot; b)significance plot (P-value). Although the R value decreases over increasing separation distance, only two of these (0 and ~8 m) in the flow-direction plot were significant (showed a corresponding P-value less than 0.05), and none in the omnidirectional plot.

correlation range was determined to be 5.8 m. For anisotropic plots (limited to pairs in the flow direction), a larger correlation range of 8.5 m ft was calculated.

ANOSIM-GS R-plots for data separated by depth, restricted to pairs in the flow direction, show that bacterial communities from sample pairs at the 1.52 m depth are more similar (have larger ANOSIM R statistics) than those from pairs at the 0.76 m depth for the same separation distance, as shown by a different shape in the R-plots (Figure 14f), and different model shape and fit in the significance plots (Figure 14f). At the 0.76 m depth, the

calculated correlation distance is 5.8 m. At the 1.52 m depth, the calculated correlation distance is 10.3 m, indicating that bacterial communities remain statistically similar at a much greater separation distance at the 1.52 m depth. Omnidirectional plots separated by depth were also created but were not substantially different to the flow direction plots, and resulted in poorer model fits, so are not shown.

ANOSIM-GS analysis of the *nosZ* data revealed no overall pattern of spatial structure. Plots showed an overall decrease in R statistics but only two points that were significant (Figure 19). The significance plots could therefore not be accurately modeled. These results suggest that while slight variation may occur, there are no significant general trends or correlations with distance for denitrifying communities, or that *nosZ* t-RFLP operates at too coarse a scale to capture them.

Based on these results, I selected a sampling distance for the 0.76 m depth of 6.1 m between samples and 10.7 m at the 1.52 m depth. These optima were the basis of our time-series sampling scheme.

4.4.4 Spatial variation in context

This is the first research to my knowledge to evaluate the spatial variation of microbial communities in woodchip biofilters receiving aqueous wastes. Franklin and Mills (2003) argue that, because microbial community spatial structure is so common within field systems, sampling approaches and experimental designs should consider its effects, particularly for certain types of ecological questions. The bacterial community in the denitrifying biofilter exhibited substantial spatial patterning that should be taken into account for future sampling schemes. Patterns of spatial variation also revealed important characteristics of the biofilter microbial community.

Perhaps most importantly, I found that the denitrifying community showed a different spatial structure than the bacterial community as a whole. At the timepoint at which the spatial dataset was taken (March 2007), the community of denitrifiers appears to be fairly consistent across the entire biofilter or is at a scale finer than can be resolved by *nosZ* t-RFLP (Figure 17, Figure 18b, d, f), whereas the overall bacterial community shows clear and significant spatial variation (Figure 17, Figure 18a, c, e). I suggest that the lesser spatial patterning of the denitrifying communities in the biofilter is due to the differing environmental requirements between denitrifiers and other organisms; denitrifiers are mostly facultative anaerobes (Zumft, 1997), and therefore may be resilient in the system. This finding is also supported by research on denitrifiers in soil habitats in which denitrifying communities varied between habitats, but not within habitats (Rich et al., 2003; Rich and Myrold, 2004). The consistency of denitrifiers in the spatial dataset suggests that the biofilter has a fairly consistent habitat for denitrifiers during the spring season when samples for this study were taken. However, in my subsequent time-series analysis, the gradient of (change in) nitrate over the length of the biofilter varied between sites and over time (max: 8.66 mg/l, FP03 17 Mar 2009; min: -1.70 mg/l, DE01 17 Mar 2009, mean: 1.25 mg/l). Under different nitrate gradients, more spatial variation in denitrifiers may occur. Because I did not measure nitrate for the spatial dataset, I cannot assess the extent to which this might occur.

The few areas showing significant denitrifying community variation were located in regions that had different conditions than the rest of the biofilter. The FP07 biofilter site is unlined and L-shaped, and its edges are not perfectly straight. The community on the edges of the biofilter may therefore be exposed to different environmental factors than on the

interior of the biofilter. Position A (found to have a slightly, but significantly different denitrifying population than positions B and C) may experience greater mixing with the nearby soil or may experience disturbances in the flow as it turns 90 degrees. This could also explain the few pairs of transects that were found to have significantly different denitrifying populations when controlling for position. These pairs mostly contained transects between the inlet or outlet of the biofilter or between the ends and the region around the 90° turn (transects 6, 7, 8 and 9).

Examining the spatial patterns in the whole bacterial community, significant differences were observed in the direction of flow (by transect) and by depth. These results suggest that hydraulic regime was influential to community structure at this particular time point.

Water flows through the biofilter when the water table in the fields draining to it exceeds the height of the outlet drainage structure. However, the outlet pipe of the biofilter is above its floor; therefore, even when water is not flowing through the biofilter, the biofilter is always partially inundated. Significant differences in microbial community at the two different sample depths may be due to continuous inundation at the 1.52 m horizon and periodic inundation at the 0.76 m horizon. Continuous inundation likely results in lower overall available oxygen than periodic inundation (in which majority of time is spent in direct contact with air). Therefore, conditions at the deeper horizon may select against strict aerobes, resulting in a different community composition. Furthermore, variety in level and period of inundation at the shallower depths of the biofilter may account for the lower population evenness at the 0.76 m depth. These conditions may increase the variety and variability in size of ecological niches, encouraging a less even

community. This hypothesis is also consistent with the results of the ANOSIM-GS analysis, which showed that the range of correlation (range over which communities were not statistically different) was larger at the 1.52 m depth.

However, differences in community by depth may also be caused by other environmental factors that may vary by depth such as temperature. To test whether community differences by depth are due to inundation regime, we could sample from two different depths that are inundated and two that are unindated and compare the communities.

Both differences in community composition and a decrease in population richness were observed in the direction of biofilter flow (increasing transect, Figure 17, ANOVA $p = 0.009$). The decreasing bacterial population richness along the flowpath of the biofilter at both depths suggests that fewer bacterial species can survive farther into the biofilter. MDS plots showed that community composition appeared to change smoothly over the length of the biofilter, with a progression from bottom left-hand to upper right hand with increasing transect number. This suggests a relatively smooth transition of habitats along the flowpath. Furthermore, there clear anisotropy of the ANOSIM-GS plots in the flowpath direction.

One explanation for these community changes may be the influence of flow through the biofilter and the gradients possibly created by it. In particular, oxygen and nitrate gradients may cause substantial differences in habitat. Data from the time-series study (November 2008-May 2010) show that DO and nitrate gradients along the flowpath of the biofilter are typical (Figure 20-Figure 22). For DO an average decrease over the biofilter of 0.579 mg/l was observed (max = 3.79 mg/l), and for nitrate an average decrease of 1.26

mg/l (max 8.66 mg/l) was measured. The substantial and significant differences in bacterial community by transect also are consistent with changes in habitat along the flowpath that could reflect gradients. DO or nitrate gradients could explain the smooth changes in bacterial community composition noted in the MDS plots and the anisotropy seen in the ANOSIM-GS plots. Decreases in DO could also explain the decreasing population richness in the direction of flow; populations that are strict aerobes would not be able to survive farther into the biofilter. That the denitrifying community did not show spatial differences in the direction of flow also supports this conclusion; denitrifiers are frequently facultative anaerobes (Zumft, 1997).

Data also suggests that the shape of the biofilter may contribute to differences in the bacterial community. As with the denitrifying populations, when controlling for transect, there were significant differences by position along a transect. This may, again, be caused by influences from the surrounding soil on the biofilter edges or by slight differences in flow characteristics at different points across the width of the biofilter, particularly when navigating the 90 degree turn. At both depths, richness appears to be lowest nearest the turn. Slight differences by position are also seen in the larger correlation distance for ANOSIM-GS plots in the direction of flow (which also restricts the pairs to those of the same position); sample communities appear to be similar for a longer distance when at the same position.

In comparison to microbial communities studied in other, similar systems, I note several similarities and differences. Firstly, the richnesses of the bacterial and denitrifying communities in the biofilter appear to be comparable to reported values. I found a total of 504 unique bacterial (ARISA) populations in the biofilter. Using 16S t-RFLP, several groups

have reported high bacterial diversity in bioremediation or denitrifying systems, including waste gas biofilters (335 unique t-RFs) (Friedrich et al., 2002), in situ bioremediation systems for PCB-contaminated soil (over 50 unique t-RFs) (Fedi et al., 2005), activated sludge (119 unique t-RFs) (Hoshino et al., 2005), and denitrifying wastewater reactors (69 unique t-RFs) (McGuinness et al., 2006).

The median values of ARISA fragments and *nosZ* t-RFs were 54 and 33 (11 for each digest), respectively; because I used three digests for the *nosZ* t-RFLP analysis, for the purposes of comparison to other methods, the total t-RF number is divided by three. The denitrifying populations in similar systems have been shown to have diversity of the same order as my results using *nosZ* t-RFLP or other methods. Two studies of denitrifying sand filters using fatty acid analysis found to have 56 and 132 isolates with denitrifying capability, respectively (Mergaert et al., 2001; Neef et al., 1996). Groups studying denitrifying wastewater reactors for life support systems reported between 50 and 70 distinct *nosZ* t-RFs from single digests (McGuinness et al., 2006; Sakano et al., 2002). Finally, in an analysis of agricultural and riparian soil and creek sediment, 74 different *nosZ* t-RFs were found with a mean of 21 per sample (Rich and Myrold, 2004). The greatest richness and diversity of *nosZ* t-RFs was found in the agricultural soils.

I suggest that the overall bacterial diversity in the biofilters is somewhat greater than most of these reported values because of differences in our methodology. ARISA is more sensitive to taxonomic differences than 16S t-RFLP (thus resulting in greater numbers of fragments). In contrast, the number of recovered *nosZ* t-RFs per digest for our system seems to be on the low side when compared to most of the previous studies (Mergaert et al., 2001; Neef et al., 1996; McGuinness et al., 2006; Sakano et al. ,2002).

However, comparison to results that derive from similar methodology (three digests, Rich et al., 2003; Rich and Myrold, 2004) suggests that the number of observed *nosZ* t-RFs per digest in this study may be comparable.

The anisotropic spatial structure found in the biofilter is also consistent with findings in similar systems. Aqueous denitrifying or other similar reactors that incorporated strong directionality of flow, like that in the biofilters, were commonly found to have community differences along the flowpath (Mergaert et al., 2001; Fedi et al., 2005; Sakano et al., 2002; McLamore et al., 2008; Hwang et al., 2009). However, using fluorescence in situ hybridization, Friedrich et al. (2003) found no substantial community gradient in waste gas biofilters, which typically have a shorter residence time and smaller overall size than aqueous biofilters. Anisotropy is also typical in field systems. Franklin and Mills (2003) found substantial differences in the spatial structure of soil communities by direction. However, the results of their analysis suggest that correlation distances for bacterial communities in cultivated soil are less that what I found for the biofilter system. In their study, correlation distances in a Virginia agricultural field were calculated to be between 2.0 and 6.3 m (Franklin and Mills, 2003), whereas correlation distances for the biofilter were approximately triple this upper value. Furthermore, I found that larger, homogenized sample sizes did not impact recovered community, in contrast with Kang and Mills (2006). This suggests larger scales of community variation in the biofilter than in soil, which may be due to media and substrates that are more homogenous than in soil systems.

In conclusion, spatial analysis of the biofilter microbial communities revealed patterns that are both useful for devising future sampling and for providing insight into the functioning of the biofilter. For the spring timepoint in which the biofilter was sampled,

denitrifying bacteria exhibited less variation across the biofilter than did the whole bacterial population. The whole bacterial population displayed substantial spatial patterning, with significant differences by sample transect and depth (Figure 14 and Figure 18). More subtle differences by position were noted when controlling for transect. From this analysis I am also able to suggest an optimal sampling scheme for bacterial populations in a denitrifying biofilter, with sampling frequencies of every 6.1 m at a 0.76 m depth and every 10.7 m at the 1.52 m depth. Although these correlation ranges were calculated for only one time point and for a particular shape of biofilter, no other similar study has been conducted and our calculations are therefore the best estimate of spatial structure in denitrifying biofilter systems.

4.5 Analyses of the Time-series Dataset

To begin to understand the relationships between community, populations within the community, and environmental and operational parameters in the biofilter, I collected time series data from three biofilters (FP03, FP07, and DE01) starting in November of 2008. These biofilters represented a range of shapes, sites, and operational characteristics. Three shapes were analyzed: linear (FP03), rectangular (DE01), and square (FP07) (Figure 4). These biofilters were from two separate locations (Decatur and Deland, Illinois), and handled drainage from differently-sized fields (Table 2). Finally, a range of operational criteria was represented, as for much of the duration of the study, the retention time of biofilter site FP03 was substantially shortened when a farmer altered the control structure.

The collected data included community samples from woodchips and water in the direction of flow, at two depths, and (for the square FP07 biofilter) in the cross-flow

direction, informed by our spatial analysis. These samples were analyzed for whole bacterial and fungal community composition. Environmental conditions and operational parameters of the biofilter were also collected. Community data were collected every 7-30 days, and some environmental data more frequently than that, providing a fine resolution for which to examine dynamic properties. This section relates the results of applying a suite of analytical techniques to the data.

4.5.1 Performance and environmental factors at the biofilter sites

The time-series study was intended to assess the relationships between microbial community and biofilter performance and environmental factors. To this end, I first assessed the variation of performance and environmental factors across different locations (biofilter and position within a biofilter) and across time.

Spatial differences in environment and performanceTable 5 summarizes the performance, environment, and meteorological factors measured for each biofilter site for the day of sampling. In terms of performance (measured by mg/L of nitrate removed), site DE01 performed the best, followed by FP07, and then by FP03. The nitrate removal of FP03 was very poor because the control structure was altered for much of the study such that the retention time was substantially shortened. Occasionally, a greater amount of nitrate was found in the outlet than in the inlet; the reason for an increase in nitrate over the biofilter is not understood. Nitrate loads were highest for DE01, and least for FP07. This may be because the FP07 site drains the smallest area of the study systems and DE01 the most (Table 2), or it may be due to unknown field management practices. The FP07 site consequently also shows the lowest outlet nitrate. Flow rates in the biofilters also show significant differences. Flow measurements taken on the day of sampling

Table 5. Summary of performance and environmental factors at biofilter sites.

Variable	Value by Biofilter Site[1]					
	DE01		FP03		FP07	
	Mean(±sd)	Range	Mean(±sd)	Range	Mean(±sd)	Range
Performance:						
Instantaneous flow (L/s)	2.22(±2.7) a	0-6.52	0.158(±0.37) b	0-1.43	0.118(±0.19) ab	0-0.881
14 d rolling avg. flow (L/s)	2.37(±2.5) a	0-6.85	1.54(±4.4) b	0-18.4	0.400(±0.89) c	0-4.23
Inlet NO_3 (mg/L)	11.1(±2.4) a	8.05-15.5	7.12(±2.6) b	3.41-11.4	4.21(±1.2) c	1.60-6.07
Outlet NO_3 (mg/L)	6.06(±2.0) a	2.24-8.97	6.07(±2.4) a	0.250-10.1	0.604(±0.65) b	0.115-2.38
Nitrate removal (mg/L)	5.83(±3.1) a	1.80-12.1	0.992(±3.1) b	-2.59-11.15	3.47(±1.2) c	1.35-5.8
Biofilter Environment:						
COD (mg/L)	25.3(±26) ab	0-107.9	20.2(±28) a	0-128.1	38.6(±56) b	0-330.6
DO (mg/L)	1.2(±0.94) a	0.14-3.9	2.0(±1.42) b	0.25-5.4	0.91(±0.99) a	0.30-8.0
Moisture (%)	61.2(±8.8) a	37.0-79.0	63.2(±14) b	0-81.0	61.1(±13) ab	0-84.0
NO_3 in port (mg/L)	3.53(±3.5) a	0.25-12.9	5.25(±3.1) b	0.25-11.8	0.95(±0.87) c	0.07-4.6
pH	7.07(±0.29) a	6.54-7.96	7.07(±0.25) b	6.38-7.38	7.18(±0.34) c	6.54-8.7
Temp in port (C)	15.2(±10.2)	1.60-38.9	14.3(±9.80)	0.40-37.8	14.4(±8.11)	2.30-44.0
Climate:						
Average Growing-degree Days	7.02(±8.9)	0-30	6.95(±9.1)	0-31	7.43(±9.3)	0-31
Average Humidity (%)	73.4(±11)	53.0-81.0	72.4(±11)	49.0-98.0	72.0(±11)	49.0-98.0
Weekly Mean Temp (C)	8.49(±10.6)	-11,1-26.7	8.66(±10.4)	-11.1-27.2	9.41(±10.1)	-11.1-27.2
Weekly Precipitation (cm)	2.23(±2.2)	0-7.92	2.68(±2.7)	0-9.93	2.81(±2.7)	0-9.93

[1] Different letters represent significant differences among biofilters at the p=0.05 level by the Kruskal-Wallis multiple comparison test; where no letters are specified, no significant differences were observed.

("instantaneous" flow) were significantly higher for the DE01 site than for the FP03 site, however DE01 and FP07 could not be distinguished, possibly because of the high variance in instantaneous flow measurements at DE01. However, because high flow periods are transient and may not have occurred on the day of sampling, a 14 d rolling average of flow was also calculated, and this showed that all three biofilters received significantly different flow rates, with DE01 having the highest and FP07 the lowest. On average, the flow rate of

DE01 was approximately 60% greater than the FP03 flow rate, and almost six times higher than the flow rate of FP07. The greatest variation in 14 d average flow was at FP03, which would be expected as there was little to no flow control at this site for much of the study.

The chemical and physical environment within biofilter ports at the different sites also varied (Table 5). COD measured was significantly higher in FP07 than in DE01 or FP03. This may be due to a difference in influent characteristics or woodchip media at FP07, or it may be that the microbial community at FP07 creates these conditions. Dissolved oxygen and port nitrate were highest at FP03, and lowest at FP07. DO was also most variable at the FP03 site. These may be a function of the flow rate through biofilters; higher velocity flows or greater variation in flow may entrain more oxygen. Moisture content of the woodchips was somewhat variable, with the FP03 site having greater moisture content than the DE01 site, and the FP07 site indistinguishable from either. However, overall the average moisture content of the woodchips was fairly similar, around 60-63%. Port temperature was similar across biofilter sites.

To determine if significant differences existed between chemical and physical environments at different ports within a biofilter, for each site and parameter, Kruskal-Wallis rank sum tests (α=0.05) for difference were conducted among ports. Some isolated differences in water chemistry were observed. Between the two 1.52 m ports at the FP03 site, DO decreased significantly ($\chi^2 = 16.18$, $p < 0.05$). Likewise, between the two 1.52 m ports at the FP07 site, nitrate was higher towards the center of the biofilter ($\chi^2 = 17.19$, $p < 0.05$). More consistent differences were found for moisture content at different ports by depth (DE01: $\chi^2 = 66.57$, $p < 0.0001$; FP03: $\chi^2 = 42.31$, $p < 0.0001$; FP07: $\chi^2 = 66.57$, $p < 0.0001$). As might be expected, ports with similar inundation regimes tended to have

similar moisture contents, with ports at the 1.52 m (continuously inundated) depth having a higher moisture content (Table 5). Between ports at the same depth, no differences in moisture content were observed at the DE01 or FP07 site, but at the FP03 site, moisture content generally decreased between the inlet and outlet (Table 5). No overall spatial differences within biofilters were observed for port temperature or pH.

Meteorological variables were not significantly different across the three biofilters, as would be expected from sites that are less than 50 miles apart (Table 5).

Temporal differences in environment and performance

As was expected, temporal variation was observed in all environmental and performance factors in the time-series dataset. To assess the level of temporal variation, Kruskal-Wallis tests were performed amongst months at different biofilters for environmental and performance variables (Table 6).

Table 6. Summary of Kruskal-Wallis tests for differences in environmental factors by month.

Variable	χ^2 statistic for differences by month		
	DE01	FP03	FP07
Performance:			
Instantaneous flow (L/s)	72.3 (p<0.0001)***	107.9 (p<0.0001)***	48.3 (p<0.0001)***
14 d rolling avg. flow (L/s)	79.9 (p<0.0001)***	67.8 (p<0.0001)***	34.6 (p<0.0001)***
Inlet NO_3 (mg/L)	58.7 (p<0.0001)***	75.9 (p<0.0001)***	44.1 (p<0.0001)***
Outlet NO_3 (mg/L)	49.1 (p<0.0001)***	45.0 (p<0.0001)***	61.9 (p<0.0001)***
Nitrate removal (mg/L)	53.2 (p<0.0001)***	74.7 (p<0.0001)***	68.1 (p<0.0001)***
Biofilter Environment:			
COD (mg/L)	3.9 (p=0.9205)	19.2 (p=0.0137)*	25.3 (p=0.0049)**
DO (mg/L)	25.3 (p=0.0014)*	17.2 (p=0.0136)*	42.0 (p<0.0001)***
Moisture (%)	8.8 (p=0.6379)	40.6 (p<0.0001)***	15.7 (p=0.1515)
NO_3 in port (mg/L)	30.8 (p=0.0003)**	45.1 (p<0.0001)***	59.2 (p<0.0001)***
pH	24.8 (p=0.0032)**	17.8 (p=0.0228)*	26.6 (p=0.0030)**
Temp in port (C)	117.2 (p<0.0001)***	176.7 (p<0.0001)***	119.6 (p<0.0001)***
Climate:			
Average Growing-degree Days	127.5 (p<0.0001)***	181.4 (p<0.0001)***	128.5 (p<0.0001)***
Average Humidity (%)	91.5 (p<0.0001)***	90.1 (p<0.0001)***	68.4 (p<0.0001)***
Weekly Mean Temp (C)	131.9 (p<0.0001)***	193.6 (p<0.0001)***	136.7 (p<0.0001)***
Weekly Precipitation (cm)	104.6 (p<0.0001)***	158.6 (p<0.0001)***	109.2 (p<0.0001)***

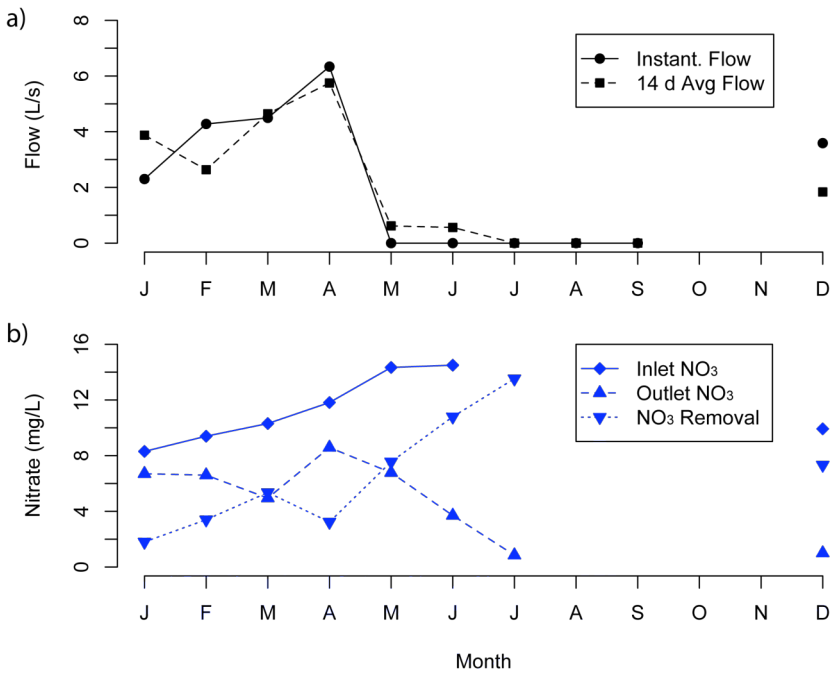

Figure 20. Monthly performance characteristics at the DE01 site between December 2007 and June 2010: a) flow variables, and b) nitrate values. Points denote average values for months where more than one year of data exists. Note different scale to reflect differences flow and nitrate between sites.

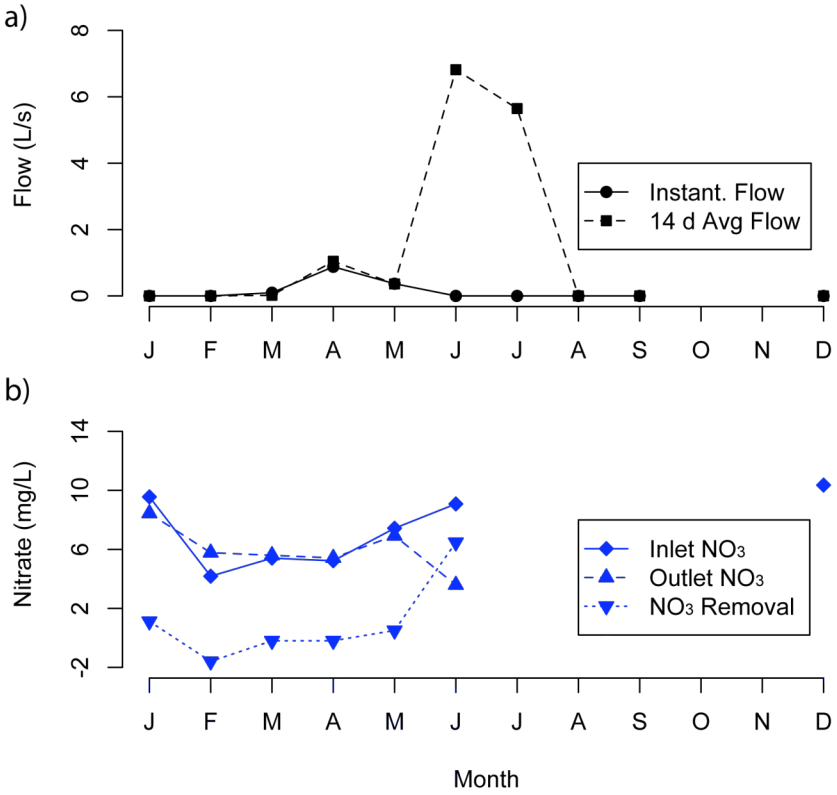

Figure 21. Monthly performance characteristics at the FP03 site between December 2008 and June 2010: a) flow variables, and b) nitrate values. Points denote average values for months where more than one year of data exists. Note different scale to reflect differences flow and nitrate between sites.

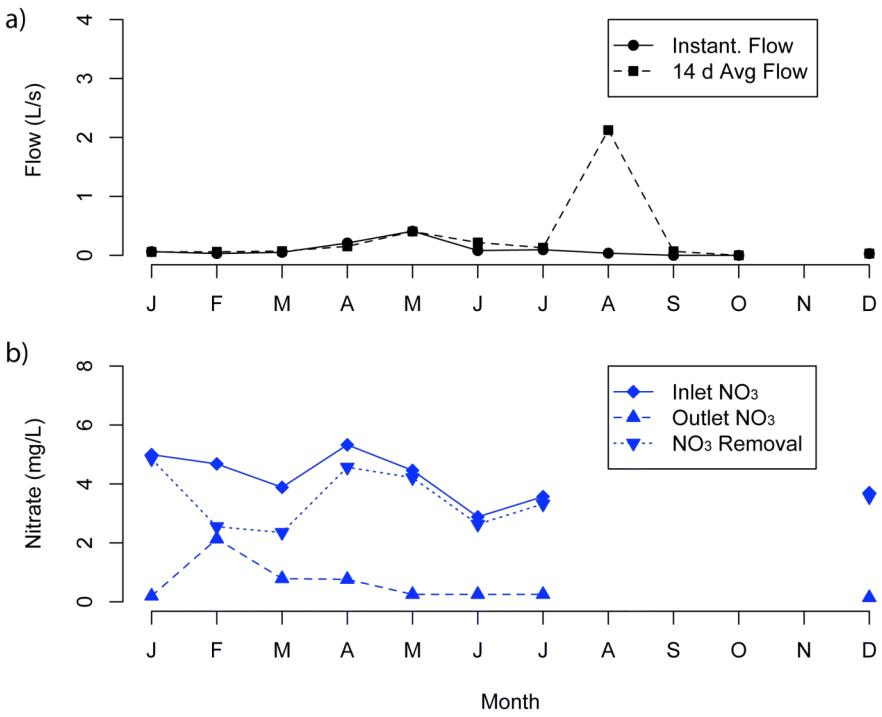

Figure 22. Monthly performance characteristics at the FP07 site between December 2008 and June 2010: a) flow variables, and b) nitrate values. Points denote average values for months where more than one year of data exists. Note different scale to reflect differences flow and nitrate between sites.

Flow and nitrate characteristics showed strong, significant month-to-month variation (Table 6, Figure 20-Figure 22). Although these data are incomplete, temporal variability is still clear. Temporal patterns in flow were different between the DE01 site, and the FP03 and FP07 sites. For the DE01 site, flow was greatest in the first four months, after which flow was minimal. For the DE01 site, the instantaneous flow (measured at the time of sample collection) and the 14 d average flow trended together. For the FP03 and FP07 sites, flow was minimal in the winter months, increasing in spring and summer. For these sites, short periods of increased flow in the summer months are shown by an increased 14 d average flow in comparison to the instantaneous flow, which stayed roughly at the same level. Inlet and outlet nitrate, and nitrate removal also showed temporal variability that differed by biofilter site (Table 6, Figure 20-Figure 22). Inlet nitrate

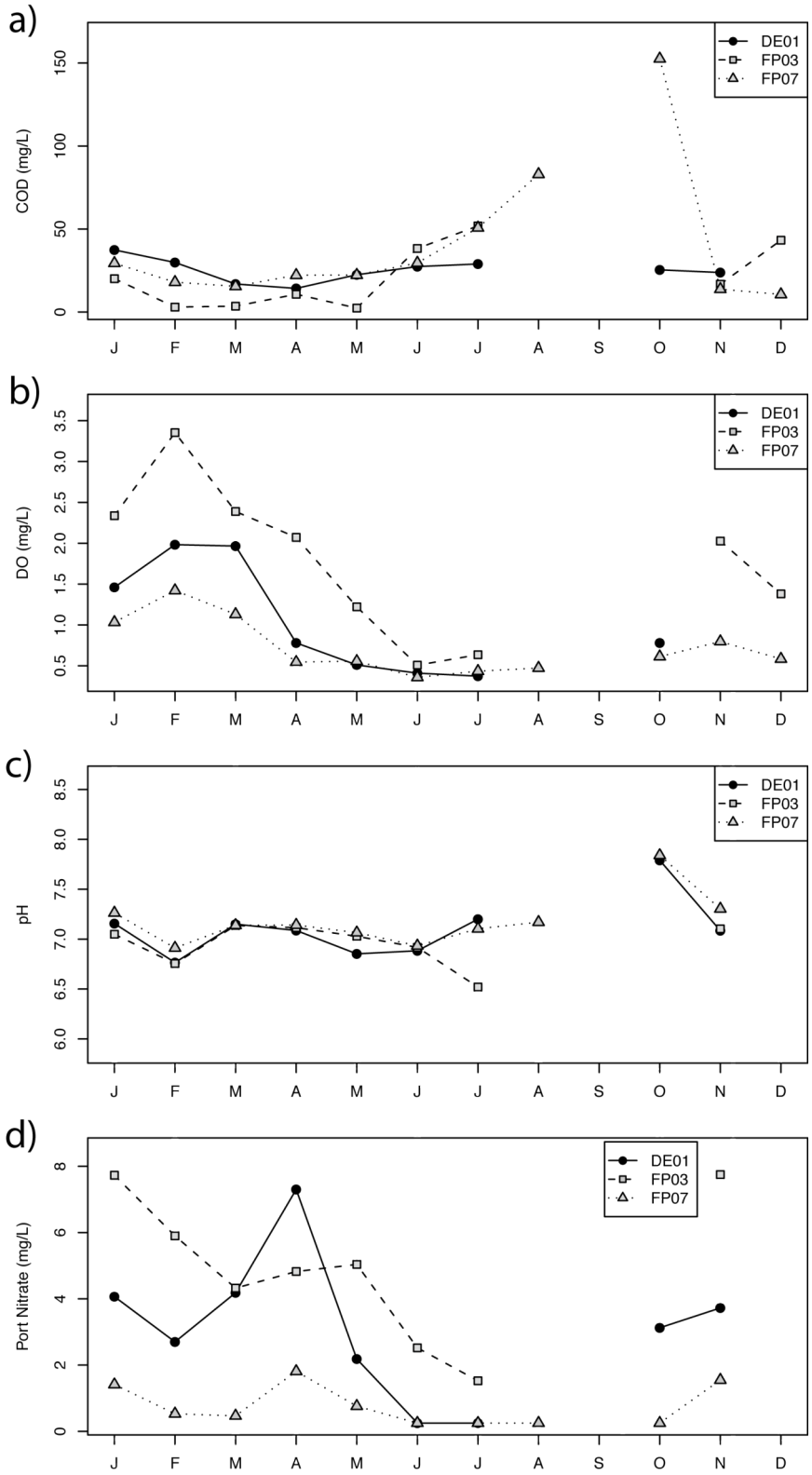

Figure 23. Average values by month for DE01, FP03, and FP07 for: a) COD, b) DO, c) pH, d) port nitrate. Values are extant only for ports that were inundated at sample collection. Points represent average values across a biofilter and across different years where recorded. Missing bars indicate months for which there were no inundated ports or where data is missing.

increased over January-June for the DE01 biofilter, whereas differences, but no clear trends were observed between inlet nitrate over time in the FP03 and FP07 biofilters. Nitrate removal generally increased during warmer periods (coincident with decreased outlet nitrate) for all three biofilter sites. However, the magnitude of this trend varied between biofilter. These variations may be due to site characteristics such as fertilizer applications or farmer behavior. The performance behavior at the FP03 site, for example, reflected the difference in operating parameters at this site for much of the study (very short residence times). The average nitrate removal at the FP03 site for the month of February was negative (higher nitrate concentrations at the outlet than the inlet). However, the average nitrate removal for June was much larger, reflecting that the appropriate hydrology was restored to the site in June of 2010.

Environmental factors within biofilter ports also showed temporal variation (Figure 23-Figure 25). Average COD values in biofilter ports showed different temporal patterns by biofilter (Figure 23). At DE01, COD variation across months was not significant, however the FP03 and FP07 sites showed generally higher COD levels for summer and autumn. At the FP07 site, this increase was smooth, however the FP03 site had inconsistent fluctuations.

Although mean DO levels were different between biofilters (Table 5), the temporal variation of DO in ports had similar trends amongst the three biofilters (Figure 23). For each site, DO was lowest in the summer months, consistent with increased biotic activity related to increased temperature. Nitrate levels inside ports also were at their lowest levels in the summer months (Figure 23), although levels increased slightly from February into March and April. This increase may be caused by increases in inlet nitrate over these

months (Figure 20-Figure 22) when temperatures may not be high enough to support increased denitrification (see Section 2.1.1). The very low port nitrate at the FP07 site is also notable, consistent with its high removal rates and low flow rates (Table 5).

Average pH in ports typically had small temporal variation, however was more elevated in October for the DE01 and FP03 site, and decreased in the FP03 biofilter in June (Figure 23). The cause of these localized variations is unknown.

The temporal patterns of temperature and moisture content within ports were different at the two different depths (Figure 24, Figure 25). Although when aggregating over all time points different ports did not have significantly different temperatures, when controlling for temporal variation, for some months temperatures at the two depths were significantly different (Figure 24). Overall, temperatures at the 1.52 m depth experienced less variation than those at the 0.76 m depth. During December and January, ports at 1.52 m were significantly warmer than those at the 0.76 m depth. Similarly, in May, June, and July, ports at the 1.52 m depth were significantly cooler than those at the 0.76 m depth.

Moisture contents at the two depths over time also showed variation (Figure 25). During each month except November, moisture content was higher at the 1.52 m depth than at the 0.76m. This was expected as ports at the 1.52 m depth were typically inundated. However, while moisture contents generally decreased in the late summer and early autumn, those ports at 0.76 m experienced more drying than those at the 1.52 m depth. A logical explanation of this variation would be that woodchips at shallower depths are more exposed to evaporation and are not as close to the water surface.

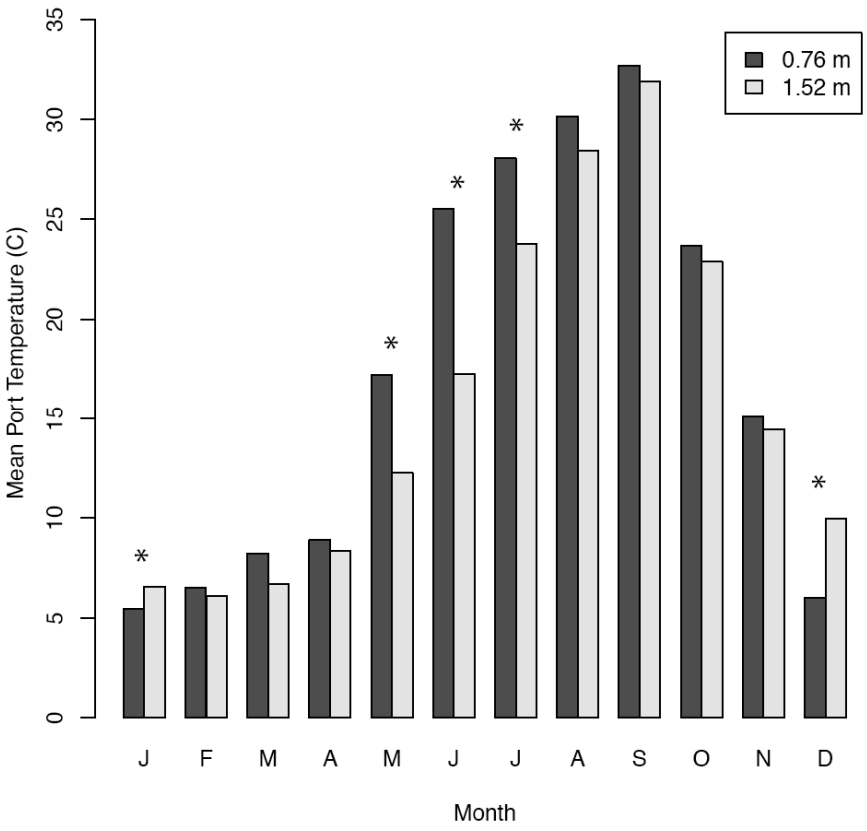

Figure 24. Variation of mean port temperature by month and depth. *denotes a significant difference between values at different depths by the Wilcoxon rank sum test.

Meteorological variables followed predictable seasonal patterns (Figure 26, Figure 27). Average growing degree days and average weekly humidity and mean weekly temperatures closely trended for each site location (De Land, IL for DE01; Decatur, IL for FP03 and FP07). Growing degree days and temperature showed a relatively smooth increase toward the summer months whereas average humidity showed more localized temporal variability. Average weekly precipitation was different for the two site locations, but both locations showed two major rainy periods—late spring and late autumn.

4.5.2 Temporal structure of community and environment

ANOSIM-GS was used to assess the degree of temporal structure in the time-series data. Bacterial and fungal community data were separated by biofilter and depth and

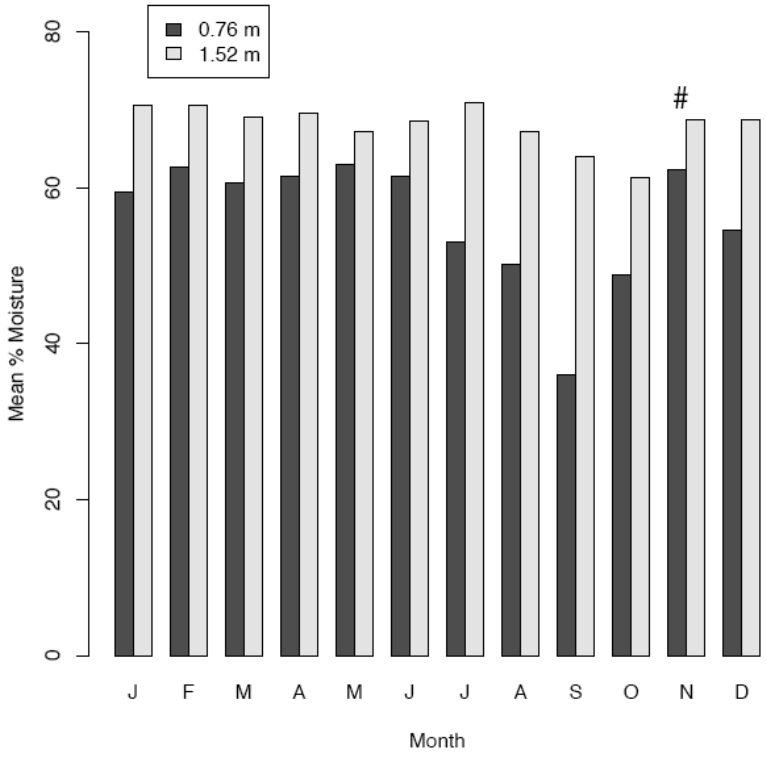

Figure 25. Variation of woodchip percent moisture by month and depth. # denotes no statistical difference using the Wilcoxon rank sum test at $\alpha = 0.05$ (November). For all other months, percent moisure at different depths are significantly different.

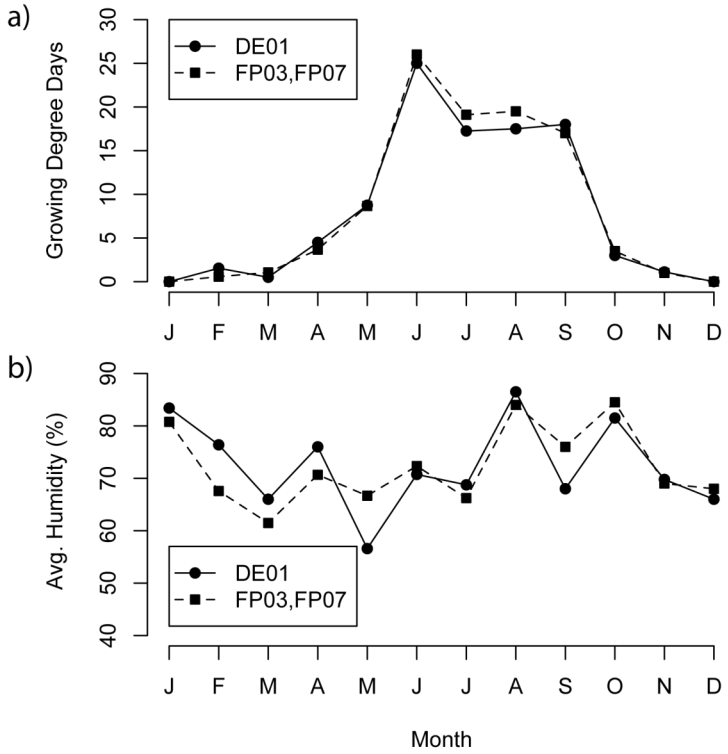

Figure 26. Variation of average growing degree days (GDD) and average humidity at biofilter sites by month.

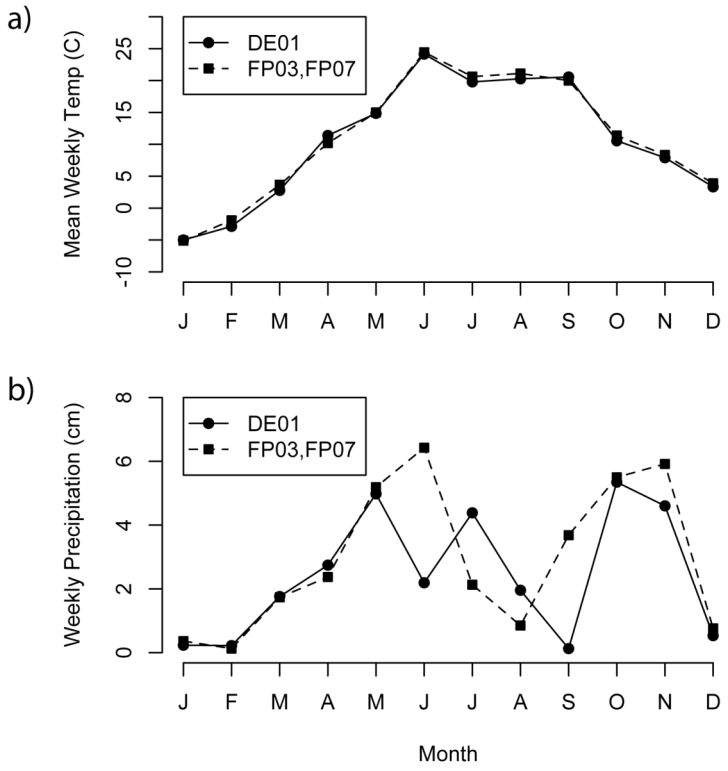

Figure 27. Variation of a) average mean weekly temperature and b) average weekly precipitation at biofilter sites by month.

analyzed with the ANOSIM-GS process. The resulting plots show the ANOSIM R metric or its significance as a function of the time separating each pair, rather than a distance separating them. The plots therefore reveal temporal patterns in the fungal and bacterial communities.

To visualize temporal variation while controlling for spatial variation within each biofilter, the analysis was restricted to pairs from the same sample location (port and biofilter) but from different sampling dates. To optimize the temporal lag size, significance plots using different lag sizes were created from bacterial community data from the DE01 biofilter (Figure 28). A lag size of 21 d was smooth but retained most structural features and was therefore chosen as the optimal lag size, used for the all following temporal plots.

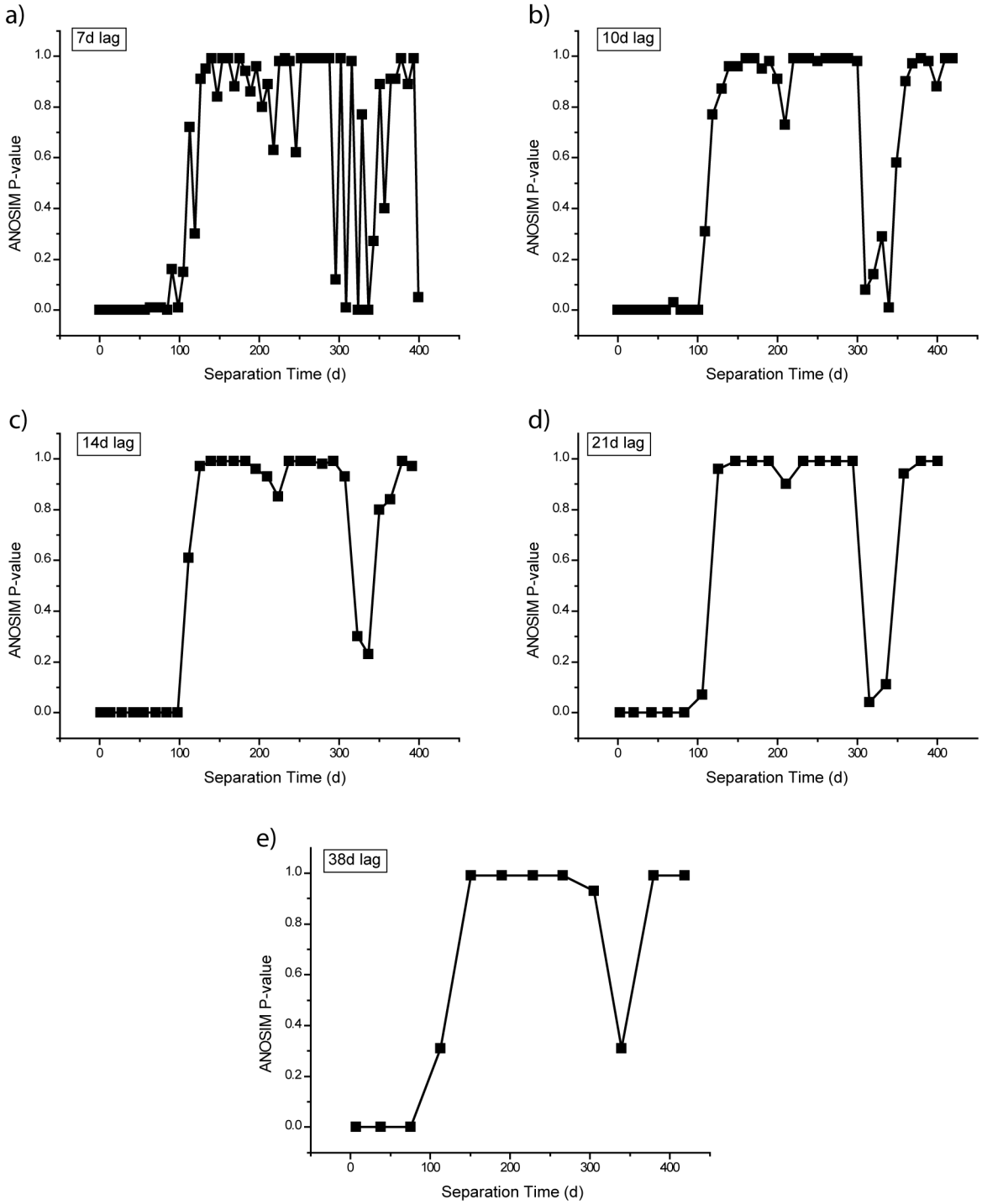

Figure 28. Optimization of temporal lag size using bacterial (ARISA) community data from the DE01 biofilter site. Lag sizes of 7 d (a), 10 d (b), 14 d (c), 21 d (d), and 38 d (e). The lag size of 21 d is the smoothest plot that retains most structural features.

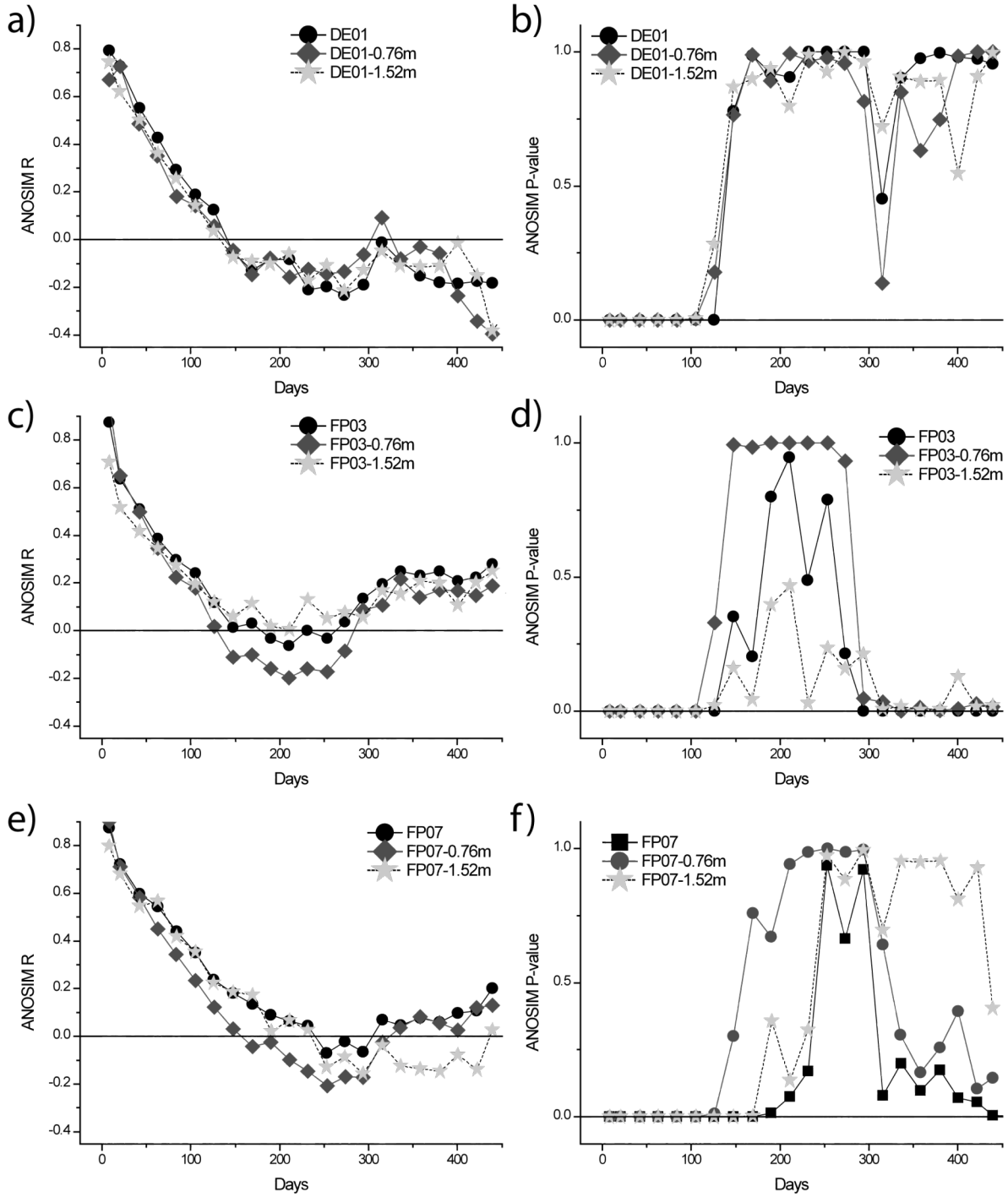

Figure 29. Temporal ANOSIM-GS plots using bacterial community (ARISA) time-series data from each biofilter site: R plots from DE01 (a), FP03 (c), and FP07 (e); and significance plots from DE01 (b), FP03 (d), and FP07 (f). Note that the horizontal axes represents time separating sample pairs in days rather than number of days into the study.

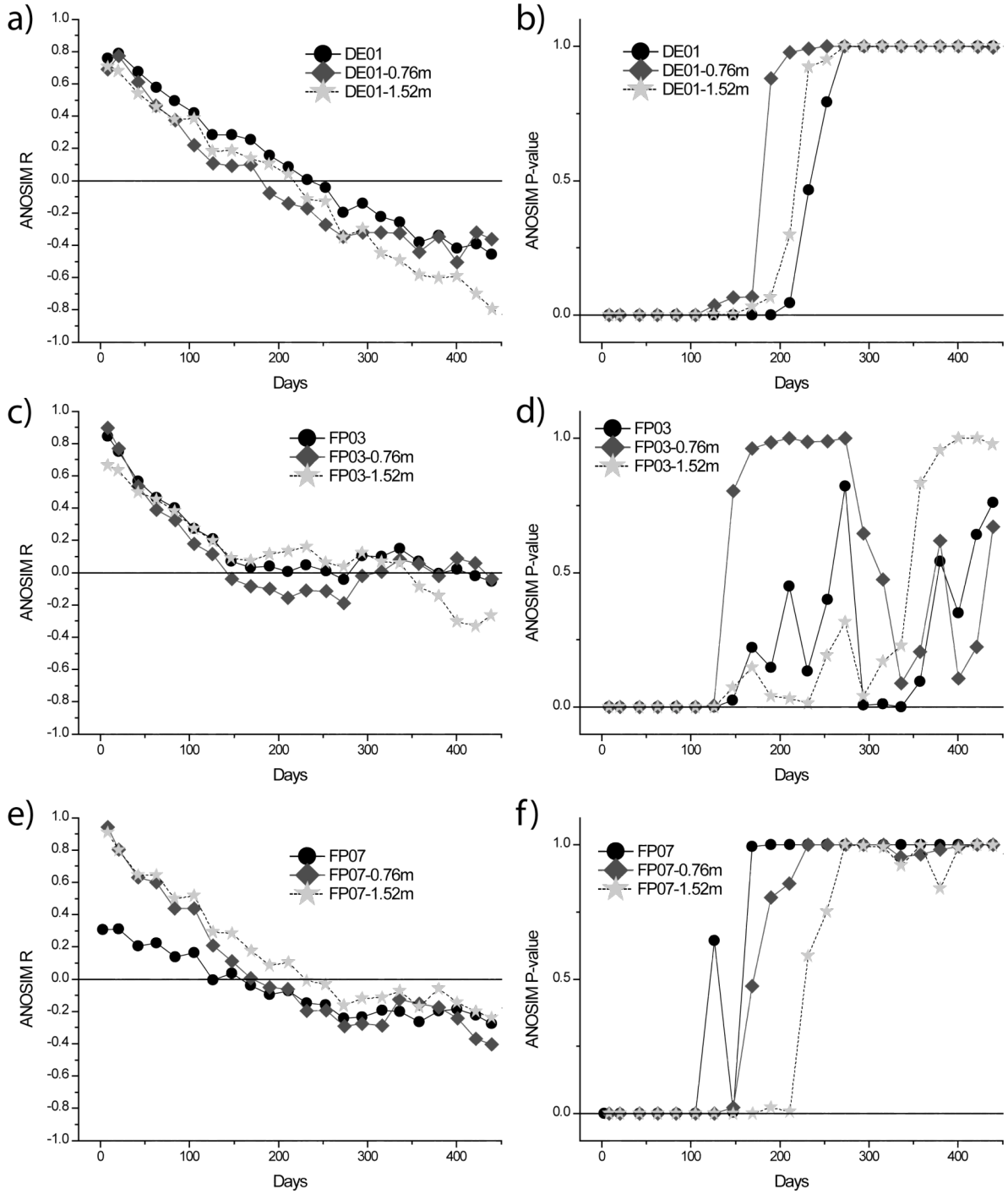

Figure 30. Temporal ANOSIM-GS plots using fungal community (fARISA) time-series data from each biofilter site: R plots from DE01 (a), FP03 (c), and FP07 (e); and significance plots from DE01 (b), FP03 (d), and FP07 (f). Note that the horizontal axes represents time separating sample pairs in days rather than number of days into the study. Fungal ARISA data courtesy of Matthew Porter.

ANOSIM plots created from bacterial community data between November of 2008 and June of 2010 show a different observed temporal community structure at different biofilter sites and by depth within each biofilter (Figure 29). These plots were limited to pairs at the same sample location (biofilter and port) but separated by different lengths of time, and show different ranges and variability of R-value and different shapes of both ANOSIM-R and its significance. The patterns showed by data combined from both depths trended with the data from the 0.76 m depth, consistent with the larger number of samples taken for each biofilter at this depth (Figure 29a, c, and e). Overall, bacterial populations in all three biofilters showed a range of significant correlations of approximately 125-150 d. Thus, communities from samples taken from less than 125-150 days apart did not show statistically significant differences.

Additionally, bacterial communities at the 0.76 m depth showed patterns of cyclic variation (Figure 29a, c, and e). The ANOSIM R metric for all three sites at 0.76 m depth began as positive (showing that sample pairs are more similar at this particular sampling distance than at other sampling distances), became negative (showing sample pairs are less similar at this particular sampling distance than at other sampling distances), and then became positive once again. That is, at a separation time of approximately a year, sample pairs became once again statistically similar. This pattern suggests that bacterial community composition cycles roughly annually, so that samples taken from the same period of the year in different years have relatively similar bacterial community composition. The extent and shape of this annual patterning varied between biofilter sites, with the pattern most suggestive of cyclic behavior seen for the FP03 biofilter, and the pattern least suggestive of cyclic behavior seen for the DE01 biofilter. Sites also differed in

the separation time at which sample pairs again became statistically dissimilar, with DE01 and FP03 sites having a return to statistical significance at approximately 300 d and the FP07 site having a return to statistical significance at approximately 425 d.

Overall, bacterial communities at the 1.52 m depth showed less temporal patterning relative to the 0.76 m depth. The DE01 and FP07 biofilters showed positive trends in the ANOSIM-R metric at approximately a year separation time for the 1.52 m bacterial community, but these were not statistically significant. At FP03, however, bacterial communities at both the 0.76 m and 1.52 m depths showed statistical similarity beginning again at approximately 300 d.

ANOSIM-GS plots constructed from fungal community time-series data (Figure 30) show that there are also differences in the temporal structure of fungal communities at different biofilter sites and by depth at each biofilter site in the range and variability of R values and the shape of cyclical patterning (or lack thereof). Fungal communities showed a somewhat greater variation in correlation range at different biofilter sites than that of bacterial communities, but the range of statistical similarity was between 100 and 200 d. The DE01 biofilter had the largest correlation range (~200 d), with the FP07 and FP03 sites having similar ranges at approximately 150 d. Thus, fungal communities of samples taken less than 150 d apart were not statistically different. The DE01 and FP07 sites did not show evidence of cyclic patterning. However at the FP03 site the fungal community at the 0.76 m depth did show slight, but unsignificant, cyclical trends. In addition, the community at the 1.52 m depth at FP03 shows a larger correlation distance (approximately 250-300 d) than in other fungal ANOSIM-GS plots (Figure 30). The smoothness of the plot from both depths (combined data) is therefore affected by substantially disparate curves.

The source of the temporal patterns in the biofilter bacterial and fungal communities and their differences by biofilter and depth cannot be identified by ANOSIM-GS analyses. However, differences in biofilter environment and age may play roles. Standardized correlograms, analogous to ANOSIM-GS R plots, constructed from meteorological and environmental variables also show cyclical patterns on the order of those in the ANOSIM-GS plots (Figure 31-Figure 33). Differences in the variation of environmental conditions with time may influence the temporal community structure at the three biofilter sites. For example, bacterial community cycles appear to occur at similar intervals as those of port temperature. However, the relative age of the biofilter sites may also partially explain differences in community correlation patterns. Annual patterning and its consistency appears to be greater with increasing biofilter age: FP03 is the oldest biofilter site, FP07 the middle, and DE01 the youngest. More cyclic patterns may therefore be a function of ecosystem age. This may also explain why the communities in the DE01 biofilter show a wider range of ANOSIM R metric than those at the other sites—the ecosystem may still be evolving. Additionally, it should be considered that the FP03 biofilter was operated under little to no flow control for most of this study. Periodicity may therefore also be influenced by retention time and consistency of hydraulic regime. For example, the extended correlation distance for fungal communities at 1.52 m at FP03 may reflect that inundation became more consistent when flow control was restored approximately 400 d into the study, changing the conditions (and affecting community) at the deeper depth.

Additionally, ANOSIM-GS plots suggest that bacteria and fungi show differences in the extent of cyclical behaviors. This may be due to differences in physiology; whereas bacterial communities exhibit comparatively rapid responses to changing environmental

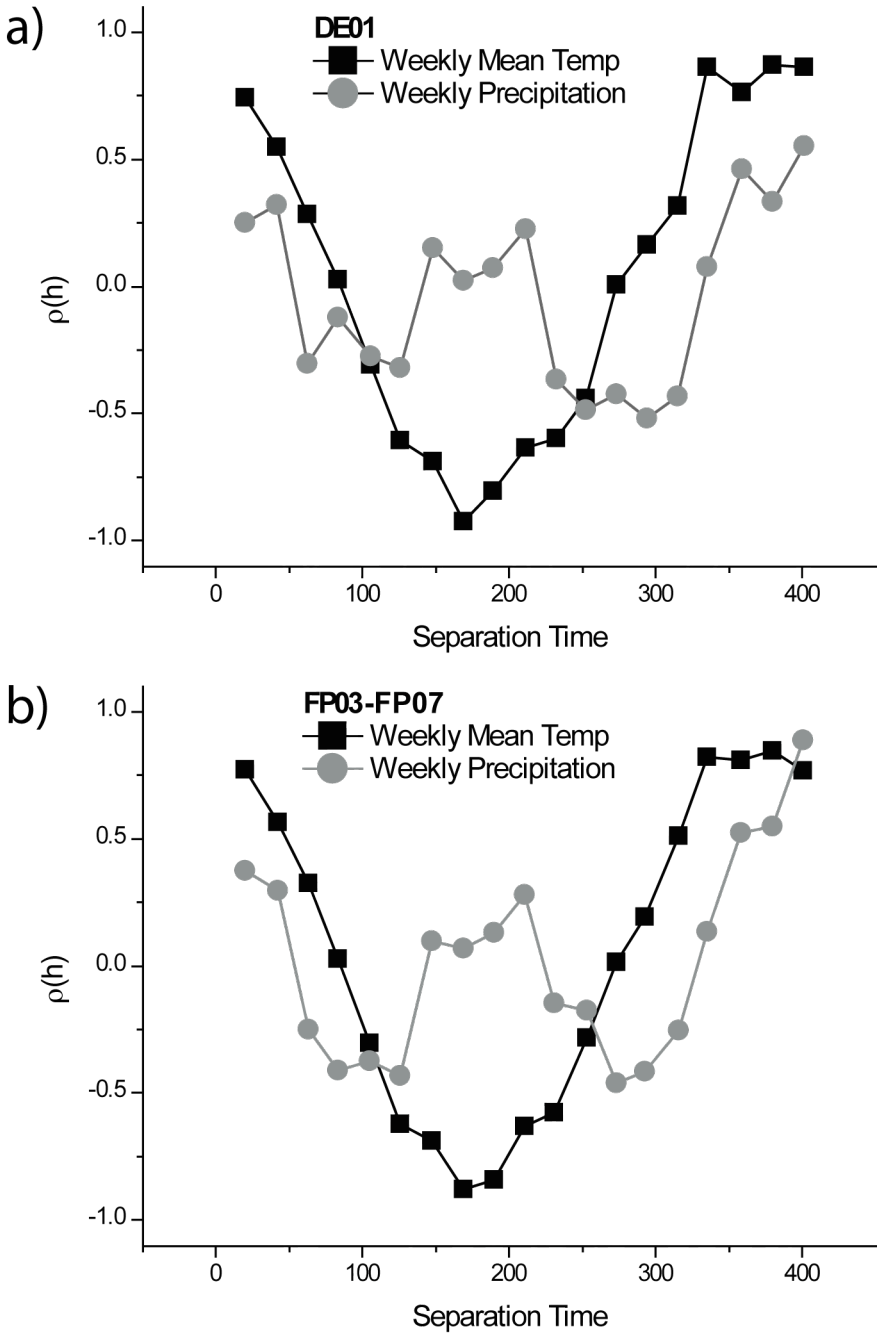

Figure 31. Standardized temporal correlograms of meteorological variables for: a) De Land, IL (DE01), and b) Decatur, IL (FP03 and FP07). Separation distance classes were identical to those used for ANOSIM-GS plots; those distance classes with fewer than 30 pairs were excluded.

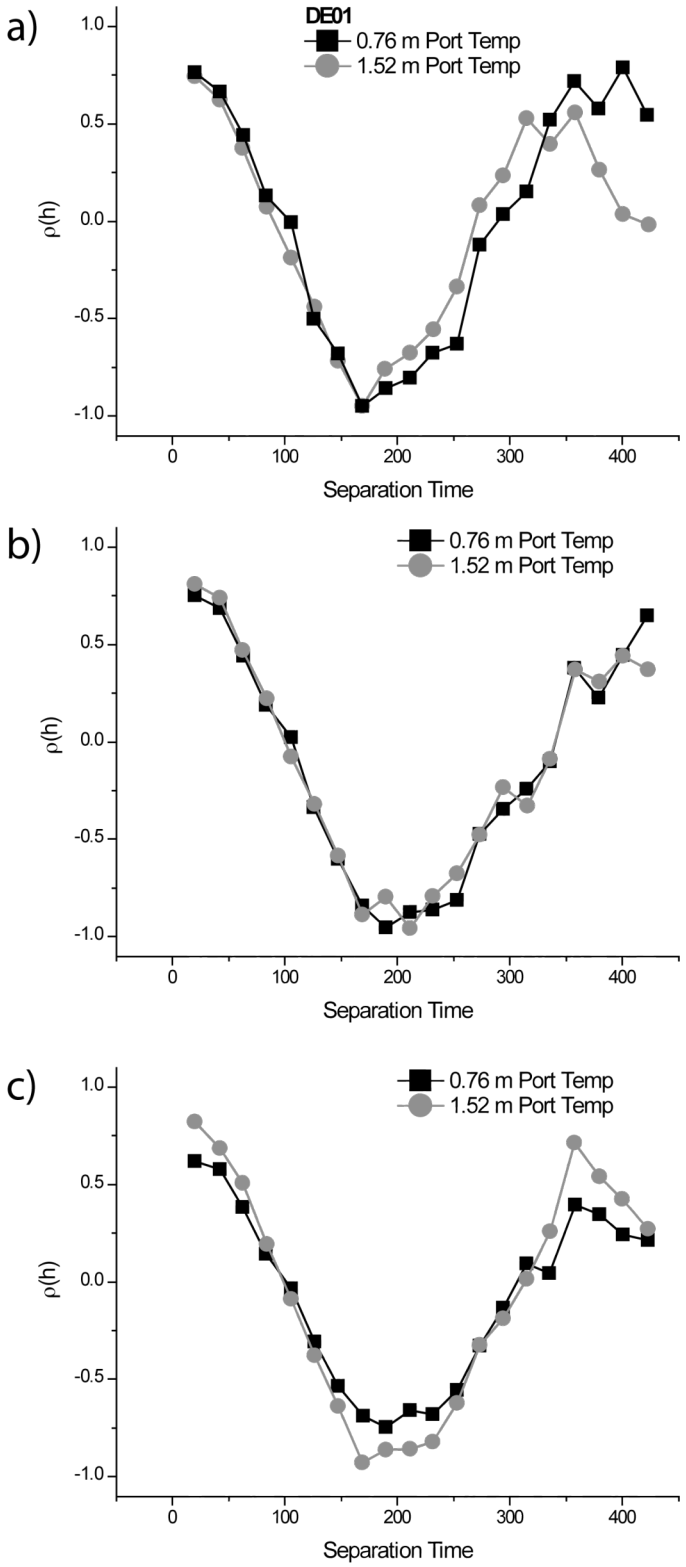

Figure 32. Standardized temporal correlograms of temperature in biofilter ports for: a) DE01, b) FP03, and c) FP07. Separation distance classes were identical to those used for ANOSIM-GS plots; those distance classes with fewer than 30 pairs were excluded.

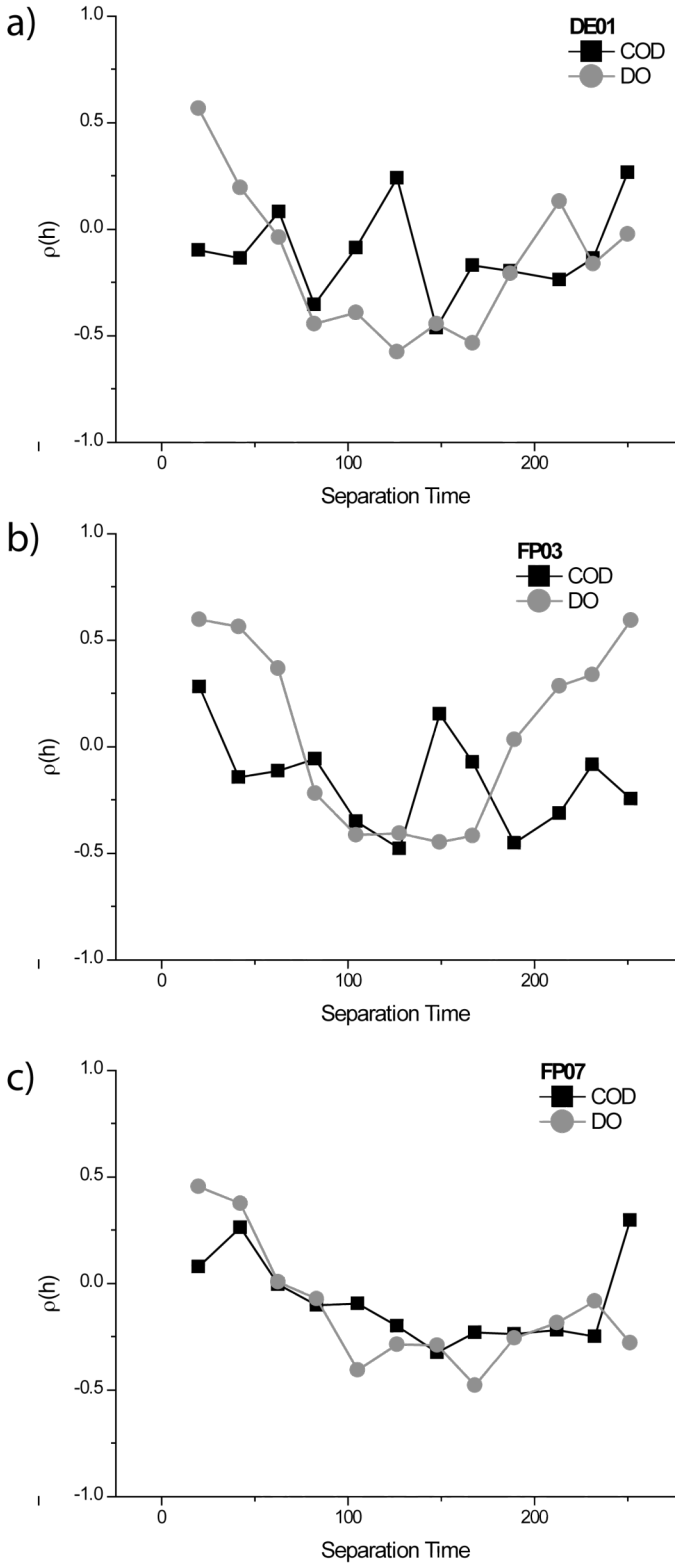

Figure 33. Standardized temporal correlograms of port COD and DO in biofilter ports for: a) DE01, b) FP03, and c) FP07. Separation distance classes were identical to those used for ANOSIM-GS plots; those distance classes with fewer than 30 pairs were excluded. Note the scale differences between this figure, Figure 31, and Figure 32; because fewer ports were inundated, fewer measurements were taken and only shorter separation times had the required number of pairs.

conditions, many fungi have persistent and extensive hyphal systems so fungal communities may exhibit less change with the seasons (Kendrick, 2001). This is consistent with the observation that bacterial communities show the greatest cyclical patterning at the shallow (0.76 m) depth. At this depth, cells may be more exposed to ambient temperatures and precipitation events and experience more seasonal variability in inundation regime (see Figure 24-Figure 25).

Patterns shown using the ANOSIM-GS method are consistent with those revealed by correspondence analysis (CA) plots constructed from the same data (Figure 35-Figure 39). Correspondence analysis is one of several ordination techniques that arrange samples along theoretical axes according to their species composition. Correspondence analysis derives in part from the theory that different species thrive in different environmental conditions. In correspondence analysis, eignenanalysis is used to plot both sample sites and populations together as points in the ordination space according to their chi-squared distance, with the axes representing environmental gradients (Legendre and Legendre, 1998). Data is typically plotted on the two or three axes (environmental gradients) that display the greatest variation.

Figure 34-Figure 39 show sample points coded both by month and by year of sample collection and separated by biofilter location. These plots reflect the patterns shown in ANOSIM-GS plots, but are much more difficult to discern. Nevertheless, evidence of both seasonal shifts in community and cyclic patterns exists in the plots.

For bacterial communities at the 0.76 m depth (Figure 34a-Figure 36a), samples represented by warmer colors (warmer months), for example, generally cluster and samples represented by cooler colors (cooler months) generally cluster, suggesting broad

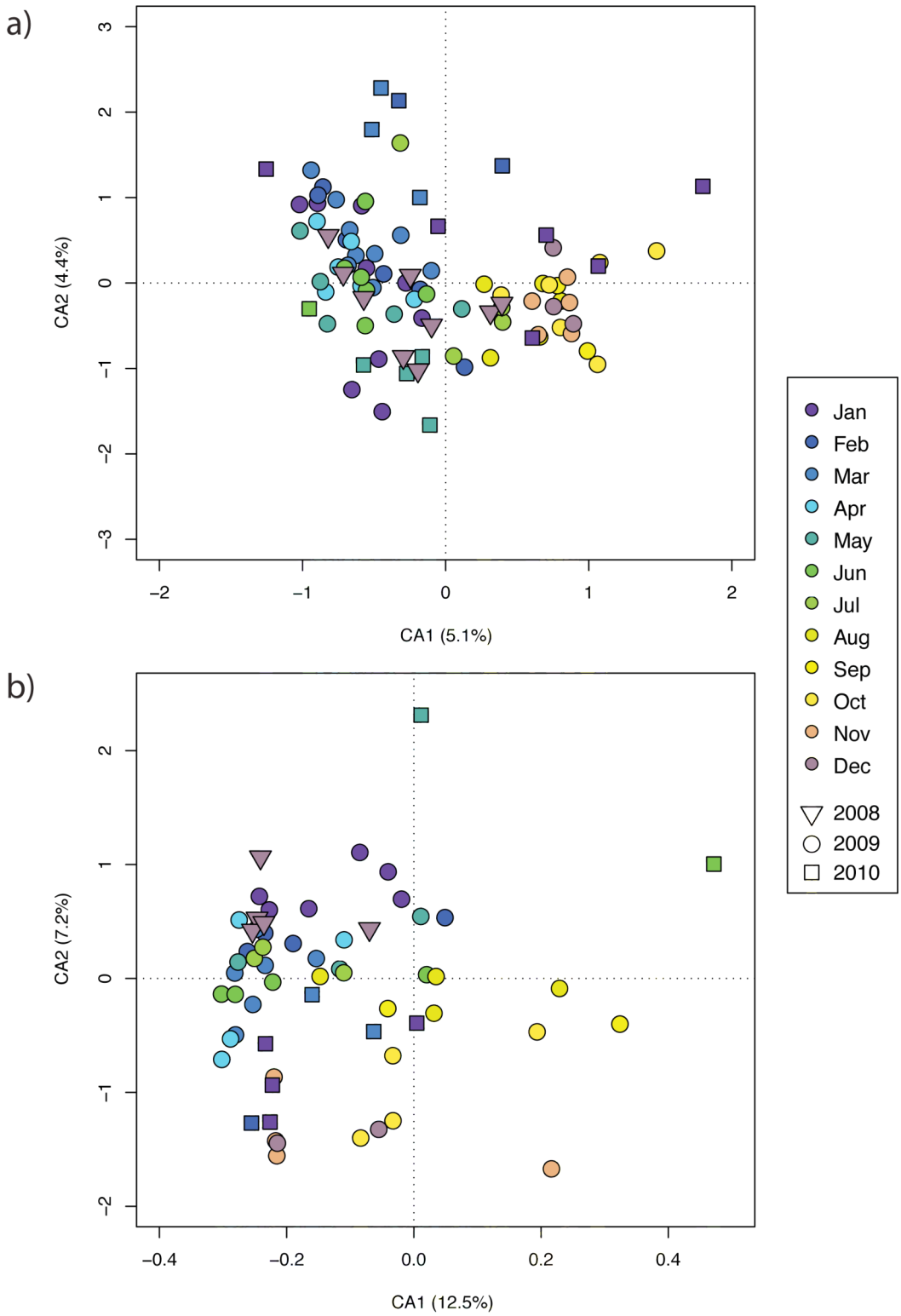

Figure 34. Correspondence analysis plots of time-series bacterial community (ARISA) data from the DE01 site at the: a) 0.76 m depth, and b) 1.52 m depth. Points represent samples and are coded both by collection month (color) and year (shape). Inertia represented by each axis is noted in parentheses. Clustering of samples by month (color) irrespective of year (shape) at the 0.76 m depth suggests annual cycles in bacterial community composition.

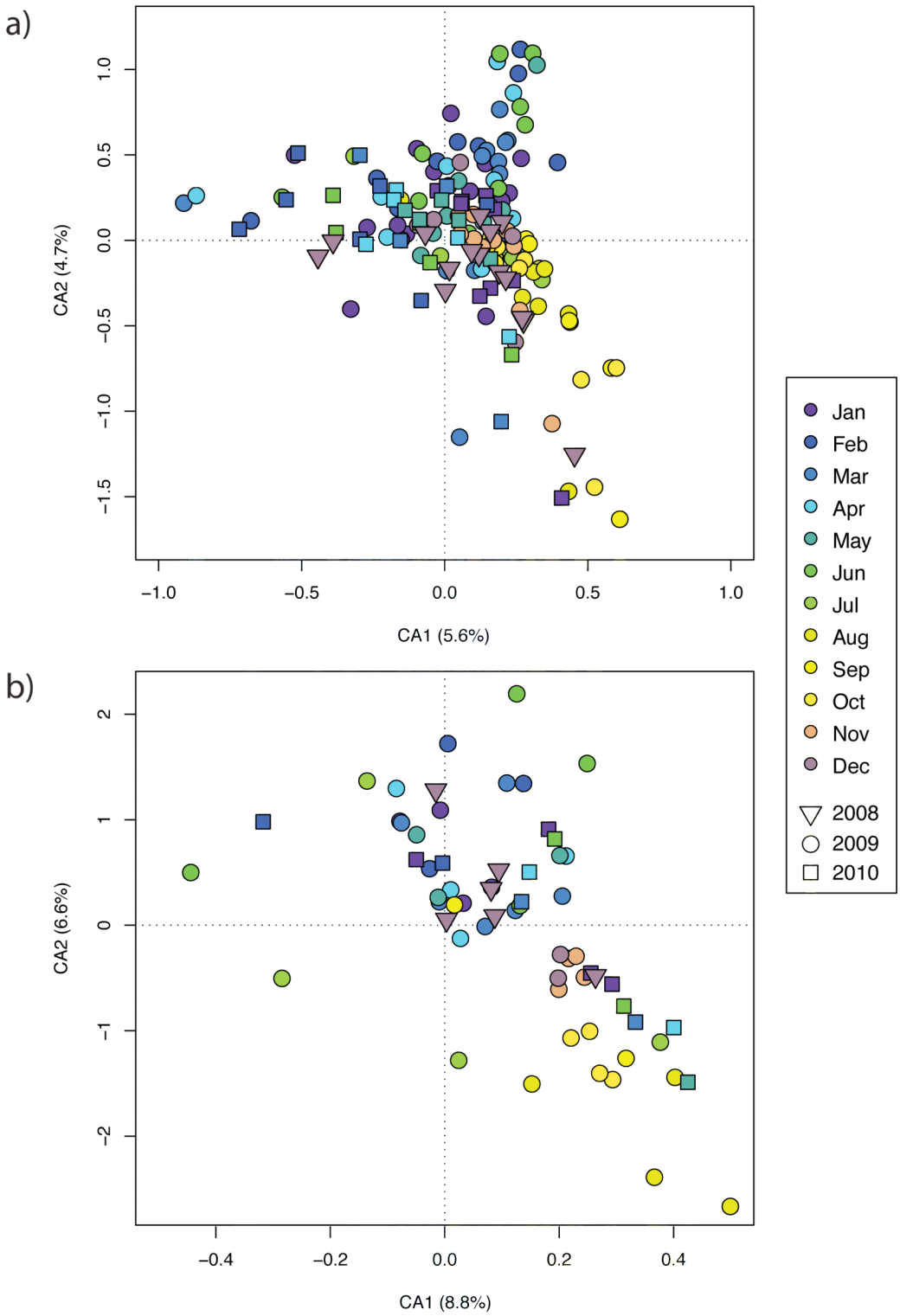

Figure 35. Correspondence analysis plots of time-series bacterial community (ARISA) data from the FP03 site at the: a) 0.76 m depth, and b) 1.52 m depth. Points represent samples and are coded both by collection month (color) and year (shape). Inertia represented by each axis is noted in parentheses. Clustering of samples by month (color) irrespective of year (shape) at the 0.76 m depth suggests annual cycles in bacterial community composition.

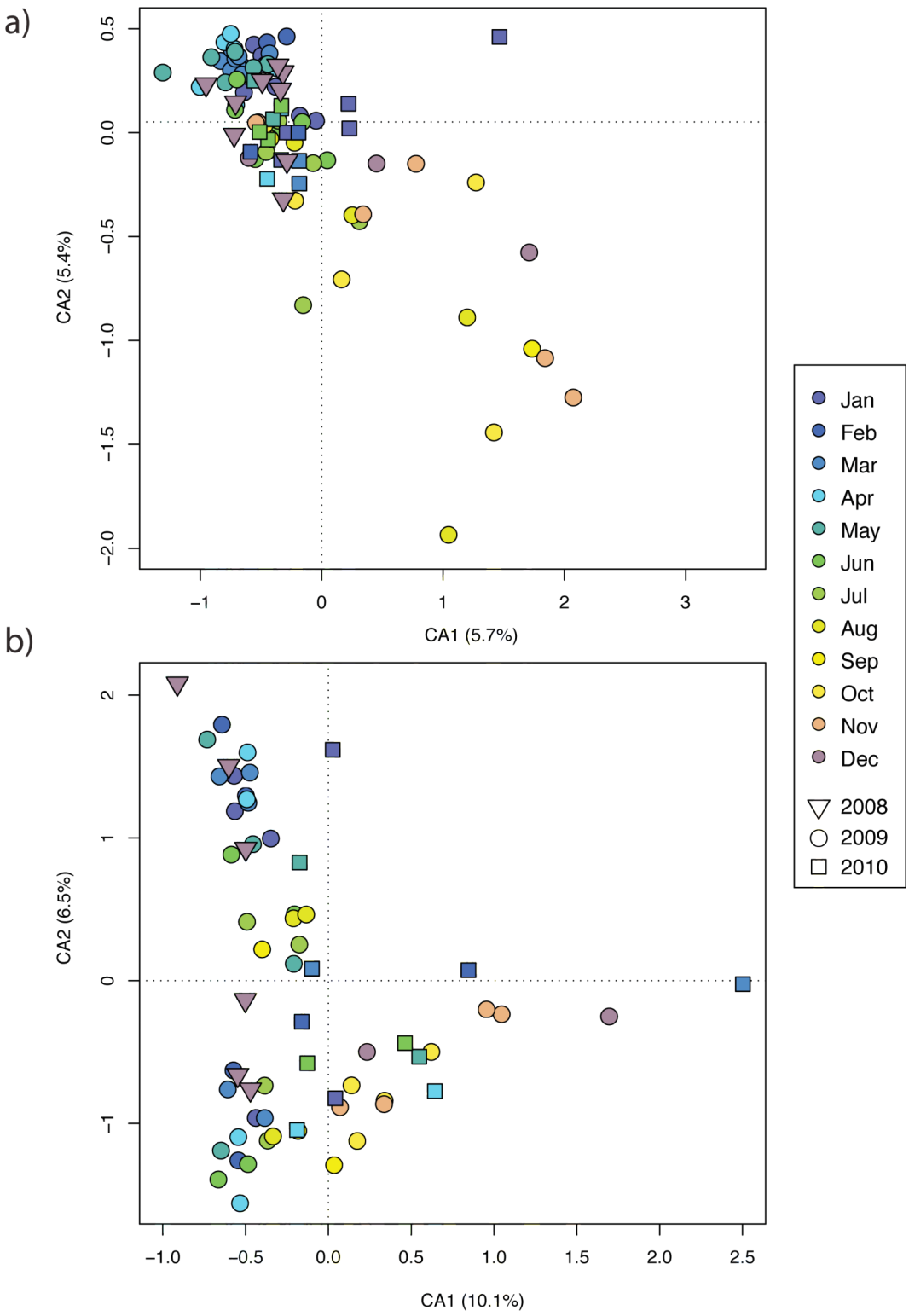

Figure 36. Correspondence analysis plots of time-series bacterial community (ARISA) data from the FP07 site at the: a) 0.76 m depth, and b) 1.52 m depth. Points represent samples and are coded both by collection month (color) and year (shape). Inertia represented by each axis is noted in parentheses. Clustering of samples by month (color) irrespective of year (shape) at the 0.76 m depth suggests annual cycles in bacterial community composition.

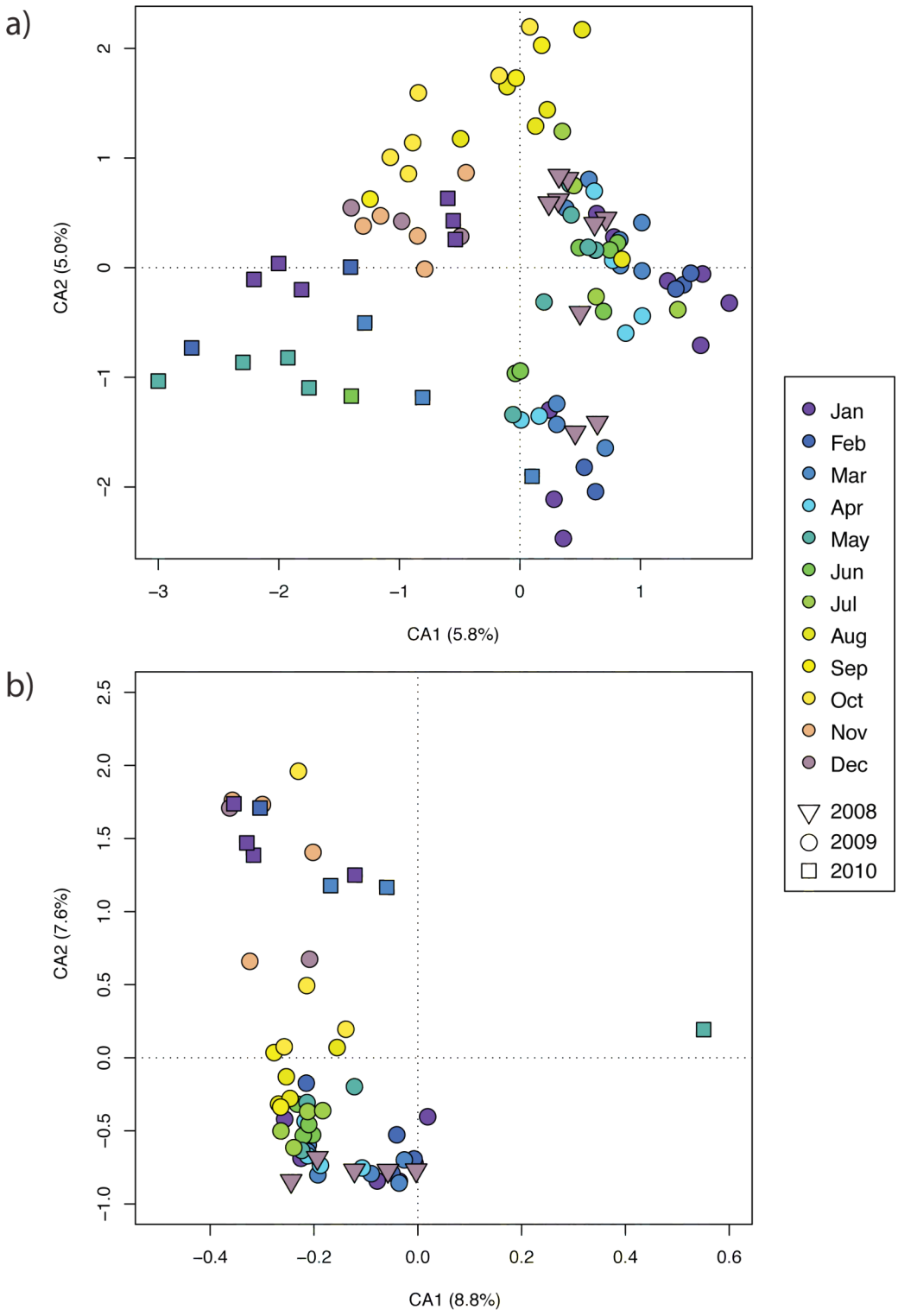

Figure 37. Correspondence analysis plots of time-series fungal community data (fARISA) from the DE01 site at the: a) 0.76 m depth, and b) 1.52 m depth. Points represent samples and are coded both by collection month (color) and year (shape). Inertia represented by each axis is noted in parentheses. Although samples of the same month and year cluster, those of the same month and differing years are not co-located, suggesting temporal autocorrelation, but not annual cycling of community composition.

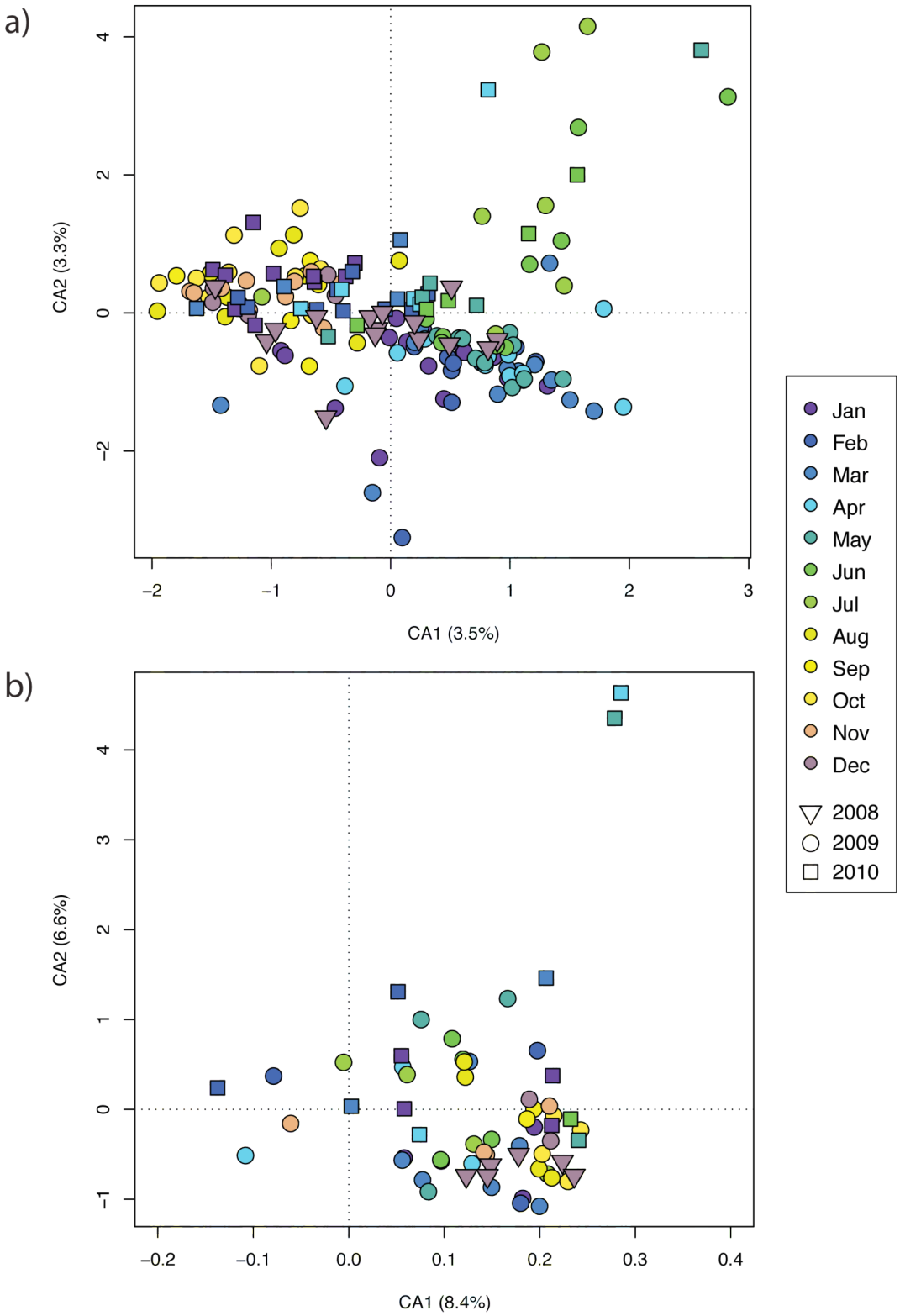

Figure 38. Correspondence analysis plots of time-series fungal community data (fARISA) from the FP03 site at the: a) 0.76 m depth, and b) 1.52 m depth. Points represent samples and are coded both by collection month (color) and year (shape). Inertia represented by each axis is noted in parentheses. Although samples of the same month and year cluster, those of the same month and differing years are not typically co-located, suggesting temporal autocorrelation, but not annual cycling of community composition.

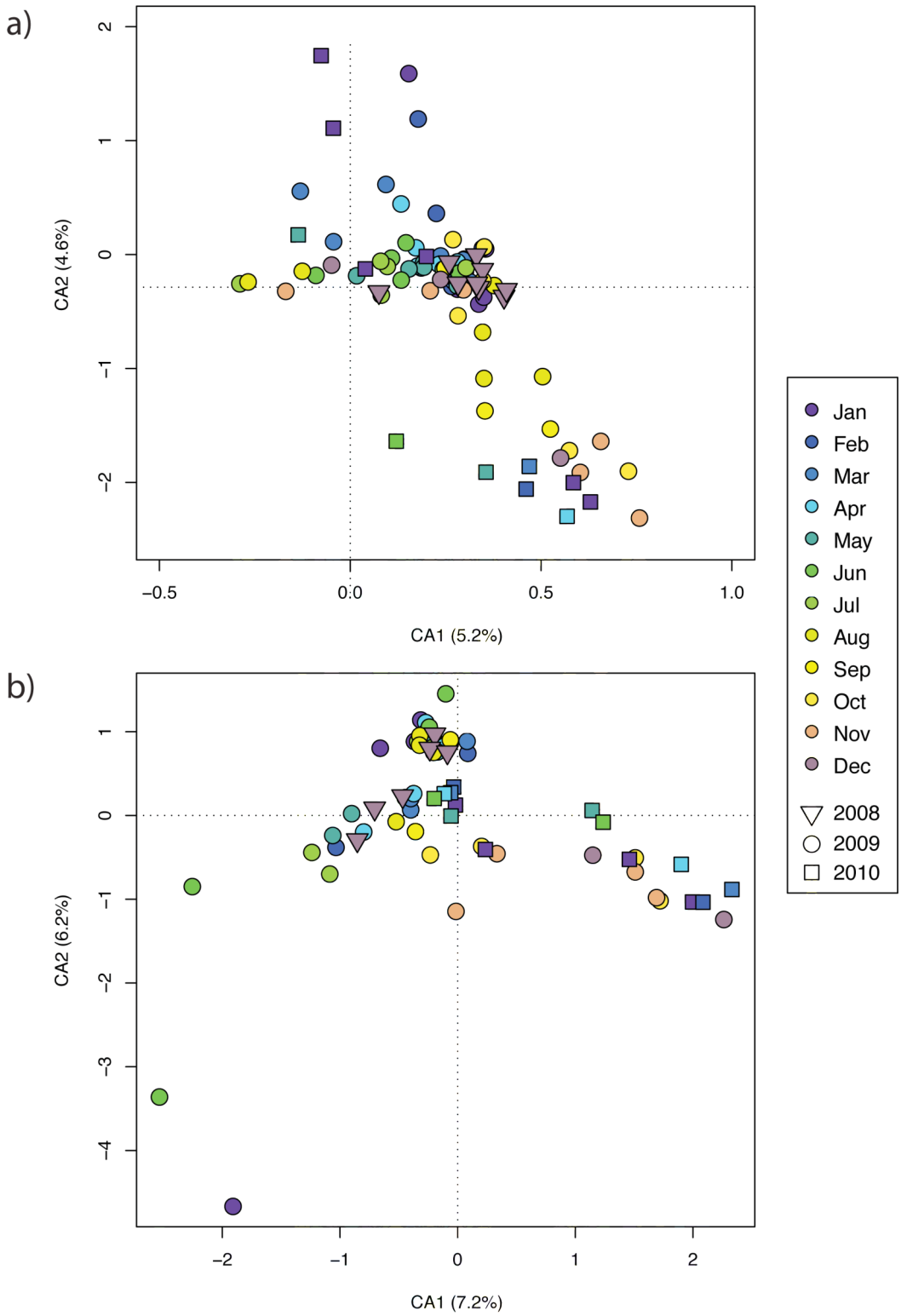

Figure 39. Correspondence analysis plots of time-series fungal community (fARISA) data from the FP07 site at the: a) 0.76 m depth, and b) 1.52 m depth. Points represent samples and are coded both by collection month (color) and year (shape). Inertia represented by each axis is noted in parentheses. Although samples of the same month and year are generally closely located, those of the same month and differing years are not typically co-located, suggesting temporal autocorrelation, but not annual cycling of community composition.

seasonal changes. Furthermore, collocation of samples from different years but the same month (see for example June and July samples at the FP07 site (Figure 36): green circles and squares are similarly positioned) support the annual cycling that is shown by the temporal ANOSIM-GS plots (Figure 29). For bacterial communities at the 1.52 m depth, on the other hand, annual patterning in community composition is not observed. However, in these plots samples of the same or adjacent months still cluster (Figure 34b-Figure 36b), indicating change in community without cyclic behavior. For fungal communities, only the FP03 site at the 0.76 m depth shows some collocation of samples from different years but the same months (Figure 37-Figure 39), notably for June and July. This is consistent with the slight annual patterning shown in the fungal community ANOSIM-GS plot for FP03 (Figure 30b). The remainder of the fungal community CA plots suggest autocorrelation but not annual patterns, as samples of the same month cluster but not those of the same month and different year (Figure 37-Figure 39).

The difficulty of discerning patterns in these CA plots show one of the strengths of the ANOSIM-GS technique. Whereas CA plots, which are a common means to display community patterns or differences, can be cluttered or result in overlapping sample groups that can obscure small scale patterns, ANOSIM-GS plots only show quantified community similarities between samples with similar separation over time or space. Therefore, ANOSIM-GS is a more sensitive technique for discriminating spatial or temporal patterns. In the case of the biofilters, I was able to discern both overall temporal shifts in community composition and also cyclic patterns. Quantifying these aspects would be difficult with the methodology typically used in community analysis.

Overall, the ANOSIM-GS plots suggest that a sampling scheme would most efficiently describe community temporal variation at 125 d between samples. At this sampling frequency, samples would not be statistically autocorrelated, but would capture important community differences over time.

4.5.3 Spatial variation in the time-series dataset

To determine if spatial variation was observed in the time-series dataset, partial Mantel tests were employed (Legendre and Legendre, 1998; Mantel, 1967). Mantel tests show the correlation between two distance matrices such that a high Mantel coefficient (R_M) indicates that samples that are more similar in one distance matrix are likely to be similar in the other distance matrix. Mantel tests can be used to show relationships between communities and environment, two different communities, or between observed data and that predicted by a model. Partial Mantel tests can also be conducted, where the relationship between two distance matrices is considered while accounting for the variability represented by one or more other matrices.

Because the temporal variation of communities in the time-series data was strong, I used a partial Mantel test accounting for temporal variation to test spatial relationships in the time-series dataset. Time-series community data was separated by biofilter, and evaluated using matrices representing distance in the flow, cross-flow, or depth directions (Table 7). Partial Mantel tests showed that spatial variation is still significantly correlated to differences in depth and position in each biofilter, but that the relative and absolute strength of these correlations varies between bacterial and fungi, and also among different biofilters. Overall, these variables explain a large part of the bacterial and fungal community variability in the DE01 and FP07 biofilters and in the fungal community of the

FP03 biofilter (between approximately 40 and 80%). Bacterial variability in the FP03 biofilter does not show correlations of a large magnitude with positions and times, suggesting that something other than these variables affects bacterial community composition.

For the bacterial community, the variable showing the largest correlation with microbial community was different for each biofilter. In the DE01 biofilter, depth had the largest magnitude correlation with community composition, followed by time, and then by a low (but still significant) correlation in the direction of flow (Table 7). This indicates that the bacterial community in DE01 is relatively similar along the flowpath with respect to the differences in depth and with time. In contrast, in the FP07 biofilter, distance in the direction of flow was correlated more strongly to community similarity (as defined by the Bray-Curtis metric) than depth was. This may be due to the topography of the FP07 biofilter site; towards the outlet end this biofilter is frequently inundated at the 0.76 m depth and thus may act more like the inundated locations at 1.52 m than like the drier 0.76 m depth locations nearer the inlet. Sample separation time was still correlated to a substantial magnitude with bacterial community similarity in the FP07 biofilter. However, in comparison to the correlation between community and distance in the flow direction, the magnitude of the correlation with distance in the cross-flow direction was substantially smaller, although still significant. This shows that, although community differences still exist in the cross-flow direction, they are less important, even in a comparatively wide biofilter, supporting the decision to largely exclude cross-flow differences from the time-series sampling scheme.

For the fungal community, the highest magnitude correlations were consistently between time and community similarity, suggesting that seasonal variability more strongly structured community composition than did position within the biofilter (Table 7). As fungal populations frequently have extensive hyphal systems (Kendrick, 2001) and some fungi may therefore exist through a single biofilter, the observation that fungal communities are less spatially structured than temporally structured is reasonable, however this result may also be due to differing resolutions between the ARISA and fARISA methods. Manter and Vivanco (2007), for example, report that fARISA may underrepresent overall fungal diversity by a factor of two due to similarities in the fragment sizes of differing species. Yet, distance in the direction of flow and depth also had substantial effects on fungal community. As with the bacterial community, the magnitude of correlation of the FP07 biofilter fungal community with distance in the cross-flow direction was much less than that in the flow direction, indicating again that communities across the width of the FP07 site were relatively similar.

Table 7. Partial Mantel tests of community versus spatial and temporal variation.

Biofilter	$R_{f.cdt}$	$R_{c.fdt}$	$R_{d.fct}$	$R_{t.fcd}$
DE01 bacterial	0.0953	--	0.382	0.169
fungal	0.154	--	0.293	0.466
FP03 bacterial	0.0996	--	0.0796	0.0675
fungal	0.169	--	0.112	0.245
FP07 bacterial	0.217	0.049 (p=0.003)	0.0770	0.183 (p=0.002)
	0.169	0.0817	0.105	0.321

Where $R_{a,bcd}$ is the partial Mantel statistic for the correlation of the community and a, accounting for b, c, and d. f = distance in the flow direction, c = distance in the cross-flow direction, d = distance in the depth direction, and t = days between samples. All tests listed were significant at the α=0.01 level, and had a p-value of p<0.001, unless otherwise noted.

4.5.4 Covariation of environmental variables, performance, and community

Understanding the spatial and temporal variation of performance and environment between biofilter sites is an important step for understanding the whole system. However,

this research was focused on identifying interactions that substantially affect performance, in particular whether the microbial community is influential. To examine the relationships among environment variables, performance and community, statistical correlations (Spearman rank and Mantel tests), ANOVA tests, and correspondence analysis plots were constructed using performance and environmental variables, and microbial populations (either all or a representative subset).

Correlations between environmental variables and performance

To better understand and account for the impact of environmental variation on performance when considering community, Spearman rank correlations were conducted between selected environment variables and nitrate removal. These tests were performed both among all biofilters and at individual sites (Table 8). These tests more quantitatively assess those relationships more generally suggested by comparison of temporal graphs of environment and ANOSIM-GS plots (Figure 20-Figure 27, Figure 14, Figure 19).

For all sites taken together, relationships between environmental variables and performance generally followed those reported in literature (see 2.1.1 Denitrification and parameters that influence it). COD, temperature (both climatic and inside ports), and increased moisture (here, rainfall), all were positively and significantly related to increased nitrate removal. DO was negatively associated with nitrate removal, reflecting that most denitrifiers are facultative anaerobes, preferring aerobic respiration. However, the relationship beween pH and nitrate removal was not significant overall. Average growing degree days was included as a factor to assess seasonality of nitrate removal; the significant and positive correlation indicates that nitrate removal is highest during the summer months.

Relationships between environmental factors and performance at DE01 and FP03 mostly reflected those overall, with some exceptions. The Spearman coefficient for COD at FP03, for example, was positive but insignificant. Additionally, pH was significantly negatively related to nitrate removal at the FP03 site. This may indicate that the denitrifying community at the FP03 site has a different or more distinct optima than that at other sites.

At the FP07 site, however, the impact of chemical and climatic factors were largely insigificant. Only the association between nitrate removal and growing degree days was significant, and notably, this was negative where at other sites the relationship was positive, indicating that the best nitrate removal did not occur during summer months.

This inconsistency between the FP07 and the DE01 and FP03 sites may partially be explained by differences in flow at the three sites. Overall, neither instantaneous nor 14 d average flow was significantly correlated to nitrate removal. However, at the DE01 site, flow was highly negatively correlated (both for instaneous and 14 d average flow), at the FP03 site, flow was negatively correlated to 14 d average flow, and at the FP07 site, flow (both instaneous and 14 d average) was *positively* correlated to nitrate removal. These correlations are reasonable in the context of the absolute flow values at the three sites (Table 5): DE01 having the greatest flow, FP03 the middle flow, and FP07 having relatively little flow. This suggests that there is a flow optimum for nitrate removal, with the DE01 and FP03 site largely operating above the optimum flow, and FP07 operating below optimum flow. The relationships at FP07 between flow and nitrate removal may also account for the lack of significant correlations between nitrate removal and other

environmental variables. For this site, the effects of limited flow impacted nitrate removal more than other variables.

It is also helpful to remember that for this analysis, nitrate removal was considered in absolute rather than relative terms. Therefore, at FP07, where inlet nitrate concentrations were less than that at other sites, less nitrate removal was possible. Additionally, times of higher load (for FP07, spring) result in higher nitrate removal, possibly explaining the negative correlation between growing degree days and nitrate removal at FP07.

Table 8. Spearman rank correlation between selected environmental factors and nitrate removal.

Factor	Coefficient ρ (p-value)			
	All Biofilters	DE01	FP03	FP07
COD	0.443 (0.0001)***	0.556 (0.0001)***	0.182 (0.1340)	0.192 (0.1226)
DO	-0.556 (0.0001)***	-0.654 (0.0001)***	-0.392 (0.0003)*	-0.209 (0.0928)
pH	0.019 (0.8551)	-0.261 (0.0543)	-0.384 (0.0007)*	0.015 (0.2433)
Port temperature	0.373 (0.0001)***	0.730 (0.0001)***	0.230 (0.030)*	0.075 (0.544)
Instantaneous flow	0.021 (0.7522)	-0.847 (0.0001)***	-0.185 (0.0754)	0.391 (0.0004)***
14 d rolling flow average	0.077 (0.2435)	-0.936 (0.0001)***	-0.208 (0.0453)*	0.328 (0.0038)*
Mean Weekly Temp	0.359 (0.0001)***	0.709 (0.0001)***	0.394 (0.0001)***	-0.193 (0.094)
Weekly precipitation	0.252 (0.0001)***	0.579 (0.0001)***	0.213 (0.0352)*	-0.085 (0.4633)
Avg. Growing Degree Days	0.318 (0.0001)***	0.663 (0.0001)***	0.458 (0.0001)***	-0.317 (0.005)**

* denotes significance at the p=0.05 level
** denotes significance at the p=0.001 level
*** denotes significance at the p=0.0001 level

Mantel tests between community, environment, and performance

To characterize the relationships between environmental variables, performance and microbial community, Mantel tests were conducted between environmental or performance factors and microbial populations (bacterial, fungal, or both; Table 9-Table

13). In particular, these tests were were intended to elucidate the relative contributions of "proximal" (environment affecting denitrification rate) and "distal" (environment affecting microbial community composition in turn affecting denitrification rate) controls on denitrification in the biofilters (Wallenstein et al., 2006b).

First, to assess whether microbial community influences nitrate removal, partial Mantel tests were performed (among all sites and for individual sites) for the relationships between bacterial community, fungal community, or environmental variables (including those with significant Spearman correlations) and nitrate removal (Table 9). As expected, the selected environmental factors were significantly related to nitrate removal both among all sites and within individual sites, indicating that proximal environmental controls are important to denitrification in the biofilter systems. The degree of association between environment and nitrate removal varied, with DE01 showing the highest partial Mantel coefficient and FP07 showing the lowest.

Among all sites, bacterial community composition was also significantly associated with nitrate removal, indicating that even accounting for environmental differences between sites, some bacterial communities were more linked to better performance than others. The partial correlations between nitrate removal and bacterial community composition and nitrate removal and environment were of approximately the same magnitude, suggesting that they are of comparable importance. At DE01, bacterial community composition was also significantly related, but at the other two sites it was not, suggesting that broad community composition changes across sites had more impact on nitrate removal than those within a site.

Fungal community composition was only significantly linked to nitrate removal at the FP07 site. At this site, the partial Mantel coefficient for fungal community composition was of roughly the same magnitude as the partial Mantel coefficient for environment.

Importantly, the sum of the partial Mantel coefficients differed from site to site. At DE01, differences in microbial communities and the included environmental variables together were associated with nearly 80% of the variation in nitrate removal. However, at FP03 and FP07 substantially less of the variation in nitrate removal (~30-40%) was

Table 9. Partial Mantel tests for relationship between nitrate removal bacterial community, fungal community, and environment.

Group	Partial Mantel Coefficient $R_{x,yz}$ (p value) against nitrate removal (mg/L)		
	Bacterial Community ($R_{b,fe}$)	Fungal Community ($R_{f,be}$)	Environment ($R_{e,bf}$)
All Biofilters	0.141 (0.001)**	0.0451 (0.150)	0.175 (0.001)**
DE01	0.180 (0.002)*	-0.518 (0.285)	0.608 (0.001)**
FP03	0.0605 (0.344)	0.0443 (0.501)	0.336 (0.001)**
FP07	-0.0663 (0.238)	0.142 (0.010)*	0.130 (0.005)*

Where $R_{x,yz}$ is the partial Mantel statistic for the correlation of factor and x, accounting for y and z, and b = bacterial populations, f = fungal populations, and e = environment. Environment includes: inlet nitrate (mg/L), COD (mg/L), DO (mg/L), woodchip moisture content (%), port temperature (C), instantaneous flow (L/s), 14 d average flow (L/s), weekly precipitation (cm), and weekly average temperature (C).
* denotes significance at the p=0.01 level
** denotes significance at the p=0.001 level

accounted for by variation in microbial community and this set of environmental parameters, suggesting that other factors may also influence nitrate removal at these sites.

Because bacterial community was associated with nitrate removal among all sites, and bacterial and fungal communities at certain sites, Mantel tests between individual environmental parameters and bacterial, fungal, or combined populations were conducted among all sites and for each site (Table 10-Table 13). These tests were designed to elucidate distal controls on microbial populations at each site (as defined in Wallenstein et al., 2006b). Among all sites (Table 10), these tests were performed as partial Mantel tests

Table 10. Partial Mantel tests for relationship between selected environmental and performance variables and microbial community (all sites).

Factor	Partial Mantel Coefficient $R_{a,b}$ (p value)			
	Bacterial Community ($R_{bac,bf}$)	Fungal Community ($R_{fun,bf}$)	All Community ($R_{all,bf}$)	Biofilter, ($R_{bf,all}$)
Inlet nitrate (mg/L)	0.0549 (0.013)*	0.111 (0.001)**	0.113 (0.001)**	0.305 (0.001)**
COD (mg/L)	-0.0119 (0.762)	0.0240 (0.526)	-0.0034 (0.929)	-0.0042 (0.845)
DO (mg/L)	-0.0699 (0.102)	0.0176 (0.669)	-0.0362 (0.374)	0.142 (0.001)**
pH	0.0151 (0.685)	0.0811 (0.029)*	0.0478 (0.196)	-0.0334 (0.147)
Moisture content (%)	0.155 (0.001)**	0.112 (0.001)**	0.165 (0.001)**	-0.0202 (0.009)**
Depth (m)	0.0524 (0.001)**	0.0642 (0.001)**	0.0682 (0.001)**	0.0035 (0.460)
Port temperature (C)	0.187 (0.001)**	0.0614 (0.001)**	0.162 (0.001)**	-0.0359 (0.001)**
Instantaneous flow (L/s)	-0.0377 (0.295)	-0.115 (0.001)**	-0.0944 (0.005)*	0.169 (0.001)**
14 d rolling avg flow average (L/s)	0.0177 (0.618)	-0.101 (0.001)**	-0.0426 (0.173)	0.137 (0.001)**
Weekly precipitation (cm)	0.0518 (0.008)*	0.0291 (0.084)*	0.0512 (0.006)*	-0.013 (0.054)
Weekly average temp (C)	0.0369 (0.013)*	0.0505 (0.001)**	0.0491 (0.002)*	-0.0131 (0.024)*

Where $R_{a,b}$ is the partial Mantel statistic for the correlation of factor and a, accounting for b, and bac = bacterial populations, fun = fungal populations, all = all populations, bf = biofilter.
* denotes significance at the p=0.05 level
** denotes significance at the p=0.001 level

Table 11. Mantel tests for relationship between microbial community composition at the DE01 site and selected environmental and performance variables.

Factor	Mantel Coefficient R_M (p value)		
	Bacterial Community	Fungal Community	All Community
Inlet nitrate (mg/L)	0.139 (0.001)**	0.148 (0.002)*	0.175 (0.001)**
COD (mg/L)	-0.0412 (0.631)	-0.0682 (0.442)	-0.069 (0.441)
DO (mg/L)	-0.0105 (0.897)	-0.0224 (0.805)	-0.0172 (0.853)
pH	0.131 (0.094)*	0.210 (0.024)*	0.177 (0.034)
Moisture content (%)	0.141 (0.001)**	0.099 (0.002)*	0.134 (0.001)**
Depth (m)	0.352 (0.001)**	0.187 (0.001)**	0.309 (0.001)**
Port temperature (C)	0.130 (0.001)**	0.0774 (0.010)*	0.118 (0.001)**
Instantaneous flow (L/s)	-0.019 (0.549)	-0.0164 (0.620)	-0.0263 (0.394)
14 d rolling avg flow average (L/s)	0.0073 (0.804)	0.0236 (0.399)	0.0176 (0.544)
Weekly precipitation (cm)	0.0886 (0.010)*	-0.0065 (0.835)	0.0492 (0.131)
Weekly average temp (C)	0.0825 (0.001)**	0.0867 (0.001)**	0.094 (0.001)**

* denotes significance at the p=0.05 level
** denotes significance at the p=0.001 level

Table 12. Mantel tests for relationship between microbial community composition at the FP03 site and selected environmental and performance variables.

Factor	Mantel Coefficient (R_M)		
	Bacterial Community	Fungal Community	All Community
Inlet nitrate (mg/L)	0.0833 (0.007)*	0.166 (0.001)**	0.159 (0.001)**
COD (mg/L)	-0.0367 (0.695)	-0.0068 (0.929)	-0.0312 (0.699)
DO (mg/L)	-0.0722 (0.259)	0.0861 (0.139)	0.0099 (0.866)
pH	-0.0221 (0.759)	-0.0176 (0.771)	-0.0305 (0.673)
Moisture content (%)	0.210 (0.001)**	0.202 (0.001)**	0.251 (0.001)**
Depth (m)	-0.0096 (0.745)	0.0525 (0.034)*	0.0142 (0.614)
Port temperature (C)	0.292 (0.001)**	0.105 (0.001)**	0.255 (0.001)**
Instantaneous flow (L/s)	-0.0487 (0.435)	-0.137 (0.019)*	-0.113 (0.052)
14 d rolling avg flow average (L/s)	0.0757 (0.148)	-0.148 (0.002)*	-0.0288 (0.600)
Weekly precipitation (cm)	0.0707 (0.017)*	0.0142 (0.585)	0.0537 (0.039)*
Weekly average temp (C)	0.0877 (0.002)*	0.0501 (0.010)*	0.0862 (0.002)*

* denotes significance at the p=0.01 level
** denotes significance at the p=0.001 level

Table 13. Mantel tests for relationship between microbial community composition at the FP07 site and selected environmental and performance variables.

Factor	Mantel Coefficient (R_M)		
	Bacterial Community	Fungal Community	All Community
Inlet nitrate (mg/L)	-0.0223 (0.587)	0.110 (0.009)**	0.054 (0.152)
COD (mg/L)	0.0846 (0.182)	0.0349 (0.588)	0.0581 (0.370)
DO (mg/L)	-0.0526 (0.403)	-0.0824 (0.181)	-0.0778 (0.189)
pH	0.102 (0.085)*	0.159 (0.014)*	0.147 (0.013)*
Moisture content (%)	0.298 (0.001)**	0.189 (0.001)**	0.304 (0.001)**
Depth (m)	0.124 (0.001)**	0.158 (0.001)**	0.164 (0.001)**
Port temperature (C)	0.217 (0.001)**	0.0416 (0.152)	0.156 (0.001)**
Instantaneous flow (L/s)	0.108 (0.043)*	-0.0168 (0.749)	0.0556 (0.269)
14 d rolling avg flow	0.207 (0.001)**	0.0171 (0.746)	0.136 (0.011)*
Weekly precipitation (cm)	0.0423 (0.256)	0.0894 (0.007)*	0.0708 (0.055)
Weekly average temp (C)	0.0218 (0.461)	0.0552 (0.045)*	0.0351 (0.214)

* denotes significance at the p=0.01 level
** denotes significance at the p=0.001 level

with differences between biofilters partialized out to account for environmental differences by site. For reference, the partial coefficient for biofilter was also listed. For individual sites (Table 11-Table 13), no partializing was conducted.

Overall, distal controls on community structure in the denitrifying biofilters appear to be inlet nitrate, pH, moisture content (in woodchips and, more weakly, rainfall), depth, and temperature (port and, more weakly, climatic). These findings are generally in line with those summarized in Wallenstein, et al. (2006b), who reported that temperature, moisture, and pH typically act to structure denitrifying communities. However, the authors also found in their metaanalysis that carbon substrate and oxygen availability functioned as distal controls. In this study, variability of COD and DO were not associated with community composition. However, because the denitrifying biofilter system is designed to provide the appropriate carbon substrates and anoxic environment for denitrification, it is possible that the variation of these parameters in this study were not enough to effect significant community differences.

Groups of variables with significant Mantel coefficients among all sites generally were also significant at individual sites, with several exceptions. The majority of these exceptions were at the FP03 site (inlet nitrate, pH, depth). One explanation for this result might be that for the majority of the time-series study, there was no flow control at FP03, meaning that the water level was very low. As increased inundation typically characterizes deeper depths in the biofilter system, drier conditions at the 1.52 m depth at FP03 may account for little community difference by depth, and by pH and inlet nitrate (as little water was actually in contact with woodchips). Supporting this conclusion is the result that moisture content was significantly, and substantially, associated with microbial communities at all biofilter sites. Therefore, those areas at FP03 that did have more inundation had different community structures, but these were not universally associated with depth.

Additionally, microbial communities at the different biofilter sites showed different associations with flow parameters. Because of different flow regimes at each of the sites (Table 5), these differences are reasonable. As a particular example, at the FP07 site, flow parameters were substantially linked to bacterial community composition, whereas they were not at other sites. Because the highest inlet nitrate concentrations at the site occurred during times of somewhat increased flow (Figure 22), this result may be due to the influence of available nitrate rather than to flow, or it may be that the comparatively low flow rates at FP07 (Table 5) affect community structure differently.

Determination of representative populations

In the previous section, I demonstrated that community composition is linked to nitrate removal, and that various environmental and operational parameters are associated with variation in this community composition. Although studying the overall microbial community in the biofilters is important, in this research we were most concerned with discerning influential populations or factors as possible points of control for the systems. Because hundreds of distinct fungal and bacterial populations were observed in the three biofilter sites studied, to analyze the relationship of each one to system performance was intractable. Therefore, an effort was made to reduce the number of populations analyzed to those that were most representative of the system.

To find the subsets of bacterial and fungal populations that were most representative of community structure, the BVStep procedure (Clarke and Warwick, 1998) was used. This method uses a stepwise Mantel test to compare subsets of communities to the overall community to identify a subset that best represents the structure of the whole community. This procedure was performed for bacteria and fungi separately, both on

samples from all sites together to identify those populations best representing community differences between sites and on samples from the same site to identify those populations that best represent fluctuations within a site. Conducting the procedure on sites individually also acknowledges a limitation of fragment analysis, namely that one cannot be assured that fragments of the same length necessarily result from identical species. Identifying representative populations for each site independently may reduce the liklihood of this error.

Table 14. Most representative populations for bacterial and fungal community structure.

Domain	Representative populatons	R_m
Bacterial:		
All sites	B488, B720, B755, B760, B765, B770, B780, B785, B793, B799, B805, B811, B848, B857, B914	0.800 ($p<0.001$)
DE01	B370, B464, B488, B755, B760, B765, B785, B793, B799, B882, B891, B914	0.806 ($p<0.001$)
FP03	B480, B646, B720, B760, B765, B770, B778, B793, B799, B805, B811, B914	0.803 ($p<0.001$)
FP07	B488, B545, B760, B765, B799, B805, B848, B878, B914	0.805 ($p<0.001$)
Fungal:		
All sites	F325, F430, F449, F462, F501, F521, F527, F554, F555, F559, F566, F613, F617, F725, F758, F771	0.803 ($p<0.001$)
DE01	F462, F527, F 566, F725, F771	0.800 ($p<0.001$)
FP03	F501, F521, F544, F554, F555, F559, F566, F613, F758, F800	0.802 ($p<0.001$)
FP07	F325, F449, F456, F527, F533, F555, F566, F613	0.813 ($p<0.001$)

F = fungal population, B = bacterial population

Populations from the BVStep procedures, numbering between five and 16 for different communities and sites, and representing approximately 80% of community variation, are listed in Table 14.

It is of note that the BVStep methodology identifies populations that best reflect fluctuations in community structure, not considering other factors (such as nitrate removal). However, because these populations represent the majority of the community variation and are of manageable number, they were used to investigate the range of

responses of biofilter populations to each other and to environmental and operational parameters.

Correspondence Analysis plots

Because many of the factors examined in this study may covary, the relationships between them are difficult to clearly delineate with standard statistical analyses. For example, as discussed above, inlet nitrate concentration at the FP07 site may obscure the true relationship between flow and community composition. Correspondence analysis plots can more clearly depict relationships in a multidimensional dataset because all variables can be visualized at once.

Correspondence analysis can either be conducted such that axes represent theoretical environmental gradients revealed by the data ("unconstrained," or "indirect gradient" correspondence analysis), or such that the environmental gradient axes are combinations of environmental factors chosen *a priori* ("constrained," "direct gradient", or "canonical" correspondence analysis—CCA) (Legendre and Legendre, 1998). Unconstrained plots are useful for assessing the overall structure of community data because the environmental gradients chosen *a priori* for a study may not be those that cause the greatest species variation. Constrained plots, on the other hand, are convenient for visualizing how communities vary with particular environmental parameters or sets of parameters.

Other explanatory factors can also be projected onto the plots as vectors to show their variation with communities and between each other. It is important to remember that these arrows are projections and thus show only the variation with respect to the axes plotted.

For CA plots in this section, only populations are shown to view their variation with each other and environmental factors; the sample points are masked. Furthermore, although all populations were used to create the plots, only representative populations are shown to simplify plots and to allow visualization of the behavior of potentially important populations. I constructed both unconstrained correspondence analysis plots (to assess the overall structure of communities) and correspondence analysis plots constrained on one axis by nitrate removal data (to show the variation of communities and other environmental and performance factors with nitrate removal). Plots were constructed both using data from all three biofilter sites, and also data separated by biofilter site to show differences in community structure and variation between sites. Plots from data among all sites include both representative populations across sites and from each individual site for completeness.

Unconstrained correspondence analysis plots

Variation in community with biofilter site, depth, and nitrate removal was observed in unconstrained correspondence analysis plots (Figure 40, Figure 41). Differences between communities at different biofilter sites are shown by vectors in the direction of increased membership in a site. These vectors show that some bacterial or fungal populations are more associated with a particular site than others. For example, bacterial population B370 is associated with the FP07 biofilter (its position is near the FP07 vector). ANOSIM tests using all bacterial or fungal populations confirm that the three biofilter sites have significantly different communities (bacterial: $R=0.186$, $p<0.001$; fungal: $R=0.250$, $p<0.001$). Additionally, the plots show that populations varied with depth and nitrate

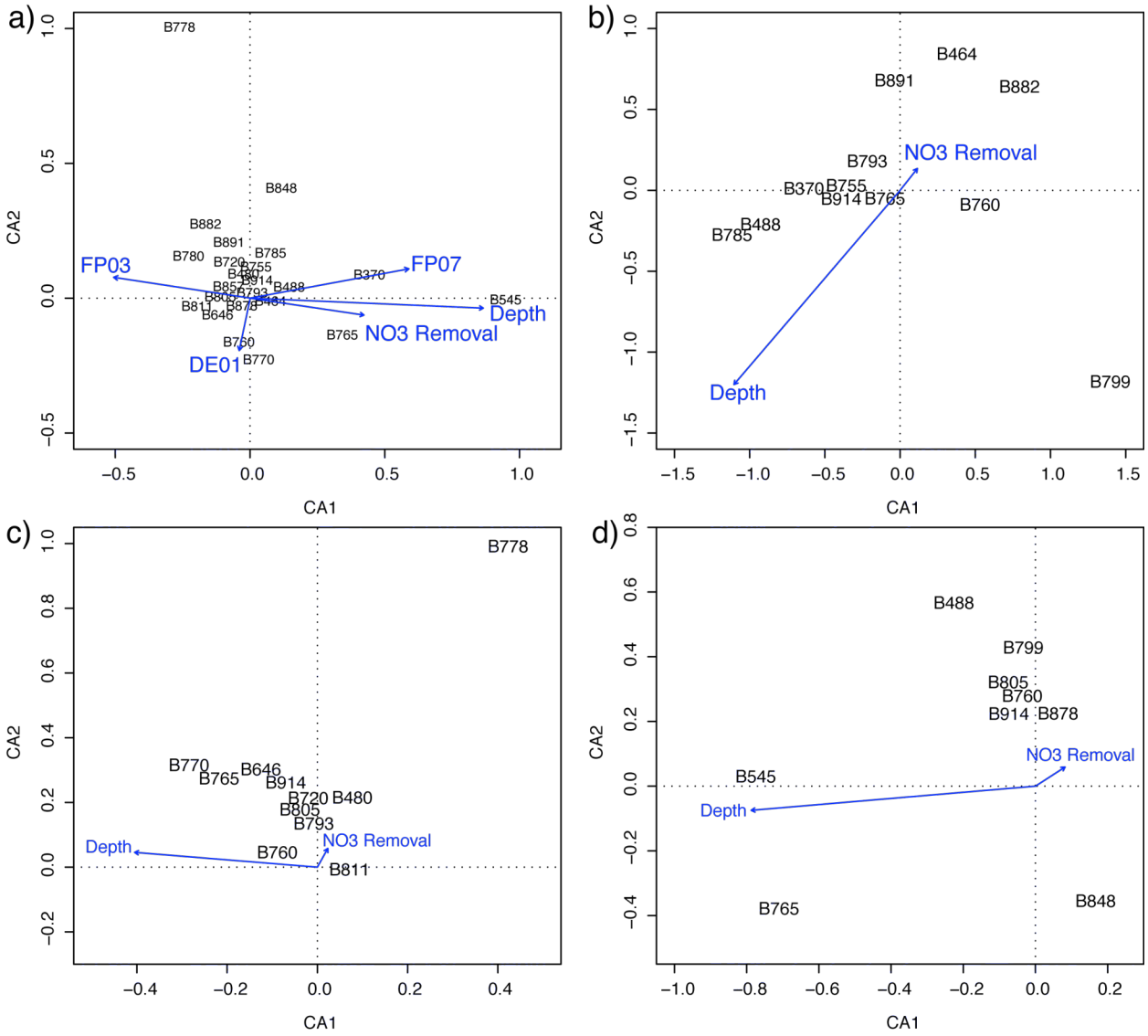

Figure 40. Correspondence analysis plots of ARISA community data from time-series biofilter woodchip samples. Axes represent theoretical environmental gradients. Plots are constructed using data from all biofilter sites (a.), or alternatively from biofilter sites DE01 (b.), FP03 (c.), or FP07 (d.). Points represent representative bacterial populations as chosen by BVStep. Arrows represent the relationship between depth, nitrate removal, or biofilter site with populations. The value of the parameter increases in the direction of the arrow, and the magnitude represents the strength of the correlation with the axes.

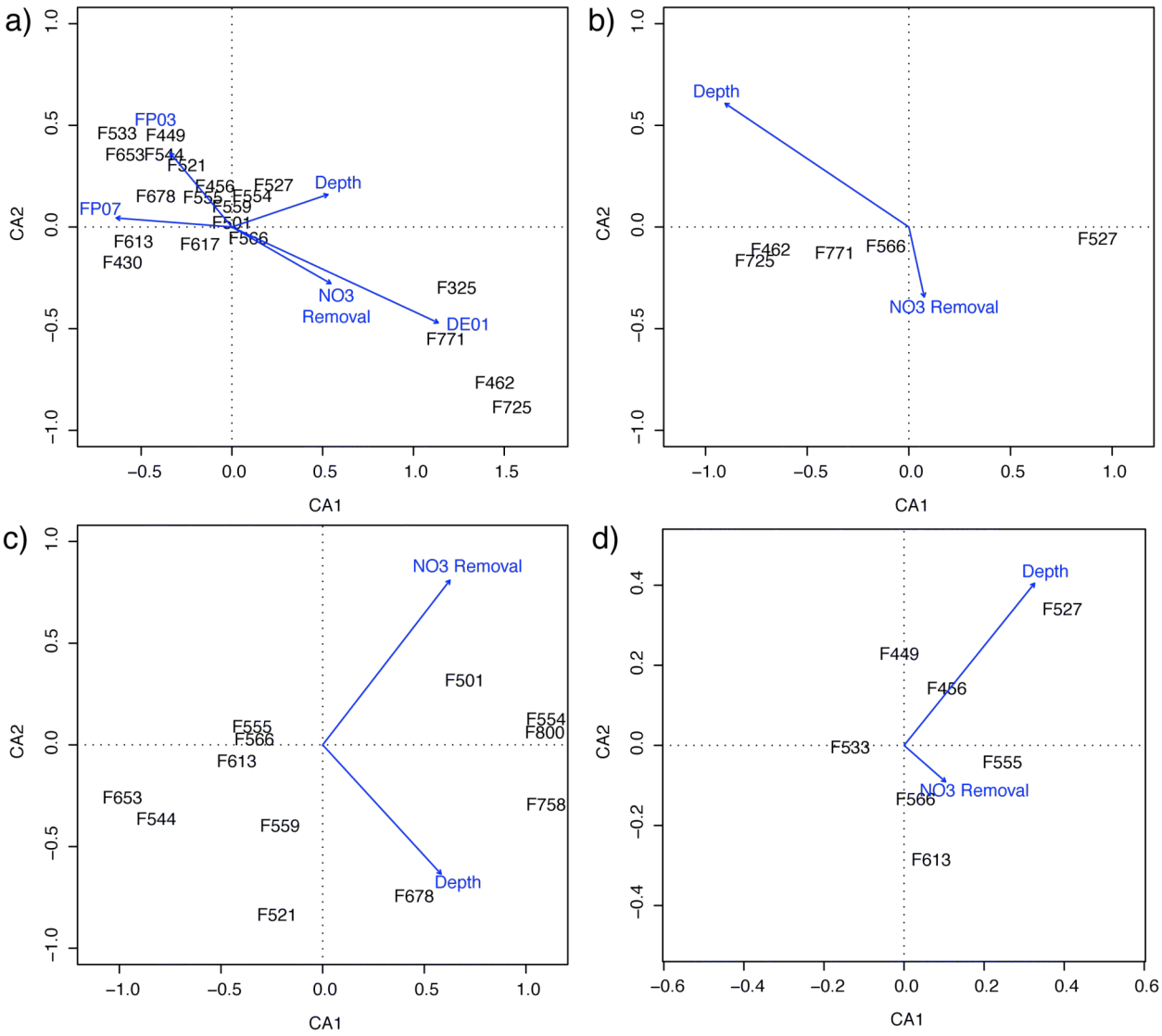

Figure 41. Correspondence analysis plots of fARISA community data from time-series biofilter woodchip samples. Axes represent theoretical environmental gradients. Plots are constructed using data from all biofilter sites (a.), or alternatively from biofilter sites DE01 (b.), FP03 (c.), or FP07 (d.). Points show representative fungal populations as chosen by BVStep. Arrows represent the relationship between depth, nitrate removal, or biofilter site with populations. The value of the parameter increases in the direction of the arrow, and the magnitude represents the strength of the correlation with the axes.

removal, as shown with vectors in the direction of increase of that factor. This indicates that certain populations are more likely to be found at different depths of the biofilter and that some populations are associated with nitrate removal.

Separating the data by biofilter shows that in all three biofilters (Figure 40b-d, Figure 41b-d), populations also showed variation with depth and nitrate removal, and that

depth has a larger relationship with variation in community than does nitrate removal. This may reflect the smaller variations in nitrate removal within the same site as opposed to between sites. Additionally, except for the bacterial community at site DE01, nitrate removal has a roughly orthogonal relationship with depth in the direction of the first two axes. This suggests that variability related to depth and variability related to variations in nitrate input and transformation have minimal connection.

A comparison of the inertias of the ordinations (which measure overall dispersion of points from the center) shows that the variability of bacterial sample communities between the three sites (All = 8.793, DE01 = 6.343, FP03 = 7.540, and FP07 = 6.656) was comparable, but was less than that of fungal sample communities (All = 21.42, DE01 = 12.03, FP03 = 14.49, FP07 = 15.1). Additionally, site DE01 showed less variability in its fungal community than did sites FP03 and FP07. Because correspondence analysis plots populations along axes of environmental gradients, differences in community patterns amongst the three sites are likely due to the variation of environmental conditions.

Correspondence analysis plots constrained by nitrate removal

Because nitrate removal is the functional goal of the denitrifying biofilter technology, to better understand factors that may influence nitrate removal, constrained correspondence plots were constructed with nitrate removal as the environmental gradient for the horizontal axis. The vertical axes of these plots are unconstrained, and therefore represent other unknown environmental gradients that are related to community variation. It is important to note that nitrate removal data was only available for part of this study, and the majority of this data was taken in the winter and spring months. However, the biofilters often have no flow during the summer and early autumn months,

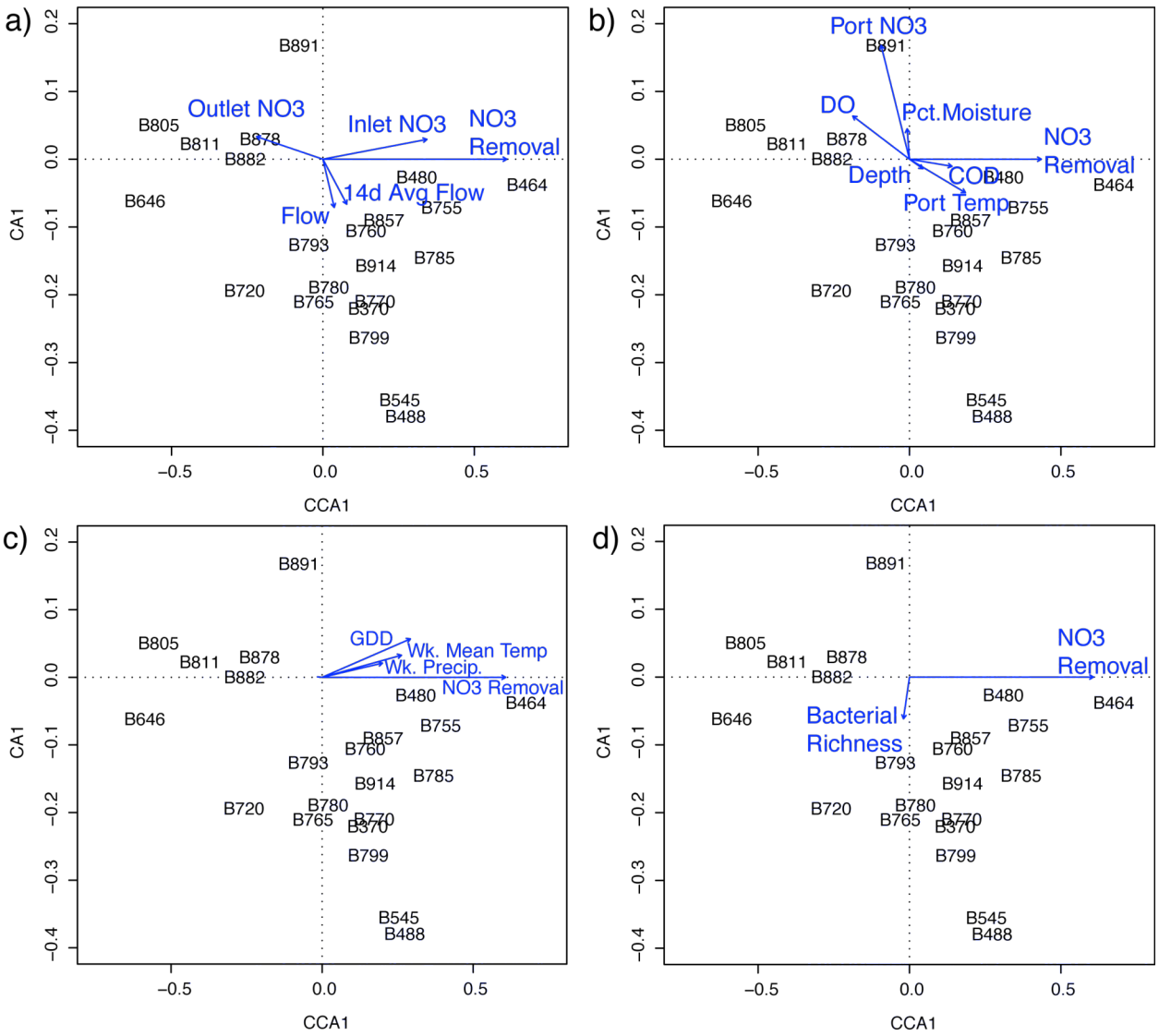

Figure 42. Constrained correspondence analyses plots of representative bacterial populations from biofilter woodchips. Correspondence analysis is constrained by nitrate removal on the horizontal axis but are unconstrained in along the vertical axis. Therefore, changes in position along the horizontal axis show changes in relationship to nitrate removal. Points show representative bacterial populations. Arrows represent the relationship of environmental factors with populations. The value of the parameter increases in the direction of the arrow, and the magnitude represents the strength of the correlation with the axes.

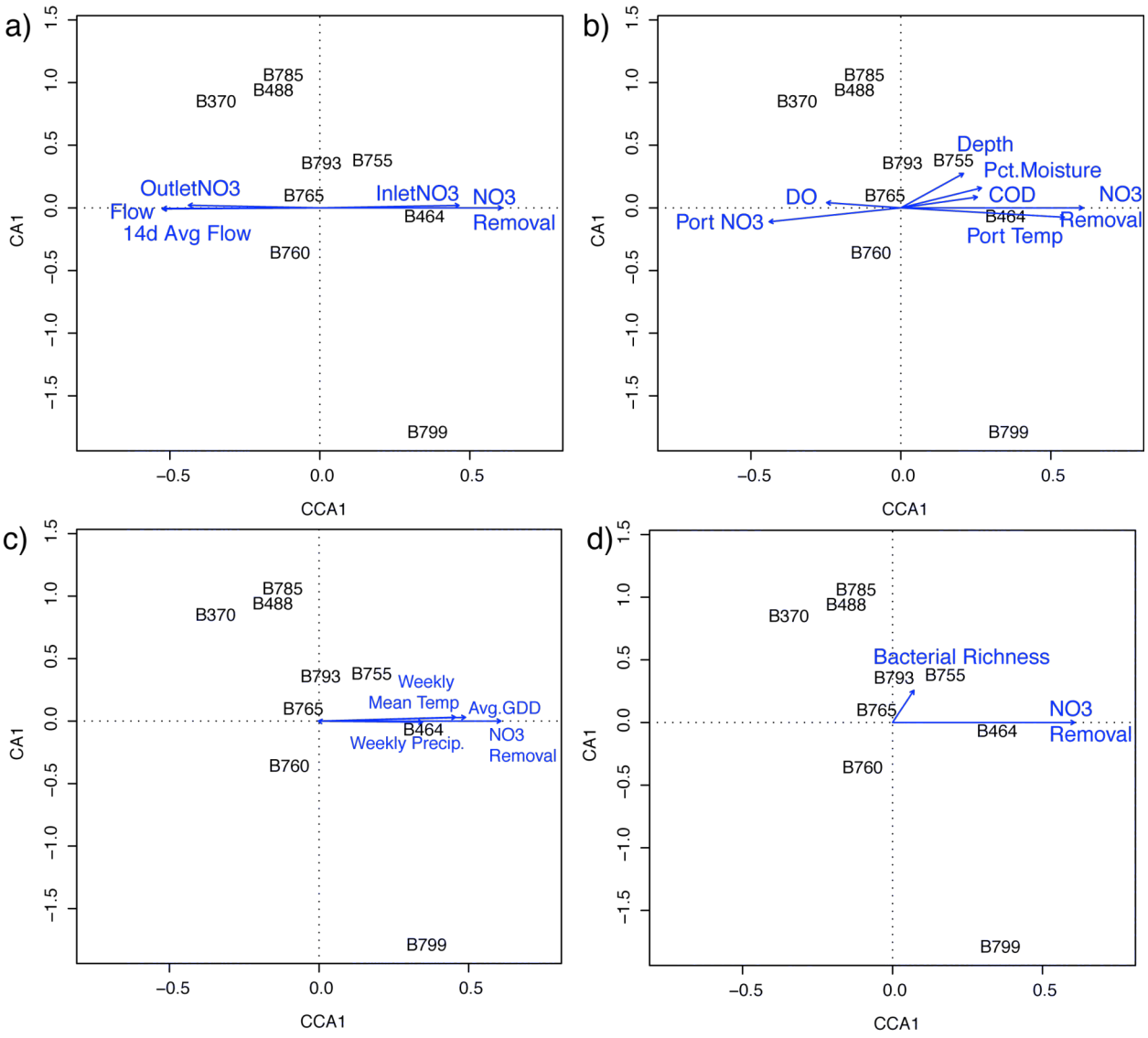

Figure 43. Constrained correspondence analyses plots of representative bacterial populations from biofilter site DE01 woodchips. Correspondence analysis is constrained by nitrate removal on the horizontal axis but are unconstrained in along the vertical axis. Therefore, changes in position along the horizontal axis show changes in relationship to nitrate removal. Points show important fungal populations. Arrows represent the relationship of environmental factors with populations. The value of the parameter increases in the direction of the arrow, and the magnitude represents the strength of the correlation with the axes.

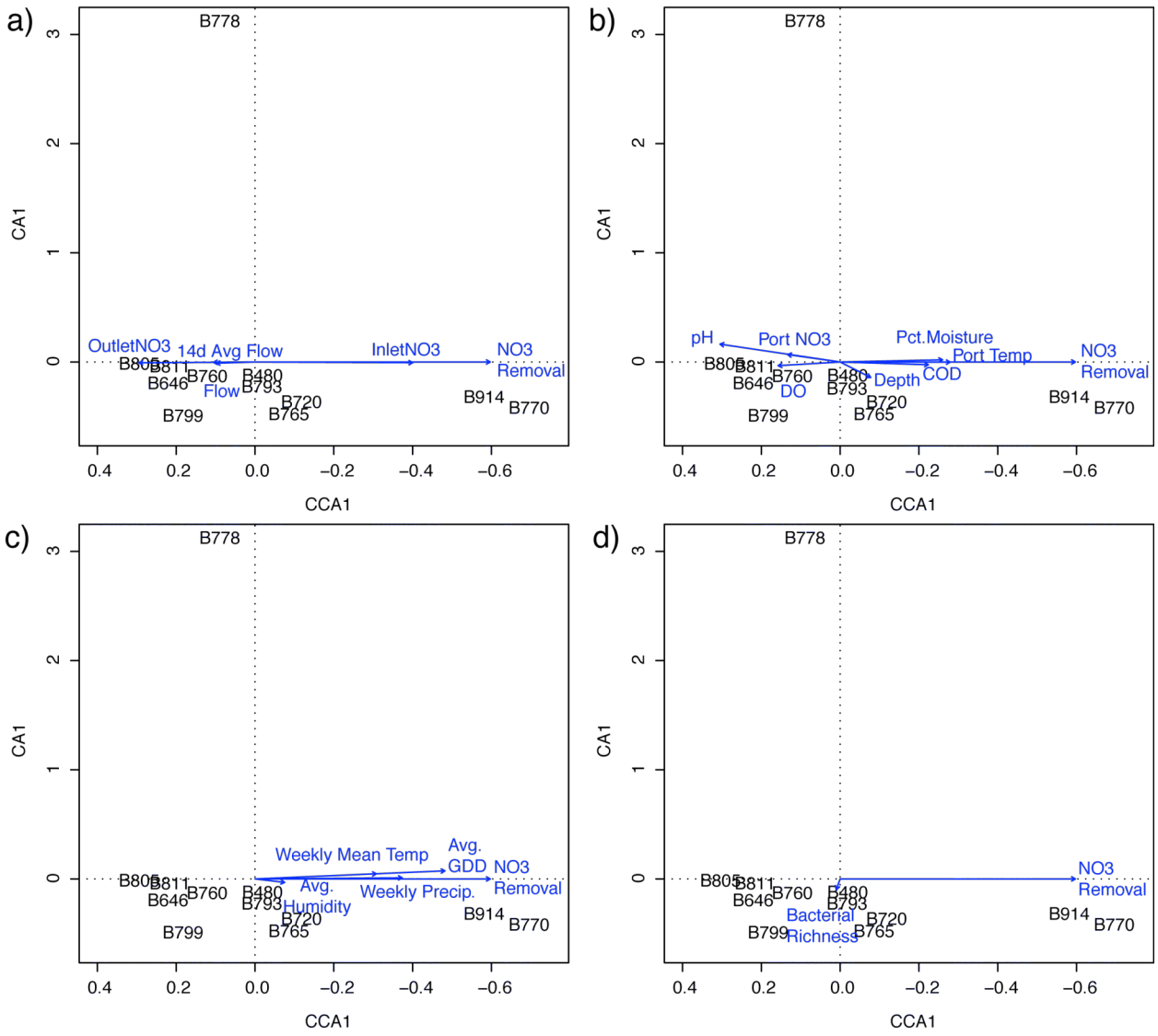

Figure 44. Constrained correspondence analyses plots of representative bacterial populations from biofilter site FP03 woodchips. Correspondence analysis is constrained by nitrate removal on the horizontal axis but are unconstrained in along the vertical axis. Therefore, changes in position along the horizontal axis show changes in relationship to nitrate removal. Points show representative fungal populations. Arrows represent the relationship of environmental factors with populations. The value of the parameter increases in the direction of the arrow, and the magnitude represents the strength of the correlation with the axes.

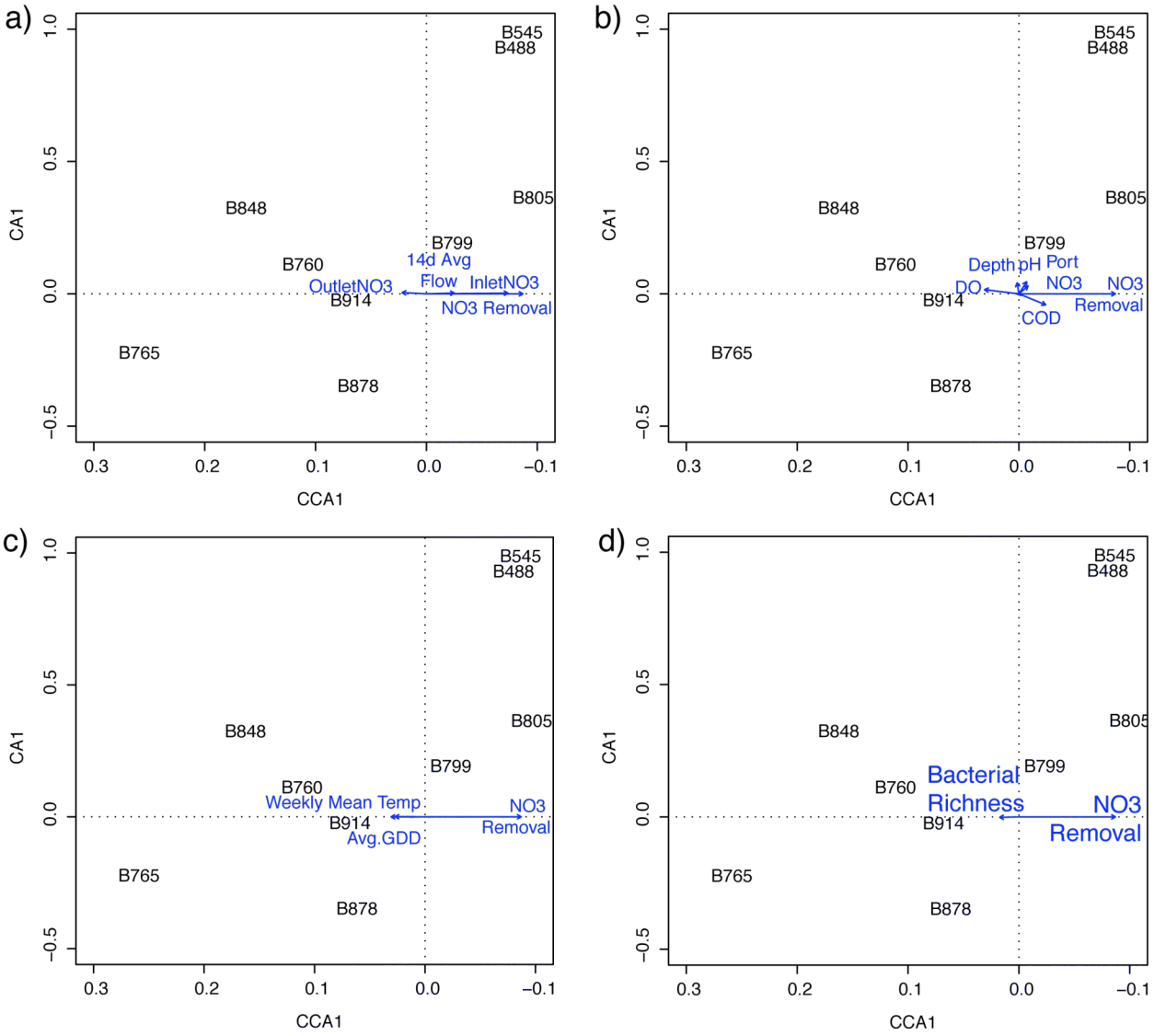

Figure 45. Constrained correspondence analyses plots of representative bacterial populations from biofilter site FP07 woodchips. Correspondence analysis is constrained by nitrate removal on the horizontal axis but are unconstrained in along the vertical axis. Therefore, changes in position along the horizontal axis show changes in relationship to nitrate removal. Points show representative fungal populations. Arrows represent the relationship of environmental factors with populations. The value of the parameter increases in the direction of the arrow, and the magnitude represents the strength of the correlation with the axes.

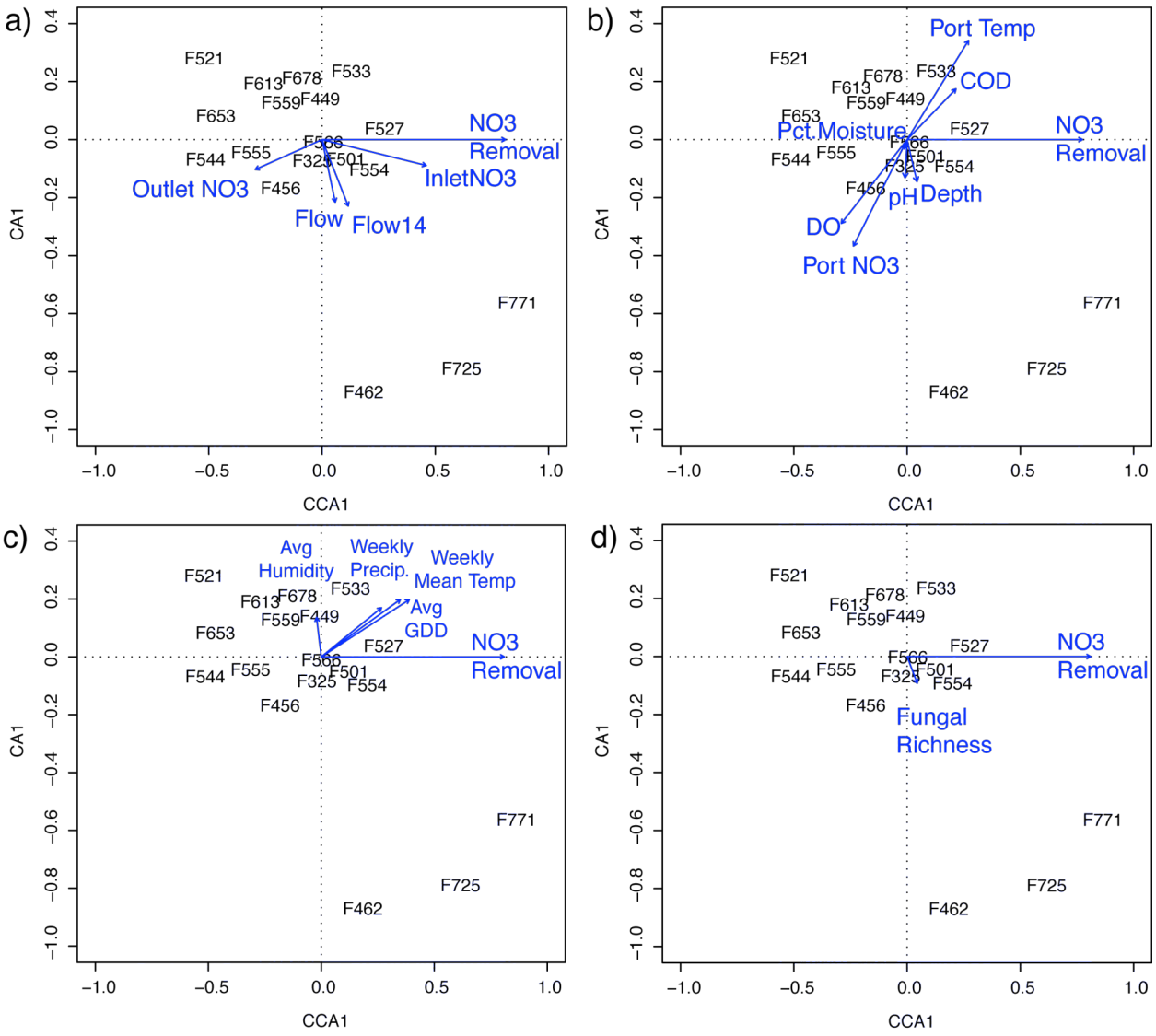

Figure 46. Constrained correspondence analyses plots of representative fungal populations from all biofilter sites. Correspondence analysis is constrained by nitrate removal on the horizontal axis but are unconstrained in along the vertical axis. Therefore, changes in position along the horizontal axis show changes in relationship to nitrate removal. Points show representative bacterial populations. Arrows represent the relationship of environmental factors with populations. The value of the parameter increases in the direction of the arrow, and the magnitude represents the strength of the correlation with the axes.

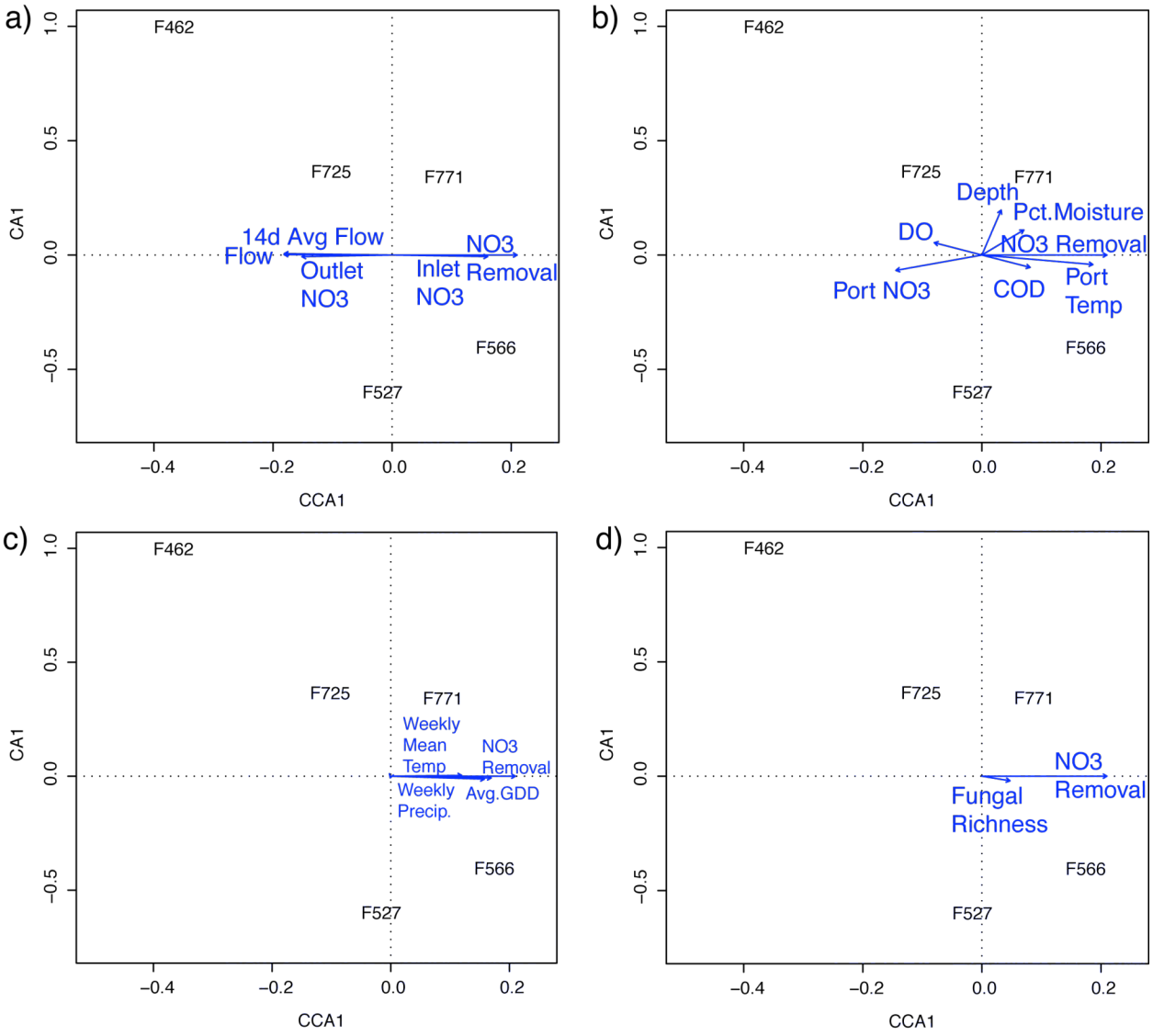

Figure 47. Constrained correspondence analyses plots of representative fungal populations from biofilter site DE01 woodchips. Correspondence analysis is constrained by nitrate removal on the horizontal axis but are unconstrained in along the vertical axis. Therefore, changes in position along the horizontal axis show changes in relationship to nitrate removal. Points show representative fungal populations. Arrows represent the relationship of environmental factors with populations. The value of the parameter increases in the direction of the arrow, and the magnitude represents the strength of the correlation with the axes.

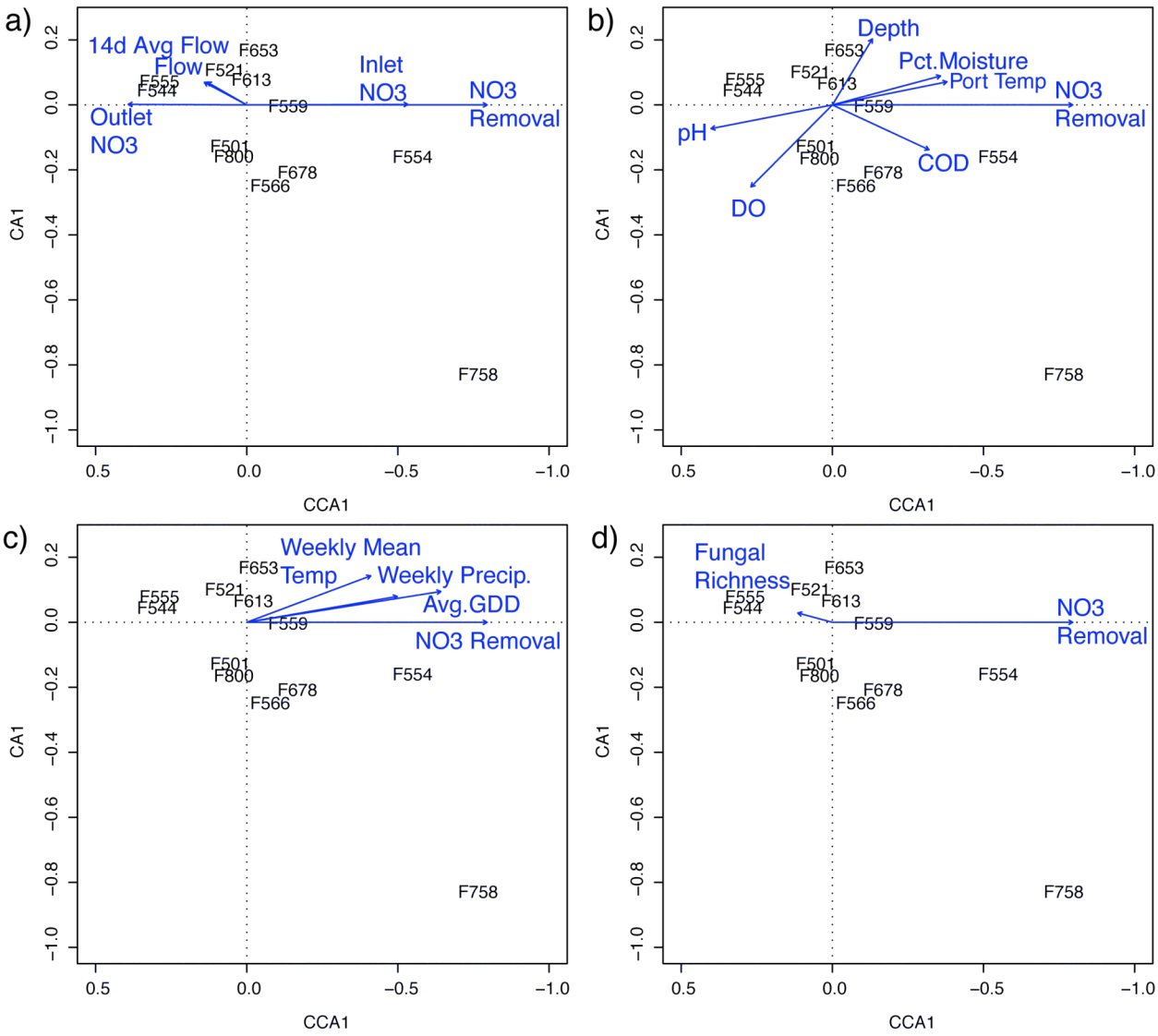

Figure 48. Constrained correspondence analyses plots of representative fungal populations from biofilter site FP03 woodchips. Correspondence analysis is constrained by nitrate removal on the horizontal axis but are unconstrained in along the vertical axis. Therefore, changes in position along the horizontal axis show changes in relationship to nitrate removal. Points show representative fungal populations. Arrows represent the relationship of environmental factors with populations. The value of the parameter increases in the direction of the arrow, and the magnitude represents the strength of the correlation with the axes.

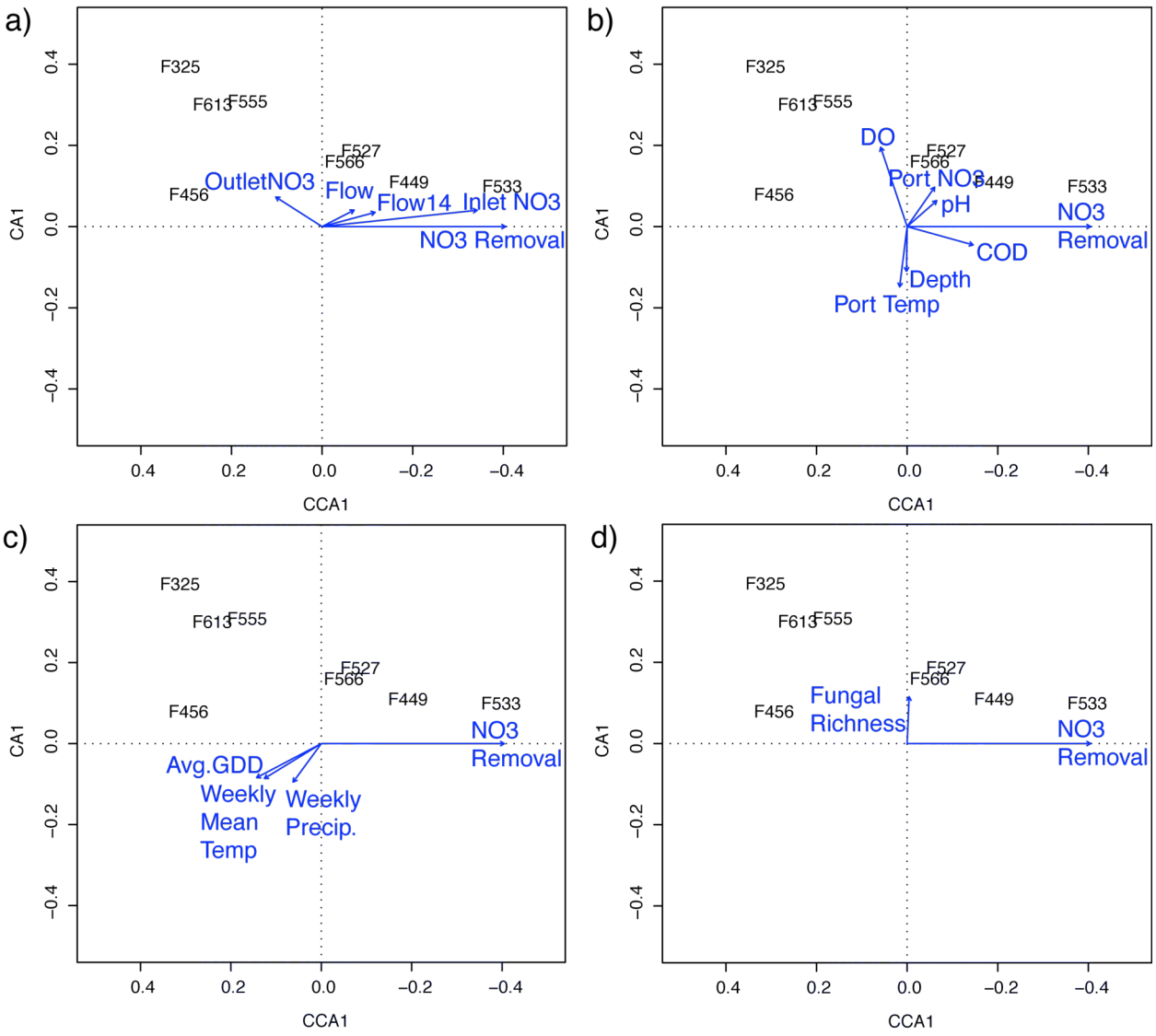

Figure 49. Constrained correspondence analyses plots of representative fungal populations from biofilter site FP07 woodchips. Correspondence analysis is constrained by nitrate removal on the horizontal axis but is unconstrained along the vertical axis. Therefore, changes in position along the horizontal axis show changes in relationship to nitrate removal. Points show representative fungal populations. Arrows represent the relationship of environmental factors with populations. The value of the parameter increases in the direction of the arrow, and the magnitude represents the strength of the correlation with the axes.

where high temperatures and crops result in drier conditions, so this data is a reasonable approximation of the nitrate removal.

When viewing plots created for individual biofilters, it is helpful to keep in mind the variation of these factors by biofilter. A particular biofilter may, for example, have significantly higher COD concentrations. Therefore, a vector showing the direction of

increased COD concentration on this plot would show COD concentration *relative to the mean value* for this site. This vector would thus not be directly comparable to the vector on a different correspondence analysis plot.

Populations associated with increased or decreased nitrate removal:

The inertia explained by the constrained (nitrate removal) axis in canonical correspondence analysis plots including samples from all sites (Figure 42, Figure 46) were 10.1% for the bacterial community and 19.7% in the fungal community. Because plots were constructed using all bacterial or fungal populations (all but representative populations are masked), these measures reflect that the composition of overall bacterial or fungal community is related to nitrate removal or conditions that increase nitrate removal. These plots therefore corroborate results of partial Mantel tests that were conducted against nitrate removal (Table 9); that is, variation in community is significantly related to differences in nitrate removal.

The CCA plots among all sites further suggest that several bacterial and fungal populations are related to increased or decreased nitrate removal (Figure 42 and Figure 46); that is, populations are found at various points along the constrained axis. However, nitrate removal appears to be unrelated to bacterial or fungal richness, as projections of richness are almost entirely orthogonal to the nitrate removal axis.

We can compare the constrained correspondence plots using data from all three biofilters with those of bacterial and fungal populations at the three different biofilter sites (Figure 43-Figure 45 and Figure 47-Figure 49). The proportions of total inertia represented by the constrained axes (nitrate removal) of these plots were generally similar

Table 15. Significant partial Mantel coefficients between individual representative populations or environment and nitrate removal, with associated CCA1 axis scores.

Population	Partial Mantel Coefficient Population, $R_{p,e}$ (p-value)	Partial Mantel Coefficient Environment, $R_{e,p}$ (p-value)	Score on CCA1 (positive NO_3 Removal)
All Sites (Bacterial):			
B480	0.216 (0.002)*	0.165 (0.001)**	0.2782
B464	0.191 (0.003)*	0.179 (0.001)**	0.6429
B755	0.109 (0.016)*	0.173 (0.001)**	0.3604
B770	0.0822 (0.036)*	0.172 (0.001)**	0.1404
B799	0.140 (0.029)*	0.175 (0.001)**	0.1210
All Sites (Fungal):			
F566	0.114 (0.020)*	0.174 (0.001)**	0.0132
F725	0.130 (0.009)*	0.172 (0.001)**	0.5748
F771	0.189 (0.002)*	0.177 (0.001)**	0.8226
DE01 (Bacterial):			
B464	0.252 (0.001)**	0.612 (0.001)**	0.3169
B755	0.168 (0.006)*	0.594 (0.001)**	0.1441
B799	0.178 (0.023)*	0.601 (0.001)**	0.3276
B891	0.273 (0.003)*	0.596 (0.001)**	0.5602
DE01 (Fungal):			
F771	0.127 (0.034)*	0.601 (0.001)**	0.0718
FP03 (Bacterial):			
B770	0.363 (0.003)*	0.355 (0.001)**	0.6715#
B914	0.247 (0.007)*	0.346 (0.001)**	0.5570#
FP03 (Fungal):			
F554	0.202 (0.018)*	0.345 (0.001)**	0.5175#
FP07 (Bacterial):			
B760	0.092 (0.055)	0.117 (0.016)**	0.1204
FP07 (Fungal):			
F613	0.173 (0.013)*	0.136 (0.010)*	0.2619

Where $R_{x,y}$ is the partial Mantel statistic for the correlation of x, accounting for y, and p = population and e = environment. Environment includes: inlet nitrate (mg/L), COD (mg/L), DO (mg/L), woodchip moisture content (%), port temperature (C), instantaneous flow (L/s), 14 d average flow (L/s), weekly precipitation (cm), and weekly average temperature (C). Mantel tests include data from all sites, or from a particular site as labeled, and the associated CCA plot using data from all sites (Figure 42, Figure 46) or from individual sites (Figure 43-Figure 45, Figure 47-Figure 49).

* denotes significance at the α=0.05 level

** denotes significance at the α=0.001 level

because the CCA1 axis for the FP03 site is in the direction of negative nitrate removal, scores are negative along the axis, but positive in the direction of nitrate removal

to those of the plots from all sites (DE01 Bacterial: 10.4%, FP03 Bacterial: 11.3%, FP07 Bacterial: 5.37%, DE01 Fungal: 15.3%, FP03 Fungal: 8.0%, and FP07 Fungal: 12.7%), except for those of the FP07 bacterial plot and the FP03 fungal plot, which were somewhat lower. This suggests that parameters other than nitrate removal (or those factors that covary with nitrate removal) have greater association with community at these sites. As in

the combined CCA plots, projections for bacterial and fungal richness in CCA plots for individual sites, are of small magnitude compared to most other factors, and do not exhibit consistent behavior.

Examining specific populations, of those populations that are representative of more than one site, several (eg. B760, B793, F555, F566) are consistently positioned along the constrained (nitrate removal) axis. However, others (eg. B765, B799, B805) have differing correlations to nitrate removal.

Because position along the nitrate removal (CCA1) axis also shows relationship to those factors that may covary with nitrate removal, it is also useful to partition out the influence of other environmental factors on nitrate removal. To quantify only the relationship between a particular population and nitrate removal, I performed partial Mantel tests between each representative population and nitrate removal, partializing out the effects of environment. These tests were performed on all 39 representative populations, whether they represent community fluctuations at all sites, or from individual sites (see Table 14). The 13 populations with significant associations with nitrate removal are shown in Table 15; that is, given similar environmental conditions, these populations are linked to higher or lower nitrate removal. For reference, both the partial Mantel coefficient of environment and the population's score on the nitrate removal (CCA1) axis on the corresponding CCA plot are also shown.

Each group of representative populations had at least one population with a significant partial Mantel statistic. The range of the significant partial Mantel statistics was between 0.109 to 0.363, which was generally on the order of the partial Mantel statistics for environment among all sites. At the DE01 site, the partial Mantel statistics for

environment were higher, as was also shown in partial Mantel tests against all populations (Table 9). The number of populations that were significantly associated with variations in nitrate removal was greater among all sites than for individual sites. This result suggests that variation between sites is greater than variation within sites either for nitrate removal (as also supported by Table 5, Figure 20-Figure 22), or community (as also supported by ANOSIM-GS and CA plots, see Figure 29, Figure 30, Figure 40, Figure 41), or both.

The range of scores on the nitrate removal (CCA1) axis in the corresponding CCA plot for populations with significant partial Mantel statistics was 0.0132 to 0.8226, showing that some populations are more strongly associated with nitrate removal than others. All axis scores were positive along the nitrate removal direction (ie, there were no populations that were significantly associated with negative variations in nitrate removal), indicating that there is no evidence that the presence of specific representative populations actively inhibit nitrate removal.

Populations that appear to be particularly influential (based upon a high partial Mantel statistic, >= 0.25, and a high score along the nitrate removal axis, >=0.5) are B464, B770, B891, B914, and F554. Because ARISA does not conclusively identify populations, but show that they are distinct, the cause of these associations cannot be presumed. However, significantly associated populations may be denitrifying species or species that have commensal relationships with denitrifying species.

Relationships between performance and climate parameters and nitrate removal in CCA plots

To further investigate conditions or combinations of conditions that favor nitrate removal and populations associated with them, I examined the overlaid environmental parameter vectors in constrained correspondence plots. The variation of performance parameters with bacterial and fungal populations and nitrate removal in the combined dataset (Figure 42a and Figure 46a) shows that while nitrate removal, as expected, was associated with high inlet nitrate, and negatively associated with outlet nitrate, both instantaneous flow and the 14 d rolling average flow were not strongly linked to nitrate removal. In contrast, for correspondence plots separated by biofilter (Figure 43a, Figure 44a, Figure 45a, Figure 47a, Figure 48a, and Figure 49a), the relationships between flow, nitrate removal, and populations varied: at DE01 and FP03, flow and nitrate removal behaved oppositely (Figure 43a-Figure 44a, Figure 47a-Figure 48a); and at FP07, flow and nitrate removal acted similarly (Figure 45a, Figure 49a). Although chemical transformations of wetlands and other similar systems are frequently decreased by high flow rates (Gutknecht et al., 2006), in our case nitrate removal does not appear to be consistently linked to flow amongst all biofilters. These results corroborate those of Spearman correlations between nitrate and flow for individual sites (Table 15).

Bearing in mind that the mean flow through FP07 is much less than that of the other two sites, the relationships between flow parameters and nitrate removal in CCA plots again suggest that nitrate removal has an optimum flow rate. In the FP07 biofilter, flow is lower than this optimum (so increased flow also increases nitrate removal), whereas flow in the DE01 and FP03 biofilters is greater than the optimum (so decreased flow decreases

nitrate removal). Furthermore, that the relationships of flow and nitrate removal to bacterial populations are sometimes not related suggests that populations may be associated with good nitrate removal regardless of flow rate. This result is also supported by the results of the partial Mantel tests in Table 15, which show significant associations between nitrate removal and certain populations, when controlling for environment.

Relationships between climate variables and bacterial and fungal populations in CCA plots are in line with the results of the Spearman correlation tests (Table 8). Weekly temperature and precipitation, and growing degree days are positively linked overall to nitrate removal, except for at FP07. At this site, while nitrate removal is consistent, it is marginally better in the winter months (Figure 22). Humidity appears to have a weak overall relationship on nitrate removal.

Relationships between biofilter environment parameters and nitrate removal

The environmental conditions within biofilter sites showed substantial relationships with community structure and with nitrate removal, corroborating Mantel tests against environmental variables (Table 10-Table 13).

Correspondence plots from both bacterial and fungal communities (Figure 42-Figure 49) show that depth and moisture content are major environmental gradients in structuring microbial communities. These two variables typically trend similarly, but not identically. As moisture content and inundation frequency generally (but not universally) increases at depth (see *Spatial differences in environment and performance*), similar trends are expected. Overall, the positions of moisture content and depth in CCA plots suggest that, while they are associated with nitrate removal, they also are associated (to various

extents depending on site) with variation in microbial community that is not linked to nitrate removal. Increases in moisture content or depth did not appear to be strongly associated with specific representative populations in this set, but some groups of populations (ex. B464, B480, B755, and F771, and F725) appear generally in the direction of increasing depth and moisture content.

For both bacterial and fungal CCA plots, the magnitude of association between pH and the variation in community along the nitrate removal (CCA1) and first unconstrained axis (CA1) is very small (in many cases, too small to show on the plot). Because pH does have some significant Mantel correlations community differences (Table 10-Table 13), the CCA plots suggest that community differences associated with pH are neither in the direction of nitrate removal (CCA axis 1) or the first unconstrained axis (CA1), but may be important to other processes.

Overall, the CCA plots show expected relationships between COD, DO, port temperature and nitrate removal (see *2.1.1 Denitrification and parameters that influence it*), where COD and temperature are positively associated with nitrate removal and DO is negatively associated. However, in fungal CCA plots (Figure 46-Figure 49), DO and COD arrows have substantial components along the first unconstrained axis (CA1). Because COD and DO also show no significant Mantel correlations with fungal community (Table 10-Table 13), arrow projections may not reflect direct influences on community composition, but perhaps are related to other processes that do influence fungal community.

Considering port temperature, projection arrows are also nearly collinear with the nitrate removal axis in CCA plots for the DE01 and FP03 sites (Figure 43, Figure 44, Figure

47, Figure 48), as expected. At the FP07 site, however, port temperature either has a minimal projection onto the first two axes (Figure 45) or projection only along the first unconstrained axis (Figure 49). This may be caused by substantially elevated port temperatures at the FP07 site at certain time points (Table 5), note the upper range of port temperature at FP07), or indicate that community variation linked to port temperature is associated with processes not captured by the first two axes. Overall CCA plots show port temperature projections that include a substantial component in the unconstrained axis direction, however, this relationship may be confounded by the inclusion of site FP07, which, as noted, shows different associations with port temperature.

Overall in the correspondence plots, elevated port nitrate is generally associated with poorer nitrate removal, although this relationship is not perfectly consistent. At the FP07 site, increased port nitrate is somewhat associated with nitrate removal. Because this biofilter has the lowest overall inlet nitrate and lowest overall nitrate in ports (Table 5), this result may indicate that this biofilter generally does not reach its nitrate removal capacity. Therefore, increased nitrate flowing through the biofilter results in greater removal.

4.5.5 Implications of relationships in time-series data

The time-series dataset provides a wealth of information about the relationships between populations, performance, and environment. While the number and complexity of these relationships may seem overwhelming, we can make several general conclusions.

First, the three biofilter sites exhibit different performance, environmental characteristics, and, importantly for this study, microbial communities. Furthermore, a large amount of microbial community variability can be represented by a set of

representative fungal and bacterial populations. The assemblages of these populations likewise display variability between the three sites. This result is consistent with many studies that show significant differences in microbial communities at different denitrifying sites (Braker et al., 2001; Franklin et al., 2002; Rich et al., 2003; Rich and Myrold, 2004; Stres et al., 2004; Enwall et al., 2005; Boyle et al., 2006; Gutknecht et al., 2006; McGuinness et al., 2006; Cao et al., 2008; Kageyama et al., 2008; Kim et al., 2008; Peralta et al., 2010).

Secondly, some of the representative populations in the biofilter samples are more associated with good nitrate removal than others. This makes intuitive sense, as we can imagine that microbial populations in the biofilter perform a variety of functions, some of which may be directly or indirectly related to denitrification, and some not. Community composition appears to be more influential for denitrification than is microbial abundance, or even specifically denitrifier abundance (Rich et al., 2003; Peralta et al., 2010; Cavigelli and Robertson, 2000; Rich and Myrold, 2004; Dandie et al., 2008). Additionally, populations that have the capability for a particular function may not actively perform that function, as has been found for denitrifiers (Nogales et al., 2002; Wertz et al. 2009). Finding that there are important populations (whether by percentage of population or importance to a function) is typical for investigations of microbial technologies (Neef et al., 1996; Mergaert et al., 2001; Sakano et al., 2002; Enright et al., 2007).

Finding populations relevant to performance of the biofilter may allow us to monitor the suitability of a biofilter microbial community through them, and they are also targets for more controlled studies of the relationship of operational characteristics to function and community. Furthermore, that there are populations related to good nitrate removal suggests that artificial seeding with “good” microorganisms could lead to better

performance. Currently, we would be unable to do this, as phylogenic assignments are not available for these populations, but further study may yield this information.

Third, although individual populations were found to be associated with nitrate removal, overall population richness was not associated with nitrate removal. While this result may seem to call into question the theories linking diversity and stability and resiliency (Elton and Elton, 1958; Macarthur, 1955; Odum ,1971; Walker, 1992; Borrvall et al., 2000; Gunderson, 2000; Loreau et al., 2001; Hooper et al., 2005), the analysis in this work only applies strictly to the magnitude of nitrate removed, regardless of conditions. It is therefore possible that richness of bacterial or fungal populations may enhance nitrate removal at times of high flow or nitrate load. A separate analysis would be required to assess the effect of richness on resistance, resilience, and functional redudance (Allison and Martiny, 2008). Furthermore, population richness may not be directly associated with nitrate removal because it includes many populations that might not participate in denitrification. It is therefore possible that, for example, there exists a relationship between denitrifying population richness and nitrate removal.

Study of the interactions between performance, environment, and microbial populations also showed that, as suggested by Wallenstein et al. (2006b) for other denitrifying systems, both distal and proximal controls on denitrification are acting in the denitrifying biofilters that were studied in this work. On the proximal side, nitrate removal was strongly influenced by COD and DO. The amount and quality of COD has long been recognized as important to denitrification rate (Firestone, 1982; Weier et al., 1993; Beauchamp et al., 1989; Wallenstein et al., 2006b; Greenan et al., 2006; Gutknecht et al., 2006). In this study, the correlation between COD and nitrate removal was the largest

magnitude relationship with performance. Similarly, DO affects denitrification by encouraging aerobic respiration over the nitrate reduction pathway (Knowles, 1982; Zumft, 1997; Firestone, 1982; Cady and Bartholomew, 1961; Wallenstein et al., 2006b; Gutknecht et al., 2006). Therefore, that DO was significantly linked to poor nitrate removal in this study is reasonable.

Significant correlations between nitrate removal and flow, port temperature, and precipitation were also observed. Flow or moisture regime are frequently found to be an important factor in denitrification for wetlands, other types of water treatment systems, and for natural systems (Janda et al., 1988; Gayle et al., 1989; Mateju et al., 1992; Schipper et al., 2004; Gutknecht et al., 2006; Ishida et al., 2006; Wallenstein et al., 2006b; Kim et al., 2008). Increased moisture is typically linked to better denitrification (Gutknecht et al., 2006), however, increased flow through treatment systems can lead to short residence time and poor performance (Mateju et al., 1992; Schipper et al., 2004; Ishida et al., 2006). Increased temperature generally also enhances denitrification rates (Ritter and Eastburn, 1988; Firestone, 1982; Knowles, 1982; Mateju et al., 1992; Wallenstein et al., 2006b; Gutknecht et al., 2006; Stres et al., 2008; Braker et al., 2010), although some results showed an upper limit for temperature for at least certain denitrifying species (Wang et al., 1995).

In our systems, there appear to be optima for temperature and hydrologic parameters, as the relationship of nitrate removal to these parameters was related to the environmental characteristics of the site. For example, the site with lowest average flow (FP07) had better nitrate removal with increased flow, while those with higher average flows (DE01 and FP03) saw reduced nitrate removal with additional flow. These results suggest that the FP07 currently operates below the optimum flow rate for nitrate removal.

Likewise, increased precipitation enhanced denitrification at the drier sites (DE01 and FP03), but not at FP07, which experienced greater inundation towards the outlet. Port temperature was strongly correlated to nitrate removal at the DE01 and FP03 sites, but did not show significant relationship with nitrate removal at the FP07 site (Table 8), perhaps because the range of operating temperatures for FP07 was broader than for the other sites.

Some environmental factors—port temperature, inlet nitrate, and moisture content—appear to be distal controls on denitrification. More weakly, pH influences community structure. These findings are supported by other studies. Temperature has been found elsewhere to influence communities in denitrifying systems (Wallenstein et al., 2006b; Braker et al., 2010). In particular, my results are consistent with Braker (2010), who found that elevated temperatures not only increased denitrification rates in agricultural soils, but also led to differences in microbial community. Variation in inlet nitrate levels also appears to be a distal control on denitrification in the biofilters. Although Wallenstein (2006b) found that community and abundance in denitrifying ecosystems are primarily controlled by factors other than nitrate, some studies have shown that chronic nitrogen inputs such as fertilizer alter denitrifying communities (Enwall et al., 2005; Wolsing and Prieme, 2004; Wallenstein et al., 2006a). In our system inlet nitrate exhibited strong associations with the fungal community, but also more weakly with the bacterial community. Wallenstein et al. (2006b) also list moisture content and pH as distal controls for denitrification; recently Peralta et al. (2010) found that these factors were related to changes in bacterial and denitrifying (*nosZ*) communities in wetlands.

The results of the time-series study suggest several options for further optimizing the performance of denitrifying biofilter systems. Firstly, that there are populations

related to improved performance leads to the possibility of seeding highly performing populations or innoculant from currently well-performing biofilters into new or underperforming biofilters. From an ecological engineering perspective, the alternative ways of controlling denitrification in the biofilter system would be to alter the environmental conditions of biofilters to encourage well-performing communities (distal control) or to increase the rate of denitrification from the population already extant. Based on the results of this study, increasing port temperature and the moisture content of the woodchips may lead to better performing microbial communities. Furthermore, improving COD release into the biofilters, reducing DO, and optimizing the flow regime of each biofilter may lead to better nitrate removal by providing optimal conditions for the microbial denitrification. Because one of the strengths of the denitrifying biofilter technology is that it requires little energy or inputs, the challenge will be to enhance the environment of these systems in a low-maintenance way.

5. CONCLUSIONS AND FURTHER WORK

5.1 MAJOR CONCLUSIONS OF THIS WORK

In this work I have made substantial progress in understanding the microbial community of denitrifying biofilters and its relationship to denitrifying performance. I have also developed methodology and analysis techniques to enable further study of the study systems and of other microbial community systems.

Based on the results of denitrification assays, I found that bacteria mediate denitrification in the biofilter, but that fungi also indirectly affect denitrification, possibly by commensal relationships or by decomposition of woodchips into substrates. Furthermore, denitrification was observed in both biofilter water and woodchip samples. Based on these results, I focused on analysis techniques optimized for bacteria and collected both woodchip and water samples. Assays also showed denitrification in woodchip washes, indicating that cells are removed from the surface of the woodchips through the woodchip wash method. This technique was able to provide cells for examination using FISH and various molecular methods.

I adapted two methodologies for analyzing woodchip microbial communities. First, I investigated the applicability of FISH to woodchip and water samples from biofilter sites. Although minimizing the effects of autofluorescence in the woodchip matrix of biofilter samples proved challenging, a sample preparation method using glass beads to assist in removing cells from woodchips was developed that allowed debris to be separated from target cells. This method dramatically improved FISH results, and initial trials showed that a majority of cells from woodchip samples were of the γ-Proteobacteria group. Second, I

extracted DNA from biofilter samples and performed ARISA and *nosZ t*-RFLP to create community fingerprints of bacterial and denitrifying populations. The extracted DNA was also used by Matthew Porter to create profiles of the fungal community using fungal ARISA.

To facilitate analysis of spatial structure in microbial communities, I developed a new geostatistical method, ANOSIM-GS. This method combines a statistical test frequently used for analysis of microbial communities with geostatistical techniques to display community difference by separation distance and to determine the range at which samples are no longer significantly correlated to each other. The result is a flexible tool for characterizing spatial or temporal structure that is particularly well-suited to the large and complex ecological datasets common in microbial ecology and that integrates well with common microbial ecology analysis approaches. Although spatial structure has been less considered in microbial ecology than in traditional ecology, I hope that the ANOSIM-GS method will provide a convenient means for microbial ecologists to integrate space into their research more effectively and frequently.

I analyzed the spatial structure of the bacterial and denitrifying communities by sampling one biofilter intensively and using ARISA and *nosZ* t-RFLP community fingerprints. The overall bacterial community and the denitrifying community exhibited different spatial patterns. For the whole bacterial community (ARISA), recovered community richness (mean 54) varied by distance from the inlet of the biofilter ($p=0.009$), and recovered community evenness (mean 0.91) was significantly higher at a depth of 1.52 m than at 0.76 m ($p=0.0165$). The evenness of the denitrifying community (*nosZ* t-RFLP) was also higher at a depth of 1.52 m ($p=0.031$), but denitrifier richness did not vary across the biofilter ($p=0.173$). The bacterial community varied by depth and in the direction of

biofilter flow, but not in the crossflow direction, as assessed by MDS plots, ANOSIM tests, and ANOSIM-GS plots. The correlation range of bacterial communities was approximately 6 m at the 0.76 m depth, and approximately 10.5 m at the 1.52 m depth. The denitrifying community, on the other hand, did not exhibit a discernable spatial structure. Very slight differences in denitrifier community were observed in the cross-flow direction.

To determine the variation of biofilter communities with time, with performance characteristics, and with environmental parameters, data was collected from three biofilters on a regular basis beginning in November of 2008. This time-series dataset included biofilter woodchip and water samples for bacterial and fungal community analysis and physicochemical analysis as well as environmental parameters. Climate and biofilter performance characteristics were also obtained from other datasets.

I used a suite of analysis techniques to characterize the relationships between microbial community, time, performance, and environmental characteristics. First, using the ANOSIM-GS method, I determined that the communities exhibited seasonal variation. Temporal structure was different between bacterial and fungal communities, between biofilter sites, and at the 0.76 m and 1.52 m depths. Bacterial communities in the three biofilters showed evidence of annual cyclical behavior, with an approximate correlation range of 125 d. Fungal communities showed less annual patterning, and had correlation ranges between 100 and 200 d. Partial Mantel tests showed that, controlling for temporal variation, spatial structure still existed in the three study biofilters. These analyses suggest that microbial community in the biofilters is variable and responsive over time.

I examined the variability of environmental parameters and nitrate removal between biofilter sites and over time using nonparametric statistical analyses, basic

graphing, and correlograms. I found that flow, nitrate loading, COD, DO, moisture content, port nitrate and temperature, pH, and nitrate removal all varied significantly between biofilter sites. Additionally, all factors measured varied temporally, and port temperature and moisture content varied significantly by depth in certain months. Correlograms of environmental data also showed similar patterning to ANOSIM-GS plots, suggesting possible relationships.

Finally, I used correspondence analysis, correlations, and Mantel tests to study the relationships between microbial populations, performance, and environment. I identified 39 key bacterial and fungal populations that accounted for 80% of variability in the community structure between biofilter sites and within individual sites. I used partial Mantel tests combined with constrained correlation analysis plots to identify several of these populations that were associated with variability in nitrate removal when controlling for environmental variaion.

Partial Mantel tests and rank correlations were utilized to determine environmental and performance parameters that were also associated with increased nitrate removal and community variability. Several proximal and distal controls (Wallenstein et al., 2006b) on denitrification in the biofilter were identified. Increased COD, temperature and moisture content, and decreased DO appeared to increase rates of denitrification. These effects were distinct from effects on microbial community composition as shown by partial Mantel tests. Evidence that flow has an optimum value for denitrification was observed, as different responses to increased flow were found depending on the average biofilter flow. A clear relationship between bacterial or fungal richness and nitrate removal was not observed. However, differences in inlet nitrate, port temperature, moisture content, depth, and pH

were associated with variation in community composition. Controlling either these proximal or distal controls on biofilter systems should improve performance, as might seeding systems with "well-performing" populations.

5.2 Further Work

This research has demonstrated that it is possible to open the black box of ecologically engineered systems and to apply various tools to understand the interactions between their components. However, while the work in this dissertation has increased the scope of our understanding of communities in the biofilter, there is still much left to do.

The community fingerprints that were constructed with samples taken for the spatial and time-series datasets yielded a great amount of information, but I did not identify the taxonomy of populations within them. The FISH technique, as well as fragment sequencing, does this. Samples were preserved for FISH at every stage of this research, and one avenue of future research should be to continue this work. One enhancement that might significantly improve signal against the woodchip background is tyramide signal amplification (Eickhorst and Tippkoetter, 2008; Schonhuber et al., 1997; Lebaron et al., 1997; van de Corput et al., 1998).

Additionally, more analyses applied to the time-series dataset would be informative. First, with the current extent of the time-series data, several investigations are possible. Statistical and other analyses in this dissertation have mostly been conducted with woodchip samples only. Because biofilter woodchip and water samples typically have different microbial communities, assessment of these samples may offer interesting and important information. It would also be interesting to attempt to group all microbial

populations into like acting groups, using the set of representative bacterial and fungal populations as examples of "type." Along these same lines, the analyses conducted in this work only briefly touched on the role of diversity on performance and stability. Analyzing the microbial populations for the level of "structural redundancy" (Clarke and Warwick, 1998) in the community dataset may yield information about the numbers of populations that are able to perform similar ecological functions, and thus, the relative reliability of biofilter ecosystems. Further statistical analyses designed to separate the effects of environmental gradients and spatial or temporal autocorrelation might also be useful to determine more precisely the effects of environment on community or performance.

Secondly, additional data collection from samples that have been already taken is possible. Community fingerprints of the *nosZ* denitrifying community for the time-series data have been begun but are incomplete. These should be finished, and DNA from these samples should also be used to create community fingerprints using *nirS/nirK* and *norB* to assess the variation of populations having different capabilities within the denitrifying pathway. Also importantly, taxonomic identification of populations that were associated with variation in nitrate removal should be attempted.

Finally, more work is needed to test the findings of the time-series study. In particular, the effect of individual environmental parameters on microbial community and nitrate removal should be conducted in lab-scale mesocosms. Although it is never possible to completely replicate a field environment in a laboratory setting, the relationships between factors in my time-series study were complex and sometimes difficult to elucidate. Experiments on community reliability and on the success of inoculation of well-performing microbial species within a controlled environment would be useful.

5.3 Final Words

Both ecological engineering and the denitrifying biofilters have the capability to make a real and positive impact upon our environment. It is my hope that by applying the tools of microbial ecology to this engineered system I have both paved the way for improving its performance and adoption, and have also furthered the discipline of ecological engineering.

6. REFERENCES

Alexander, R. B., R. A. Smith, G. E. Schwarz, E. W. Boyer, J. V. Nolan and J. W. Brakebill. 2008. Differences in phosphorus and nitrogen delivery to the Gulf of Mexico from the Mississippi river basin. *Environmental Science & Technology* 42(3): 822-830.

Allison, S. D. and J. B. H. Martiny. 2008. Resistance, resilience, and redundancy in microbial communities. *Proceedings of the National Academy of Sciences of the United States of America* 10511512-11519.

Amann, R. I., L. Krumholz and D. A. Stahl. 1990. Fluorescent-oligonucleotide probing of whole cells for determinative, phylogenetic, and environmental-studies in microbiology. *Journal of Bacteriology* 172(2): 762-770.

Amman, R. I., B. J. Binder, S. W. Olsen, S. W. Chrisholm, R. Devereux and D. A. Stahl. 1990. Combination of 16S rRNA-targeted oligonucleotide probes with flow cytometry for analyzing mixed microbial populations. *Applied and Environmental Microbiology* 56(6): 1919-1925.

Bailey, V. L., J. L. Smith and H. Bolton. 2002. Fungal-to-bacterial ratios in soils investigated for enhanced C sequestration. *Soil Biology & Biochemistry* 34(7): 997-1007.

Bardgett, R., W. Bowman, R. Kaufmann and S. Schmidt. 2005. A temporal approach to linking aboveground and belowground ecology. *Trends in Ecology & Evolution* 20(11): 634-641.

Barnes, R., S. Baxter and R. Lark. 2007. Spatial covariation of *Azotobacter* abundance and soil properties: A case study using the wavelet transform. *Soil Biology & Biochemistry* 39(1): 295-310.

Beauchamp, E. G., J. T. Trevors and J. W. and Paul. 1989. Carbon sources for bacterial denitrification. *Advances in Soil Science* 10113-142.

Bell, T., J. A. Newman, B. W. Silverman, S. L. Turner and A. K. Lilley. 2005. The contribution of species richness and composition to bacterial services. *Nature* 436(7054): 1157-1160.

Bertaux, J., U. Gloger, M. Schmid, A. Hartmann and S. Scheu. 2007. Routine fluorescence in situ hybridization in soil. *Journal of Microbiological Methods* 69(3): 451-460.

Blowes, D. W., W. D. Robertson, C. J. Ptacek and C. Merkley. 1994. Removal of agricultural nitrate from tile-drainage effluent water using in-line bioreactors. *Journal of Contaminant Hydrology* 15(3): 207-221.

Bollag, J. M., S. Drzymala and L. T. Kardos. 1973. Biological versus chemical nitrite decomposition in soil. *Soil Science* 116(1): 44-50.

Borrvall, C., B. Ebenman and T. Jonsson. 2000. Biodiversity lessens the risk of cascading extinction in model food webs. *Ecology Letters* 3(2): 131-136.

Boyle, S. A., J. J. Rich, P. J. Bottomley, K. Cromack and D. D. Myrold. 2006. Reciprocal transfer effects on denitrifying community composition and activity at forest and meadow sites in the Cascade Mountains of Oregon. *Soil Biology & Biochemistry* 38(5): 870-878.

Braker, G., J. Z. Zhou, L. Y. Wu, A. H. Devol and J. M. Tiedje. 2000. Nitrite reductase genes (*nirK* and *nirS*) as functional markers to investigate diversity of denitrifying bacteria in Pacific Northwest marine sediment communities. *Applied and Environmental Microbiology* 66(5): 2096-2104.

Braker, G. and J. M. Tiedje. 2003. Nitric oxide reductase (*norB*) genes from pure cultures and environmental samples. *Applied and Environmental Microbiology* 69(6): 3476-3483.

Braker, G., J. Schwarz and R. Conrad. 2010. Influence of temperature on the composition and activity of denitrifying soil communities. *FEMS Microbiology Ecology* 73(1): 134-148.

Braker, G., H. L. Ayala-Del-Rio, A. H. Devol, A. Fesefeldt and J. M. Tiedje. 2001. Community structure of denitrifiers, Bacteria, and Archaea along redox gradients in Pacific Northwest marine sediments by terminal restriction fragment length polymorphism analysis of amplified nitrite reductase (*nirS*) and 16S rRNA genes. *Applied and Environmental Microbiology* 67(4): 1893-1901.

Bray, J. R. and J. T. Curtis. 1957. An ordination of the upland forest communities of southern Wisconsin. *Ecological Monographs* 27(4): 326-349.

Bremner, J. M. and K. Shaw. 1958. Dentrification in soil. I. Methods of investigation. *Journal of Agricultural Science* 51(1): 22-39.

Brezonik, P. L., V. J. V.J. Bierman, R. Alexander, J. Anderson, J. Barko, M. Dortch, L. Hatch, D. Keeney, D. Mulla, V. Smith, C. Walker, T. Whitledge and W. Wiseman. 1999. Effects of reducing nutrient loads to surface waters within the Mississippi River Basin and the Gulf of Mexico (Report of Task Group 4 to the White House Committee on Environment and Natural Resources, Hypoxia Work Group). Federal Register 6423834-23835.

Cady, F. and W. Bartholomew. 1961. Influence of low pO2 on denitrification processes and products. *Proceedings of the Soil Science Society of America* 25(5): 362-365.

Cameron, S. G. and L. A. Schipper. 2010. Nitrate removal and hydraulic performance of organic carbon for use in denitrification beds. *Ecological Engineering* 36(11): 1588-1595.

Cao, Y., P. G. Green and P. A. Holden. 2008. Microbial community composition and denitrifying enzyme activities in salt marsh sediments. *Applied and Environmental Microbiology* 74(24): 7585-7595.

Cavigelli, M. A. and G. P. Robertson. 2000. The functional significance of denitrifier community composition in a terrestrial ecosystem. *Ecology* 81(5): 1402-1414.

Cavigelli, M. A., G. P. Robertson and M. J. Klug. 1995. Fatty-acid methyl-ester (FAME) profiles as measures of soil microbial community structure. *Plant and Soil* 170(1): 99-113.

Chang, F. H. and F. E. Broadbent. 1982. Influence of trace-metals on some soil-nitrogen transformations. *Journal of Environmental Quality* 11(1): 1-4.

Cho, J. C. and J. M. Tiedje. 2000. Biogeography and degree of endemicity of fluorescent *Pseudomonas* strains in soil. *Applied and Environmental Microbiology* 66(12): 5448-5456.

Chun, J. A., R. A. Cooke, J. W. Eheart and J. Cho. 2010. Estimation of flow and transport parameters for woodchip-based bioreactors: II. Field-scale bioreactor. *Biosystems Engineering* 105(1): 95-102.

Clarke, K. R. 1993. Nonparametric multivariate analyses of changes in community structure. *Australian Journal of Ecology* 18(1): 117-143.

Clarke, K. R. and R. M. Warwick. 1998. Quantifying structural redundancy in ecological communities. *Oecologia* 113(2): 278-289.

Clarke, K. R. and R. H. Green. 1988. Statistical design and analysis for a biological effects study. *Marine Ecology-Progress Series* 46(1-3): 213-226.

Collins, D., B. Jacobsen and B. Maxwell. 2003. Spatial and temporal population dynamics of a phyllosphere colonizing *Bacillus subtilis* biological control agent of sugar beet *Cercospora* leaf spot. *Biological Control* 26(3): 224-232.

Cooke, R. A., A. M. Doheny and M. C. Hirschi. 2001. Bio-reactors for edge-of-field treatment of tile outflow. ASABE paper #0120181-17.

Cooper, D. W. 1968. Significance level in multiple tests made simultaneously. *Heredity* 23614-617.

Couteron, P. and S. Ollier. 2005. A generalized, variogram-based framework for multi-scale ordination. *Ecology* 86(4): 828-834.

Crump, B. and J. Hobbie. 2005. Synchrony and seasonality in bacterioplankton communities of two temperate rivers. *Limnology and Oceanography* 50(6): 1718-1729.

Daims, H., A. Bruhl, R. Amann, K. H. Schleifer and M. Wagner. 1999. The domain-specific probe EUB338 is insufficient for the detection of all Bacteria: Development and evaluation of a more comprehensive probe set. *Systematic and Applied Microbiology* 22(3): 434-444.

Dandie, C. E., D. L. Burton, B. J. Zebarth, S. L. Henderson, J. T. Trevors and C. Goyer. 2008. Changes in bacterial denitrifier community abundance over time in an agricultural field and their relationship with denitrification activity. *Applied and Environmental Microbiology* 74(19): 5997-6005.

Dandurand, L., D. Schotzko and G. Knudsen. 1997. Spatial patterns of rhizoplane populations of *Pseudomonas fluorescens*. *Applied and Environmental Microbiology* 63(8): 3211-3217.

D'Angelo, E. M., A. D. Karathanasis, E. J. Sparks, S. A. Ritchey and S. A. Wehr-McChesney. 2005. Soil carbon and microbial communities at mitigated and late successional bottomland forest wetlands. *Wetlands* 25(1): 162-175.

Danovaro, R., A. Dell'anno, A. Trucco, M. Serresi and S. Vanucci. 2001. Determination of virus abundance in marine sediments. *Applied and Environmental Microbiology* 67(3): 1384-1387.

David, M. B. and L. E. Gentry. 2000. Anthropogenic inputs of nitrogen and phosphorus and riverine export for Illinois, USA. *Journal of Environmental Quality* 29(2): 494-508.

de los Reyes, F. L., W. Ritter and L. Raskin. 1997. Group-specific small-subunit rRNA hybridization probes to characterize filamentous foaming in activated sludge systems. *Applied and Environmental Microbiology* 63(3): 1107-1117.

Deutsch, C. V. and A. G. Journel. 1998. *GSLIB geostatistical software library and user's guide.* Oxford: Oxford University Press.

Diaz, R. J. and R. Rosenberg. 2008. Spreading dead zones and consequences for marine ecosystems. *Science* 321(5891): 926-929.

Doheny, A. M. 2003. Amerlioration of tile nitrate and atrazing using inline biofilters. MS thesis. Urbana-Champaign, Illinois: University of Illinois, Department of Agricultural Engineering.

Eickhorst, T. and R. Tippkoetter. 2008. Improved detection of soil microorganisms using fluorescence in situ hybridization (FISH) and catalyzed reporter deposition (CARD-FISH). *Soil Biology & Biochemistry* 40(7): 1883-1891.

Elgood, Z., W. D. Robertson, S. L. Schiff and R. Elgood. 2010. Nitrate removal and greenhouse gas production in a stream-bed denitrifying bioreactor. *Ecological Engineering* 36(11): 1575-1580.

Ellingsoe, P. and K. Johnsen. 2002. Influence of soil sample sizes on the assessment of bacterial community structure. *Soil Biology & Biochemistry* 34(11): 1701-1707.

Elton, C. S. and C. S. Elton. 1958. *The ecology of invasions by animals and plants.* Chicago: University of Chicago Press.

Enright, A. M., G. Collins and V. O'Flaherty. 2007. Temporal microbial diversity changes in solvent-degrading anaerobic granular sludge from low-temperature (15 degrees C) wastewater treatment bioreactors. *Systematic and Applied Microbiology* 30(6): 471-482.

Enwall, K., L. Philippot and S. Hallin. 2005. Activity and composition of the denitrifying bacterial community respond differently to long-term fertilization. *Applied and Environmental Microbiology* 71(12): 8335-8343.

Ettema, C. and D. Wardle. 2002. Spatial soil ecology. *Trends in Ecology & Evolution* 17(4): 177-183.

Faith, D. P., P. R. Minchin and L. Belbin. 1987. Compositional dissimilarity as a robust measure of ecological distance. *Vegetatio* 69(1-3): 57-68.

Fedi, S., V. Tremaroli, D. Scala, J. R. Perez-Jimenez, F. Fava, L. Young and D. Zannoni. 2005. t-RFLP analysis of bacterial communities in cyclodextrin-amended bioreactors developed for biodegradation of polychlorinated biphenyls. *Research in Microbiology* 156(2): 201-210.

Firestone, M. K. 1982. Biological denitrification. In *Nitrogen in Agricultural Soils*, 289-326. ed. J. Stevenson, Madison, WI.: American Society of Agronomy.

Fisher, M. M. and E. W. Triplett. 1999. Automated approach for ribosomal intergenic spacer analysis of microbial diversity and its application to freshwater bacterial communities. *Applied and Environmental Microbiology* 65(10): 4630-4636.

Floyd, M. M., J. Tang, M. Kane and D. Emerson. 2005. Captured diversity in a culture collection: Case study of the geographic and habitat distributions of environmental isolates held at the American type culture collection. *Applied and Environmental Microbiology* 71(6): 2813-2823.

Franklin, R. B. and A. L. Mills. 2003. Multi-scale variation in spatial heterogeneity for microbial community structure in an eastern Virginia agricultural field. *FEMS Microbiology Ecology* 44(3): 335-346.

Franklin, R. B., L. K. Blum, A. C. McComb and A. L. Mills. 2002. A geostatistical analysis of small-scale spatial variability in bacterial abundance and community structure in salt marsh creek bank sediments. *FEMS Microbiology Ecology* 42(1): 71-80.

Frey, S. D., E. T. Elliott and K. Paustian. 1999. Bacterial and fungal abundance and biomass in conventional and no-tillage agroecosystems along two climatic gradients. *Soil Biology & Biochemistry* 31(4): 573-585.

Friedrich, U., H. Van Langenhove, K. Altendorf and A. Lipski. 2003. Microbial community and physicochemical analysis of an industrial waste gas biofilter and design of 16S rRNA-targeting oligonucleotide probes. *Environmental Microbiology* 5(3): 183-201.

Friedrich, U., K. Prior, K. Altendorf and A. Lipski. 2002. High bacterial diversity of a waste gas-degrading community in an industrial biofilter as shown by a 16S rDNA clone library. *Environmental Microbiology*, 2002 Nov.

Gayle, B. P., G. D. Boardman, J. H. Sherrard and R. E. Benoit. 1989. Biological denitrification of water. *Journal of Environmental Engineering-ASCE* 115(5): 930-943.

Gonod, L., J. Chadoeuf, C. Chenu and V. Gonod. 2006. Spatial distribution of microbial 2,4-dichlorophenoxy acetic acid mineralization from field to microhabitat scales. *Soil Science Society of America Journal* 70(1): 64-71.

Goovaerts, P. 1997. *Geostatistics for natural resources evaluation*. Oxford, England: Oxford University Press.

Gower, J. C. and P. Legendre. 1986. Metric and euclidean properties of dissimilarity coefficients. *Journal of Classification* 3(1): 5-48.

Grant, M. A. and W. J. Payne. 1982. Effects of pesticides on denitrifying activity in salt-marsh sediments. *Journal of Environmental Quality* 11(3): 369-372.

Green, J. L., A. J. Holmes, M. Westoby, I. Oliver, D. Briscoe, M. Dangerfield, M. Gillings and A. J. Beattie. 2004. Spatial scaling of microbial eukaryote diversity. *Nature* 432(7018): 747-750.

Greenan, C. M., T. B. Moorman, T. C. Kaspar, T. B. Parkin and D. B. Jaynes. 2006. Comparing carbon substrates for denitrification of subsurface drainage water. *Journal of Environmental Quality* 35(3): 824-829.

Grundmann, G. and D. Debouzie. 2000. Geostatistical analysis of the distribution of NH_4 and NO_2--oxidizing bacteria and serotypes at the millimeter scale along a soil transect. *FEMS Microbiology Ecology* 34(1): 57-62.

Gu, B., D. B. Watson, L. Wu, D. H. Phillips, D. C. White and J. Zhou. 2002. Microbiological characteristics in a zero-valent iron reactive barrier. *Environmental Monitoring and Assessment* 77(3): 293-309.

Gunderson, L. H. 2000. Ecological resilience - in theory and application. *Annual Review of Ecology and Systematics* 31425-439.

Gutknecht, J. L. M., R. M. Goodman and T. C. Balser. 2006. Linking soil process and microbial ecology in freshwater wetland ecosystems. *Plant and Soil* 289(1-2): 17-34.

Hahn, D., R. I. Amann, W. Ludwig, A. D. L. Akkermans and K. H. Schleifer. 1992. Detection of microorganisms in soil after in situ hybridization with ribosomal-RNA-targeted, fluorescently labeled oligonucleotides. *Journal of General Microbiology* 138 879-887.

Henry, S., D. Bru, B. Stres, S. Hallet and L. Philippot. 2006. Quantitative detection of the *nosZ* gene, encoding nitrous oxide reductase, and comparison of the abundances of 16S rRNA, *narG*, *nirK*, and *nosZ* genes in soils. *Applied and Environmental Microbiology* 72(8): 5181-5189.

Hooper, D. U., F. S. Chapin, J. J. Ewel, A. Hector, P. Inchausti, S. Lavorel, J. H. Lawton, D. M. Lodge, M. Loreau, S. Naeem, B. Schmid, H. Setala, A. J. Symstad, J. Vandermeer and D. A. Wardle. 2005. Effects of biodiversity on ecosystem functioning: A consensus of current knowledge. *Ecological Monographs* 75(1): 3-35.

Horner-Devine, M. C., K. M. Carney and B. J. M. Bohannan. 2004a. An ecological perspective on bacterial biodiversity. *Proceedings of the Royal Society of London Series B-Biological Sciences* 271(1535): 113-122.

Horner-Devine, M. C., M. Lage, J. B. Hughes and B. J. M. Bohannan. 2004b. A taxa-area relationship for bacteria. *Nature* 432(7018): 750-753.

Hoshino, T., T. Terahara, S. Tsuneda, A. Hirata and Y. Inamori. 2005. Molecular analysis of microbial population transition associated with the start of denitrification in a wastewater treatment process. *Journal of Applied Microbiology* 99(5): 1165-1175.

Hunter, W. J., R. F. Follett and J. W. Cary. 1997. Use of vegetable oil to remove nitrate from flowing groundwater. *Transactions of the ASAE* 40(2): 345-353.

Hwang, C. C., W. M. Wu, T. J. Gentry, J. Carley, G. A. Corbin, S. L. Carroll, D. B. Watson, P. M. Jardine, J. Z. Zhou, C. S. Criddle and M. W. Fields. 2009. Bacterial community succession during in situ uranium bioremediation: spatial similarities along controlled flow paths. *ISME Journal* 3(1): 47-64.

Ishida, C. K., J. J. Kelly and K. A. Gray. 2006. Effects of variable hydroperiods and water level fluctuations on denitrification capacity, nitrate removal, and benthic-microbial community structure in constructed wetlands. *Ecological Engineering* 28(4): 363-373.

Jackson, J. 1994. Community Unity. *Science* 264(5164): 1412-1413.

Janda, V., J. Rudovsky, J. Wanner and K. Marha. 1988. In-situ denitrification of drinking water. *Water Science and Technology* 20(3): 215-219.

Janssen, P. H. 2006. Identifying the dominant soil bacterial taxa in libraries of 16S rRNA and 16S rRNA genes. *Applied and Environmental Microbiology* 72(3): 1719-1728.

Jaynes, D. B., T. C. Kaspar, T. B. Moorman and T. B. and Parkin. 2004. Potential methods for reducing nitrate losses in artificially drained fields. In *Drainage Management for the Midwest U. S., Proceedings of the 8th International Drainage Symposium*, 56-69. St. Joseph, MI: American Society of Agricultural Engineers.

Jaynes, D. B., T. C. Kaspar, T. B. Moorman and T. B. Parkin. 2008. In situ bioreactors and deep drain-pipe installation to reduce nitrate losses in artificially drained fields. *Journal of Environmental Quality* 37(2): 429-436.

Journel, A. G. and C. J. Huijbregts. 1978. *Mining Geostatistics*. San Diego, CA: Academic Press.

Kageyama, S. A., N. R. Posavatz, K. E. Waterstripe, S. J. Jones, P. J. Bottomley, K. Cromack Jr. and D. D. Myrold. 2008. Fungal and bacterial communities across meadow-forest ecotones in the western Cascades of Oregon. *Canadian Journal of Forest Research-Revue Canadienne De Recherche Forestiere* 38(5): 1053-1060.

Kang, S. and A. L. Mills. 2006. The effect of sample size in studies of soil microbial community structure. *Journal of Microbiological Methods* 66(2): 242-250.

Kangas, P. C. 2004. *Ecological Engineering: Principles and Practice*. Boca Raton, FL: CRC Press.

Keeney, D. R. and T. H. Deluca. 1993. Des-Moines River nitrate in relation to watershed agricultural practices - 1945 versus 1980s. *Journal of Environmental Quality* 22(2): 267-272.

Kendrick, B. 2001. *The Fifth Kingdom.* 3rd ed. Waterloo, Ontario: Mycologue.

Kent, A., S. Jones, G. Lauster, J. Graham, R. Newton and K. McMahon. 2006. Experimental manipulations of microbial food web interactions in a humic lake:

shifting biological drivers of bacterial community structure. Environmental *Microbiology* 8(8): 1448-1459.

Kent, A. D., A. C. Yannarell, J. A. Rusak, E. W. Triplett and K. D. McMahon. 2007. Synchrony in aquatic microbial community dynamics. *ISME Journal* 1(1): 38-47.

Kent, A. D., S. E. Jones, A. C. Yannarell, J. M. Graham, G. H. Lauster, T. K. Kratz and E. W. Triplett. 2004. Annual patterns in bacterioplankton community variability in a humic lake. *Microbial Ecology* 48(4): 550-560.

Kent, M., R. A. Moyeed, C. L. Reid, R. Pakeman and R. Weaver. 2006. Geostatistics, spatial rate of change analysis and boundary detection in plant ecology and biogeography. *Progress in Physical Geography* 30(2): 201-231.

Kim, H. H., E. A. Seagren and A. P. Davis. 2003. Engineered bioretention for removal of nitrate from stormwater runoff. *Water Environment Research* 75(4): 355-367.

Kim, S., S. Lee, C. Freeman, N. Fenner and H. Kang. 2008. Comparative analysis of soil microbial communities and their responses to the short-term drought in bog, fen, and riparian wetlands. *Soil Biology & Biochemistry* 40(11): 2874-2880.

Knowles, R. 2005. Denitrifiers associated with methanotrophs and their potential impact on the nitrogen cycle. *Ecological Engineering* 24(5): 441-446.

Knowles, R. 1982. Denitrification. *Microbiological Reviews* 46(1): 43-70.

Kobabe, S., D. Wagner and E. M. Pfeiffer. 2004. Characterisation of microbial community composition of a Siberian tundra soil by fluorescence in situ hybridisation. FEMS Microbiology Ecology 50(1): 13-23.

Krause, S., C. Luke and P. Frenzel. 2009. Spatial heterogeneity of methanotrophs: a geostatistical analysis of *pmoA*-based t-RFLP patterns in a paddy soil. *Environmental Microbiology Reports* 1(5): 393-397.

Kruskal, W. H. and W. A. Wallis. 1952. Use of ranks in one-criterion variance analysis. *Journal of the American Statistical Association* **47** (260): 583–621.

Lam, P. and J. P. Cowen. 2004. Processing deep-sea particle-rich water samples for fluorescence in situ hybridization: Consideration of storage effects, preservation, and sonication. *Applied and Environmental Microbiology* 70(1): 25-33.

Laughlin, R. J. and R. J. Stevens. 2002. Evidence for fungal dominance of denitrification and codenitrification in a grassland soil. *Soil Science Society of America Journal* 66(5): 1540-1548.

Lebaron, P., P. Catala, C. Fajon, F. Joux, J. Baudart and L. Bernard. 1997. A new sensitive, whole-cell hybridization technique for detection of bacteria involving a biotinylated oligonucleotide probe targeting rRNA and tyramide signal amplification. *Applied and Environmental Microbiology* 63(8): 3274-3278.

Legendre, P. 1993. Spatial autocorrelation—Trouble or new paradigm. *Ecology* 74(6): 1659-1673.

Legendre, P. and M. J. Fortin. 1989. Spatial Pattern and Ecological Analysis. *Vegetatio* 80(2): 107-138.

Legendre, P. and L. Legendre. 1998. *Numerical ecology*. 2nd English edition. Volume 20, Developments in Environmental Modelling. Amsterdam: Elsevier.

Lichstein, J. W. 2007. Multiple regression on distance matrices: a multivariate spatial analysis tool. *Plant Ecology* 188(2): 117-131.

Lilleskov, E. A., T. D. Bruns, T. R. Horton, D. L. Taylor and P. Grogan. 2004. Detection of forest stand-level spatial structure in ectomycorrhizal fungal communities. *FEMS Microbiology Ecology* 49(2): 319-332.

Lindahl, V. 1996. Improved soil dispersion procedures for total bacterial counts, extraction of indigenous bacteria and cell survival. *Journal of Microbiological Methods* 25(3): 279-286.

Lipski, A., U. Friedrich and K. Altendorf. 2001. Application of rRNA-targeted oligonucleotide probes in biotechnology. *Applied Microbiology and Biotechnology* 56(1/2): 40-57.

Liu, W. T., T. L. Marsh, H. Cheng and L. J. Forney. 1997. Characterization of microbial diversity by determining terminal restriction fragment length polymorphisms of genes encoding 16S rRNA. *Applied and Environmental Microbiology* 63(11): 4516-4522.

Lloyd, M. and R. Ghelardi. 1964. A table for calculating the equitability component of species-diversity. *The Journal of Animal Ecology* 33(2): 217-225.

Lohrenz, S. E., G. L. Fahnenstiel, D. G. Redalje, G. A. Lang, X. G. Chen and M. J. Dagg. 1997. Variations in primary production of northern Gulf of Mexico continental shelf waters linked to nutrient inputs from the Mississippi River. *Marine Ecology Progress Series* 15545-54.

Loreau, M., S. Naeem, P. Inchausti, J. Bengtsson, J. P. Grime, A. Hector, D. U. Hooper, M. A. Huston, D. Raffaelli, B. Schmid, D. Tilman and D. A. Wardle. 2001. Ecology - Biodiversity and ecosystem functioning: Current knowledge and future challenges. *Science* 294(5543): 804-808.

Macarthur, R. 1955. Fluctuations of animal populations, and a measure of community stability. *Ecology* 36(3): 533-536.

Mackas, D. 1984. Spatial auto-correlation of plankton community composition in a composition in a continental-shelf ecosystem. *Limnology and Oceanography* 29(3): 451-471.

Manly, B. 1991. *Randomization and Monte Carlo Methods in Biology.* Boca Raton, FL: CRC Press.

Mantel, N. 1967. Detection of disease clustering and a generalized regression approach. *Cancer research* 27(2P1): 209-220.

Manter, D. K. and J. M. Vivanco. 2007. Use of the ITS primers, ITS1F and ITS4, to characterize fungal abundance and diversity in mixed-template samples by qPCR and length heterogeneity analysis. *Journal of Microbiological Methods* 717-14.

Manz, W., R. Amann, W. Ludwig, M. Wagner and K. H. Schleifer. 1992. Phylogenetic oligodeoxynucleotide probes for the major subclasses of Proteobacteria - problems and solutions. *Systematic and Applied Microbiology* 15(4): 593-600.

Martiny, J. B. H., B. J. M. Bohannan, J. H. Brown, R. K. Colwell, J. A. Fuhrman, J. L. Green, M. C. Horner-Devine, M. Kane, J. A. Krumins, C. R. Kuske, P. J. Morin, S. Naeem, L. Ovreas, A. L. Reysenbach, V. H. Smith and J. T. Staley. 2006. Microbial biogeography: putting microorganisms on the map. *Nature Reviews Microbiology* 4(2): 102-112.

Mateju, V., S. Cizinska, J. Krejci and T. Janoch. 1992. Biological water denitrification. A review. *Enzyme and Microbial Technology* 14(3): 170-183.

May, R. M. 1973. Stability and complexity in model ecosystems. *Monographs in Population Biology* 61-235.

Mcardle, B. H., K. J. Gaston and J. H. Lawton. 1990. Variation in the size of animal populations - patterns, problems and artifacts. *Journal of Animal Ecology* 59(2): 439-454.

McGrady-Steed, J., P. M. Harris and P. J. Morin. 1997. Biodiversity regulates ecosystem predictability. *Nature* 390(6656): 162-165.

McGuinness, L. M., M. Salganik, L. Vega, K. D. Pickering and L. J. Kerkhof. 2006. Replicability of bacterial communities in denitrifying bioreactors as measured by PCR/t-RFLP analysis. *Environmental Science & Technology* 40(2): 509-515.

McLamore, E., S. Sharvelle, Z. Huang and K. Banks. 2008. Simultaneous treatment of graywater and waste gas in a biological trickling filter. *Water Environment Research* 80(11): 2096-2103.

Mergaert, J., A. Boley, M. C. Cnockaert, W. R. Muller and J. Swings. 2001. Identity and potential functions of heterotrophic bacterial isolates from a continuous-upflow fixed-bed reactor for denitrification of drinking water with bacterial polyester as source of carbon and electron donor. *Systematic and Applied Microbiology* 24(2): 303-310.

Mistral, M., O. Buck, D. C. Meier-Behrmann, D. A. Burnett, T. E. Barnfield, A. J. Scott, B. J. Anderson and J. B. Wilson. 2000. Direct measurement of spatial autocorrelation at the community level in four plant communities. *Journal of Vegetation Science* 11(6): 911-916.

Mitchell, J. K., G. F. McIsaac, S. E. Walker and M. C. Hirschi. 2000. Nitrate in river and subsurface drainage flows from an east central Illinois watershed. *Transactions of the ASAE* 43(2): 337-342.

Mitsch, W. J. and S. E. Jorgensen. 2004. *Ecological Engineering and Ecosystem Restoration.* 2nd ed. Hoboken, NJ: Wiley.

Moorman, T. B., T. B. Parkin, T. C. Kaspar and D. B. Jaynes. 2010. Denitrification activity, wood loss, and N_2O emissions over 9 years from a wood chip bioreactor. *Ecological Engineering* 36(11): 1567-1574.

Mouser, P. J., D. M. Rizzo, W. F. M. Roling and B. M. Van Breukelen. 2005. A multivariate statistical approach to spatial representation of groundwater

contamination using hydrochemistry and microbial community profiles. *Environmental Science & Technology* 39(19): 7551-7559.

Myrold, D. D. and J. M. Tiedje. 1985. Establishment of denitrification capacity in soil - effects of carbon, nitrate and moisture. *Soil Biology & Biochemistry* 17(6): 819-822.

Myrold, D. D. and N. R. Posavatz. 2007. Potential importance of bacteria and fungi in nitrate assimilation in soil. *Soil Biology & Biochemistry* 39(7): 1737-1743.

Naeem, S. and S. B. Li. 1997. Biodiversity enhances ecosystem reliability. *Nature* 390(6659): 507-509.

Nanos, N., F. Pardo, J. A. Nager, J. A. Pardos and L. Gil. 2005. Using multivariate factorial kriging for multiscale ordination: a case study. *Canadian Journal of Forest Research-Revue Canadienne De Recherche Forestiere* 35(12): 2860-2874.

Neef, A., A. Zaglauer, H. Meier, R. Amann, H. Lemmer and K. H. Schleifer. 1996. Population analysis in a denitrifying sand filter: Conventional and in situ identification of *Paracoccus* spp. in methanol-fed biofilms. *Applied and Environmental Microbiology* 62(12): 4329-4339.

Nekola, J. C. and P. S. White. 1999. The distance decay of similarity in biogeography and ecology. *Journal of Biogeography* 26(4): 867-878.

Nogales, B., K. N. Timmis, D. B. Nedwell and A. M. Osborn. 2002. Detection and diversity of expressed denitrification genes in estuarine sediments after reverse transcription-PCR amplification from mRNA. *Applied and Environmental Microbiology* 68(10): 5017-5025.

Nunan, N., K. Wu, I. Young, J. Crawford and K. Ritz. 2003. Spatial distribution of bacterial communities and their relationships with the micro-architecture of soil. *FEMS Microbiology Ecology* 44(2): 203-215.

Oakley, S. M., A. J. Gold and A. J. Oczkowski. 2010. Nitrogen control through decentralized wastewater treatment: Process performance and alternative management strategies. *Ecological Engineering* 36(11): 1520-1531.

Obrien, P. C. 1992. Robust procedures for testing equality of covariance matrices. *Biometrics* 48(3): 819-827.

Oden, N. L. 1984. Assessing the significance of a spatial correlogram. *Geographical Analysis* 16(1): 1-16.

Oden, N. L. and R. R. Sokal. 1986. Directional autocorrelation - an extension of spatial correlograms to 2 dimensions. *Systematic Zoology* 35(4): 608-617.

Odum, E. P. 1971. *Fundamentals of Ecology*. 5th ed. Philadelphia: Saunders.

Olson, C. L. 1974. Comparative robustness of 6 tests in multivariate-analysis of variance. *Journal of the American Statistical Association* 69(348): 894-908.

Orum, T., D. Bigelow, P. Cotty and M. Nelson. 1999. Using predictions based on geostatistics to monitor trends in *Aspergillus flavus* strain composition. *Phytopathology* 89(9): 761-769.

Ovreas, L. 2000. Population and community level approaches for analysing microbial diversity in natural environments. *Ecology Letters* 3(3): 236-251.

Pace, N. R. 1997. A molecular view of microbial diversity and the biosphere. *Science* 276(5313): 734-740.

Parkin, T. B. and J. J. Meisinger. 1989. Denitrification below the crop rooting zone as influenced by surface tillage. *Journal of Environmental Quality* 18(1): 12-16.

Paver, S. F. and A. D. Kent. 2010. Temporal patterns in glycolate-utilizing bacterial community composition correlate with phytoplankton population dynamics in humic lakes. *Microbial Ecology* 60(2): 406-418.

Peralta, A. L., J. W. Matthews and A. D. Kent. 2010. Microbial community structure and denitrification in a wetland mitigation bank. *Applied and Environmental Microbiology* 76(13): 4207-4215.

Philippot, L., S. Piutti, F. Martin-Laurent, S. Hallet and J. C. Germon. 2002. Molecular analysis of the nitrate-reducing community from unplanted and maize-planted soils. *Applied and Environmental Microbiology* 68(12): 6121-6128.

Philippot, L., D. Bru, N. Saby, J. Cuhel, D. Arrouays and M. Simek. 2009. Spatial patterns of bacterial taxa in nature reflect ecological traits of deep branches of the 16S rRNA bacterial tree. *Environmental Microbiology* 11(12): 3096-3104.

Pickles, B., D. Genney, J. Potts, J. Lennon, I. Anderson and I. Alexander. 2010. Spatial and temporal ecology of Scots pine ectomycorrhizas. *The New Phytologist* 186(3): 755-768.

Pimm, S. L., J. H. Lawton and J. E. Cohen. 1991. Food web patterns and their consequences. *Nature* (London) 350(6320): 669-674.

Pinhassi, J. and A. Hagstrom. 2000. Seasonal succession in marine bacterioplankton. *Aquatic Microbial Ecology* 21(3): 245-256.

Rabalais, N. N. and R. E. Turner, eds. 2001. *Coastal Hypoxia: Consequences for living resources and ecosystems.* Washington, D.C.: American Geophysical Union.

Rabalais, N. N., R. E. Turner and D. Scavia. 2002. Beyond science into policy: Gulf of Mexico hypoxia and the Mississippi River. *Bioscience* 52(2): 129-142.

Rees, G. N., D. S. Baldwin, G. O. Watson, S. Perryman and D. L. Nielsen. 2004. Ordination and significance testing of microbial community composition derived from terminal restriction fragment length polymorphisms: application of multivariate statistics. *Antonie Van Leeuwenhoek International Journal of General and Molecular Microbiology* 86(4): 339-347.

Rich, J. J. and D. D. Myrold. 2004. Community composition and activities of denitrifying bacteria from adjacent agricultural soil, riparian soil, and creek sediment in Oregon, USA. *Soil Biology & Biochemistry* 36(9): 1431-1441.

Rich, J. J., R. S. Heichen, P. J. Bottomley, K. Cromack Jr. and D. D. Myrold. 2003. Community composition and functioning of denitrifying bacteria from adjacent meadow and forest Soils. *Applied and Environmental Microbiology* 69(10): 5974-5982.

Ricklefs, R. E. 2008. *The Economy of Nature.* 6th ed. New York: W. H. Freeman.

Ritter, W. F. and R. P. Eastburn. 1988. A review of denitrification in on-site wastewater treatment systems. *Environmental Pollution* 51(1): 49-61.

Ritz, K., W. McNicol, N. Nunan, S. Grayston, P. Millard and D. Atkinson. 2004. Spatial structure in soil chemical and microbiological properties in an upland grassland. *FEMS Microbiology Ecology* 49(2): 191-205.

Robertson, W. D. 2010. Nitrate removal rates in woodchip media of varying age. *Ecological Engineering* 36(11): 1581-1587.

Robertson, W. D. and M. R. Anderson. 1999. Nitrogen removal from landfill leachate using an infiltration bed coupled with a denitrification barrier. *Ground Water Monitoring and Remediation* 19(4): 73-80.

Robertson, W. D. and J. A. Cherry. 1995. In situ denitrification of septic-system nitrate using reactive porous media barriers: field trials. *Ground Water* 33(1): 99-111.

Robertson, W. D., J. L. Vogan and P. S. Lombardo. 2008. Nitrate removal rates in a 15-year-old permeable reactive barrier treating septic system nitrate. *Ground Water Monitoring and Remediation* 28(3): 65-72.

Robertson, W. D., D. W. Blowes, C. J. Ptacek and J. A. Cherry. 2000. Long-term performance of in situ reactive barriers for nitrate remediation. *Ground Water* 38(5): 689-695.

Rodrigue, A. L. 2006. Effects of sampling frequencies in the evaluation of nitrate-N transport from drainage-related BMP. MS thesis. Urbana-Champaign, Illinois: University of Illinois, Department of Agricultural and Biological Engineering.

Rosch, C., A. Mergel and H. Bothe. 2002. Biodiversity of denitrifying and dinitrogen-fixing bacteria in an acid forest soil. *Applied and Environmental Microbiology* 68(8): 3818-3829.

Rossi, R. E., D. J. Mulla, A. G. Journel and E. H. Franz. 1992. Geostatistical tools for modeling and interpreting ecological spatial dependence. *Ecological Monographs* 62(2): 277-314.

Saetre, P. and E. Baath. 2000. Spatial variation and patterns of soil microbial community structure in a mixed spruce-birch stand. *Soil Biology & Biochemistry* 32(7): 909-917.

Sakano, Y., K. D. Pickering, P. F. Strom and L. J. Kerkhof. 2002. Spatial distribution of total, ammonia-oxidizing, and denitrifying bacteria in biological wastewater treatment reactors for bioregenerative life support. *Applied and Environmental Microbiology* 68(5): 2285-2293.

Sambrook and Russell. 2001. *Molecular Cloning: A Laboratory Manual*. 3rd ed. Cold Spring Harbor, NY: Cold Spring Harbor Laboratory Press.

Schimel, J. and J. Gulledge. 1998. Microbial community structure and global trace gases. *Global Change Biology* 4(7): 745-758.

Schipper, L. and M. Vojvodic-Vukovic. 1998. Nitrate removal from groundwater using a denitrification wall amended with sawdust: Field trial. *Journal of Environmental Quality* 27(3): 664-668.

Schipper, L. A. and M. Vojvodic-Vukovic. 2001. Five years of nitrate removal, denitrification and carbon dynamics in a denitrification wall. *Water Research* 35(14): 3473-3477.

Schipper, L. A. and M. Vojvodic-Vukovic. 2000. Nitrate removal from groundwater and denitrification rates in a porous treatment wall amended with sawdust. *Ecological Engineering* 14(3): 269-278.

Schipper, L. A., G. F. Barkle and M. Vojvodic-Vukovic. 2005. Maximum rates of nitrate removal in a denitrification wall. *Journal of Environmental Quality* 34(4): 1270-1276.

Schipper, L. A., W. D. Robertson, A. J. Gold, D. B. Jaynes and S. C. Cameron. 2010. Denitrifying bioreactors-An approach for reducing nitrate loads to receiving waters. *Ecological Engineering* 36(11): 1532-1543.

Schipper, L. A., G. F. Barkle, J. C. Hadfield, M. Vojvodic-Vukovic and C. P. Burgess. 2004. Hydraulic constraints on the performance of a groundwater denitrification wall for nitrate removal from shallow groundwater. *Journal of Contaminant Hydrology* 69(3-4): 263-279.

Schonhuber, W., B. Fuchs, S. Juretschko and R. Amann. 1997. Improved sensitivity of whole-cell hybridization by the combination of horseradish peroxidase-labeled oligonucleotides and tyramide signal amplification. *Applied and Environmental Microbiology* 63(8): 3268-3273.

Shade, A., C. Chiu and K. McMahon. 2010. Seasonal and episodic lake mixing stimulate differential planktonic bacterial dynamics. *Microbial Ecology* 59(3): 546-554.

Shannon, C. and W. and Weaver. 1963. *The Mathematical Theory of Communication*. 5th ed. Chicago: University of Illinois Press.

Shelley, R. C. L. and J. A. Perry. 2000. Evaluation of bacterial recovery efficiency and counting precision from decaying leaf litter in Little Rock Lake, Wisconsin, USA. *Journal of Freshwater Ecology* 15(2): 157-169.

Siegel, S. and N. J. Castellan, Jr. 1988. *Non parametric statistics for the behavioural sciences.* New York: MacGraw Hill.

Sikora, L. J. and D. R. Keeney. 1976. Denitrification of nitrified septic tank effluent. *Journal of the Water Pollution Control Federation* 48(8): 2018-2025.

Soares, M. I. M., A. Brenner, A. Yevzori, R. Messalem, Y. Leroux and A. Abeliovich. 2000. Denitrification of groundwater: pilot-plant testing of cotton-packed bioreactor and post-microfiltration. *Water Science and Technology* 42(1): 353-359.

Spain, A. M., L. R. Krumholz and M. S. Elshahed. 2009. Abundance, composition, diversity and novelty of soil *Proteobacteria*. *ISME Journal* 3(8): 992-1000.

Stahl, D. A. and R. Amann. 1991. Development and application of nucleic acid probes. In *Nucleic Acid Techniques in Bacterial Systematics*, 205-208. ed. E. Stackebrandt and Goodfellow, M., Chichester, England: Wiley.

Starr, R. C. and J. A. Cherry. 1994. In situ remediation of contaminated ground water: the funnel-and-gate system. *Ground Water* 32(3): 465-476.

Stepanauskas, R., M. Moran, B. Bergamaschi and J. Hollibaugh. 2003. Covariance of bacterioplankton composition and environmental variables in a temperate delta system. *Aquatic Microbial Ecology* 31(1): 85-98.

Stres, B., I. Mahne, G. Avgustin and J. M. Tiedje. 2004. Nitrous oxide reductase (*nosZ*) gene fragments differ between native and cultivated Michigan soils. *Applied and Environmental Microbiology* 70(1): 301-309.

Stres, B., T. Danevcic, L. Pal, M. M. Fuka, L. Resman, S. Leskovec, J. Hacin, D. Stopar, I. Mahne and I. Mandic-Mulec. 2008. Influence of temperature and soil water content on bacterial, archaeal and denitrifying microbial communities in drained fen grassland soil microcosms. *FEMS Microbiology Ecology* 66(1): 110-122.

Susyan, E. A., N. D. Ananyeva and E. V. Blagodatskaya. 2005. The antibiotic-aided distinguishing of fungal and bacterial substrate-induced respiration in various soil ecosystems. *Microbiology* 74(3): 336-342.

Tchobanoglous, G., F. L. Burton and H. D. Stensel. 2003. *Metcalf & Eddy Wastewater Engineering, Treatment and Reuse.* 4th ed. New York: McGraw-Hill.

Thurnheer, T., R. Gmur and B. Guggenheim. 2004. Multiplex FISH analysis of a six-species bacterial biofilm. *Journal of Microbiological Methods* 56(1): 37-47.

Tiedje, J. M., S. Simkins and P. M. Groffman. 1989. Perspectives on measurement of denitrification in the field including recommended protocols for acetylene based methods. *Plant and Soil* 115(2): 261-284.

Tiedje, J. M., S. Asuming-Brempong, K. Nusslein, T. L. Marsh and S. J. Flynn. 1999. Opening the black box of soil microbial diversity. *Applied Soil Ecology* 13(2): 109-122.

Torneman, N., X. Yang, E. Baath and G. Bengtsson. 2008. Spatial covariation of microbial community composition and polycyclic aromatic hydrocarbon concentration in a creosote-polluted soil. *Environmental Toxicology and Chemistry* 27(5): 1039-1046.

Torsvik, V., J. Goksoyr and F. L. Daae. 1990. High diversity in DNA of soil bacteria. *Applied and Environmental Microbiology* 56(3): 782-787.

Tuckfield, R. and J. McArthur. 2008. Spatial analysis of antibiotic resistance along metal contaminated streams. *Microbial Ecology* 55(4): 595-607.

Turner, R. E. and N. N. Rabalais. 1994. Coastal eutrophication near the Mississippi River delta. *Nature* 368(6472): 619-621.

van de Corput, M. P. C., R. W. Dirks, R. P. M. van Gijlswijk, E. van Binnendijk, C. M. Hattinger, R. A. de Paus, J. E. Landegent and A. K. Raap. 1998. Sensitive mRNA detection by fluorescence in situ hybridization using horseradish peroxidase-labeled oligodeoxynucleotides and tyramide signal amplification. *Journal of Histochemistry & Cytochemistry* 46(11): 1249-1259.

van der Heijden, M. G. A., J. N. Klironomos, M. Ursic, P. Moutoglis, R. Streitwolf-Engel, T. Boller, A. Wiemken and I. R. Sanders. 1998. Mycorrhizal fungal diversity determines plant biodiversity, ecosystem variability and productivity. *Nature* 396(6706): 69-72.

van Driel, P. W., W. D. Robertson and L. C. Merkley. 2006. Denitrification of agricultural drainage using wood-based reactors. *Transactions of the ASABE* 49(2): 565-573.

Vogan, J. 1993. The use of emplaced denitrifying layers to promote nitrate removal from septic effluent. MS thesis. Waterloo, Ontario: University of Waterloo, Department of Earth Science.

Volokita, M., S. Belkin, A. Abeliovich and M. I. M. Soares. 1996a. Biological denitrification of drinking water using newspaper. *Water Research* 30(4): 965-971.

Volokita, M., A. Abeliovich, M. Ines and M. I. M. Soares. 1996b. Denitrification of groundwater using cotton as energy source. *Water Science and Technology* 34(1-2 pt 1): 379-385.

Wagner, H. H. 2004. Direct multi-scale ordination with canonical correspondence analysis. *Ecology* 85(2): 342-351.

Wagner, H. H. 2003. Spatial covariance in plant communities: Integrating ordination, geostatistics, and variance testing. *Ecology* 84(4): 1045-1057.

Wainwright, M., K. Killham and M. F. Diprose. 1980. Effects of 2450-mhz microwave-radiation on nitrification, respiration and s-oxidation in soil. *Soil Biology & Biochemistry* 12(5): 489-493.

Wakatsuki, T., H. Esumi and S. Omura. 1993. High-performance and N-removable and P-removable on-site domestic wastewater treatment system by multi-soil-layering method. *Water Science and Technology* 27(1): 31-40.

Walker, B. H. 1992. Biodiversity and ecological redundancy. *Conservation Biology* 6(1): 18-23.

Wallenstein, M. D., W. T. Peterjohn and W. H. Schlesingeri. 2006a. N fertilization effects on denitrification and N cycling in an aggrading forest. *Ecological Applications* 16(6): 2168-2176.

Wallenstein, M. D., D. D. Myrold, M. Firestone and M. Voytek. 2006b. Environmental controls on denitrifying communities and denitrification rates: Insights from molecular methods. *Ecological Applications* 16(6): 2143-2152.

Wang, J. H., B. C. Baltzis and G. A. Lewandowski. 1995. Fundamental denitrification kinetic-studies with *Pseudomonas denitrificans*. *Biotechnology and Bioengineering* 47(1): 26-41.

Ward, D. M., R. Weller and M. M. Bateson. 1990. 16S ribosomal-RNA sequences reveal numerous uncultured microorganisms in a natural community. *Nature* 345(6270): 63-65.

Wardle, D., R. Bardgett, J. Klironomos, H. Setala, W. van der Putten and D. Wall. 2004. Ecological linkages between aboveground and belowground biota. *Science* 304(5677): 1629-1633.

Weier, K. L., J. W. Doran, J. F. Power and D. T. Walters. 1993. Denitrification and the dinitrogen nitrous-oxide ratio as affected by soil-water, available carbon, and nitrate. *Soil Science Society of America Journal* 57(1): 66-72.

Weier, K. L., J. W. Doran, A. R. Mosier, J. F. Power and T. A. Peterson. 1994. Potential for bioremediation of high nitrate irrigation water via denitrification. *Journal of Environmental Quality* 23(1): 105-110.

Wertz, S., C. E. Dandie, C. Goyer, J. T. Trevors and C. L. Patten. 2009. Diversity of *nirK* denitrifying genes and transcripts in an agricultural soil. *Applied and Environmental Microbiology* 75(23): 7365-7377.

Whiteley, A. S., R. I. Griffiths and M. J. Bailey. 2003. Analysis of the microbial functional diversity within water-stressed soil communities by flow cytometric analysis and CTC plus cell sorting. *Journal of Microbiological Methods* 54(2): 257-267.

Wildman, T. A. 2002. Design of field-scale bioreactors for bioremediation of nitrate in tile drainage effluent. MS thesis. Urbana-Champaign, Illinois: University of Illinois, Department of Agricultural Engineering.

Woese, C. R. 1987. Bacterial evolution. *Microbiological Reviews* 51(2): 221-271.

Woli, K. P., M. B. David, R. A. Cooke, G. F. McIsaac and C. A. Mitchell. 2010. Nitrogen balance in and export from agricultural fields associated with controlled drainage systems and denitrifying bioreactors. *Ecological Engineering* 36(11): 1558-1566.

Wolsing, M. and A. Prieme. 2004. Observation of high seasonal variation in community structure of denitrifying bacteria in arable soil receiving artificial fertilizer and cattle manure by determining t-RFLP of nir gene fragments. *FEMS Microbiology Ecology* 48(2): 261-271.

Yannarell, A., A. Kent, G. Lauster, T. Kratz and E. Triplett. 2003. Temporal patterns in bacterial communities in three temperate lakes of different trophic status. *Microbial Ecology* 46(4): 391-405.

Yannarell, A. C. and E. W. Triplett. 2005. Geographic and environmental sources of variation in lake bacterial community composition. *Applied and Environmental Microbiology* 71(1): 227-239.

Yannarell, A. C., A. D. Kent, G. H. Lauster, T. K. Kratz and E. W. Triplett. 2003. Temporal patterns in bacterial communities in three temperate lakes of different trophic status. *Microbial Ecology* 46(4): 391-405.

Yeomans, J. C., J. M. Bremner and G. W. McCarty. 1992. Denitrification capacity and denitrification potential of subsurface soils. *Communications in Soil Science and Plant Analysis* 23(9-10): 919-927.

Zarda, B., D. Hahn, A. Chatzinotas, W. Schonhuber, A. Neef, R. I. Amann and J. Zeyer. 1997. Analysis of bacterial community structure in bulk soil by in situ hybridization. *Archives of Microbiology* 168(3): 185-192.

Zhou, Z., M. N. Pons, L. Raskin and J. L. Zilles. 2007. Automated image analysis for quantitative fluorescence in situ hybridization with environmental samples. *Applied and Environmental Microbiology* 73(9): 2956-2962.

Zhou, Z. 2007. Evaluation of macrolide-lincosamide-streptogramin B (MLSB) antimicrobial resistance at swine farms. PhD dissertation. Urbana-Champaign, Illinois: University of Illinois, Department of Civil and Environmental Engineering.

Zumft, W. G. 1997. Cell biology and molecular basis of denitrification. *Microbiology and Molecular Biology Reviews* 61(4): 533-616.